Sampling Visual Space

Topography, colour vision and visually guided predator avoidance in fiddler crabs (*Uca vomeris*)

Jochen Smolka

A thesis submitted for the degree of Doctor of Philosophy of

The Australian National University

June 2009

Title page: Regional specialisations in the *Uca vomeris* compound eyes exploit the differences in information content in different parts of the visual world (right image half, see chapter II). In the lateral visual field, facets are largest, increasing contrast sensitivity for the detection of approaching territory intruders. Frontally, resolution is highest and finely tuned to the short wavelengths that are provided by the crabs' blue carapace patterns (spectra in left image half) and picked up by the crabs' unusual trichromatic colour vision system (spectral sensitivities depicted between eyes, see chapter III). The dorsal eye features poor resolution, but comparatively large facets, leading to a patchy, undersampled visual field, but good sensitivity for the detection of small moving objects like approaching predators (see chapter IV and V).

Declaration

This thesis is an account of research undertaken between March 2005 and May 2009 at the Research School of Biological Sciences, The Australian National University, Canberra, Australia. Except where acknowledged in the customary manner, the material presented in this thesis is, to the best of my knowledge, original and has not been submitted in whole or in part for a degree at any other university. I am the senior author and the principal contributor to all aspects of the co-authored papers within.

…….

Jochen Smolka

Abstract

Many animals use vision to guide their behaviour and to collect relevant information about their environment. The diversity of visual environments and of visually guided tasks has led to a large variety of specialisations of eyes and visual systems. Our knowledge, however, about how the anatomical and physiological properties of eyes and the behavioural strategies of animals relate to the visual signals that are important to them in their natural environment, is extremely limited. In this thesis, I make use of optical, physiological and behavioural analyses to reconstruct the flow of visual information that the fiddler crab *Uca vomeris* experiences during its daily life on the mudflat. I present a detailed analysis of the first stage of visual processing, the sampling by the ommatidial array of the crabs' compound eye and demonstrate how regional specialisations of optical and sampling resolution reflect the information content and behavioural relevance of different parts of the visual field. Having developed the first intracellular electrophysiological preparation in fiddler crabs, I then examine the spectral sensitivities of photoreceptors – the basis for colour vision. I show that the crabs possess an unusual trichromatic colour vision system featuring a UV-sensitive and a variety of short-wavelength receptor types based on the co-expression of two short-wavelength sensitive pigments. Finally, the natural visual signals that predatory and non-predatory birds present to fiddler crabs are described. The visual cues the crabs use when deciding whether and when to respond to these potential predators are analysed and compared to those used in dummy predator experiments. The crabs use a decision criterion that combines multiple visual cues – including retinal speed, elevation and visual flicker. Neither of these cues accurately predicts risk, but together they reflect the statistical properties of the natural signals the crabs experience.

The complex interactions between the design of the crabs' visual system, the stimuli they experience in their natural context and their behaviour demonstrate that neither of them can be understood without knowledge of the other two.

Acknowledgements

This thesis would not have been possible without the support from a great number of people.

First and foremost, I would like to thank my PhD supervisors Jan Hemmi and Jochen Zeil for their marvellous support, their continual encouragement and invaluable advice. Jan's fantastic support, analytical zeal and incredible impetus – whether in the lab, on the mudflat or chasing me up New Zealand's mountains – were an invaluable, constant source of motivation and made this thesis possible. Equally, without Jochen's scientific enthusiasm, inspiration and wisdom, this project would have been impossible. I would also like to thank my PhD advisor Michael Jennions for providing motivation through keen interest and valuable discussions.

A great number of others have contributed to this work in many ways. I am indebted to Justin Marshall, Sonja Kleinlogel and Daniel Tomsic for initiating and training me in the mysteries of electrophysiology. Many others, at ANU and elsewhere have provided help or advice along the way, including Eric Warrant, Ajay Narendra, Cecile Bordier, Richard Berry, Angelique Paulk, Debjani Das, Shaowu Zhang, Waltraud Pix, Tobias Merkle, Richard Peters and Willi Ribi. For his astonishing crab-catching skills, I am also much indebted to Juri Hemmi. I would also like to thank Robert Parker, Mark Snowball, Istavan Zaveczky, Shane Green and the RSBS workshop, as well as the RSPhysE workshop, especially Ron Cruikshank, Richard Kolterman and Tony Barling for helping in the design and construction of my laboratory and field equipment.

I would also like to thank my fellow students, who have helped keep me (mostly) sane through the duration of my PhD and supported me in many ways, including Mario Pahl, Pinar, Johannes and Laila (almost a student) Letzkus, Martin How,

Wiebke Ebeling, Shaun New, Lisa Vlahos, Riccardo Natoli, Sam Reid, Ali Alkaladi, Marianne Peso, Nicole Carey, Yu-Shan Hung and Amir Mohammadi, to name but a few.

I would like to thank my parents, my brother and all my friends in Germany for continuously supporting me both before and during my PhD.

Finally, I would like to thank the Research School of Biological Sciences (RSBS, now RSB), and the Australian National University for providing funding through an ANU PhD scholarship; further the Australian Department of Education, Employment and Workplace Relations for an International Postgraduate Research Scholarship; the German National Academic Foundation and the Zeiss Foundation for support through a Heinz-Dürr Scholarship; and the Australian Institute of Marine Sciences for providing accommodation and facilities during fieldwork in Queensland.

Contents

List of figures

List of tables

Chapter I

Introduction

I.1 Sensory systems and natural stimuli

Animals have evolved a large number of senses to provide them with information about their environment. Because these sensory systems are limited by the developmental and energetic costs they impose, they are not general information processing devices, but are highly specialised to efficiently extract the information that is relevant to the animal in the context of its behaviour and ecology. In the words of Simoncelli and Olshausen (2001):

> *"The use of such ecological constraints is most clearly evident in sensory systems, where it has long been assumed that neurons are adapted, at evolutionary, developmental, and behavioral timescales, to the signals to which they are exposed. Because not all signals are equally likely, it is natural to assume that perceptual systems should be able to best process those signals that occur most frequently."*

This, of course, is true not only for neurons, but equally for the sensory organs themselves and for the animal's behaviour that is guided by and guiding the sensory experience. However, there are only very few circumstances where we know enough about the signals in a natural environment to understand the complex interactions that shape the animal's sensory systems and behaviour. This thesis aims to contribute to our understanding of sensory ecology by examining visual sampling – from optics to colour vision – and the visually guided behaviour of the fiddler crab *Uca vomeris* in its natural environment.

I.1.1 Visual sampling

Vision is arguably one of most important senses that animals use to collect information about their environment. As one of the few senses that can collect and locate information over long distances, it is frequently used for navigation, food localisation, predator avoidance, communication, mate detection and many other

functions (Land and Nilsson, 2006). Even more so than in other sensory modalities, the adaptations to different visual ecologies are immediately apparent by the immense range of eye types in the animal kingdom (reviewed by Land and Nilsson, 2002) and the regional specialisations within these eyes. As John Lythgoe (1979) puts it:

> *"A large predator armed in tooth and claw is unlikely to share the same visual preoccupations as a grazing rodent, and an animal of the open plains has to cope with a different kind of visual scene than one that lives in the middle-layer of the forest."*

Whether in the intricate spatial arrangement of photoreceptors in the retinae of vertebrates (reviewed by Hughes, 1977) and invertebrates (reviewed by Land, 1997), in their spectral (e.g. Kelber et al., 2003) or polarisation sensitivity (reviewed by Labhart and Meyer, 1999), regional specialisation of eyes are extremely common. However, considering this diversity of adaptations, there is very limited evidence of how the global design of eyes and the distribution of different regional specialisations reflect the informational ecology of animals and affect their the behavioural strategies.

I.2 The visual world of fiddler crabs

The 97 species of fiddler crabs (Crustacea; Malacostraca; Decapoda; Brachyura; Ocypodidae; *Uca*) are extremely colourful and social crabs that can be found in dense colonies on tropical intertidal mudflats around the world. Each crab occupies a burrow from which it emerges shortly after the mudflat is exposed by the low tide. This burrow is the central hub around which the crabs centre most of their daily activities. It serves as a refuge from predators and plays an important role as a resource in the crabs' mating system (e.g. Christy, 1982; Backwell and Passmore, 1996). It is therefore defended vigorously against territory intruders. During their

excursions on the mudflat the crabs constantly keep track of the direction and distance of their burrow (Zeil, 1998; Zeil and Layne, 2002; Layne et al., 2003a, b) and return to it immediately when threatened by a predator (Christy, 1982; Hemmi, 2005a, b) or when another crab approaches the burrow (Salmon, 1984; Hemmi and Zeil, 2003a, b; Yamaguchi and Tabata, 2004). Whilst active on the mudflat, crabs feed by scraping mud from the mudflat surface using their small feeding claws, of which females have two and males have only one. The males' second claw is enormously enlarged and used as a weapon in territorial disputes and as a signalling device in the males waving displays. These extremely variable displays serve the crabs to attract females to their burrow and to deter competing males (Berglund et al., 1996; Pope, 1998; How et al., 2007; How et al., 2008).

Fiddler crabs are highly visual animals. They use visual cues in their complex courtship behaviour and to detect other crabs intruding into their territory. Most importantly, their predator avoidance system is exclusively based on visual cues[1] (Land and Layne, 1995; Hemmi, 2005a,b). The crabs carry their compound eyes on long stalks above their body. Each eye covers a 360°, panoramic field of view, removing the need for any directed or scanning eye movements. The eyestalks are kept perpendicular to the visual horizon at all times (Nalbach et al., 1989). Provided a detailed knowledge of the properties of the visual system, this therefore allows us to reconstruct what the crabs see at any point in time by simply recording their position and orientation.

I.2.1 Life in a dangerous world

The fiddler crab predator avoidance system thus gives us the unique opportunity to study a purely visual signal in a model system where we can monitor both the visual signal and the receiver for extended periods of time. The compound eyes of fiddler crabs provide us with the additional advantage of a comparatively low resolution. This allows us to manipulate elements of the predator recognition and risk assessment

[1] Although vibratory cues might play a role in the detection of walking birds, they are of no use in the detection of aerial predators. Similarly, chemical cues provide no useful information about fast-approaching predators. The use of auditory cues, finally, is easily disproved in the field: Fiddler crabs do not display flight behaviour in response to any sounds.

process using dummy predators in the field. Although these dummies have no resemblance to real birds – they are in fact small plastic or Styrofoam balls – the crabs react to them the same way they would to an actual predator (Hemmi, 2005a,b). This clearly demonstrates how limited the information is that fiddler crabs have available when they are making decisions about whether and when to flee from an approaching predator. These dummy experiments allow us to carefully manipulate and examine the visual cues that the crabs could potentially be using and to easily and strictly test the effect of individual cues. Because of this, however, such controlled experiments tend to focus on single cues rather than the complex interactions that natural visual stimuli entail. Animals that rely on these cues for their survival, on the other hand, require a reliable, robust and adaptable response criterion, and this is usually more likely to be provided by a complex combination of multiple cues. The only way, therefore, to know what the natural consequences of certain decision criteria are, is to look at the natural interactions between fiddler crabs and their predators.

I.3 Thesis outline

This thesis represents four years of work on the topography of vision and visual behaviour in the fiddler crab *Uca vomeris*. It aims to provide a detailed analysis and a basis for future modelling of the visual sampling process in the fiddler crab compound eye, all the way from the signal through the spatial and spectral processing in the ommatidial array to the behavioural decisions in a natural setting. In Chapter II, I conduct an in-depth examination of the *U. vomeris* sampling array. Using *in vivo* optical techniques, I have mapped viewing directions and lens diameters and reconstructed the first full eye map of sampling and optical resolution for any crustacean. The results of this analysis are compared to behavioural data from other studies and used to speculate on the role of different eye regions in the behaviour of the crabs. This chapter has been submitted for journal publication and is presented as

a manuscript. In Chapter III, I present the first intracellular electrophysiological preparation in a fiddler crab eye. I elucidate the spectral sensitivities of individual photoreceptors. These reveal an unusual trichromatic colour vision system, including a UV-sensitive receptor class previously undescribed in crabs, and a wide variety of blue receptors, most likely created by differential co-expression of two visual pigments. The chapter ends with a demonstration of the new setup's potential for measurements of polarisation sensitivity and light responses in visual interneurons. In Chapter IV and V, I investigate the visual signal that crabs experience when making decisions during one of their most important visual tasks, predator avoidance. In the first of these chapters, I examine the natural signal during bird approaches at an Australian beach and find that in the presence of incomplete and imperfect information fiddler crabs use a multiple-cue response criterion including visual flicker which might help them to more efficiently balance early detection against the costs of false alarms. Then, in Chapter V, I use a well-established dummy-predator system (Hemmi, 2005a, b) to determine the contribution of flicker when compared to other decision criteria. Finally, I conclude with Chapter VI, a general discussion of the close link between visual sampling, natural images and behaviour and an outlook on possible future studies.

Chapter II

Topography of fiddler crab vision and its relation to behaviour

II.1 Summary

Given the great range of visual systems, tasks and habitats, there is surprisingly little experimental evidence of how sensory limitations affect behavioural strategies. Fiddler crabs present a well-studied and easily accessible experimental system for the synchronous measurement of visually elicited behaviour and the underlying visual cues. To quantify these cues from a crab's perspective, however, it is necessary to understand the processing of the signal in the visual system. We examined the first stage of visual processing, the sampling by the ommatidial array, in the compound eye of *Uca vomeris*. Using an *in vivo* pseudopupil method we determined sizes and viewing directions of ommatidia and created a complete eye map of optical and sampling resolution. Vertical resolution is maximal in a narrow visual streak along the horizon and decreases rapidly in the dorsal and ventral eye. This streak also contains the largest facets (max. 32 μm). There are clear differences between the frontal and lateral visual field within the streak. Resolution is highest frontally (1.54 c/º compared to 1.36 c/º laterally), whereas the lateral visual field features the largest facets and therefore highest contrast sensitivity. We argue that, under global eye space constraints, these regional optimisations reflect the information content and behavioural relevance of the corresponding parts of the visual field. In demonstrating the tight link between visual sampling, visual cues and behavioural strategies, our analysis highlights how the study of natural behaviour and natural stimuli is essential to our understanding and interpretation of the evolution and ecology of animal behaviour and the design of sensory systems.

II.2 Introduction

All animals rely on sensory information to guide their behaviour. However, sensory systems are limited in the amount and quality of information they can provide about the state of the environment. To understand an animal's behaviour, we therefore have to understand the design and limitations of the sensory systems guiding it. Conversely, the design of sensory systems can be expected to reflect important stimuli the animal is confronted with in natural situations (e.g. Gibson, 1950; Lythgoe, 1979; Loew and Lythgoe, 1985; Lythgoe and Partridge, 1989; Simoncelli and Olshausen, 2001; Körding et al., 2004) and the organisation of its behaviour (e.g. Srinivasan, 1993; Eckert and Zeil, 2001; Sparks, 2005). Both sensory systems and behavioural strategies also depend on an animal's evolutionary history and are under physiological and developmental constraints. In particular, eyes and visual systems are energetically costly (Niven and Laughlin, 2008), which has led to a wide variety of global (e.g. for optic flow processing, Franz and Krapp, 2000) and regional (Walls, 1942; Hughes, 1977; Land, 1989) specialisations in the eyes of many animals. All of these specialisations exploit the fact that biologically relevant information is not randomly distributed in visual space. Whether through ecological and topological constraints or through active movements of eyes, head and body, similar events tend to happen in similar regions of the visual field. An example is the streak of high acuity at the visual horizon found in the eyes of many flat-world inhabitants, be they grazing mammals such as kangaroos (Hughes, 1975), rabbits and horses (Hughes, 1977) or invertebrates like water striders (Dahmen, 1991), locusts (Krapp and Gabbiani, 2005) and fiddler crabs (Zeil et al., 1986; Land and Layne, 1995a; Zeil and Al-Mutairi, 1996). In a flat environment any approaching object, including predators, will first be seen close to the horizon. Increasing resolution in this area will therefore increase detection and recognition threshold distances and give the animal an advantage in both predator and social interactions. Interestingly, this specialisation seems to go one step further in invertebrates than in most vertebrates. The horizontal visual streaks of compound eyes feature an increased **vertical** resolution only (i.e. the

ability to distinguish objects of small vertical distances), whereas **horizontal** resolution is usually similar to the rest of the eye. In the visual streaks of most vertebrate eyes the random nature of the retinal arrangement of photoreceptors seems to prevent such a peripheral distinction (e.g. Hughes, 1977). A difference between vertical and horizontal resolution might, however, be introduced later during processing in the visual pathway (Mark et al., 1993). Other examples of regional eye specialisations are abundant both in vertebrates and invertebrates, be they regionalisations of acuity and sensitivity as in the foveae of many vertebrates (Walls, 1942) and in acute zones for target-tracking in predatory and mate-chasing insects (reviewed in Land, 1989), or regionalisations of colour vision abilities (e.g. Arikawa, 2003; Marshall et al., 2007), of polarisation sensitivity (e.g. Labhart, 1980; Dacke et al., 2003; Marshall et al., 2007) or of temporal resolution (e.g. Burton et al., 2001).

Fiddler crabs present an ideal model system for long-term studies of visually guided behaviour (review Zeil and Hemmi, 2006). They live in dense colonies on tropical and subtropical intertidal mudflats around the world. Each crab occupies a small territory centred on a burrow which it defends vigorously. During their excursions on the mudflat, they always keep the burrow in their lateral visual field and return to it in a straight line when a predator approaches or another crab moves towards the burrow (Altevogt and von Hagen, 1964; von Hagen, 1967; Land and Layne, 1995b; Zeil, 1998; Hemmi and Zeil, 2003a, b). This burrow-centred, small home-range lifestyle makes it possible to monitor an individual animal's whole behavioural range continuously for extended periods of time.

The crabs' compound eyes offer an additional experimental advantage. They are situated on long stalks which are kept perpendicular to the visual horizon (Nalbach et al., 1989; Zeil and Al-Mutairi, 1996). Each eye has a panoramic visual field, making it unnecessary for the animal to perform directed eye movements. Provided that the detailed sampling array of the compound eye is known, this makes it possible to reconstruct the complete visual information available to crabs at any one time. This approach has been used to examine a large range of visual behaviours including predator avoidance (Land and Layne, 1995a, b; Hemmi, 2005a, b), homing

(Zeil, 1998; Layne et al., 2003a, b), territory defence (e.g. Land and Layne, 1995a, b; Hemmi and Zeil, 2003a, b), mate choice (Detto et al., 2006) and courtship signalling (How et al., 2007; How and Hemmi, 2008). All of these behaviours are limited in different ways by the capabilities and accuracy of the visual system (e.g. Land and Layne, 1995b; Hemmi, 2005a, b; Hemmi and Zeil, 2005). In some *Uca* species, for example, individual recognition is based on the coloured patterns on the crabs' carapaces (Detto et al., 2006; Detto et al., 2008). Distinguishing these fine patterns requires high visual acuity and likely a finely tuned colour vision system. Predator avoidance, on the other hand, does not require the formation of a coloured or high-resolution image at all, but rather relies on high sensitivity in individual receptors to detect a small object as early as possible.

This study examines the regional specialisations of resolving power and contrast sensitivity in the *U. vomeris* compound eye and their relation to behaviour, social signals and colour vision. Resolving power is limited by the number of receptors per visual angle (sampling resolution) and by their receptive field sizes (optical resolution). The latter also directly constrains local contrast sensitivity and the detection of small objects. Previous studies (Zeil et al., 1986; Land and Layne, 1995a; Zeil and Al-Mutairi, 1996) have examined the distribution of optical and vertical sampling resolution along selected transects, focussing on the strong horizontal visual streak. In this study we have used a pseudopupil method similar to these earlier studies to determine sampling resolution and optical resolution over almost the entire *U. vomeris* compound eye. Our results show several differences between the frontal and lateral visual field that are closely associated with aspects of the crabs' behaviour. We will argue that different regions of the *U. vomeris* compound eye are specialised for different behavioural tasks. The design of their compound eye exploits the differences in the spatial distribution of different visual events. This is one of very few examples of a complete eye map in an invertebrate (Dahmen, 1991; Petrowitz et al., 2000; Krapp and Gabbiani, 2005) and, to our knowledge, the first full eye map published for any crustacean. This map can be used to accurately determine the visual cues that crabs receive in natural and experimental

situations, to predict maximum detection and recognition distance thresholds with respect to different visual events and to examine in fine detail the relation between local specialisations of the retinal sampling array and behavioural strategies.

II.3 Materials and methods

II.3.1 Animals, morphology and optical apparatus

Fiddler crabs *Uca vomeris* (McNeill) (Ocypodidae: Brachyura: Decapoda) of both sexes and of a wide range of sizes (10-25 mm carapace width, measured between lateral carapace spines) were collected from intertidal mudflats near Cungulla (19°24’S, 147°6’E), south of Townsville, Queensland, Australia and Redland Bay (27°37’S, 153°17’E) near Brisbane, Queensland, Australia. The animals were kept in individual plastic containers in the laboratory in Canberra for up to 6 weeks before experiments. During this period they were regularly provided with fresh seawater and fish food.

We took frontal macro-photographs of a total of 73 crabs from the two collection sites in several sessions in the field and the lab. The relation of eye height, width, separation, and eyestalk length to carapace width was analysed in a linear mixed model in R (R Development Core Team, Vienna, Austria) using experimental session as a random parameter and crab sex, carapace width, and handedness (the side of the larger claw in males) as variables. Variables were only included in the model when they were significant ($p < 0.05$) when added to the model last.

All optical measurements were performed on live and intact animals. To restrain the crabs, their legs and claws were tied together with tape. The males were forced to autotomise their larger claw by pinching the merus with forceps. An aluminium bar was then glued to the carapace and one eye stalk fixed to the metal with Blu-Tack and tape in an approximately natural position. During the experiment the eye was kept moist while taking care that no drops formed on the eye that would distort the microscope image and change the position of the pseudopupil. Using the

attached aluminium bar, the crab was fixed with its eye upright in the rotation centre of a goniometer microscope (Figure II.1, Dahmen, 1991). This allowed us to rotate the microscope along a horizontal and a vertical axis around the eye and thereby adjust its optical axis to different angles of azimuth and elevation. The microscope was fitted with a 1.3 Megapixel USB camera to monitor focus, position the microscope and rapidly acquire a large number of images.

II.3.2 Optical measurements

We examined the equatorial and dorsal field of view in one large adult female (19 mm carapace width). Through the microscope and even with the naked eye the principal pseudopupil (Franceschini, 1975; Stavenga, 1979) can be observed as a dark spot that follows the observer around the eye (Figure II.2; Zeil and Al-Mutairi, 1996). Only the ommatidia whose optical axes are aligned with the axis of observation appear black as all light is absorbed by the photopigment in the rhabdom. Ommatidia that are viewed off-angle appear in the colour of the secondary screening pigment covering the primary pigment cell layer (Alkaladi, 2008). By observing the position of the pseudopupil from many different angles around the eye, the optical axes of all ommatidia can thus be inferred (Franceschini, 1975).

Starting at the medial rim of the eye, we took consecutive measurements, first every 5° of azimuth along the eye equator (0° elevation), and then along 13 vertical strips every 30° of azimuth. Every strip included measurements at a maximum of 18 elevations in 5° steps between -10° and 70°. At each elevation we took three measurements with a horizontal offset of -5°, 0° and 5° azimuth, resulting in three adjacent vertical transects 5° apart. Each one of the resulting 780 measurements (Figure II.3B,C, grey circles) consisted of two photographs: one at the level where the principal pseudopupil could be observed clearest, and one at the focus level of the facets. The large depth of field of our microscope allowed us to identify, count, measure and connect all facets between strips and thus account for a total of 6925 individual ommatidia. This produced a continuous map of ommatidia filling almost the entire dorsal and part of the ventral visual field.

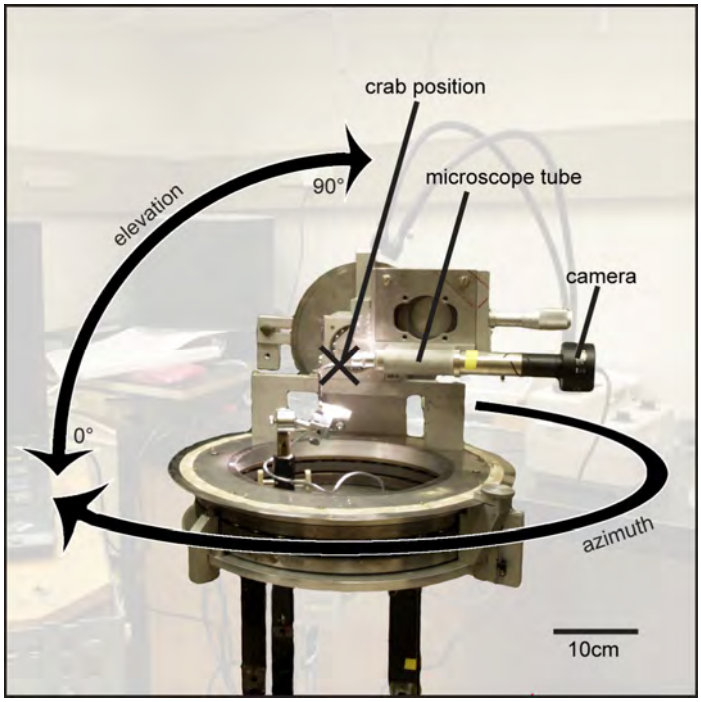

Figure II.1: The goniometer microscope. The goniometer allowed for a microscope with attached digital camera to be rotated to defined angles of azimuth and elevation. The restrained live crab was fixed in the rotation centre with its eye in a natural upright position. The frontal viewing direction was defined as 0° azimuth, with angles increasing along the lateral visual field towards the rear. The visual horizon was defined as 0° elevation with negative values in the ventral and positive in the dorsal visual field.

Selected parts of the visual field were measured in five additional animals (three males and two females between 14 mm and 22 mm carapace width). In three of these animals we took measurements along the eye equator and two vertical strips, one frontal (0° azimuth), one lateral (90° azimuth). In the other two animals we measured only the lateral strip. In all of these additional crabs we reduced our minimum vertical step size to 1.25° for increased measurement accuracy in the equatorial acute zone.

II.3.3 Analysis

In every photograph, the centres of all visible facets and of the pseudopupil were marked using custom software in MATLAB 7.4 (The MathWorks, Natick,

Massachusetts, USA). We then used natural irregularities in the eye as markers to identify individual facets that were visible in adjacent images. With at least three such common facets for each pair of neighbouring images we could individually label all 6925 observed facets, relate them to their neighbours and combine them with the measured pseudopupil positions into a single map similar to a retinal wholemount (Appendix A, Figure A.1). The area of every facet was measured as the area of its Voronoi cell (the cell containing all points that are closer to this than to any other facet). All photographs were calibrated using images of a microscope calibration slide.

In most cases, the positions of the pseudopupil centres developed smoothly on this map, but some deviations were clearly visible. Especially near the eye equator, where the pseudopupil is large and tear-shaped, its centre was often difficult to determine accurately. Similarly, in some parts of the dorsal eye the dark pigmentation made it hard to clearly identify facets and pseudopupils. We therefore adjusted the positions of our measured pseudopupil centres by smoothing their positional function using a two-dimensional thin-plate spline (Wahba, 1990). Great care was taken not to introduce artefacts during this procedure and all splined pseudopupil centres were checked against the original images. Viewing directions could now be assigned to a total of 5132 ommatidia that lay within the grid of measured pseudopupils. The viewing direction of a facet at a pseudopupil centre is equal to the pseudopupil's 'viewing direction', i.e. the optical axis of the microscope when the pseudopupil was observed. For facets that lay between measured pseudopupils, we linearly interpolated between adjacent viewing directions.

Once an animal is fixed in the goniometer, the optics of the eye starts degrading within hours, even when eye and animal are constantly kept moist. A quick procedure is therefore essential for the quality of the obtained images, making it difficult to perfectly align the eye centrally and upright at the beginning of the experiment. In our final map, the acute zone of highest vertical resolution was sinusoidally modulated in a way that could be fully explained by a 6° tilt of the eye in the goniometer. Previous studies (Land and Layne, 1995a; Zeil and Al-Mutairi, 1996)

have shown that under natural conditions crabs align this acute zone with the visual horizon. We therefore rotated our map accordingly to adjust for this tilt.

II.3.4 Extrapolation to a full eye model

Apparatus constraints and limited time before the eye degrades (as described above) prevented us from measuring the full ventral visual field in our main animal. We therefore included the ventral part of the frontal and lateral strips that we had measured in a size-matched female. To achieve a full description of the *U. vomeris* sampling grid, we splined and extrapolated the functions describing the vertical distance between rows and the horizontal distance between facets. Parameters of the splines were carefully adjusted to smoothly continue observed resolution curves and, where known, approximate the total number of rows we had observed in the main female. Ommatidia were then consecutively added according to the smoothed functions until the visual field was filled to the rim. These extrapolations thus created a full eye model based on measurements from two females.

II.4 Results

II.4.1 Morphology of the eye

The compound eyes of *U. vomeris* (Figure II.2 inset) are vertically elongated ellipsoids situated on long eyestalks. The ommatidial array wraps around the cylindrical eye, leaving only a narrow band of cuticle free from ommatidia at the median surface of the eyestalk. All anatomical dimensions scale linearly with animal carapace width (*cw*, in mm) and all except eye separation are slightly, but significantly larger in males than in females (Table II.1, Figure II.2). In males, we found no difference between the eye on the side of the major claw and the opposite eye in any of the measured parameters. As determined from linear mixed models, the eyes are 0.055**cw*+0.844 mm high and 0.030**cw*+0.632 mm wide in the mid-frontal plane in females. In males they are 0.063 mm higher and 0.068 mm wider respectively. The lower rim of the facet-bearing surface is held 0.34**cw*-0.38 mm

(+0.27 mm in males) above the animal's carapace. In a flat, natural environment, the eyestalks are held almost perfectly vertical, placing the centres of the eyes 0.17**cw*+2.4 mm apart.

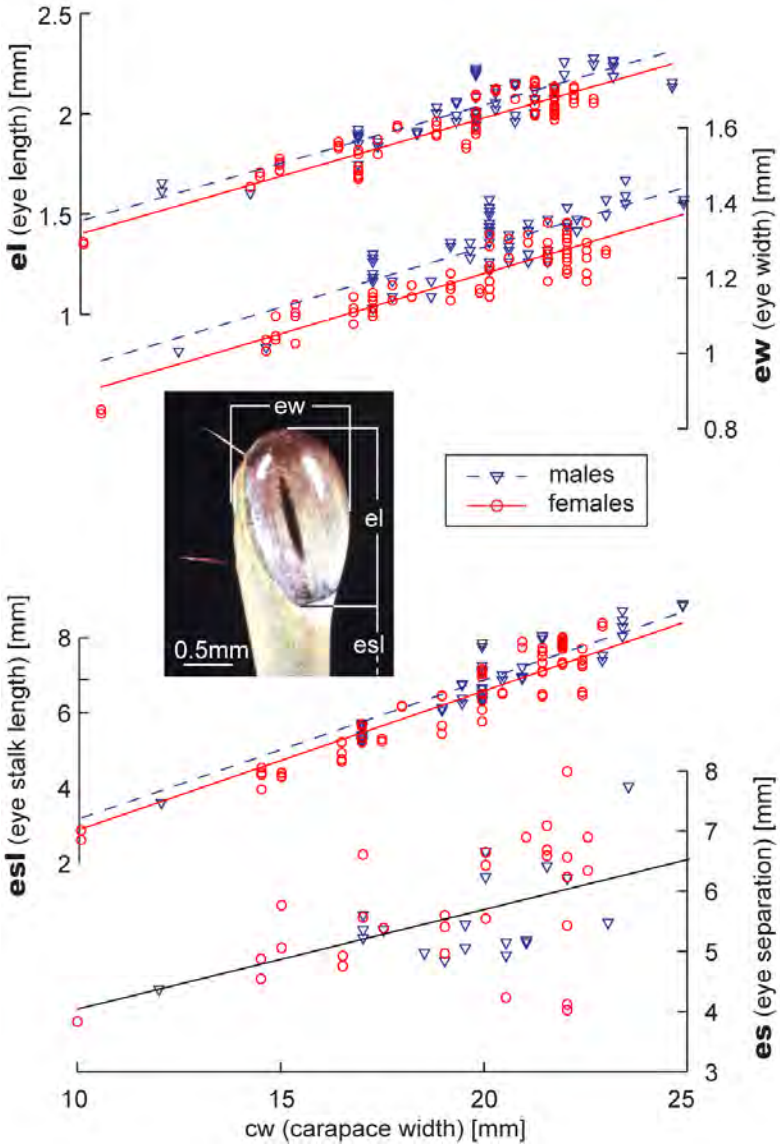

Figure II.2: Anatomical eye parameters. Eye width (***ew***, horizontal width of the eye at the widest point), eye length (***el***, vertical extent of the facet-bearing surface), eye stalk length (***esl***, distance between carapace and the lower end of the facet-bearing surface) and eye separation (***es***, distance between the centres of the eyes in a natural position) were measured as a function of carapace width in frontal macro photographs (inset) for male (triangles) and female (circles) *U. vomeris*. Regression lines are shown dashed for males and solid for females. All parameters were significantly dependent on carapace width and all measurements except eye separation (the distance between the eye centres in a natural position) were significantly larger for males than for females (for statistics see Table II.2).

Table II.1: Anatomical eye parameters. Results of the linear mixed model analysis (REML; random model: crab identity + setup identity). All measurements increase linearly with body size. 74 crabs between 10 and 25 mm carapace width (cw) were measured in frontal macro-photographs of the eyes. All parameters except eye separation are significantly larger in males. Regression lines are given by $\beta_1+\beta_2*cw+\beta_3*sex$, where sex is 0 for females and 1 for males. *** = $p<0.001$

	β_1	β_2	β_3	range	res. df
Eye length (el)	0.844 ***	0.055 ***	.063 ***	1.35-2.25	145
Eye width (ew)	0.632 ***	0.030 ***	.068 ***	0.86-1.4	45
Stalk length (esl)	-0.378 ***	0.343 ***	.270 ***	3.0-8.64	134
Eye separation (es)	2.395 ***	0.166 ***	0 (p=0.16)	3.85-8.0	50

II.4.2 Visual field and facet numbers

We determined the dorsal rim of the visual field in the goniometer micrographs and confirmed and extended these measurements to the full extent of the visual field in a second female crab (see Methods). Figure II.3 shows how the visual axes of ommatidia in the compound eye are distributed in visual space on a flat (Figure II.3A) and spherical projection (Figure II.3B,C). It also indicates which visual tasks are relevant in different areas of visual space (see discussion). Horizontally, the ommatidia cover a full 360° panoramic field of view between -20° and 40° of elevation. The fields of view of the two ends of the facet-bearing surface adjacent to the medial ridge overlap by at least 30° at the visual horizon. Dorsally, the frontal visual field extends to just over 70° of elevation, slowly decreasing toward about 50° caudally and even lower at the caudo-medial border of the medial cuticle ridge.

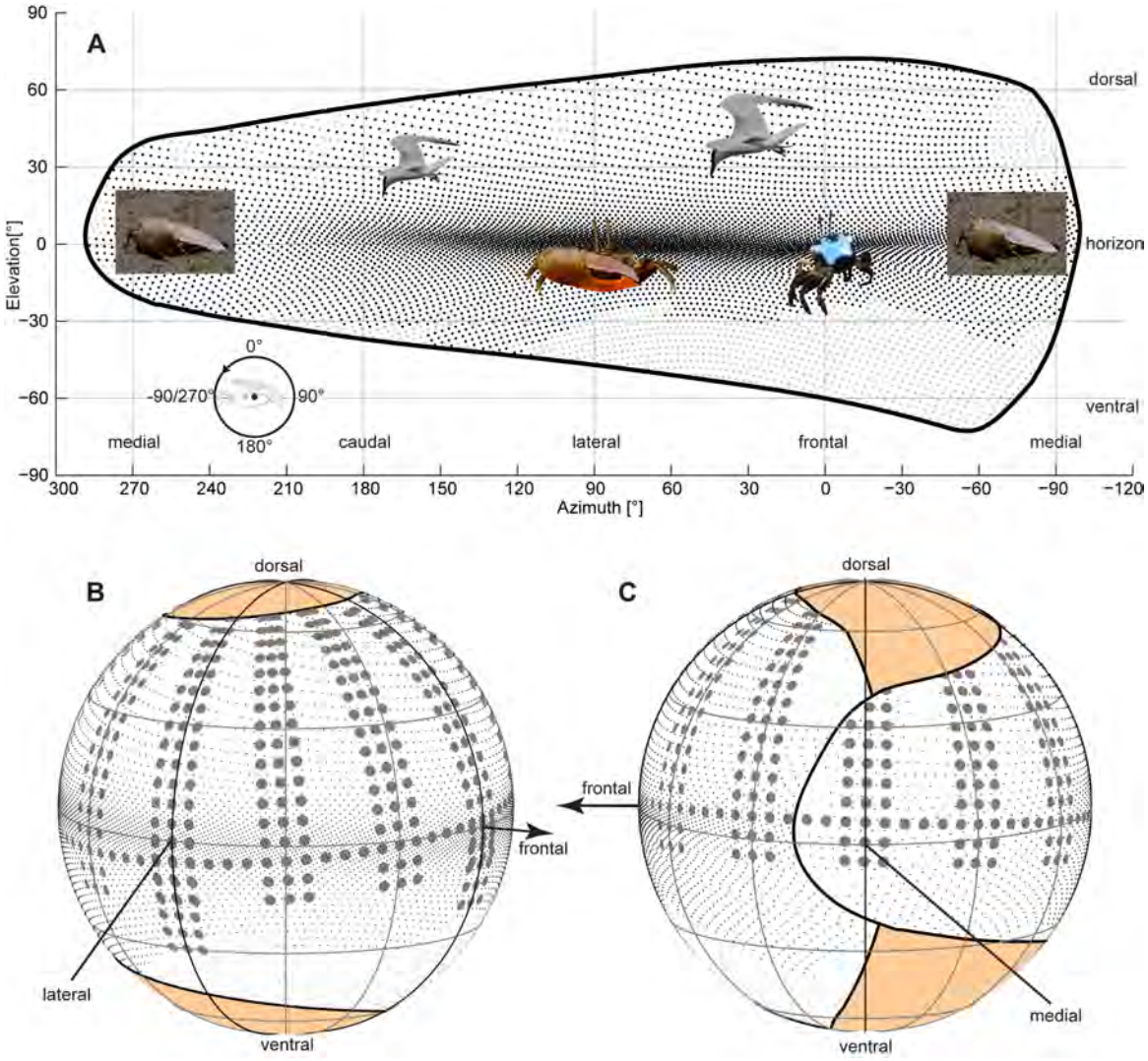

Figure II.3: Optical axes of ommatidia. (A) Equirectangular map of the reconstructed optical axes of an *U. vomeris* female. Black dots represent facets that were observed and whose size was measured on microscope photographs, grey dots represent facets added in an iterative extrapolation process to smoothly continue resolution gradients. The rim of the visual field (thick black line) is defined at the last position where a clear pseudopupil can be observed, the total visual field is likely to be up to 10° larger in all directions, but with a much lowered density of optical axes. Image insets indicate the relevant behaviours in specialised areas: Individual recognition frontally (female carapace pattern), burrow defence laterally (male with large claw), eye stalk orientation medially (crab on slope), predator avoidance dorsally (tern). See discussion for details. Optical axes are also displayed in spherical maps seen from fronto-lateral **(B)** and medial point of view **(C)**. Dots and rim as in A, large grey dots represent the visual directions at which microscope images were taken. Meridians and parallels are shown every 30° (grey lines) and emphasised every 90° (black lines). Note the 30° overlap of the two ends of the receptive surface in the medial visual field.

Ventrally, the field of view extends to -70° of elevation in a small corner looking about 45° medio-frontally towards the area directly in front of the animal's mouthparts. The ventral extension of the field of view shrinks drastically to about -45° laterally, -35° at the back and less than -20° close to the medial ridge. Because the eyestalks are situated at the front of the carapace, these angles essentially cut out that part of the field of view that is blocked by the animal's own body.

When reaching the border of the visual field the pseudopupil broadens and merges into the rim of the ommatidial array, making it hard to reliably determine pseudopupil positions and reconstruct optical axes. To exclude these facets, we defined the border of the field of view as the last point at which we could identify a clear pseudopupil. This method leads to an underestimation of the true field of view of the eye by 1-2 rows. The facets in these rows, however, probably have a very large receptive field of more than 10° diameter. Consequently, and contrary to what our maps (Figure II.3) suggest, the dorsal visual field is probably fully covered, but by ommatidia that will likely only provide very basic detection of changes in light level (e.g. due to movement of large, close objects).

We found 90 horizontal rows in the front (0° azimuth) and 74 in the lateral eye (90° azimuth), with a maximum of 138 ommatidia per row at the eye equator (Table II.2). Most facets look into an extremely narrow band around the visual horizon. Out of the total number of ommatidia, 33% / 50% / 75% are devoted to the central ±6.5° / ±13° / ±29° of elevation (Figure II.4). The number of facet rows inside this acute streak can be used as a simple anatomical indicator of resolution differences between frontal and lateral eye. In the central ±20° of elevation, there were on average 56 rows frontally and 48.2 rows laterally (difference 7.8, Welch two-sample t-test, $t = -10.08$, $df = 4.90$, $p < 0.0005$, 95% CI: [5.8 - 9.8]). The numbers varied only slightly and irrespectively of body size (Table II.2, see also Land and Layne, 1995a). Our final reconstruction (Figure II.3), in comparison, has a total of 79 rows frontally (54 in the 40° band) and 69 laterally (52 in band). These numbers are within or very close to the observed range, with the exception of the frontal total, suggesting that our extrapolation of the fronto-ventral visual field slightly

underestimated the sampling resolution and/or extent of the dorsal and/or ventral visual field outside the 40° band. The reconstructed eye contains a total of 7971 ommatidia.

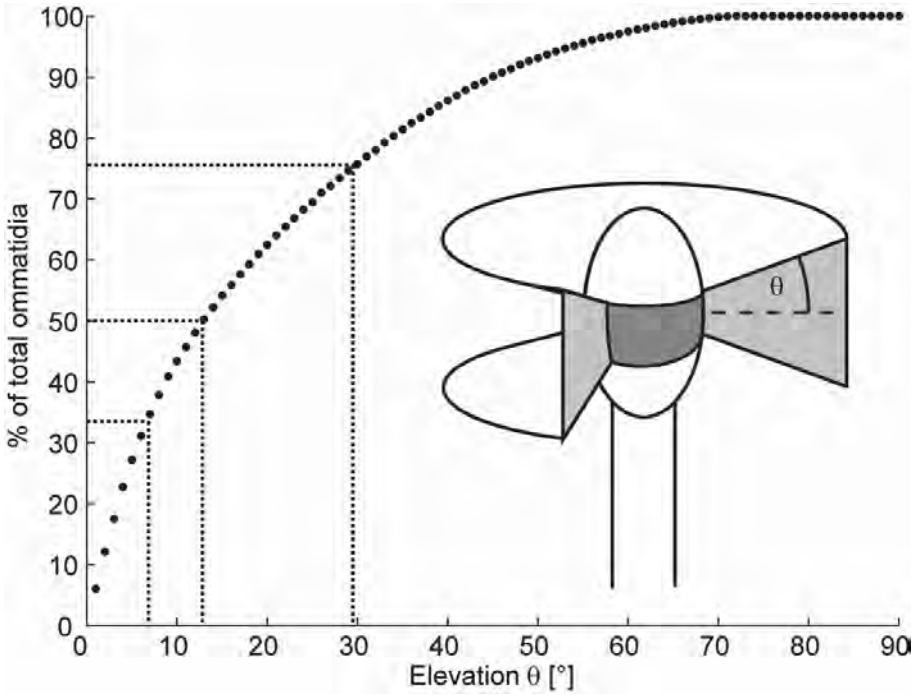

Figure II.4: Most ommatidia sample the horizon. The percentage of the total number of ommatidia looking into a symmetric band of viewing direction around the visual horizon. Note that even though the visual field extends to a maximum of ±70°, 50% of all facets are sampling the central ±13°, highlighting once more the importance of the visual horizon for the crabs.

Table II.2: Horizontal ommatidial row counts compared. Counts in experimental animals and our final reconstruction of the eye agree well. Rows were counted as total number of rows along two vertical transects (lateral and frontal eye surface) and as number of rows between the pseudopupils at +20° and -20° of elevation.

		Total rows	range	+-20° rows	range	n
Measured	Lateral	73.6	65-79	49.3	47-55	6
	Frontal	89.7	86-93	56	55-57	3
Model	Lateral	69	-	52	-	-
	Frontal	79	-	54	-	-

II.4.3 Variation in sampling resolution

We determined the partial interommatidial angle $\Delta\varphi$ (following Stavenga, 1979) in the vertical direction by calculating the distance between horizontal ommatidial rows and in the horizontal direction as half the distance between ommatidia along these rows (Figure II.5G). Vertical and horizontal sampling resolution in cycles/degree (c/°) follow as $\nu_s = 1/(2\Delta\varphi)$.

Vertical sampling resolution (Figure II.5A-C) peaks in a very narrow band around the visual horizon with a full width at half maximum (FWHM) of 11° laterally and 9° frontally (Figure II.5B). If we follow this streak horizontally along the equator, there appear to be two peaks, the first one frontally (0°) with a maximum of 1.54 c/° and the second laterally (60-90°) with a maximum of 1.48 c/°. Towards the backwards-facing visual field, peak resolution declines to 1.2 c/° caudo-laterally (135°), 0.45 c/° caudally (180°) and finally to about 0.2 c/° when approaching the medial end (270°) of the sampling area. Note that there are two parts of the eye sampling the medial visual field, referred to here by -90° (coming from the frontal eye) and 270° (coming from the rear). Outside of this horizontal acute streak, resolution declines rapidly to a minimum of about 0.3 c/° ventrally and 0.2 c/° in the dorsal visual field. To more accurately estimate the difference in peak vertical resolution between the lateral and frontal visual fields, we supplemented our data with measurements in an additional five animals, with increased measurement resolution in the visual streak. A detailed analysis including a discussion of potential errors inherent in the pseudopupil method can be found in Appendix B. Our analysis confirmed that frontal peak resolution (1.54 c/° on average) is always higher than the lateral resolution (1.36 c/° on average). Average peak FWHMs were slightly larger than measured above with 13° in the frontal and 12.5° in the lateral visual field.

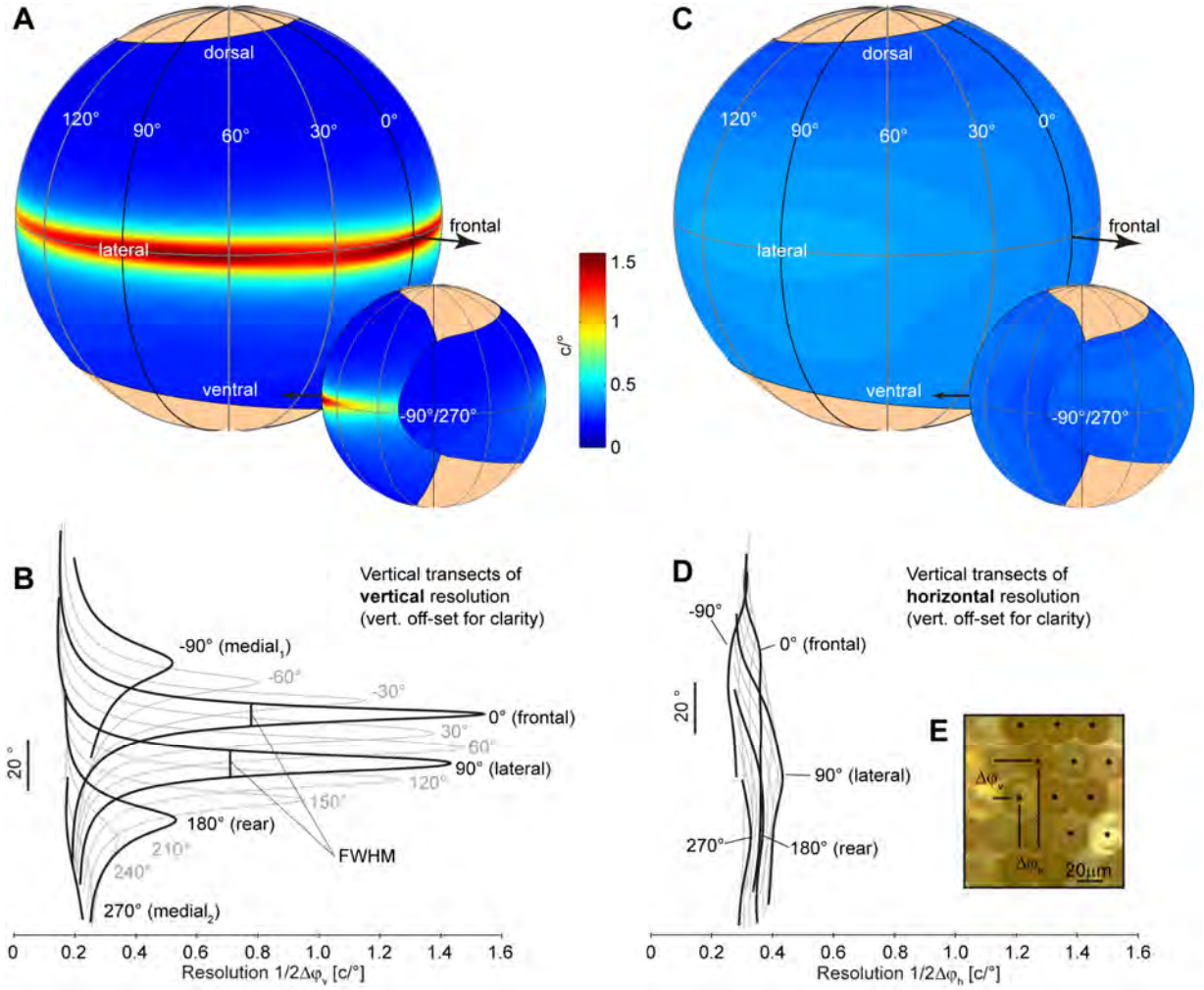

Figure II.5: Vertical and horizontal sampling resolution. Vertical **(A-B)** and horizontal **(C-D)** sampling resolution (in c/°) on spherical maps from fronto-lateral and medial (insets) point of view and as vertical transects **(B, D),** vertically off-set for clarity, every 30° of elevation (grey lines, with black lines every 90°). Resolution was determined from partial interommatidial angles (definition in **E**) measured as the angular distance between rows ($\Delta\varphi_v$: vertical resolution) and half the horizontal angular distance between facets in these rows ($\Delta\varphi_h$: horizontal resolution). Note the two distinct peaks (frontal and lateral) in the horizontal visual streak of vertical resolution. Horizontal resolution is up to four times lower at the horizon, but about 50% larger than vertical resolution in the dorsal and ventral visual field.

Two interesting observations concern the asymmetry of the resolution profile between the dorsal and ventral visual field. Firstly, as Zeil and Al-Mutairi (1996) also observed in *U. lactea annulipes*, resolution declines much slower ventrally than dorsally. In *U. vomeris* this effect is strongest in the frontal visual field (Figures II.5B, II.9). Secondly, the largest facets and therefore the peak of optical resolution in the frontal visual field are not at the visual horizon, but about 5° below. This means that the region of highest sensitivity points in a direction that corresponds to the body of a crab about 10 cm away, which agrees well with evidence about the functional significance of this zone in social interactions (see Discussion).

Horizontal sampling resolution (Figure II.5D-F) is generally much lower and more uniformly distributed than vertical resolution, but follows a similar trend. There is a global peak at the lateral horizon (90°) with a resolution of 0.45 c/°, declining to 0.4 c/° in the front (0°), 0.35 c/° in the rear (180°) and to a minimum of around 0.25-0.3 c/° in the far dorsal, ventral and medial (-90°/270°) visual field.

II.4.4 Optical vs. sampling resolution

Beside the number of receptors per visual angle (sampling resolution) the resolving power of an eye is limited by the receptors' angular sensitivities. The wider the angular sensitivity functions (usually represented by their half-width $\Delta\rho$, the acceptance angle), the more the image is blurred. Contrast is thus reduced at higher spatial frequencies, until at a spatial cut-off frequency $\nu_{co} = 1/\Delta\rho$, no contrast remains (Sparrow limit, see Snyder, 1979; Warrant and McIntyre, 1993). The acceptance angle depends partly on the amount of blur produced by diffraction in the lens as it focuses light onto the receptors (Warrant and McIntyre, 1993). In a lens of diameter D, a point source of monochromatic light (wavelength λ) is blurred onto an area known as the Airy disc or Fraunhofer diffraction pattern with a FWHM of $\Delta\rho_l = 1.02\lambda/D$.

Due to waveguide effects, the full acceptance angles $\Delta\rho$ are not easily determined theoretically (Stavenga, 2003a, b, 2004). However, the acceptance angle can be approximated by the half-width of the Airy disc in three circumstances: when

the eye is strongly light adapted, when the rhabdom is very thin and propagates mostly the fundamental waveguide mode, and/or when the focal lengths of the lenses are large compared to their diameters (Stavenga, 2003a, b, 2004). In the case of *Uca vomeris*, all these conditions are likely to be satisfied since these crabs are active on bright beaches, they have rhabdoms that are extremely thin and their focal length is about 5-6 times larger than the lens diameter (Alkaladi, 2008). In this study, we have therefore used Airy disc half-widths to estimated acceptance angles[2].

We determined the facet diameter (D, in μm) from facet area (A, in μm^2) as the diameter of a round facet of equal area ($D = 2\sqrt{(A/\pi)}$; Figure II.6C). In some parts of the eye facets were asymmetric, but the diameter along their largest dimension was never more than 10% larger than D. Facets were largest around the visual horizon. This strip of large facets coincides with the streak of highest visual acuity, but is much broader (Figure II.6A,B). Average facet diameter was 32.4 ± 0.33 μm (s.d.) in the lateral (n = 80 in a 5° radius around 90° azimuth / 0° elevation), and 30.9 ± 0.21 μm (s.d.) in the frontal (n = 54 in a 5° radius around 0° azimuth / -5° elevation) visual field (difference 1.5 μm, Welch two-sample t-test, t = -31.33, df = 131.56, p < 1e-15, 95% CI: [1.38 1.56]). The smallest measured facets in the far dorsal parts of the eye are about half that diameter.

[2] A more accurate description of acceptance angles would require either detailed electrophysiological measurements or a theoretical analysis of waveguide effects in fiddler crab eyes like that of Stavenga for *Drosophila* eyes. The exact size of acceptance angles, however, is not crucial for this study and even a substantial increase of 20-40% would not alter our general conclusions.

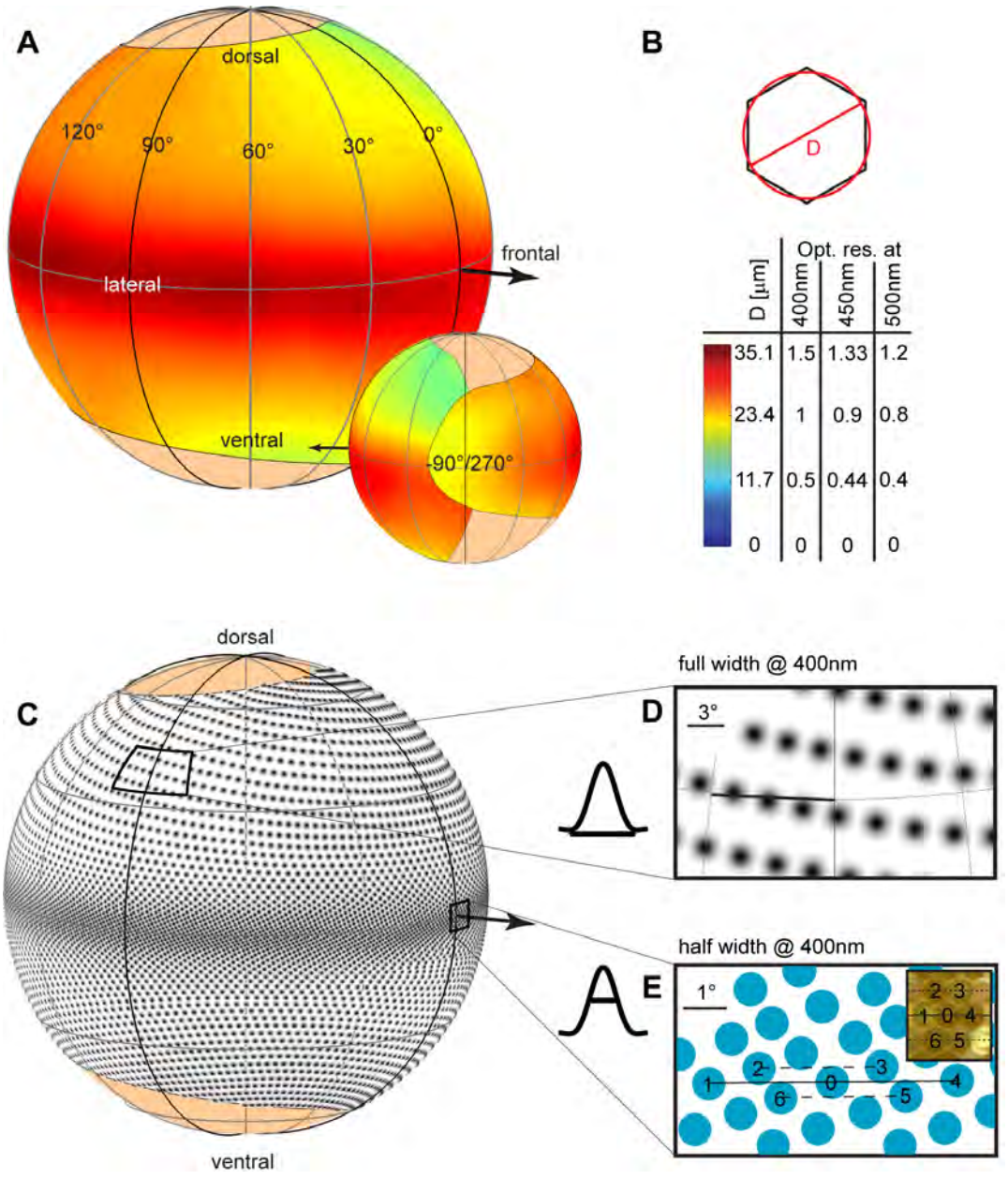

Figure II.6: Optical resolution and Airy discs. (A) Spherical maps of facet diameter in a female *U. vomeris* (*cw* = 19 mm) from fronto-lateral and medial (inset) points of view. **(B)** Facet diameter was determined from facet area as the diameter of a round facet of equal area. Optical resolution is directly proportional to the ratio of the wavelength of light to the facet diameter, and is listed for three exemplary wavelengths beside the colour bar coding facet diameter. **(C)** Spherical map of Airy discs from fronto-lateral point of view calculated for 400 nm light. **(D)** Magnification of a part of the dorsal visual field showing full Airy discs. These represent minimum acceptance angles of ommatidia, demonstrating that there is considerable undersampling of the visual field. **(E)** Magnification of the fronto-equatorial visual field. The seven numbered ommatidia show how the row structure on the eye translates into visual space. For a perfect match of vertical sampling and optical resolution, next-but-neighbour facets (e.g. #2 and #6) should show no vertical overlap. The fact that they do overlap demonstrates that even for 400 nm light, vertical resolution in the frontal acute zone is diffraction limited in an animal of this size (compare also Figure II.7B).

Figure II.6D illustrates how for blue light (400 nm) the visual space is covered by the Airy discs, representing the acceptance angles of individual ommatidia. For longer-wavelength light, Airy discs and acceptance angles will be larger (see below). In an ideal imaging system the acceptance angles should just cover the visual space with minimal or no overlap (see Land, 1981; Warrant and McIntyre, 1993). If they are larger, resolution will be limited below what could be achieved with the given sampling array. If they are smaller, visual space will be undersampled, i.e. there will be gaps in the field of view. In *U. vomeris*, Airy discs (Figure II.6D,E) are indeed far smaller than interommatidial angles in most of the visual field, suggesting that the visual surroundings are drastically undersampled (Dahmen, 1991; Zeil and Al-Mutairi, 1996). There are some regions of space that are effectively not sampled at all. Only at the horizon, visual space is fully covered with little overlap between the half-widths of Airy discs (Figure II.6E). Airy disc diameters, however, increase linearly with the wavelength of transmitted light and a direct comparison between sampling and optical resolution for different wavelengths suggests that in an animal of the size of our studied female (19 mm carapace width) the frontal peak of sampling resolution can only be fully utilized for ultra-violet light (Figure II.7).

As larger animals (and males) have larger eyes and facets, the cut-off will be less dramatic, but even in a 25 mm male (the largest we have observed in our study) the eyes are only 20% longer and, assuming facets grow linearly with eye length, the frontal limit would be at about 450 nm. Conversely, in small animals this problem will be exaggerated. In animals smaller than about 13 mm, frontal resolution would be diffraction limited for all relevant wavelengths.

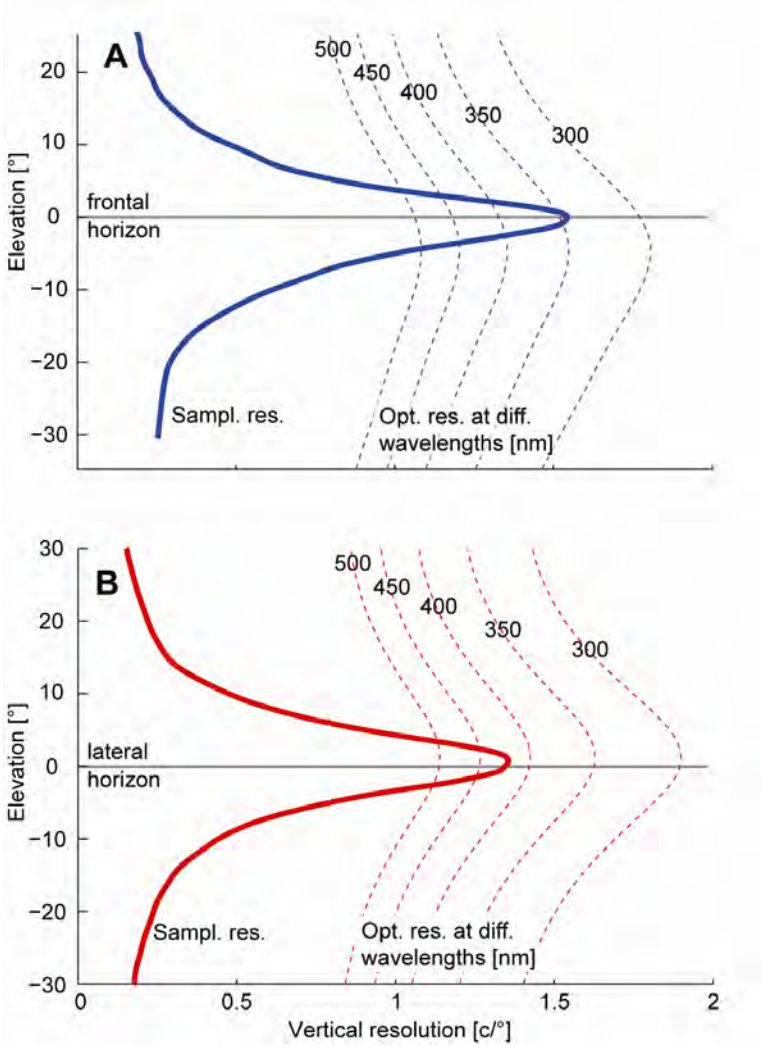

Figure II.7: Comparison of vertical sampling resolution and optical resolution. Sampling resolution (solid lines) was determined from averaged pseudopupil measurements in six animals (Appendix B, Figure B.1) along a lateral **(A)** and a frontal **(B)** transect. Optical resolution (dashed lines) is expressed as cut-off frequency and was determined from lens diameters (Figure II.6) measured in a female crab (*cw* = 19 mm). Optical resolution depends on the wavelength of sampled light and is shown for several different wavelengths. Note that the peak of optical, but not sampling resolution is shifted by about 5° below the horizon in the frontal visual field (since facet diameters are maximal at this location).

II.4.5 Eye shape

Facet size and sampling resolution compete for eye space in the sense that for a given maximum eye radius any increase in the number of facets (and therefore sampling resolution) must be compensated for by a reduction in facet size (and therefore optical resolution) and vice versa. Turning this dependence around, once we know the

distribution of ommatidial size and sampling resolution, we should be able to predict eye size and shape with few assumptions. We did this in an iterative computer model, starting with a horizontal row of ommatidia at the visual horizon and adding rows dorsally and ventrally under the constraint that visual axes must be perpendicular to the eye surface (Zeil and Al-Mutairi, 1996). Horizontal resolution and ommatidial width were considered constant for computational simplicity and an estimate of horizontal eye radius had to be fixed (0.5 mm) in the model. Given the simplicity of our assumptions the model gives a very close approximation of the shape of the *U. vomeris* eye (Figure II.8).

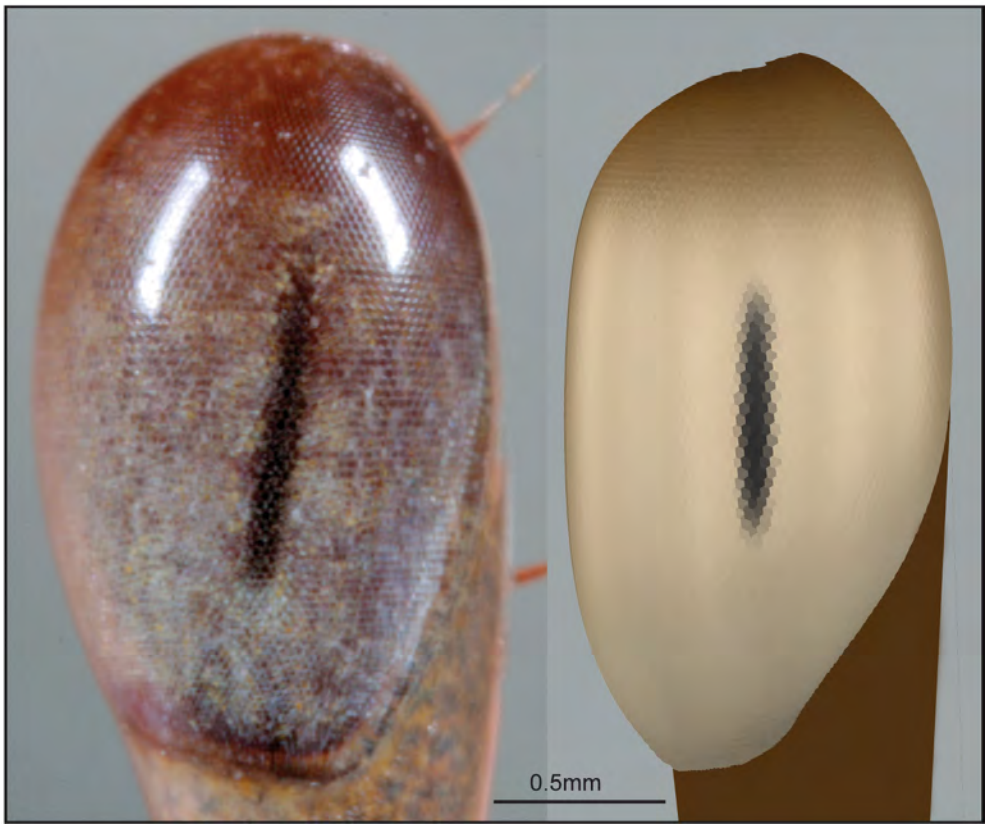

Figure II.8: Eye model. Comparison of the eye of a large *U. vomeris* male (*cw* = 22.25 mm) with our eye model for a similarly sized animal. Note that despite the very simple assumptions of our model (details in text) the eye shape is very similar. However, the model does not fully account for changes in eye radius and can not predict the tilt of the pseudopupil.

II.5 Discussion

The compound eyes of *Uca vomeris* have a narrow acute streak along the visual horizon in both vertical sampling resolution (determined from interommatidial angles) and optical resolution (determined from facet diameters). Vertical sampling resolution peaks in a 13° wide (FWHM) band along the frontal and lateral visual field. It declines rapidly towards ventral, dorsal, caudal and medial visual field and this gradient is shallowest in the fronto-ventral visual field. Horizontal sampling resolution is comparatively uniform across the eye with a broad, but shallow peak at the lateral horizon. It is four times lower than peak vertical resolution at the horizon, but up to 50% higher in the dorsal and ventral visual field. Facet diameter, and thus optical resolution, peaks in an equally wide strip along the visual horizon with a maximum in the lateral visual fields. Optical resolution and vertical sampling resolution are matched in the horizontal acute zone, although in the frontal visual field this match only holds for short-wavelength (blue and ultraviolet) light. In the dorsal, ventral and caudal visual fields, optical resolution is much higher than vertical sampling resolution.

II.5.1 Comparison with earlier studies

U. vomeris is similar in most major features of eye organisation to those fiddler crabs examined in earlier studies (*U. pugilator*, Land and Layne, 1995a; *U. lactea annulipes*, Zeil and Al-Mutairi, 1996) and to several other ocypodid and mictyrid crabs (Zeil et al., 1986). However, using a live crab instead of separated eyestalks allowed us to look at almost the whole eye and develop the first full model of a crab eye sampling array. Our detailed map reveals several differences to the previously studied species and highlights several novel aspects of the sampling array organisation.

Firstly, with a peak of 1.54 c/° the maximum vertical sampling resolution is higher than in *U. pugilator* (1.0 c/°, Land and Layne, 1995a), *U. lactea annulipes* (1.2 c/°, Zeil and Al-Mutairi, 1996) and another *Uca* species (1.2 c/°) studied by Zeil et al.

(1986). Also, the visual streak in *U. vomeris* is much narrower (13° FWHM) than in *U. pugilator* (30°) and the unidentified *Uca* species (22°, Zeil et al., 1986). The latter study examined a number of semi-terrestrial crabs and found that species that live in cluttered environments have short, well-separated eyestalks and little developed acute zones ('broad-fronted' crabs), while crabs in flat environments have long, narrowly-separated eyestalks and strong horizontal acute zones ('narrow-fronted' crabs). In this sense, *U. vomeris* is an extreme example of a narrow-fronted crab, featuring long, very close eyestalks and a highly developed, narrow visual streak. Secondly, we observed a horizontal offset in the peaks of optical and sampling resolution. While vertical sampling resolution is highest in the frontal visual field, both horizontal sampling resolution and optical resolution are higher in the lateral field of view. Additionally, the peak of optical, but not sampling resolution, in the frontal visual field is shifted by about 5° ventrally.

II.5.2 The visual information zones

Due to the physiological costs of developing and maintaining a large eye (Niven and Laughlin, 2008), eye space is a valuable physiological resource. In this context, the above regional specialisations of the sampling array can be interpreted as a heavily constrained optimisation of eye space use. For an eye to collect information effectively, it should (i) use more eye space to sample more important regions of visual space and (ii) trade off different uses of the available eye space (e.g. facet number vs. facet size) depending on the nature of information that is relevant in a certain region of the visual field. In the following, we will discuss five specialised regions of the *U. vomeris* compound eye in this context (Figure II.3A).

II.5.3 Ventral zone

The ventral limits of the visual field approximately coincide with the visible contour of the crab's own body (Land and Layne, 1995a). Away from the horizon, vertical sampling resolution declines rapidly to a minimum of about 0.3 c/°. Zeil and Al-Mutairi (1996) suggested that this gradient towards the ventral (and also the dorsal)

visual field follows an inverse sine function. In a flat environment, a distant object is seen at the horizon. As it comes closer, the lower edge of its retinal image moves downwards away from the visual horizon. At the same time it subtends an increasingly large visual angle, but is sampled at lower resolution. If vertical interommatidial angles $\Delta\varphi_v$ vary with the sine of elevation θ as $\Delta\varphi_v = \tan^{-1}(s/h)*\sin(\theta)$, this will result in size constancy (Schwind, 1989), i.e. an object at a fixed height above ground would be sampled by the same number of ommatidia irrespective of its distance (Zeil et al., 1986; Schwind, 1989; Dahmen, 1991). The only parameter adjusted in this fit is the linear scaling constant $\tan^{-1}(s/h)$, the arctangent of the size *s* (in cm) of an object at height *h* (relative to eye height, in cm) that is projected onto one interommatidial angle. Our results confirm this hypothesis (Figure II.9). The inverse sine functions fit astonishingly well using the same value for *s*/*h* (0.11) in the latero-ventral, latero-dorsal and fronto-dorsal eye, but require a smaller value for *s*/*h* (0.09), corresponding to generally higher resolution, in the fronto-ventral visual field. For perfect size constancy, resolution would have to be infinitely large at the horizon. Due to eye size constraints, size constancy therefore breaks down at about ±5°. Objects closer to the horizon (i.e. further away from the observer) appear smaller on the retina. This rule of size constancy has important consequences for the detection of social signals. This means that the vertical part of a conspecific's back pattern will look exactly the same no matter how far away that crab is, as long as it is closer than about 9-18 cm (see below).

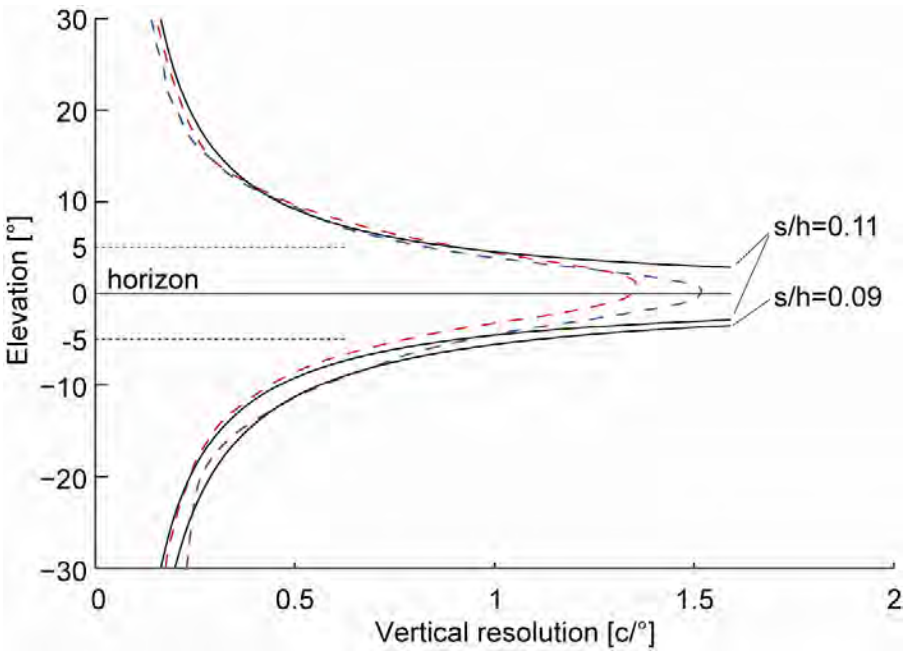

Figure II.9: Vertical sampling resolution predicts size-constancy. The decline of vertical sampling resolution (dashed lines, blue frontal, red lateral) can be predicted by an inverse sine-function assuming that objects at constant height above ground are sampled by the same number of ommatidia irrespective of their distance (solid lines). Functions can be scaled by a single parameter s/h (indicated beside the fits). See text for details.

II.5.4 Dorsal zone

At the edges of the visual field, our maps (Figures II.4-II.6) are limited to those ommatidia for which a viewing direction could be accurately determined using the pseudopupil method. The few ommatidia that are not included at the dorsal rim, sample the space directly above the crab with widely spaced and very large receptive fields, presumably closing the visual field completely.

As in the ventral visual field, vertical sampling resolution declines rapidly with increasing elevation. In the far dorsal visual field, a minimum of 0.2 c/° is reached, making vertical resolution lower than horizontal resolution. Facet diameter does not decrease at the same rate and the minimum facet diameter of about 15 µm results in an optical resolution several times larger than the vertical sampling resolution. Visual space is thus sampled by small receptive fields with large gaps between neighbouring viewing directions (Figure II.6E). This effect, however, is not

restricted to the highest elevations. Already at 10° elevation, optical resolution is more than twice as good as vertical sampling resolution (Figure II.7A).

The simplest explanation - that 15 μm represents a minimum functional size and thus only a widely spaced facet array can cover the entire visual space – is questionable, as many small insects have far smaller facets (e.g. 8 μm in Hymenopterans, Barlow, 1952). An alternative, functional hypothesis is suggested by the visual ecology of the crabs (Zeil and Hemmi, 2006). The crabs' most important task in the dorsal visual field is the early detection of predators. Fiddler crabs will start dashing home towards the safety of their burrow when birds subtend a visual angle of only 1-2° (Land and Layne, 1995a; Hemmi, 2005a). The task of the visual system is therefore not to extract detailed image information, but to detect small objects against a very bright, uniform background. Neither high sampling resolution nor seamless coverage of the visual field are necessary for this task. However, small acceptance angles and high contrast resolution, as provided by comparatively large facets, are essential for early detection. In other words, an approaching bird will not be seen continuously by this sampling grid. When it is seen, however, it is seen at high contrast and high signal-to-noise ratio and therefore will be spotted at a much safer distance (Land, 1981; Zeil, 1983).

II.5.5 Frontal zone

In contrast to the ventral and dorsal areas discussed so far, the frontal and lateral horizontal parts of the visual field have been assigned a huge proportion of eye space. This space, however, is utilised with a different trade-off between facet number and size. In the frontal visual field the balance is biased towards more rather than larger facets, resulting in smaller interommatidial angles and the highest overall sampling resolution. The comparatively small facets, however, lead to resolution being diffraction-limited for long wavelengths (Figure II.7A). The actual cut-off wavelength, where no contrast remains at the highest spatial frequency that could be sampled, depends linearly on the size of the eye and thus the size of the crab. However, even in very large animals the full sampling resolution will only be

available if the sampled light is restricted to short wavelengths. This restriction could be achieved by having a purely blue and UV signal, or by sampling with a short-wavelength sensitive visual pigment. Indeed, using intracellular electrophysiology, we have recently found a UV-sensitive class of photoreceptors in *U. vomeris* (Smolka and Hemmi, 2008). In addition, behavioural evidence suggests that in *U. capricornis* this frontal zone is involved in the individual identification of conspecifics by their intricate, blue/UV back patterns (Detto et al., 2006). In *U. vomeris*, the reflectance spectrum of these patterns peaks at about 450 nm and extends to below 350 nm (Hemmi et al., 2006), providing an ideal signal for full use of the resolution of the frontal acute zone. When a conspecific approaches their burrow, resident male fiddler crabs (*U. pugilator*) start differentiating behaviourally between male and female wanderers at a distance of 10-15 cm (Land and Layne, 1995a). How et al. (2007) found in *U. perplexa* that this sex identification is accompanied by a change in body orientation; residents kept the side of the body that carries the major claw towards intruding males, but turned their front towards approaching female wanderers. Our results complement these observations in several ways.

Firstly, the gradient of vertical sampling resolution towards the ventral visual field is less steep in the frontal eye than either of the gradients in the frontal-dorsal, lateral-dorsal and lateral-ventral eye. Sampling resolution is therefore highest in the frontal visual field for any given elevation below the horizon (i.e. for any given distance of an approaching crab). Furthermore, we found the frontal peak of optical resolution to be below the visual horizon, at about -5° of elevation. On flat ground this corresponds to looking at the top of another crab's carapace at a distance of about 9 cm or at the bottom edge of the carapace at about twice that distance (Figure II.10A). -5° of elevation is also where size constancy begins (see above). The retinal image of a crab approaching from far away (0° elevation) will cover more and more facets until it reaches an elevation of about -5°. At closer distances, the image is always seen by the same number of facets. The vertical component of individual patterns will therefore always be sampled by the same number of ommatidia, as long

as the observed crab is closer than 9-18 cm (Figure II.10A). This is likely to significantly reduce the neural complexity of the underlying pattern matching task.

In conclusion, the frontal eye region is the zone best equipped for recognising individual conspecifics and it is likely that the re-orientation behaviour of courting males not only directs the waving signal towards the target female, but also centres her within his frontal acute zone.

II.5.6 Lateral zone

Conversely to the frontal visual field, the lateral zone has larger rather than more facets, leading to higher optical resolution and contrast sensitivity. Horizontal resolution is also highest in this part of the visual field. Again, the visual ecology of the crabs suggests a possible function for these anatomical features. With few exceptions, fiddler crabs always align themselves to keep their burrow in a lateral position (Land and Layne, 1995b; Zeil, 1998; Zeil and Layne, 2002; How et al., 2007). When another crab approaches, the resident rushes back to defend its burrow from the intruder (Crane, 1975; Zeil and Layne, 2002; Hemmi and Zeil, 2003a, b). To provide a safe time margin to return home and defend the burrow, this decision is made when the intruding crab is a fixed distance away from the burrow. The crabs that are furthest away – often in excess of 50 cm at the time of response (Hemmi and Zeil, 2003a, b) – and thus hardest to detect, are consequently seen across the burrow, i.e. in the lateral visual field. To reliably detect intruding crabs at this distance on a low-contrast mudflat background, high contrast sensitivity is essential. Additionally, when compared to the frontal zone, the different trade-off between facet size and interommatidial angles means that laterally the full resolution can be used at longer-wavelengths of light without being limited by lens diffraction. This would allow a large crab to optimally sample light up to about 550 nm (Figure II.7B), which is practically the whole range of light sampled by *U. vomeris* photoreceptors (Jordão et al., 2007; Smolka and Hemmi, 2008), and thereby further increase sensitivity.

II.5.7 Medial zone

Although there is an anatomical gap in the ommatidial array at the medial cuticular ridge, the visual field at the horizon is fully covered. In fact, the visual fields of the two ends of the eye surface overlap by at least 30° (see also Zeil and Al-Mutairi, 1996). Given the very low resolution and small facets in this region when compared to the lateral part of the other eye, which looks into the same region of the crab's visual environment, what could be the function of this region? Before leaving their burrow after escaping from a perceived threat, crabs can frequently be observed sitting in the burrow entrance and cautiously raising one eye while the rest of the body remains in the safety of their home. Full coverage of the visual field in each individual eye is essential for this strategy that might have evolved against sit-and-wait (and therefore close-by) predators (Zeil and Al-Mutairi, 1996). This does not, however, explain the extent of the overlap. A possible use of this monocular overlap is stereoptic distance perception. The distance between the pseudopupils on the two sides of the ridge is about 0.5 mm, and a simple calculation (Burkhardt et al., 1973) shows the maximum distance for stereopsis with a horizontal interommatidial angle of 3-4° to be between 7-9.5 mm. The only object within this distance, however, is the other eye. In a natural environment, crabs keep the vertical axis of their eyes very accurately perpendicular to the visual horizon (Zeil and Al-Mutairi, 1996) using visual and statocyst reflexes (Nalbach et al., 1989), even when the body is tilted at a large angle (e.g. on a slanted surface or in the burrow entrance, Zeil et al., 1989). It is thus possible that the medial zones monitor the position and distance of the other eye to help synchronising their visual fields.

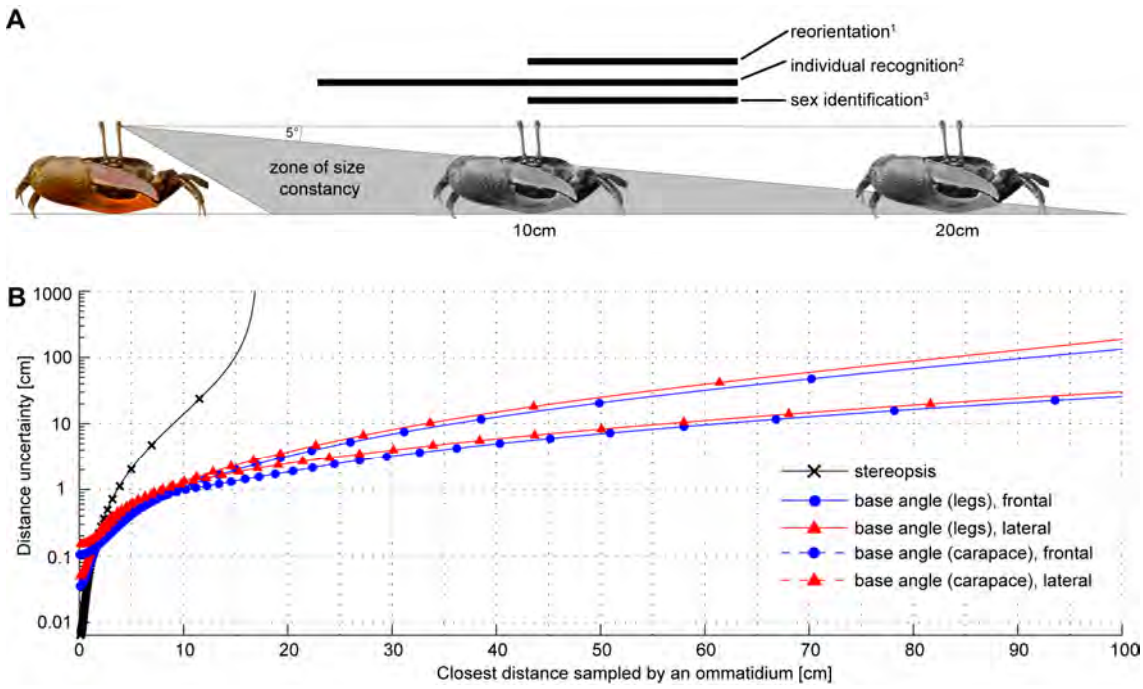

Figure II.10: Size constancy and distance estimation. (A) Size constancy in the *U. vomeris* eye begins at about 5° below the horizon. This corresponds to a distance of an observed crab of about 10-20 cm. At this distance crabs start differentiating between male and female intruders ([2], Land and Layne, 1995a), changing body orientation accordingly ([1], How et al., 2007) and recognising individuals ([3], Detto et al., 2006). In the frontal visual field (which is turned towards females) the largest facets (highest sensitivity) are facing this direction. It is likely that this zone is involved in individual recognition. **(B)** Comparison of accuracy of distance measurement using stereopsis (black line), elevation of legs (solid red and blue line) or elevation of carapace (dashed red and blue lines) in the frontal (blue) and lateral (red) visual field. Markers on lines indicate one possible set of ommatidia along this curve. By rotating the eye within an ommatidial angle, these points can be shifted along the line. See text for details. Stereopsis only performs better for distances shorter than about 2 cm.

II.5.8 Distance estimation in crab compound eyes

Due to the limited resolution and small eye separation of invertebrates, stereoptic distance cues are only useful to them at very close distances (Collett and Harkness, 1982; Schwind, 1989), or when enhanced by peering movements, for example when striking at prey (e.g. Rossel, 1996). For flat-world inhabitants like fiddler crabs, an alternative possibility is the estimation of distance from retinal elevation (Collett and Harkness, 1982; Zeil et al., 1986; Ooi et al., 2001; Hemmi and Zeil, 2003c). The closer an object gets to the observer while staying at constant height above ground, the further away it moves from the visual horizon. While the accuracy of stereopsis depends on horizontal resolution and eye separation, estimation from elevation relies

(in a similar fashion) on vertical resolution and eye height above ground. Figure II.10B shows the uncertainty of both these measures, expressed as the depth of ommatidial receptive fields, i.e. the range of distances along the ground that is sampled by an ommatidium. While the functions are continuous, in a real eye they are discrete, with one point for each relevant ommatidium (Figure II.10B, crosses, triangles and dots). By rotating the eye, these points can be shifted along the curve.

Stereopsis (for a horizontal interommatidial angle of 1.1° and an eye separation of 6.6 mm, corresponding to a 25 mm male crab) is only useful at very short distances (Figure II.10B, black line). The error exceeds 10 cm at 10 cm distance, indicating that the distance of small objects between 10 cm and 20 cm away can not be distinguished in this way. Stereopsis accuracy declines even further when the observed object is not exactly in front of the animal. In the lateral visual field, where the most important distance judgements have to be made for burrow defence (see above), stereopsis is not available at all.

Retinal elevation (for vertical interommatidial angles as measured in the frontal (blue) and lateral (red) visual field, and an eye height above ground of 25 mm) provides a far more accurate estimation of distance up to a distance of several meters (Figure II.10B, red and blue solid lines). However, the base of an object, which is seen at the largest angles below the horizon and would therefore provide the most accurate results, might not always be seen due to ground undulations or insufficient contrast (Zeil et al., 1989). Using the top of the carapace (estimated 8.4mm below eye height, corresponding to a 25 mm male crab) instead, makes the measurements less accurate (about three times larger error at 50 cm distance), but still far more reliable than stereopsis (Figure II.10B, red and blue dashed lines).

Note that these calculations determine the error for **absolute** distance estimation. The retinal elevation of ommatidia could instead be used as a **threshold** indicator: Whenever an ommatidial row measures a stronger signal than its dorsal neighbours, the observed object has approached below a certain threshold distance (Figure II.10B, triangles, dots and crosses). The accuracy of this measurement is not limited by resolution, but by noise in the visual system, local contrast sensitivity and,

most importantly, by the flatness of the terrain. If the ground undulates by 50% of eye height, distance threshold measurements will have an uncertainty of ±50%. When observing a moving object, however, this uncertainty could be partly overcome by temporal summation. Even with this limitation, retinal elevation provides more accurate absolute and threshold distance cues for all distances longer than about 2 cm. At shorter distances, stereopsis might provide useful information, e.g. for fights or feeding.

In this study, we have analysed the sampling array of the fiddler crab compound eye in extensive detail and provided, to our knowledge, the first full map of a crab compound eye. Our analysis has shown several novel aspects of how different zones of the eye may be adapted to process specific, behaviourally relevant information that occurs in different parts of the crabs' visual field. The results of this study can be used to accurately model visual cues while recording natural behaviours *in situ*, to predict visual response thresholds and to compare how behavioural strategies relate to visual information and eye design in different species. Most importantly, in showing how sampling by the ommatidial array is related to the visual cues in the animal's environment and to the animal's behavioural strategies, our analysis highlights the tight link between vision and behaviour.

Chapter III

Uca vomeris – an unusual trichomat

(incl. preliminary data on polarisation sensitivity and visual interneurons)

III.1 Summary

Fiddler crabs use their striking body colouration in a number of visual displays to communicate with one another. However, even 35 years after the first experiments on colour vision in fiddler crabs, the fundamental properties of their colour vision system are still unknown. To determine the spectral sensitivities of individual photoreceptors – the basis for any colour vision system – I developed the first intracellular electrophysiological preparation for fiddler crabs in *Uca vomeris*. The results indicate the presence of at least three visual pigments: an ultra-violet sensitive pigment with an absorption maximum at about 345 nm (UV), and two pigments with effective peak absorptions at 410 nm (B1) and 460 nm (B2). Most unusually, B1 and B2 seem to be co-expressed in the majority of receptors in different ratios, creating a wide spectrum of blue spectral receptor classes. There was no evidence for a middle-wavelength (green) sensitive receptor class as it has been found in many other crabs. I suggest that the B2 sensitivity originates (either through genetic mutation or filtering by screening pigments) from the same gene that creates the green sensitivity in other crabs. Shifting the spectral sensitivity towards shorter wavelengths increases spectral and spatial resolution in the blue to facilitate individual recognition by carapace patterns. The new electrophysiological preparation also allowed me to demonstrate the polarisation sensitivity of photoreceptors and to record light responses from interneurons in the optical neuropils, thus paving the way for the study of the neural basis of behaviour in this well-established *in situ* behavioural model system.

III.2 Introduction

One of the most conspicuous features of fiddler crabs is their colourful appearance. The males' one enlarged claw (Figure III.1A), often bright red, orange or yellow in colour and waved in complex patterns to attract females, can be seen from far away on the tropical mudflats around the world – the semi-terrestrial crabs' preferred habitat. This, however, is not the only colourful mark the crabs bear. In the Australasian species *Uca vomeris*, for example, both males and females have a bright blue pattern on their otherwise brownish-black carapaces (Hemmi et al., 2006). Their fronts are often white and the males' minor claw, as well as both of the females' claws, shines bright orange, pink or blue (Figure III.1A). Both the carapace patterns and the dactyl of the males' major claw also reflect strongly in the UV (Zeil and Hofmann, 2001). Not surprisingly, these colours play an important role in the crabs' social life. Females in *U. mjoebergi* recognise conspecific males by the colours of their claws (Detto et al., 2006; Detto, 2007), and *U. capricornis* males recognise individual females by their particular back patterns (Detto et al., 2006). Although these observations have been made in different fiddler crab species, and not in *U. vomeris*, the fact that *U. vomeris* changes its colouration depending on the level of predation (Hemmi et al., 2006) makes it likely that colours play an important social function in this species, as well; provided, of course, that they do possess colour vision.

III.2.1 Crustacean colour vision

Colour vision is the ability to discriminate between stimuli based purely on their spectral composition and irrespective of their intensity (Kelber et al., 2003). To achieve this task, an animal needs to compare the signals of at least two different types of photosensitive cells with different spectral sensitivities. While colour vision has been extensively studied in vertebrates and insects (for reviews see Menzel, 1979; Kelber et al., 2003; Osorio and Vorobyev, 2008), relatively little is known about the abilities of crustaceans to see colours. Behavioural demonstrations – the only way to

conclusively show that an animal possesses colour vision – are exceedingly rare in this clade and essentially limited to *Daphnia* (Lubbock, 1888; Storz and Paul, 1998), shrimp (Koller, 1927), hermit crabs (Koller, 1928), stomatopods (Marshall et al., 1996), and fiddler crabs (Hyatt, 1975; Detto et al., 2006; Detto, 2007). The behavioural ability to distinguish colours requires an animal to compare receptors with different spectral sensitivities. A photoreceptors sensitivity, however, is affected by a number of factors and, as will become clear later, can realistically only be determined by directly measuring the intracellular response of photoreceptors. While a variety of methods have been used to determine these factors in a number of crustacean species, intracellular information is available for only a few species. Both behaviour and electrophysiological information – together providing a comprehensive overview of the capabilities relevant to the animal – exists only for *Daphnia* (Smith and Macagno, 1990) and stomatopods (reviewed in Marshall et al., 2007). Within the Decapoda, with 8000 species (including crayfish, shrimps and crabs) one of the largest groups of extant Crustacea, there is no example combining behaviour and intracellular information. Our knowledge about the physiological basis of colour vision in decapods crustaceans is limited to pigment absorption spectra and genetic studies.

According to a recent molecular phylogeny of arthropod opsins (Porter et al., 2007), the ancestors of insects and crustaceans were trichromatic with a ultra-violet sensitive (UV), a middle-wavelength sensitive (MWS) and a long-wavelength sensitive (LWS) visual pigment. While insects and branchiopods (like *Daphnia*) kept these three opsins and developed an additional short-wavelength sensitivity (SWS), the UV opsin was supposedly lost in the Malacostrata, incl. crabs. The results of this study, as well as recent *in-situ* hybridisation in the fiddler crab *Uca pugilator* (Rajkumar et al., 2008) challenge this hypothesis (see Appendix C for a brief phylogenetic overview of the Crustacea and their colour vision systems).

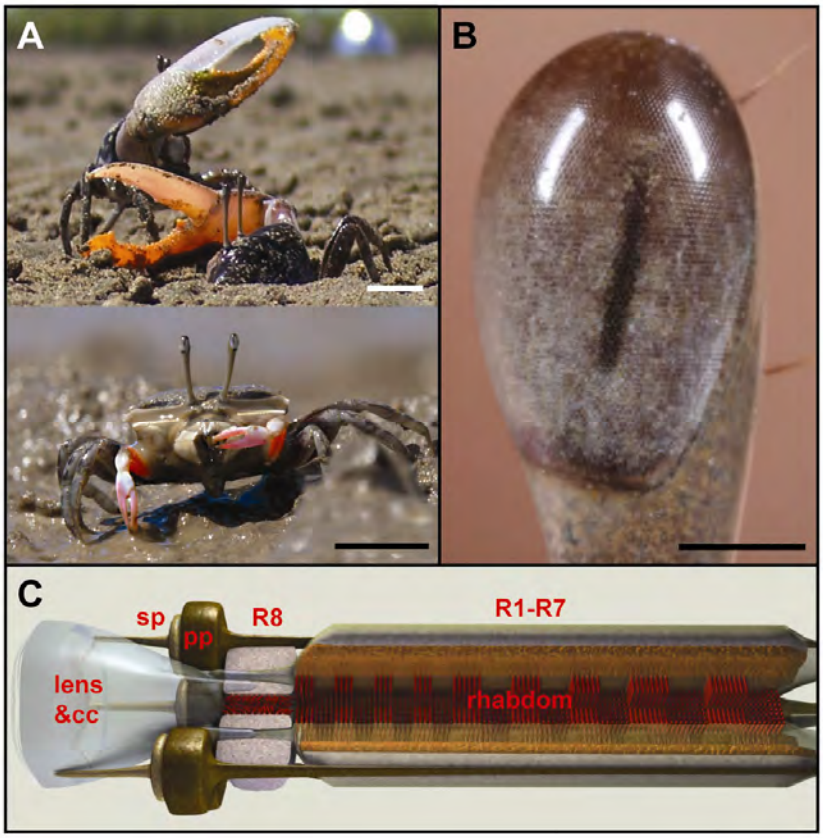

Figure III.1: *U. vomeris* compound eye. (A) Fiddler crabs carry their eyes on long stalks above their body. **(B)** 9000 ommatidia in each eye provide a 360°, dorsally closed field of view with a horizontal visual streak of high acuity. **(C)** In each ommatidium, light is focused onto the light-absorbing rhabdom by a lens and a long crystalline cone. Stray light is absorbed by the primary (PP) and secondary (SP) pigment cells. Seven retinula cells (R1-R7) contribute microvilli to the main rhabdom in alternating, orthogonal bands. The eighth and smallest retinula cell R8 sits distally on top of the others with its microvilli in random orientations. 3D ommatidium model by Thomas Magill and Sharyn Wragg after Alkaladi (2008). Scale bars are approximately 1 cm (A), and 0.5 mm (B), respectively.

III.2.2 Fiddler crab colour vision

Despite the wealth of information on the fiddler crab visual system, the details of their colour vision system remain controversial. Behaviourally, their ability to distinguish colours has been shown using a phototactic (Hyatt, 1975) and a mate-choice related (Detto et al., 2006; Detto, 2007) protocol, but both are based on the animals' natural preferences and thus unsuitable for the examination of the underlying spectral sensitivities. Physiologically, only four studies have so far attempted to characterise the visual pigments or spectral sensitivities. Scott and Mote

(1974) examined the electroretinogram (ERG) in *U. pugnax* and *U. pugilator* and suggested that both species possessed only a single visual pigment with a peak sensitivity around 510 nm. However, their study suffered from several methodological difficulties (reviewed in Horch et al., 2002) making it likely that they missed additional pigments. Two other ERG studies (Hyatt, 1975; Horch et al., 2002) have since found evidence of a second pigment sensitive to much shorter wavelengths in *U. thayeri*, *U. pugilator*, *U. pugnax* and *U. minax*. A microspectrophotometry (MSP) study (Jordão et al., 2007) has recently characterised the absorption of the LWS pigment expressed in the R1-R7 retinula cells of *U. pugilator*, *U. pugnax*, *U. tangeri* and *U. vomeris*. Interestingly, the maximum sensitivity of the *U. vomeris* pigment was shifted towards shorter wavelengths by at least 10-20 nm compared to the other three species. Due to technical difficulties, the small size of the rhabdoms, this study unfortunately could not measure the pigments in R8.

Each fiddler crab ommatidium is comprised of eight retinula cells (Alkaladi, 2008, Figure III.1C), seven of which (R1-R7) contribute their rhodopsin-carrying microvilli to a common, central rhabdom in alternating, orthogonal bands in the typical crustacean fashion (e.g. Stowe, 1980). As microvilli preferably absorb light that is polarised parallel to their orientation, this orthogonal organisation makes R1-R7 highly sensitive to the polarisation vector of incoming light (Wald et al., 1963). The eighth and smallest retinula cell R8 sits distally on top of the others with its microvilli in random orientations, thus cancelling out its polarisation sensitivity.

Two *U. vomeris* opsins (MWS and LWS) were recently isolated and *in-situ* hybridised (Alkaladi et al., in prep.), demonstrating that they are co-expressed in most photoreceptors. A parallel *in-situ* hybridisation study on *U. pugilator* found four opsin genes, one of which was closely related to the insect UV opsin gene (Rajkumar et al., 2008). Unfortunately, the UV part of the spectrum has never been examined in any detail in either MSP or ERG.

While the methods discussed so far can determine visual pigment absorption spectra (MSP), pigment distribution (*in-situ* hybridisation), the absorbance of spectral filters (histological and optical studies) and the summed responses of large numbers

of different receptors (ERG), they can only give indirect information about the individual receptor sensitivities. Both MSP and ERG are also likely to miss or average out rare and similar sensitivities, and ERG does not allow for the characterisation of regional variations in the eye. Neither of them measures the actual, physiologically relevant spectral sensitivities of individual photoreceptors.

In this study I have established an *in vivo* intracellular electrophysiological preparation of the fiddler crab compound eye. This technique allowed me to directly determine photoreceptor spectral sensitivities by recording intracellular responses to monochromatic light stimuli. The results show that *U. vomeris* possess an ultra-violet sensitive photoreceptor class (λ_{max} 345 nm, **UV**) and a variety of blue-sensitive receptors that can be fully modelled by co-expression of two short-wavelength sensitive pigments (λ_{max} 410 nm, **B1**, and 460 nm, **B2**). To my knowledge, this is the first time that a UV receptor class has been demonstrated in a brachyuran crab, and the first example of potential trichromacy in any decapod crustacean (Appendix C). I argue that this unusual colour vision system is tuned to facilitate social communication both in the individual recognition of blue/UV, fine spatial patterns, and in enhancing the contrast of UV-bright claws against a dark mudflat. The new electrophysiological protocol also allowed me to demonstrate the high polarisation sensitivity of *U. vomeris* photoreceptors and to obtain for the first time recordings from interneurons in the optical neuropils, thus paving the way for the study of the neural basis of behaviour in an already well-established *in-situ* behavioural model system.

III.3 Materials and methods

III.3.1 Animals

Large adult male and female fiddler crabs *Uca vomeris* (McNeill) (Ocypodidae: Brachyura: Decapoda) were collected from the mudflats near Cungulla (19°24'S, 147°6'E), south of Townsville, Queensland, Australia and Redland Bay (27°37'S, 153°17'E) near Brisbane, Queensland, Australia. I preferably used large animals (18-23 mm carapace width) as they generally provided more stable physiological preparations. The animals were kept in individual plastic containers in the laboratory in Canberra, in some cases for several weeks prior to experiments. During this period they were exposed to natural daylight through a window (thus cutting out especially the UV part of the spectrum) and regularly provided with fresh seawater and fish food. After the experiments, animals were euthanised on ice.

III.3.2 Preparation and recording setup

For the electrophysiological recordings, animals were held either with an aluminium bar glued to the carapace (Figure III.2B) or in an adjustable metal clamp (Berón de Astrada et al., 2001). In the latter case, additional support was provided by a layer of beeswax between clamp and animal. To restrain the crabs, a drop of superglue was applied to the merus-carpus joint of each leg. One or two days before the experiment, males were forced to autotomise their larger claw by pinching the merus with forceps. Only fully recovered males (judged by their general activity and willingness to accept food) were used in the experiments. The claws of females were held together with a small strip of rubber to restrict their movement. Both eye-stalks were fixed in a natural upright position with a drop of superglue at the base of the stalk and an aluminium angle was glued to the stalk and to the carapace. During recordings the eye was kept moist and clean with seawater, taking care to ensure that no drops formed on the eye that would refract or filter the incoming light.

The animals were positioned in the centre of a motorised cardan arm (Figure III.2A, see below) and a glass electrode inserted into the eye through a small hole either in

the dorsal part of the cornea or in the small 'peninsular' strip of cuticle on top of the eye (Berón de Astrada et al., 2001). The neutral electrode was inserted into a small hole in the carapace and glued into place. Glass electrodes were pulled on a Flaming/Brown micropipette puller (Model P-97, Sutter Instruments, Novato, California, USA) with tip resistances of 80-100 MΩ when filled with 2 mol/l potassium acetate. The glass microelectrode was connected to the head stage of a Getting Model 5A amplifier (Getting Instruments, San Diego, California, USA) via a Ag/AgCl electrode. Signals were then digitised through a 12-bit data acquisition card (NI-6025E, National Instruments, Austin, Texas, USA) and recorded and displayed on a computer monitor through a LabView (National Instruments, Austin, Texas, USA) interface. Signals were also monitored on a digital oscilloscope (Tektronix, Brighton, East Sussex, UK). After inserting the electrode, the hole was often sealed with soft Vaseline to minimise bleeding. The animals were then dark adapted for at least 20 minutes prior to the start of experiments. All experiments were carried out during the day.

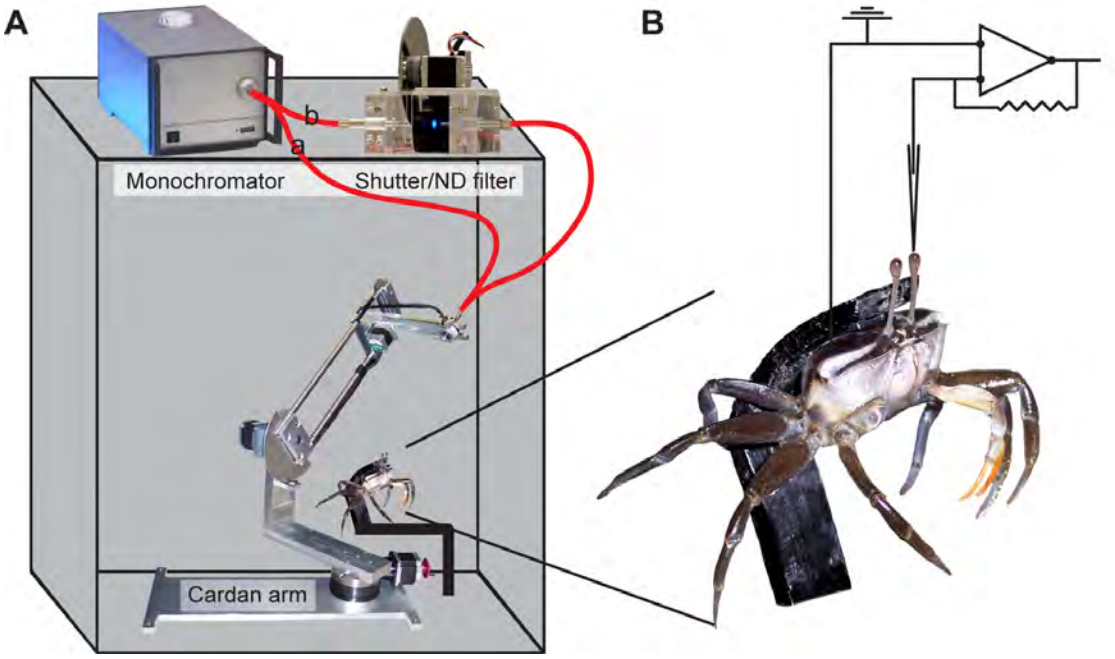

Figure III.2: The electrophysiological setup. (A) Light was produced by a monochromator and intensity regulated either by either **(a)** the internal slits of the monochromators, or **(b)** by an external shutter and a 0-4ND motorised variable neutral density filter wheel (in later experiments). The stimulus was then transmitted through a UV-transmitting fibre optic cable to the end of an automatic cardan arm, where a motorised linear polarisation filter could be mounted to determine the polarisation of the stimulus. The whole setup was positioned in an optically and electrically isolated Faraday cage. From the cardan arm the stimulus was centred onto the receptive fields of recording units. **(B)** The crab was held by an aluminium strip glued to its back and a small metal bracket held the eyes upright in a natural position. A glass electrode was inserted into the eye through a small cut in the cornea; the reference electrode was inserted into the carapace.

III.3.3 Optical stimulation

Light stimuli were produced using a computer-controlled TILL Polychrome V monochromator (TILL Photonics GmbH, Gräfelfing, Germany) with a 150 W Xenon high-stability lamp, providing illumination between 330 nm and 680 nm at 0.1 nm wavelength resolution and 400 nm/ms maximal scanning speed. The entrance slit was fully opened, producing light with a spectral full width at half maximum (FWHM) of approximately 15 nm. The exit slit can be controlled in 97 steps resulting in an approximately linear output intensity range between 0% and 100%. By setting the monochromator to resting wavelength (247 nm) before closing entrance and exit slits, intensity can be dropped below 0.1% in a few milliseconds. In early experiments (cells PR1-9), I used these internal mechanisms to produce flashes of controlled

intensity and duration. In later experiments, an SC10 solenoid shutter (Thorlabs Inc., Newton, New Jersey, USA) and a motorised variable neutral density filter wheel (Thorlabs Inc., Newton, New Jersey, USA) were introduced into the light path, allowing for light flashes as short as 1 ms, at 4800 intensity steps over a range of four log units. Light is imaged onto the eye through a 0.22 NA, 1.1 mm diameter, UV-transmitting quartz light guide (TILL Photonics GmbH, Gräfelfing, Germany) mounted on a motorised cardan arm allowing for accurate angular positioning of the stimulus in the receptive field of the cell I recorded from. A motorised, UV-transparent polarisation filter (Knight Optical, Harrietsham, UK) can be inserted into the light path for polarisation sensitivity measurements. The polarisation angle changes at a minimum step size of 0.9°. Output intensities of the optical setup were calibrated using a USB2000 spectrometer (Ocean Optics, Dunedin, Florida, USA) which itself was calibrated for intensities against a LS-1-CAL Tungsten Halogen calibration lamp (Ocean Optics, Dunedin, Florida, USA) and spectrally against a CAL-2000 Mercury-Argon lamp (Ocean Optics, Dunedin, Florida, USA). All devices (monochromator, shutter, ND-wheel, polariser and cardan arm) were controlled via serial port through a LabView (National Instruments, Austin, Texas, USA) interface. The physiological setup was isolated optically and electrically in a closed Faraday cage (Figure III.2A).

III.3.4 Experimental protocol

Using a manual Leitz micromanipulator, the electrode was slowly advanced through the tissue until a drop in voltage indicated penetration of a cell. Photoreceptors were identified by their large, fast, graded responses to flashes of light and their extremely narrow receptive fields. Upon impalement of a photoreceptor, the centre of its receptive field was determined using a white strobe light and the cardan arm's position adjusted to maximise the cell's response to a monochromatic test stimulus (470 nm or 350 nm depending on cell type). Only photoreceptors that yielded a stable response for several minutes were considered further. The spectral sensitivity of a photoreceptor was determined using 40 ms (early experiments, cells PR1-9) or 300

ms flashes of monochromatic light according to the following protocol[3]: First, in an **initial intensity run**, responses to flashes of up to 24 different intensities at a wavelength near the sensitivity maximum (estimated from a number of test flashes) were recorded. These measurements were used to calculate the cell's ***V/log(I)*-function**, which characterises the cell's non-linear response to different light intensities. After this, one or several ***spectral runs*** were performed, each consisting of up to 36 monochromatic, equal-photon (exceptions see below) flashes at different wavelengths of light. In most experiments, these were divided into two halves. Each half covered the entire wavelength range, the first half with increasing wavelengths (upward sweep), the second half with decreasing wavelengths interspersed between those of the first half (downward sweep). Differences in the response curves between these two sweeps could be used to identify time-dependent changes in the cell, e.g. due to changing penetration, physiology or adaptation state. Lastly, in a **final intensity run**, the *V/log(I)*-function was measured again. Generally, I only accepted cells for analysis when both intensity runs resulted in a similar *V/log(I)*-function[4]. For polarisation sensitivity measurements, spectral runs were replaced by ***polarisation runs*** with flashes at the wavelength of maximum sensitivity at 10-20 different orientations of the polarisation filter.

Spacing between individual flashes was 5 s in early experiments, and eventually reduced to 1 s, the minimum duration at which no adaptation of the light response was visible. All flashes in spectral and polarisation runs were photon-matched and adjusted such that they produced responses in the linear part of the *V/log(I)*-function. The only exception to this was at 330 nm, where intensity was 10-60% lower (depending on the target intensity).

[3] Although in insect photoreceptors a 'light clamp' protocol, where at each wavelength intensity is adjusted to produce a preset membrane potential, has been shown to be faster and more reliable (Menzel et al., 1986), noise and large random fluctuations in the base potential prevented me from using this method.

[4] Despite the apparently comparatively low number of intensity runs when compared to spectral runs, there are often actually more intensity than spectral runs for a given cell. This is due to the fact that both wavelength resolution and target intensity was tuned separately for each cell, and many initial spectral runs therefore had to be discarded in the final analysis. Their respective intensity runs, however, were still used in the analysis.

III.3.5 Data analysis

Raw voltage traces were offset in voltage to align resting potential (RP) and in time to align response onset. Traces were then averaged for every individual condition (intensity in intensity runs, wavelength in spectral runs, polarisation angle in polarisation runs) and low-pass filtered with a 5 ms half-width gaussian. The response to 40 ms flashes was determined as the difference between the response peak (maximum between 30-50 ms after response onset) and the RP (average of 100 ms before response onset). Although the cell response was low-pass filtered, this measure was quite sensitive to noise. I therefore changed flash length to 300 ms in later experiments (cell no. 10 onwards) and measured response as the difference between plateau response (average between 100 ms and 250 ms after response onset) and RP. To separate variability due to differences in the cell's physiological state in different runs from variability due to recording noise, individual half-runs were scaled to fit the mean of all half-runs in spectral and polarisation runs. Intensity runs were not scaled to maintain a measure of the absolute error in response size, as this influences the shape of the *V/log(I)*-function and thereby the shape and width of the sensitivity function.

V/log(I)-functions were fitted using a hyperbolic function of the form

$$\frac{V}{V_{\max}} = \frac{(R * I)^n}{(R * I)^n + 1} \qquad \text{(III.1)}$$

with variables ***I*** (intensity as quantal flux) and ***V*** (response amplitude in mV), and fit parameters $\boldsymbol{V_{max}}$ (saturated response amplitude in mV), ***R*** (reciprocal of the intensity yielding a half-maximum response), and slope constant ***n*** (Naka and Rushton, 1966a, b; Lipetz, 1971; Matić and Laughlin, 1981; Menzel et al., 1986). Note that this hyperbolic tangent function is equivalent to a sigmoidal function in log-space of the form

$$\frac{V}{V_{\max}} = \frac{1}{1 + \frac{e^{-\ln(I)*n}}{R^n}} \qquad \text{(III.2)}$$

(with variables and fit parameters as above; see Appendix E.1), which might be a more intuitive fit when examining the function in log-space (e.g. Figure III.4B).

The spectral sensitivity function of a cell ***S(λ)*** describes the percentage of quanta absorbed at any given wavelength compared to that percentage at the wavelength of maximum sensitivity (Menzel et al., 1986). To determine sensitivity, receptor responses ***V(λ)*** were transformed into equivalent intensities $\boldsymbol{I_{eq}(\lambda)}$ using the inverse of the fitted *V/log(I)*-function ('equivalent' because a flash of this intensity, at the wavelength at which the *V/log(I)*-function was measured, would evoke an equivalent receptor response). Sensitivity is then determined as

$$S(\lambda) = \frac{I_{eq}(\lambda)}{I(\lambda)} * \frac{1}{S_{\max}} \qquad \text{(III.3)}$$

where ***I(λ)*** is the real quantal flux of the stimulus, $\boldsymbol{I_{eq}(\lambda)}$ the equivalent intensity as described above and $\boldsymbol{S_{max}}$ a constant to normalize maximum sensitivity to 1.

Sensitivity to polarised light is calculated in an equivalent way for all angles ***Φ*** of polarisation as

$$P(\Phi) = \frac{I_{eq}(\Phi)}{I(\Phi)} * \frac{1}{P_{\max}} \qquad \text{(III.4)}$$

The polarisation sensitivity ***PS*** of a cell is defined as the ratio of maximum and minimum sensitivity

$$PS = \frac{P(\Phi_{\max})}{P(\Phi_{\min})} \qquad \text{(III.5)}$$

III.3.6 Sensitivity modelling

Rhodopsin absorption was modelled using nomogram templates (Govardovskii et al., 2000). Photoreceptor sensitivities $S_{PR}(\lambda)$ can be calculated for each receptor from these individual rhodopsin absorptions using Snyder's formulas (Snyder et al., 1973), taking into account any absorbing material in the light path (visual pigments, optical filters, screening pigments, metarhodopsins):

$$S_{PR}(\lambda) = k_{PR} \sum_{R,in} \frac{C_R}{C} \alpha_R(\lambda) \frac{1 - e^{-\xi(\lambda) l}}{\xi(\lambda)} \tag{III.6}$$

with total absorption

$$\xi(\lambda) = \sum_{R,in/out} C_R \alpha_R(\lambda) \frac{A_R}{A} + \sum_F C_{RF} \alpha_F(\lambda) \frac{A_F}{A} \tag{III.7}$$

where $S_{PR}(\lambda)$ is a photoreceptor's spectral sensitivity, k_{PR} a dimensionless scaling factor to normalise $S_{PR}(\lambda)$ to a maximum of 1, C_R the peak absorption per unit length of rhodopsin R (in μm^{-1}, depending only on its concentration), C_R/C the relative concentration of a pigment inside a cell, $\alpha_R(\lambda)$ the rhodopsin's absorbance function (modelled by a nomogram template), l the rhabdom length (in μm), and A_R/A the combined relative area of the retinula cells in a rhabdom expressing this rhodopsin. C_F, $\alpha_F(\lambda)$ and A_F/A represent the equivalent factors for the lateral screening pigments that might work as spectral filters for the rhabdom. Note that in Eq. 6 absorptions are only summed up over pigments inside one *electrical* unit (i.e. a single retinula cell or several electrically coupled cells), whereas Eq. 7 includes all pigments in an ommatidium expressed inside an *optical* unit / one ommatidium (i.e. all rhodopsins and screening pigments). Unless otherwise specified, I assumed a rhabdom length of 150 μm (Alkaladi, 2008), a rhodopsin peak absorbance of 0.006 μm^{-1} (Cronin and Forward, 1988; Jordão et al., 2007) and a screening pigment peak absorbance of 0.1 μm^{-1} (Jordão et al., 2007).

III.3.7 Interneuron recordings

Inserting the microelectrode at a different angle, the same recording setup can be used to target interneurons in the optic neuropils. In collaboration with Daniel Tomsic, I recorded from these interneurons in one crab to test my preparation as a model for recordings from the optic pathway. Upon impalement of a neuron, its response to light flashes, sustained illumination and motion in different parts of the visual field was tested.

III.4 Results

I successfully recorded from 23 photoreceptors (PR) in twelve compound eyes of eleven fiddler crabs (six males, five females). Spectral sensitivities were recorded from 21 photoreceptors (PR1, PR3-4, PR6-23) and full polarisation sensitivities from two cells (PR5-6). In addition, two cells (PR9, 22) were preliminarily tested for differential sensitivity to horizontally and vertically polarised light. Finally, I recorded light responses from five interneurons (DN1, SN1-4) in crab 11. Impalements of the cells reported here usually lasted between 10-20 minutes, sometimes up to several hours (e.g. PR23).

III.4.1 Photoreceptor properties

The resting potentials of most photoreceptors were between -20 and -40 mV (mean ± s.e.m. -33.6 ± 2.3 mV). Maximal light responses varied between 5 mV and 30 mV (mean ± s.e.m. 10.9 ± 1.5 mV). I adjusted the maximum intensity of my stimuli to elicit maximal responses in the central (most linear) part of the *V/log(I)*-function. The only exceptions were PR15 and PR16, which had a much lower resting potential of -80 mV. I often found similar cells with resting potentials as low as -90 mV and small (1-3 mV), but very reliable flash responses, directly adjacent to photoreceptors – they might be screening pigment cells that are weakly electrically coupled with the

photoreceptors. However, the identity of these cells can only be reliably determined by intracellular dye injection.

All cells I report here had their receptive field near the frontal or lateral visual horizon. Dorsal and ventral looking cells are difficult to reach due to their small number and their position. Dorsal receptors are most likely to be damaged during preparation, whereas ventral cells are difficult to reach because of the long way the electrode has to travel through the tissue (about 1.5 mm from the top of the eye to the first ventral photoreceptors).

The temporal shape of the depolarising response to a flash of light varied between photoreceptors. Figure III.3 shows several examples of mean responses to 40 ms (Figure III.3A) and 300 ms (Figure III.3B) flashes (see Appendix D for the full raw data set of all cells). These responses are normalised to the start of the response, as I collected direct information (using a photodiode) about the relative timing of flash and cell response only in one experiment (PR9). While most cells showed a gradually rising depolarisation that reached a maximum plateau after about 40-60 ms (e.g. Fig 3A, green, black and red line), some cells reliably exhibited a fast, phasic peak, after which they dropped to a plateau (e.g. Figure III.3A, blue line). Off-responses varied even more widely. In many recordings the membrane potential dropped back to RP (e.g. Figure III.3A, black line) or below RP (e.g. Figure III.3A, green line, Figure III.3B, blue line) within 10-20 ms. However, there were several cells that consistently took much longer to recover, in some cases up to several hundred milliseconds (e.g. Figure III.3A, red line). It is likely that rather than indicating different cell types or states, these differences in light responses reflect different cell penetration sites and different or minor damage to the cell membrane.

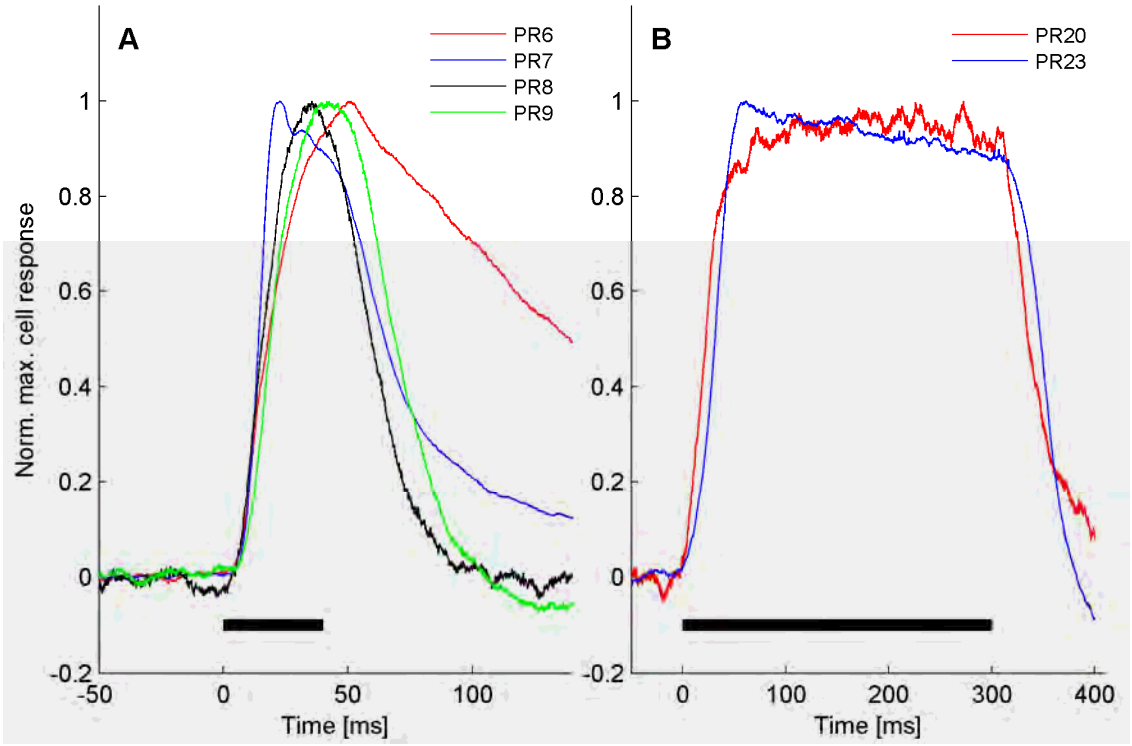

Figure III.3: Photoreceptor light responses. Normalised responses of six photoreceptors to either 40 ms **(A)** or 300 ms **(B)** flashes of monochromatic light. The relative timing of the light stimulus (black bar) is only known for PR9 (green line), all other receptors were aligned at the response start. Note that while most receptors slowly rise to a plateau response, PR 7 (blue line) shows a fast, transient spike and only drops to a plateau afterwards. Similarly, the recovery time to (or below) RP is highly variable between different cells. These differences might reflect different cell penetration sites.

III.4.2 Spectral sensitivities

The analysis from raw data to initial fits of visual pigment templates is demonstrated for PR9 in Figure III.4. This was the only cell where light responses were recorded with a photodiode, allowing me to measure response latency. For this cell, I evaluated five spectral runs and ten intensity runs. The means (± s.e.m.) of scaled spectral response curves (blue for upwards, red for downwards sweeps) are shown superimposed on the mean voltage traces (grey and black lines, off-set to position their response peak at the corresponding stimulation wavelength) in Figure III.4A. Note that due to the way in which responses were measured (maximum within a 20 ms interval), the mean of responses (mean of maxima) is not always the same as the maximum of the mean traces (maximum of mean). The response latency between the

start of the light stimulus (Figure III.4A, black bars) and the peak of the cell's response (Figure III.4A, black lines) was about 40 ms. The same analysis was performed for the intensity runs, with the exception that intensity response curves of different runs were not scaled. Mean voltage traces (grey lines), mean responses (± s.e.m., blue and red dots and error bars) and three representative stimuli with their corresponding responses (black bars and lines) are shown in Figure III.4B. A sigmoidal *V/log(I)*-function was fitted to the responses (Figure III.4B, dotted line) and applied to transform spectral responses into sensitivities (Fig 4C, black dots ± s.e.m.). The sensitivity function has a broad maximum (FWHM 118 nm) around 410 nm and is asymmetric with a long tail on the long-wavelength side. The best fit assuming a single photo-pigment is provided by a 425 nm nomogram (Figure III.4C, dashed red line). While this fit clearly does not predict the long-wavelength slope, a much better explanation is provided by a superposition of two nomograms (405 nm + 455 nm, Fig 4C, solid line).

The reliance on a *V/log(I)*-function when measuring spectral sensitivities using equal-photon flashes creates two fundamental problems. Firstly, very small errors at the peak of the voltage response curve are transformed into much larger errors in sensitivity due to the exponential nature of the *V/log(I)*-function. Secondly, an error in the slope of the *V/log(I)* fit will change the width of the sensitivity function. To check if this might be the reason for the poor single fit observed in PR9, I compared the measured *V/log(I)*-function (Figure III.5, black dots and solid line) to the function that would be needed to make the single nomogram fit the data (Figure III.5, red dots and dotted line). The slope of this hypothetical *V/log(I)*-function is clearly far outside the range of the observed data, especially the points corresponding to the long-wavelength tail, indicating that no realistic error in my intensity response measurements will allow a single pigment to fit. This analysis can be found for all 23 photoreceptors in Appendix D.

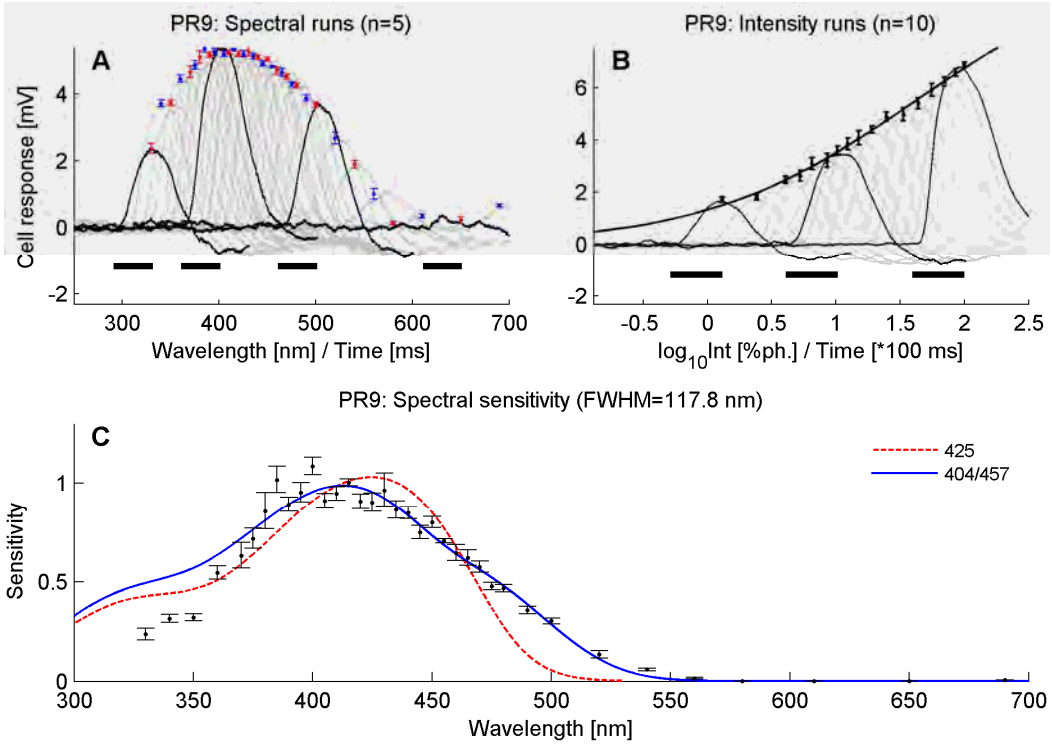

Figure III.4: Spectral sensitivity analysis in a short-wavelength receptor (PR9). (A) Evaluation of five spectral runs. Means (± s.e.m.) of scaled spectral response curves (blue for upwards, red for downwards sweeps) are overlayed on mean voltage traces (grey and black lines, off-set to position response peaks at corresponding wavelengths). Response latency between light stimulus (black bars) and response peak (black lines) is shown for four example wavelengths and was about 40 ms. **(B)** The same analysis for ten intensity runs. A sigmoidal *V/log(I)*-function was fitted to the responses (black line) and applied to transform spectral responses into sensitivities. **(C)** The sensitivity function (black dots ± s.e.m.) has a broad maximum (FWHM 118 nm) around 410 nm and is asymmetric with a long tail on the long-wavelength side. The best single-pigment fit assumes a 425 nm pigment (dashed red line). The long-wavelength slope is explained much better by a superposition of two nomograms (405 nm + 455 nm, solid line).

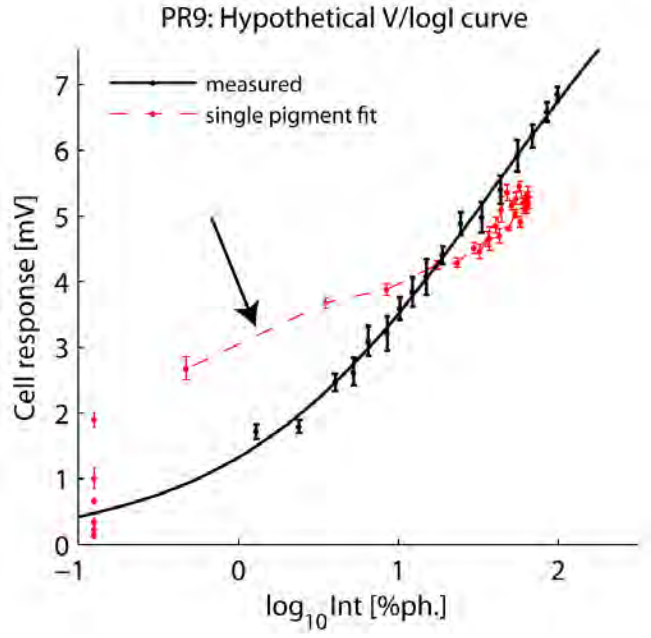

Figure III.5: *V/log(I)* measurement error does not explain poor single-pigment fit. To check if *V/log(I)*-function measurement errors explain the poor single fit, I compared the measured function (black dots and solid line) to the one needed to make the single nomogram fit the data (red dots and dotted line, unconnected red dots outside axis limit). The hypothetical function's slope is far outside the observed data range, especially the points corresponding to the long-wavelength tail (arrow).

III.4.3 Spectral receptor classes and visual pigments

The surprising range of spectral sensitivities of *U. vomeris* photoreceptors (Figure III.6A) shows at least two distinct classes of photoreceptor types. **UV receptor** sensitivities (e.g. Figure III.6B) peak in the UV below 350 nm and have a secondary peak around 440 nm (PRs 8, 22, 23). **Blue receptors** (e.g. Figures 6B-D) show a diversity of sensitivity peaks (410 - 460 nm), widths (FWHM 72-177 nm, mean ± s.e.m. 124 nm ± 4.9 nm) and shapes. While some have narrow sensitivities that are well explained by a single pigment fit (e.g. PR11, Figure III.6C), others show broad sensitivities that end in a long tail on the short-wavelength (e.g. PR20, Figure III.6D) or on the long-wavelength side (e.g. PR9, Fig. 6E) and are much better fitted assuming the presence of two co-expressed pigments. There was no indication of a pigment with a sensitivity peak at 500 nm or longer, as it can be found in many other crabs (see Discussion). Red and orange objects, like the males own claws, will

therefore only present a very weak signal to the *U. vomeris* eye. I will discuss the ecological implications of this observation later.

Considering this variety of photoreceptor types, what is the most parsimonious explanation for the observed spectral sensitivities? The range of possible factors affecting spectral sensitivities in compound eyes is very large. Without extensive histological and physiological examination, including all potential factors therefore make modelling these spectral sensitivities extremely flexible and practically meaningless. The possible role of several of these factors (rhabdom length and pigment density, screening pigments and absorption in cornea and crystalline cone, adaptation, optical and electrical coupling, metarhodopsins) will be considered in the Discussion. I will restrict the following analysis to finding the minimal number of visual pigments that must be present to explain all observed sensitivities.

Firstly, the strong UV peak in the UV cells could either be generated by a UV pigment or by a hypothetical screening pigment inside or around the rhabdom which filters out most of the visible light in some photoreceptors. Evidence from a recent genetic study in *Uca pugilator* suggests that a UV opsin is present and expressed in fiddler crabs (Rajkumar et al., 2008), leading me to believe that the UV receptors' sensitivity is based on a pigment.

In addition, there appears to be a large variation in blue sensitivities. At first glance, these either represent a number of additional photopigments or have to be explained by the presence of noise in the recordings (far more than the variability within individual receptors' sensitivity measurements would suggest). Upon closer inspection, however, many blue receptors have one flank that agrees with a single pigment and one that is too long. Systematically, this long tail points towards the long-wavelength side in shorter-wavelength receptors (e.g. Fig 6E) and to the short-wavelength side in longer-wavelength receptors (e.g. Fig 6D). This observation led me to believe that all blue receptors could be modelled as a superposition of the spectra of only two different visual pigments.

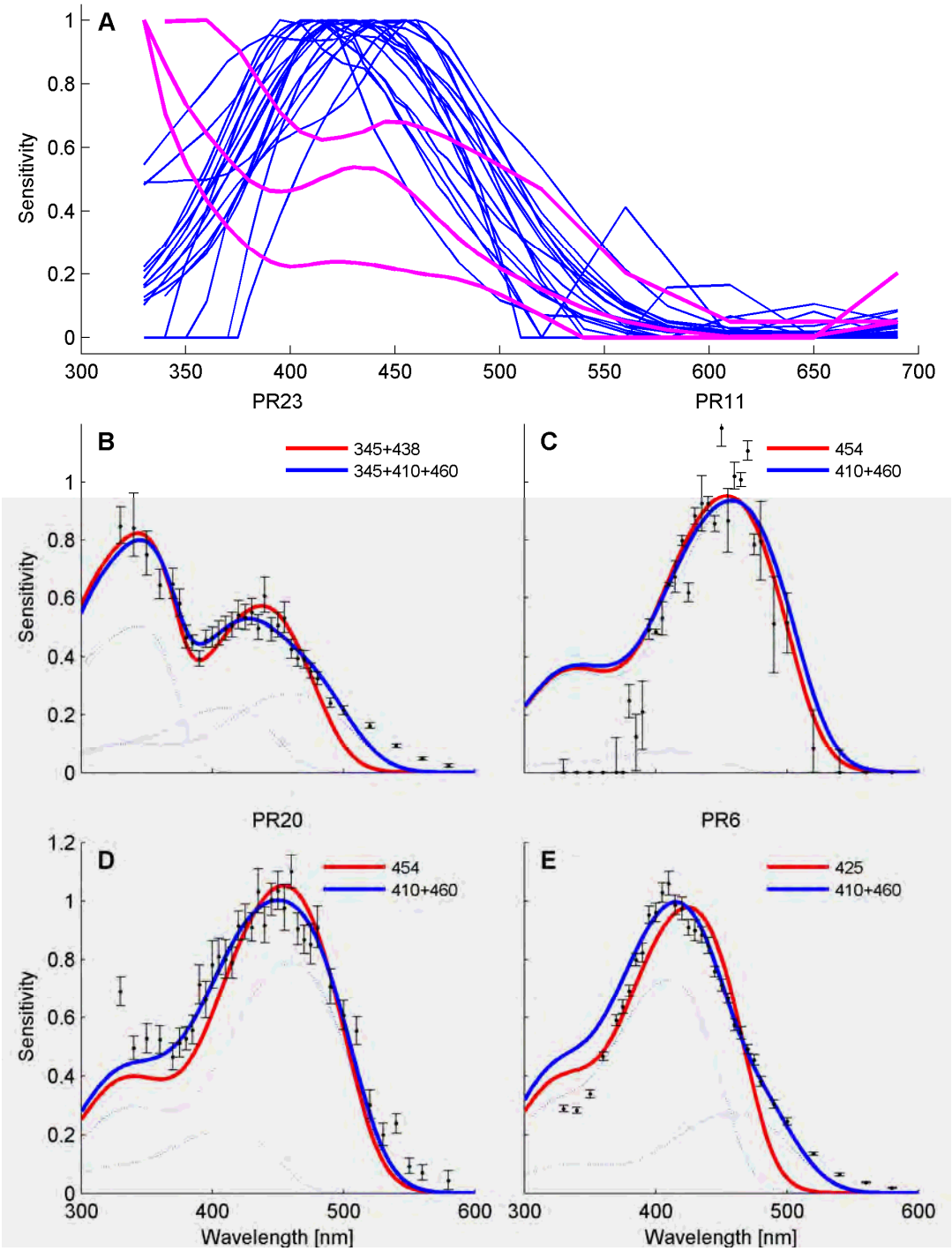

Figure III.6: Photoreceptor spectral types. *U. vomeris* photoreceptors classes in overview **(A)** and in four example cells fitted by the best single pigment (red lines) and by a combination of a 410 nm and a 460 nm pigment (blue lines): **(B)** UV receptor, peaking in the UV below 350 nm with a secondary peak at 440 nm (PRs 8, 22, 23) **(C,D,E)** blue receptors, showing the wide variety of spectral peaks, widths and shapes (see text for detail). Pigment ratios (UV/B1/B2) fitted were as follows. B: 50.4%/22.4%/27.2%; C: 7.3%/92.7%; D: 21.4%/78.6%; E: 72.7%/27.3% (dotted blue lines indicate individual pigment contributions)

To test this hypothesis and to find the best pigment combination, I calculated the normalised residual for all cells when fitted by a single pigment or by any combination of two pigments with maximum sensitivities at wavelengths λ_{max} between 300 nm and 500 nm (see Appendix E.2 for complete mathematical detail). The residuals were averaged for all those cells where I deemed the spectral sensitivity reliably measured, i.e. where more than one spectral scan was recorded (this was the case in nine cells).

For the single pigment case, the average fitting error is shown in Figure III.7A. The residual function has a broad minimum at a λ_{max} of 440 nm, suggesting that this pigment represents the best explanation of all cells' sensitivities (assuming that the variation in blue receptors is due to noise). The addition of a second pigment drastically improves the fits. The error surface for this case is shown in Figure III.7B. Red colours represent pigment combinations that resulted in a poor fit to the recorded data, while blue colours represent combinations that give a comparatively good fit. The diagonal, where both pigments are the same, shows the same data as the residual line for the single case (Figure III.7A). The minimum of the error surface is clearly away from the diagonal, at a combination of a 410 nm and a 460 nm pigment (Figure III.7B, black square). As fits to the spectral sensitivities of individual cells confirm (Figures 6B-E and Appendix D, blue lines), combining these two pigments in various ratios results in satisfactory fits to practically all recorded sensitivities, including the secondary peak of UV cells (e.g. Figure III.6B).

In conclusion, all measured sensitivities can be explained by co-expression of three individual spectral units at 345 nm (UV), 410 nm (B1) and 460 nm (B2). My data do not allow me to decide whether the sensitivity maxima of these units are directly provided by the underlying pigments, or whether pigment spectra are shifted, for instance by screening pigments (see Discussion).

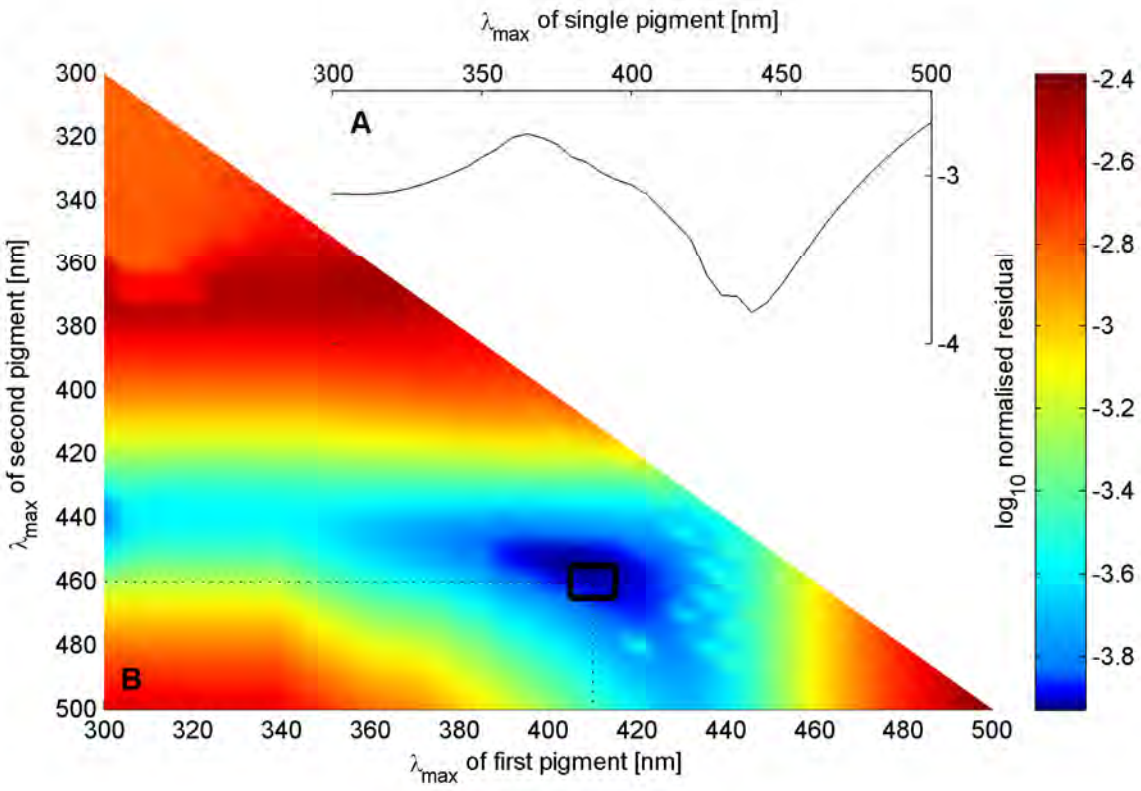

Figure III.7: Two-pigment fit error surface. (A) Mean normalised residuals for all combinations of two pigments between 300 nm and 500 nm (detail in Appendix E.2), averaged for all cells with more than one spectral scan. **(B)** Best single pigment fit (minimum of the diagonal / black line) at λ_{max} 440 nm. A second pigment improves the fit, with a minimum normalised error at a combination of a 410 nm and a 460 nm pigment (black square).

III.4.4 Polarisation sensitivity

Polarisation sensitivity was determined in an analysis equivalent to that for spectral sensitivity (compare Figures 4 and 8). I examined PS in detail in two cells (PR5 and 6[5], Figure III.8). Both were more sensitive to vertically than to horizontally polarised light with PS 5.4 and 2.9, respectively, and thus were either R1, R2, R5 or R6 (Alkaladi, 2008). Two additional cells, PR9 and PR22, were briefly tested by comparing (on the oscilloscope) the responses to several horizontally and vertically polarised test flashes. PR9 (λ_{max} 410 nm) was found to be more sensitive to horizontally and PR22 (a UV receptor) to vertically polarised light. As all four cells were found to be polarisation sensitive, they must be retinula cells R1-R7. We have no confirmed recording of polarisation insensitive cells (i.e., R8).

III.4.5 Visual interneurons

Spiking interneurons in the visual neuropils were simpler to penetrate and far more stable than photoreceptors. This may be due to their larger size. In the shore crab *Chasmagnathus*, for example, many of the interneurons in the lamina and medulla are more than 10 μm in diameter (Sztarker et al., 2005; Sztarker et al., 2009). I recorded the light responses of five interneurons with resting potentials between -30 and -60 mV and observed several others. The neurons' responses to flashes of light were similar to those observed in other crustaceans (e.g. Wiersma and Yamaguchi, 1967a, b; Berón de Astrada et al., 2001). The majority of observed neurons showed no response to the start of a light pulse, but responded to the end of illumination with a large, graded depolarisation that lasted several seconds (dimming neurons, e.g. DN1, Figure III.9A, B).

[5] PR6 had a broad, asymmetric spectral sensitivity peaking at 410 nm with a long tail towards longer wavelengths (Appendix D). PR5's spectral sensitivity was not determined to facilitate more accurate measurements of the polarisation sensitivity.

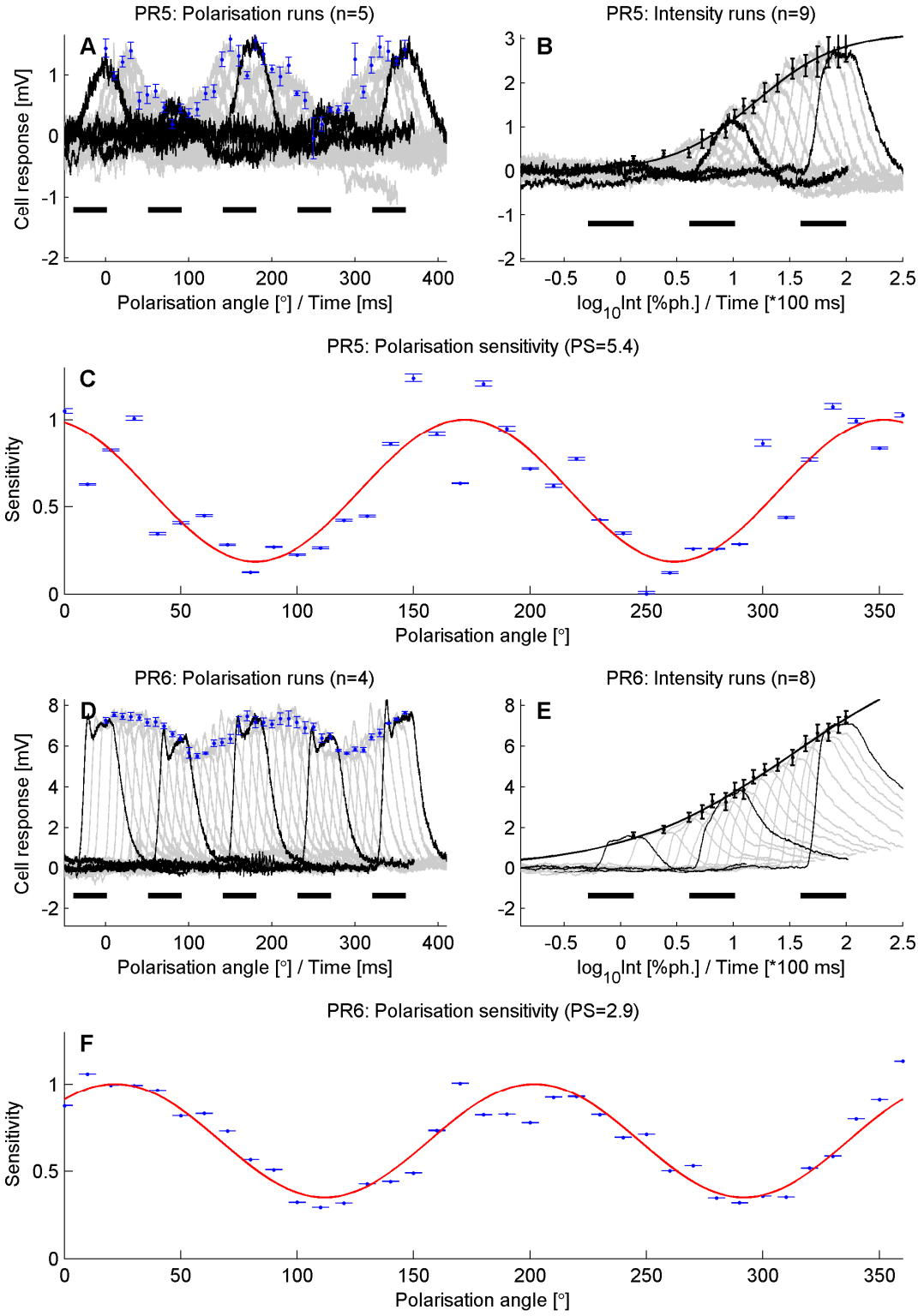

Figure III.8: Polarisation sensitivity of *U. vomeris* photoreceptors. Analysis equivalent to that for spectral sensitivity (Figure III.4). Both PR5 **(A,B,C)** and PR6 **(D,E,F)** are more sensitive to vertically than to horizontally polarised light with PS 5.4 and 2.9, respectively**.**

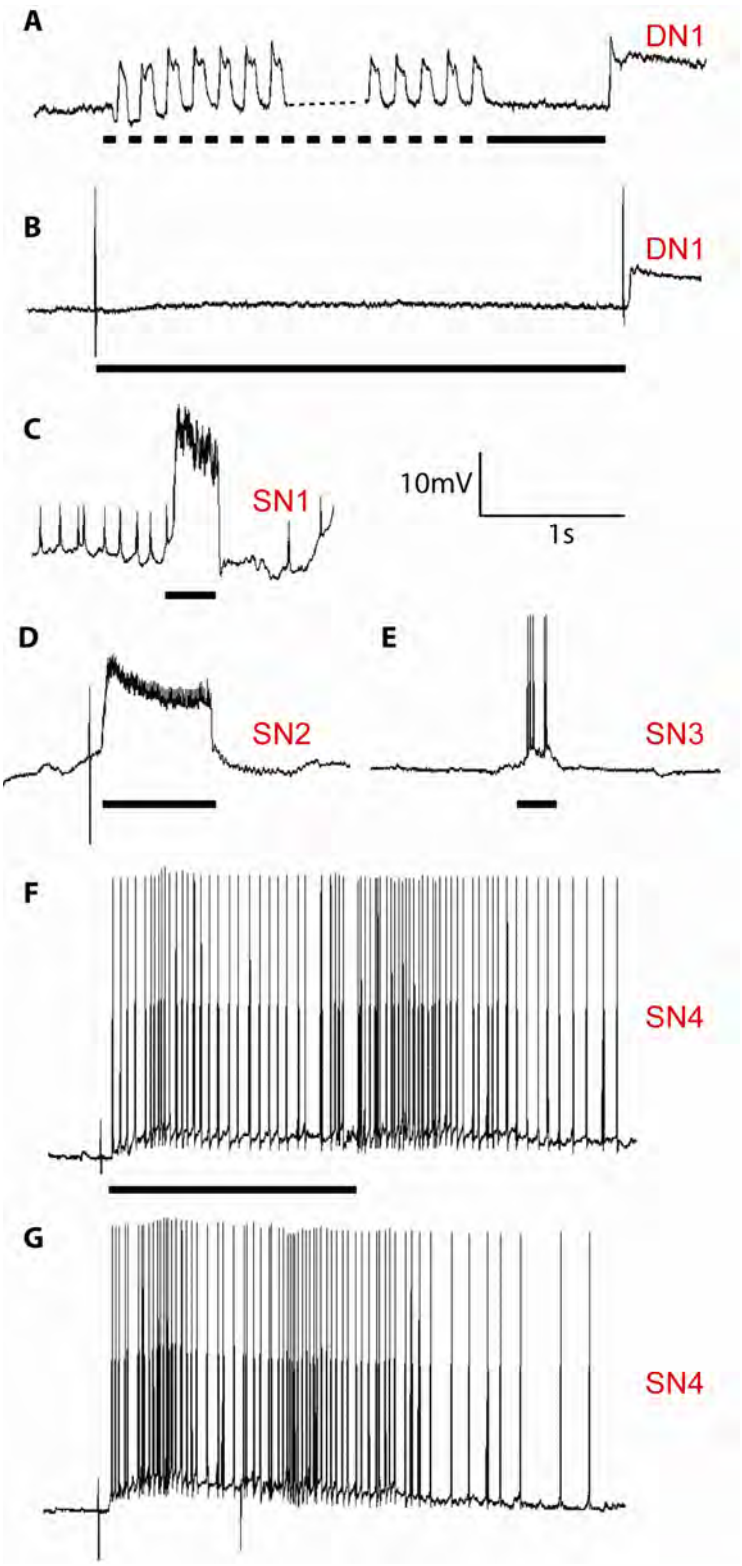
A
DN1
B
DN1
C
SN1
10mV
1s
D
SN2
E
SN3
F
SN4
G
SN4

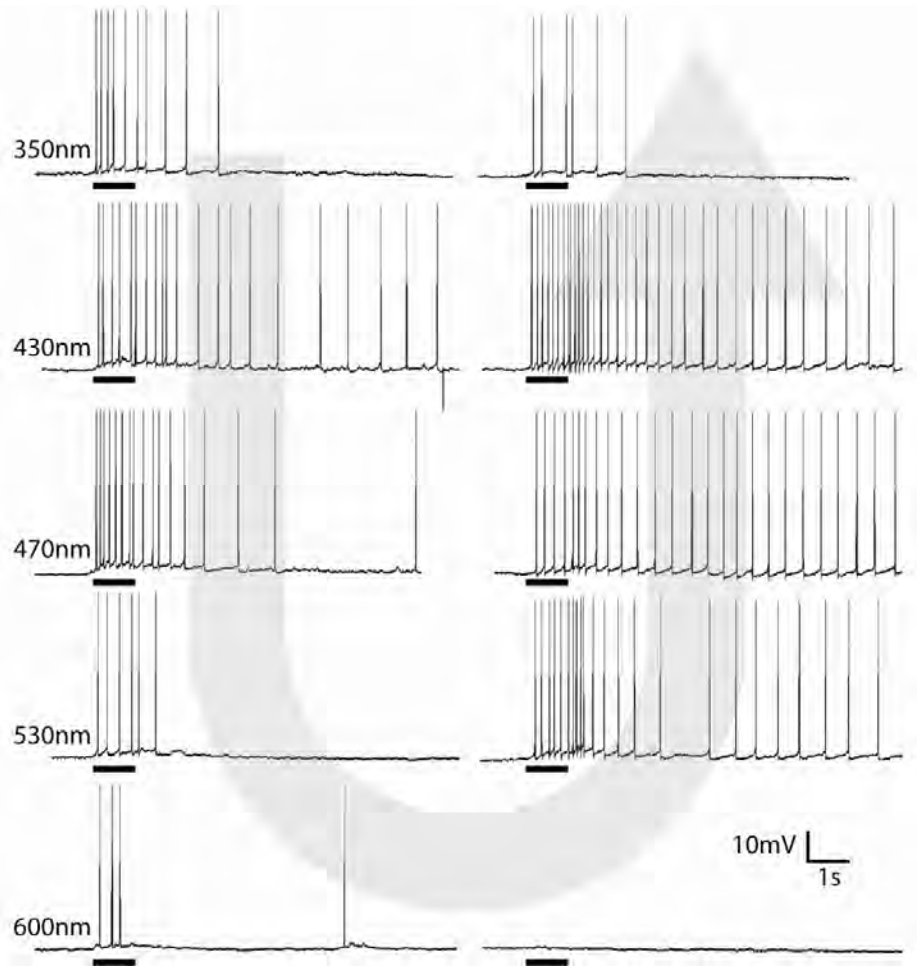

Figure III.10: Wavelength-specificity of a sustaining neuron's (SN4) flash response. When stimulated with monochromatic light of five different wavelengths (two repetitions at each wavelength, order indicated by arrow), SN4's responded most strongly in the blue, almost as strongly in the UV and practically not at all at 600 nm. Consistent with the spectral sensitivity measurements, there was no indication of an underlying green sensitivity.

Figure III.9: Light responses of five *U. vomeris* interneurons. A large part of the observed neurons showed no response to the start of a light pulse, but responded to the end of illumination with a large, graded depolarisation lasting several seconds (dimming neurons, e.g. DN1, **A,B**). Sustaining neurons (e.g. SN1-4, **C-G**) showed a sustained, graded depolarisation in response to light, overlayed by spikes with a frequency related to the amplitude of the graded response. Larger 'spikes' at the start of B,D,F and G and at the end of B are electrical artefacts induced by the light source.

Many other neurons (e.g. SN1-4, Figures 9C-G, 19) were sustaining neurons (SNs), showing a sustained, graded depolarisation in response to light, overlayed by spikes with a frequency that is related to the amplitude of the graded response.

These two cell types are most likely equivalent to dimming and sustaining neurons in the medulla of crayfish and crabs (Kirk et al., 1982; Berón de Astrada et al., 2001). Responses of the SNs varied between recordings from small (~2 mV) spikes riding on large (10-15 mV) graded responses (Figure III.9C,D) to large (20 mV) spikes on very small or negligible graded responses (Figures 9E-G,10). In the latter case, spiking often continued well beyond the end of the light stimulus. Despite these obvious differences, both types of responses are likely produced by the same cell type (Sandeman, 1969; Grossman et al., 1979; Berón de Astrada et al., 2001).

I stimulated one of these cells (SN4) with monochromatic light of five different wavelengths (Figure III.10). Consistent with the spectral sensitivities measured in photoreceptors, its response was strongest in the blue and essentially gone at 600 nm.

III.5 Discussion

III.5.1 Electrophysiological preparation

The first important contribution of this study lies in establishing the first intracellular electrophysiological preparation in a fiddler crab. Apart from recording from photoreceptors, this setup allowed me to penetrate and hold visual interneurons for extended periods of time. Although the stability of the preparations is still delicate (all my recordings were obtained from only 11 crabs out of a total of more than 70 preparations), I have recently developed several improvements to my electrodes, holding apparatus and experimental protocol that have considerably improved the success of my recordings. In combination with a recently established behavioural protocol on a crab tread-mill (Liang, 2008), this preparation will allow me to examine the neural mechanisms underlying fiddler crab behaviour in the laboratory; in an

animal that is already well established as an *in-situ* behavioural model (Zeil and Hemmi, 2006).

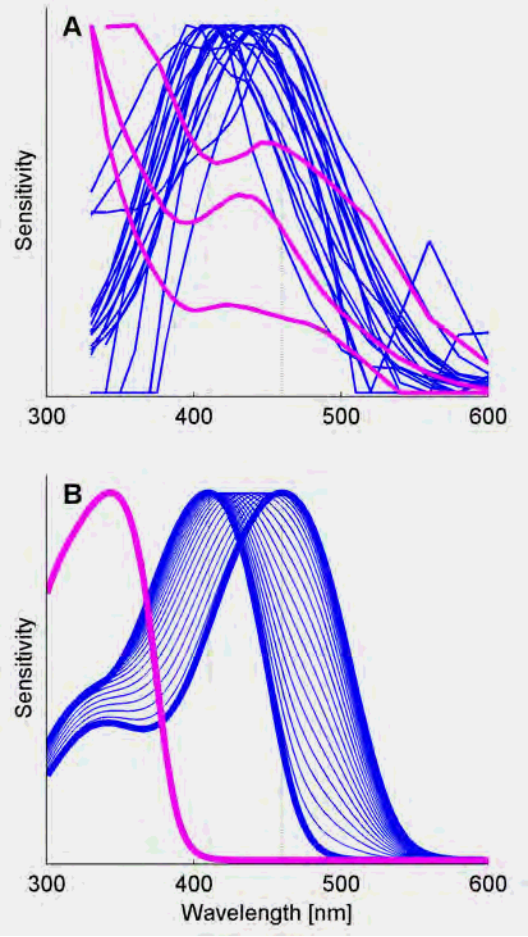

Figure III.11: The unusual trichromatic colour vision system of *Uca vomeris*. The proposed colour vision system **(A)** is in good agreement with all recorded spectral sensitivities **(B)**. The variability of blue receptors is unusual in colour vision systems and its ecological significance has yet to be examined.

III.5.2 Uca vomeris spectral sensitivities

The second contribution of this study is the first intracellular measurement of spectral and polarisation sensitivities in the fiddler crab compound eye. My recordings

revealed the presence of an unusual, potentially[6] trichromatic colour vision system in *Uca vomeris* (Figure III.11). Apart from a UV-sensitive receptor type (λ_{max} 345 nm) the crabs possess a wide variety of blue-sensitive receptors that are most likely created by co-expression of different ratios of two blue-sensitive visual pigments (λ_{max} 410 nm, B1, and 460 nm, B2). There was no indication of a pigment with a sensitivity peak around 500 nm, as it can be found in many other crabs (see below). Although I cannot directly verify the mechanism by which these spectral sensitivities are created, I will discuss several possible alternative effects that I have considered in my modelling. The factors that have been shown to influence spectral sensitivities of photoreceptors in compound eyes are extremely diverse:

Several pigments can be **co-expressed** in individual photoreceptors (Kirschfeld et al., 1977; Hardie, 1979; Sakamoto et al., 1996; Arikawa, 2003), resulting in a spectral sensitivity that is effectively the sum of the two pigments absorptions. A similar summation of spectral sensitivities can result from **electrical coupling** between several photoreceptors[7] (Shaw, 1969; Snyder et al., 1973). The spectral sensitivity of a photoreceptor further depends on the length of its rhabdom and the pigment concentration, which determine the amount of **self-screening** (Snyder et al., 1973). In a long and densely packed receptor, light of the preferred wavelength is largely depleted in the distal part of the rhabdom. Light of a wavelength that the receptor is less sensitive to, on the other hand, travels much further through the rhabdom and is absorbed there, resulting in a broader spectral sensitivity. In contrast to self-screening, spectral sensitivities can be sharpened by **optical coupling** (Snyder et al., 1973). If receptors of different spectral types are present within the same rhabdom, each receptor will deplete a large percentage of the light of its preferred wavelength, thereby decreasing the absorption of this wavelength in all other receptors. In other words, each photoreceptor acts as a

[6] Whether and how these three sensitivities are compared neurally to form a trichromatic colour vision system will, of course, have to be confirmed in behavioural experiments.

[7] Similarly, the broad spectra could be a recording artefact caused by double recordings from two adjacent cells. This possibility, however, is extremely unlikely, as I have never observed any changes in the spectral sensitivities during the course of a recording, even when the strength of the response clearly indicated that the electrode had changed position and was penetrating the cell better. Also, co-expression is strongly supported by the results of in-situ hybridisation.

spectral filter for all other receptors within the same ommatidium. Similarly, spectral sensitivities can be modified by actual **spectral filters** in or around the light path. These filters can be realized as screening pigments in or around the rhabdom (Snyder et al., 1973; Stavenga, 2002), absorption by the lens or crystalline cone (Walls, 1942; Douglas and Marshall, 1999), or by metarhodopsins in the rhabdom (Goldsmith and Bruno, 1973; Stavenga, 2002). Lastly, **competition for extracellular Na^+** (Hamdorf et al., 1973) and **synaptic interactions** on the level of the retinula axons (Menzel, 1974; 1979) have been shown to modify spectral sensitivities in some invertebrates.

What then is the possible impact of these various effects on spectral sensitivities in *U. vomeris*?

- Self-screening: *U. vomeris* rhabdoms are between 250 and 350 μm long at the eye equator, with individual receptors contributing alternating packages of rhabdomeres; the effective length of a single rhabdomere is therefore on average 50% of the total length, 150 μm. The pigment concentration has been measured in several decapod species with results varying between 0.003 μm^{-1} and 0.023 μm^{-1} (reviewed in Warrant and Nilsson, 1998). I used a value of 0.006 μm^{-1}, inferred from MSP in isolated rhabdoms of the brachyuran crab *Sesarma reticulatum* (Cronin and Forward, 1988; Jordão et al., 2007). The effects of self-screening on the modelled sensitivities were minor. They helped in explaining the width of the sensitivity functions, but cannot account for their asymmetry. Changing either parameter value by even a factor of 2 does not change the qualitative results of my analysis.
- Optical coupling: I did not include the effects of optical coupling in my models, as the information I have about the distribution of different spectral types within individual ommatidia is very limited. A detailed study comprising intracellular dye injections, *in-situ* hybridisation and/or the measurement of the wavelength dependence of polarisation sensitivity (Menzel, 1975) would be necessary to resolve this question. However, while optical coupling might sharpen and separate similar spectral sensitivities

within one ommatidium, it cannot account for the broad sensitivities and long tails I observed in many cells and can therefore not be considered as an alternative explanation to co-expression.

- Spectral filters: The eyes of fiddler crabs are packed with screening pigments (Alkaladi, 2008), including the dark primary pigment, the golden secondary pigment surrounding the crystalline cones and a red screening pigment surrounding the rhabdoms (Figure III.1C). While these screening pigments are clearly an adaptation to an extremely bright light environment (Zeil and Hemmi, 2006), the functional significance of their spectral filtering properties remains unknown. To complicate things even further, the screening pigments do not immediately encircle the rhabdom, but are separated from it by a 1 μm thick palisade (Alkaladi, 2008) that appears transparent (its actual transmission, however, particularly in the UV, is unknown!). What effect this peculiar arrangement has on the spectral sensitivities as well as the polarisation sensitivity, acceptance angles and total light absorption, is currently unknown. I will argue below that the red screening pigments in *U. vomeris* eyes might shift the sensitivity of the green pigment found in other crabs to provide the B2 sensitivity, thereby increasing spectral and spatial resolution in the blue, while keeping the ability to retract the screening pigments in the dark to increase sensitivity. Filter pigments might also explain the variability in the secondary UV peak of many cells I recorded from. Unfortunately, we currently have very little information on the absorption spectra of any of the *U. vomeris* screening pigments. The only screening pigment measured so far (Jordão et al., 2007) has a peak absorption close to the maximum of B2 and would only broaden, but not shift a 460 nm pigment sensitivity. The measurement also did not include the UV part of the spectrum.
- Na^+ competition and synaptic interactions: Our knowledge of fiddler crab photoreceptor physiology is currently too limited to allow us to predict these effects. However, their effects would be very similar to those of optical

coupling and therefore could not explain the broad, assymetric sensitivities I found.

- Co-expression: There is strong evidence from *in-situ* hybridization experiments (Alkaladi et al., in prep.) that at least two non-UV pigments with very similar opsin sequences are co-expressed in most photoreceptors in *U. vomeris* (as in another grapsid crab, Sakamoto et al., 1996). In my models, co-expression of two blue pigments was the most likely single effect that could satisfactorily explain the variability of blue receptor types.

In conclusion, the combined effects of self-screening and co-expression seem sufficient to explain the variation in the observed sensitivities. Co-expression is also well-supported by evidence from *in-situ* hybridisation. However, screening pigments might play a role in shifting a long-wavelength sensitive pigment – as it has been found in previous studies in related species – towards shorter wavelengths and thus creating the B2 sensitivity. Before I discuss this possibility, I will compare my results to the results of these previous studies.

III.5.3 Comparison to previous studies

For easier comparison, I have extracted the data from the four previous studies (Scott and Mote, 1974; Hyatt, 1975; Horch et al., 2002; Jordão et al., 2007, reviewed in the introduction), fitted pigments using my algorithms and replotted them in Figure III.12. My fit agrees well with Scott and Mote's interpretation (Figure III.12A) of a single pigment peaking at 500-510 nm. Hyatt offered no guess as to the underlying pigments; my fits (Figure III.12B) predict a 510-525 nm long-wavelength and a 430-480 nm short-wavelength pigment depending on species. Horch and his colleagues interpreted their ERG data from both graded responses and spikes (when fitted in logarithmic space) as demonstrating a 430 nm and a 500-530 nm pigment. My template fits (Figure III.12C) favour a similar long-wavelength pigment (510 nm), but a short-wavelength pigment peaking at 460 nm for the graded and 470 nm for the spike responses[8].

[8] though it seems bold to fit two pigments to four data points

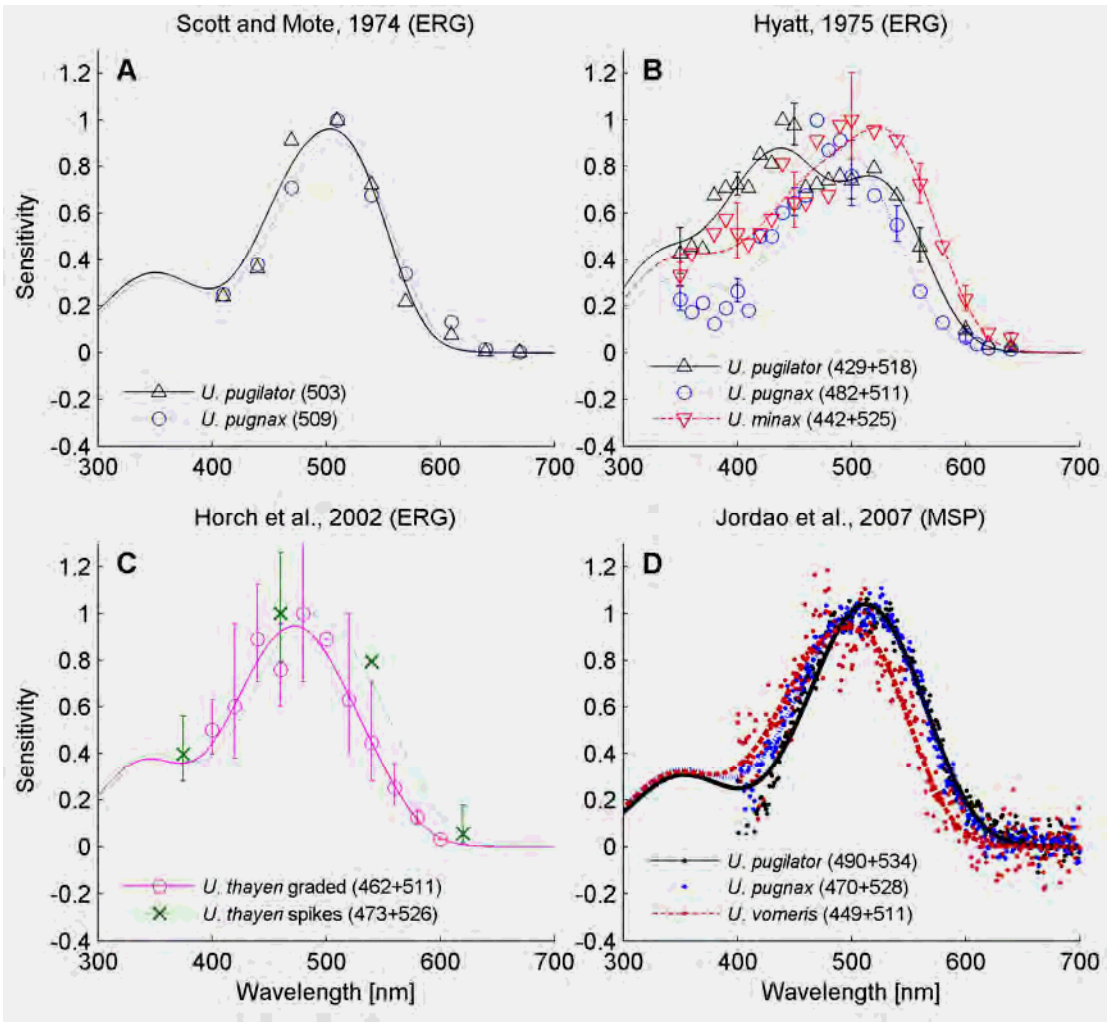

Figure III.12: Previous studies re-evaluated. Data from four previous studies on fiddler crab colour vision using ERG **(A,B,C)** and MSP **(D)**. Nomogram fits were recalculated with our algorithms. See text for details.

Cronin and Forward (1988) measured the absorption of the long-wavelength sensitive pigment of 27 crab species by MSP in isolated rhabdoms. They found the λ_{max} to be between 473 nm and 515 nm (Figure III.13). Unfortunately, they could not determine *Uca* absorption due to the dense screening pigments. Only very recently, Jordão and her colleagues (2007) were able to finally measure *Uca* absorbances in frozen sections. They decided to only fit a single pigment to their MSP measurements. Their measured absorbances, however, seem very broad and are indeed much better

predicted by a combination of two pigments[9] (Figure III.12D). Again, the long-wavelength pigment has a maximum sensitivity at about 510-530 nm, while the short-wavelength pigment peaks between 450 and 490 nm. This last study was also the only one so far to consider my study species *U. vomeris*. However, their data on this species was limited to eight measurements in only a single crab.

Considering that all previous studies indicated a dichromatic blue/green visual system, it was quite surprising to find a trichromatic UV/blue/blue arrangement instead. The UV receptor type was probably least surprising, as only one of the earlier studies had looked at the UV part of the spectrum (Hyatt, 1975). In an ERG based study, a relatively rare UV receptor could easily be confused with the secondary UV peaks in other receptor types. The absence of a green receptor, however, was unexpected and made me consider whether I could have 'missed' it or whether it could be expressed in R8 (for which I have no confirmed recordings). There are several reasons why I think this is unlikely:

- In most invertebrates with more than one visual pigment, R8 expresses a shorter-wavelength pigment than R1-R7 (e.g. in the crayfish Procambarus, Cummins and Goldsmith, 1981; in the crabs Callinectes and Carcinus, Martin and Mote, 1982; and in the spiny lobster Panulirus, Cummins et al., 1984).
- Whenever a light response was observed in my experiments, extra- or intracellularly, I immediately observed the responses to equi-quantal test flashes at 430 nm and 530 nm, and never observed a larger response to the green flash.
- I briefly checked spectral sensitivities of some visual interneurons (e.g. Figure III.10), and never found indications of a long-wavelength sensitivity. In most vertebrates and invertebrates, higher-order functions like motion and form processing are colour blind and only receive input from long-wavelength receptors (reviewed in Osorio and Vorobyev, 2005). I would have therefore

[9] As these measurements represent pigment absorptions, not receptor sensitivities, I assumed a 'rhabdom length' of 1 μm for this fit (as opposed to 150 μm in all other fits).

expected at least some interneurons in the lamina or medulla to respond to longer wavelength light beyond 550 nm.

The long-wavelength sensitive photoreceptors found in other crabs could have been shifted in *U. vomeris* towards shorter wavelengths (i) by one or several mutations of the opsin gene, or (ii) by the filtering effect of screening pigments (similar to the situation in mantis shrimps, Marshall et al., 2007, Figure III.13). As this screening would reduce the absolute sensitivity of the pigment, the latter solution would require a much higher concentration of the green-sensitive pigment compared to the co-expressed blue-sensitive pigment. This would also explain differences between my results and those reported by Jordão and colleagues (2007). MSP would have measured the unfiltered absorbance of the pigment and therefore due to the higher concentration mostly a green sensitivity. This hypothesis can be tested by comparing recordings performed at night with those made during the day. In the shore-crab *Leptograpsus*, screening pigments have been shown to move in a circadian and light-dependent rhythm, leaving the rhabdom almost completely exposed at night and in the dark, and closely surrounding the rhabdom in bright light during the day (Stowe, 1980). Although my crabs were briefly dark-adapted before experiments, all recordings were done during the day and my stimuli were bright and quite frequent. In a fully dark-adapted crab (i.e. at night), I would expect a much stronger green sensitivity, if that sensitivity is indeed shifted by screening pigments.

III.5.4 Uca vomeris 'spectral ecology'

If most crustaceans have a green-sensitive long-wavelength receptor (Figure III.13), why is *U. vomeris*' shifted towards the blue, decreasing absolute sensitivity and the range of wavelengths that can be perceived? The first point to note is that this species' visual system is extreme among the species studied so far in another way: Longer eyestalks, smaller eye separation and higher vertical resolution in the horizontal visual streak (chapter II) make *U. vomeris* an extreme example of a narrow-fronted crab, adapted more than usual to a life in a flat world. One purpose of

the higher resolution in the frontal visual field is the identification of conspecifics from their individual carapace patterns. These patterns reflect most strongly in the blue and UV. In chapter II I have demonstrated that the maximum resolution is available for these blue/UV wavelengths only due to diffraction in the lenses. Shifting a ubiquitously expressed visual pigment's sensitivity from the green to the blue would thus increase spatial resolution and contrast for a difficult pattern detection task. It would also increase the spectral resolution, i.e. the ability to discriminate similar colours, in the blue. To see what important social stimuli look like to *U. vomeris'* colour vision system, spectrograph measurements (kindly provided by Jan Hemmi and Jochen Zeil) were transformed into fiddler crab colour space (Figure III.14) using equations from Kelber et al (2003). A larger distance in these chromaticity diagrams indicates a better discriminability of two colours.

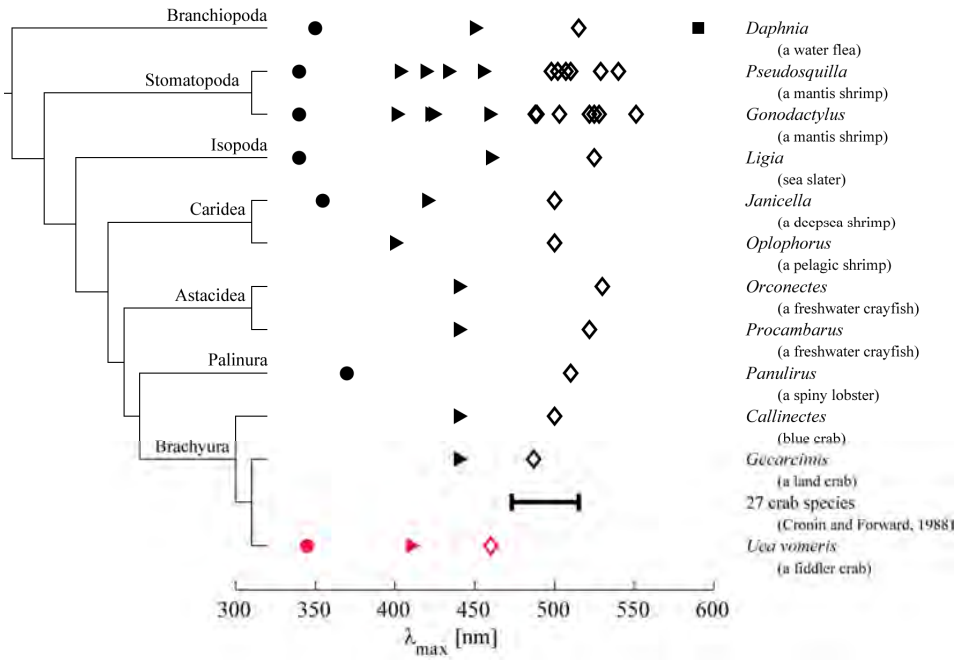

Figure III.13: Visual pigments in crustaceans (modified from Chittka, 1996). A long-wavelength sensitive (diamonds) and a short-wavelength sensitive (triangles) pigment have been identified in many crustaceans (data from electrophysiology and MSP). Note the extreme diversity of spectral sensitivities created by optical filters in stomatopods. Several groups have an additional UV pigment (circles). The maximum wavelength of the long-wavelength sensitive pigment has been measured in 27 crab species using MSP in isolated rhabdoms (Cronin and Forward, 1988). For comparison, the fiddler crab pigments proposed in this study have been added to the diagram (red symbols).

The first important signal I examined concerns the colours of the males' enlarged claws (Figure III.14A). While the dactyl (the upper 'finger' of the claw) appears light pink and has a relatively flat reflectance with a large amount of reflected UV, the pollex (the lower part of the claw) is bright orange and has no UV component (Zeil and Hofmann, 2001). The main contrast within the claw is therefore in the UV and blue and the fiddler crab colour vision system is exquisitely tuned to pick it up (Figure III.14A, pink crosses and orange plusses) and to distinguish it from the mudflat background (brown stars) and most mangrove leaves lying on the ground (green triangles). This contrast between a UV-bright dactyl and a dark pollex could increase the visibility of the motion signal of the males' claw-waving display. The question remains, however, why the claws of *U. vomeris* are orange. This colouration makes them highly conspicuous on the mudflat for the human observer, and quite likely for birds, as well. For the colour vision system of the crabs, however, light above 550 nm (orange) would hardly excite any of the photoreceptors. If, as in *U. mjoebergi* (Detto et al., 2006; Detto, 2007), the claw colouration is a species marker in *U. vomeris*, a shorter wavelength would make claws more easily identifiable for the crabs. One possible explanation for this paradox is that *U.vomeris'* spectral sensitivities might be exceptional for fiddler crabs. I have described in chapter II how (with an extremely narrow acute streak and very high vertical sampling resolution that is tuned to short wavelengths) *U. vomeris* is exceptional in its sampling grid organisation. The tuning of the colour vision system might be targeted to the same task and cohabiting species might actually see longer wavelengths better. Retaining a long-wavelength claw could in this context interpreted as an inter-specific signal.

Figure III.14: Chromaticity diagram of claws and back patterns. Positions in fiddler crab colour space were calculated for the colours of different fiddler crab body parts from spectrograph reflectance measurements (shown in insets). Larger distance in colour space indicates better discriminability of colours. **(A)** The dactyl (pink crosses) and pollex (orange plusses) of male claws are clearly distinct from one another, from the mudflat background (brown stars) and from most mangrove leaves (green triangles). Some yellow leaves scattered on the ground closely resemble claw colours and frequently fool the (human) observer. **(B)** While the bright blue patterns on fiddler crab carapaces (blue dots) are distinct from the black background of the carapace (black circles) largely by their UV components (i.e. along a vertical axis in colour space) and by their intensity (not shown), there is considerable variation between different blue measurements. Whether this variation exists mainly between different parts of the carapace or different females remains unknown, but the two blue spectral sensitivities of the fiddler crab colour vision system seem well tuned to differentiate between these different shades of blue.

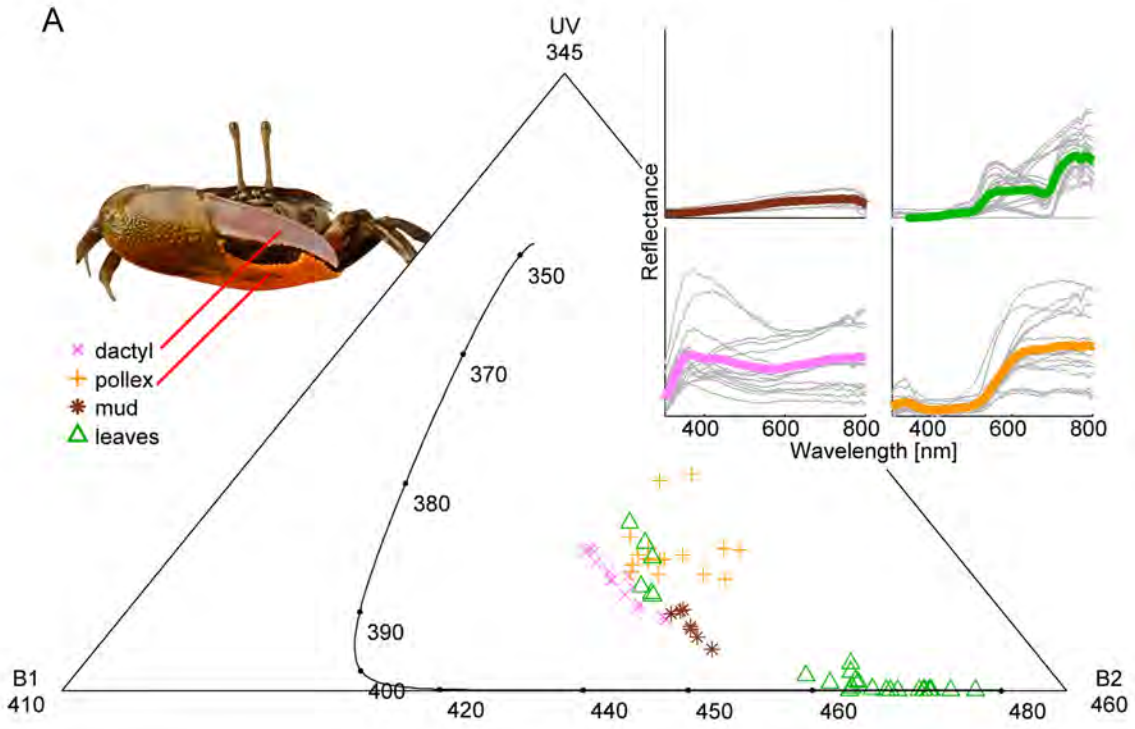
A
UV
345
dactyl
pollex
mud
leaves
350
370
380
390
400
B1
410
420
440
450
460
480
B2
460
Reflectance
400
600
800
Wavelength [nm]

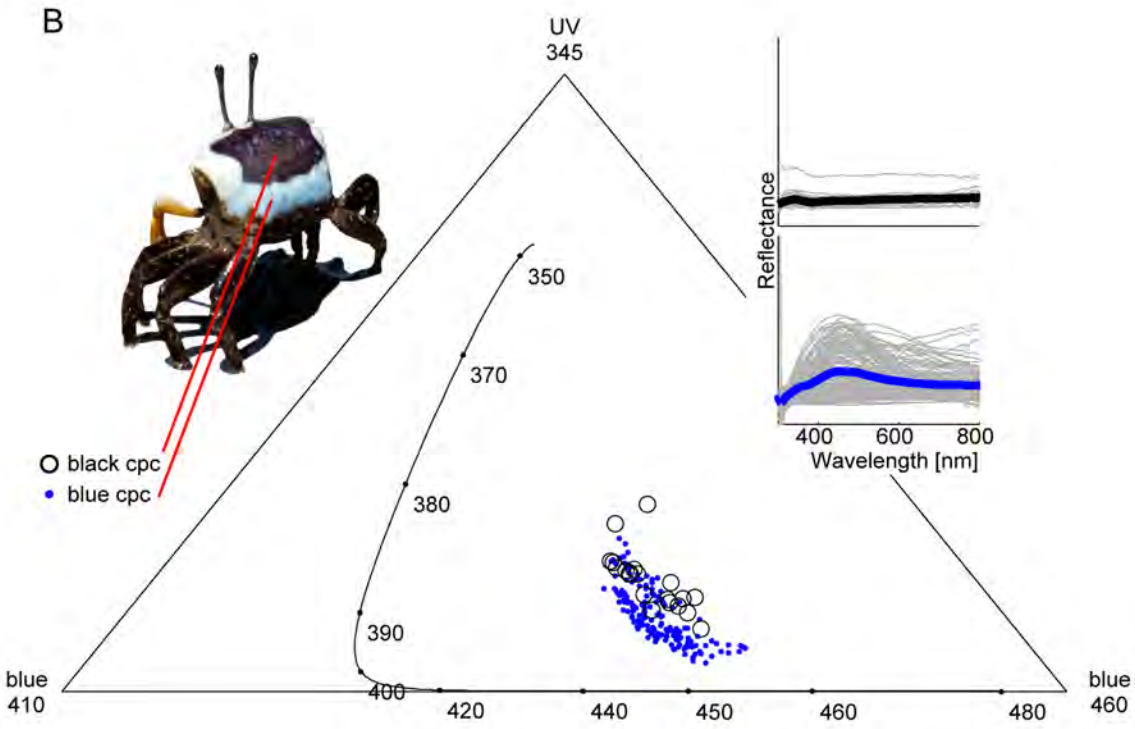
B
UV
345
black cpc
blue cpc
350
370
380
390
400
blue
410
420
440
450
460
480
blue
460
Reflectance
400
600
800
Wavelength [nm]

An alternative possibility is the existence of a physiological limitation. The pigments that crabs have available to create a large UV reflectance might be limited. Unfortunately, the chemistry of the cuticular pigment underlying the claw colours in these animals is yet unknown. Lastly, the long-wavelength tail of the blue receptors samples the region where the orange/red reflectance of the pollex begins. A possible function of the "array" of different blue receptors could therefore be to detect the exact point at which the pollex begins to reflect. To examine these hypotheses, further behavioural experiments will be necessary.

The second signal I considered is the blue/UV carapace pattern. While the blue (Figure III.14B, blue dots) is distinct from the black background of the carapace (Figure III.13B, black circles) mostly in intensity, not colour, there is a substantial variation in colour between different blue measurements. Apart from differences in the brightness of these colours, mainly due to a fading in response to increased predation level and stress (Hemmi et al., 2006), there is considerable variation between individual crabs. Whether, however, this variation could be an indicator of mate quality or mating status and is evaluated as such by the crabs, is unknown. In any case, the two blue spectral sensitivities of the fiddler crab visual system appear well tuned to differentiate between these different shades of blue. Additionally, as described in chapter II, the sampling grid in the frontal eye seems to be involved in the individual identification of conspecifics from these carapace patterns. The sampling grid organisation in this eye region relies on short-wavelength signals to be able to utilise the maximum resolution. The presence of two short-wavelength sensitive pigments could therefore be interpreted as an adaptation to facilitate fine spatial vision.

III.5.5 Polarisation sensitivity

I found highly polarisation sensitive photoreceptors with PS up to 5.4. While polarisation sensitivity can be inferred from the rhabdom anatomy (Alkaladi, 2008), and has been shown behaviourally in the dorsal visual field (Korte, 1965), it has not yet been demonstrated directly in the remaining field of view. The experimental

protocol developed here will allow us to analyse how colour, polarisation and intensity interact in the fiddler crab eye to efficiently extract relevant information from a bright, colourful and polarised world.

III.5.6 Future directions

To consolidate the spectral sensitivity data presented here, the recording setup and experimental protocol can be significantly improved. A large part of the noise in my final sensitivity curves is due to the exponential transformation through the *V/log(I)*-function. To reduce this effect, the *V/log(I)*-function can either be measured with higher accuracy, or a new experimental protocol can be adapted that does not require a *V/log(I)* transformation, e.g. by comparing each wavelength individually against a central wavelength or white light. To establish the validity of my UV/blue/blue model, it will have to conclusively shown that additional green receptor is absent and/or that this green receptor undergoes a spectral shift through the filtering by rhabdomeral screening pigment. The two most important steps here are to perform ERG measurements on *U. vomeris* and to identify individual photoreceptors. This identification can be achieved by measuring the polarisastion sensitivity of cells. Based on anatomical data (Alkaladi, 2008), R1,2,5,6 are most sensitive to vertically polarised, R3,4,7 to vertically polarised light and R8 is polarisation insensitive. Another option to identify individual cells is to inject fluorescent dyes intracellularly and subsequently examine histological sections. Finally, it is likely that spectral and polarisation sensitivities are different in the dorsal and ventral eye. To examine this, both recordings and cell identification in these eye regions have to be performed.

In the medium-term this preparation will also enable us to record from optical neuropils, especially the motion-pathway, to examine the neural basis of fiddler crab predator avoidance responses. While these responses are well-studied in the field (Land and Layne, 1995a; Hemmi, 2005a; Hemmi, 2005b, chapter IV), the neural mechanisms that trigger different stages of the escape response have yet to be identified.

III.5.7 Conclusions

The photoreceptor basis of colour vision in *U. vomeris* involves a **UV** receptor (λ_{max} 345 nm) and a variety of short-wavelength sensitive receptors that most likely co-express two pigments (**B1** with λ_{max} 410 nm and **B2** with λ_{max} 460 nm) in different ratios. There was no evidence for a long-wavelength (green) receptor. The B2 sensitivity might originate (through mutation or filtering) from the long-wavelength sensitive gene in other crabs. Shifting the spectral sensitivity towards shorter wavelengths increases spectral and spatial resolution in the blue to facilitate individual recognition by carapace patterns. The new electrophysiological preparation allowed me to demonstrate the polarisation sensitivity of photoreceptors and to record light responses from interneurons in the optical neuropils. This new possibility of recordings from the fiddler crab optic pathway will allow us to uncover the neural mechanisms underlying the complex behaviour of fiddler crabs.

Chapter IV

Natural visual cues eliciting predator avoidance in fiddler crabs

IV.1 Summary

To a wide range of animals, vision provides crucial information for navigation, feeding, social communication and predator avoidance. The type of information animals need to extract to make behavioural choices depends strongly on the task and the environment. The design of visual system can therefore be expected to reflect these ecological constraints. However, our knowledge about the signals that animals experience in their natural environments is extremely limited. Especially in a predator defence context, it has so far been impossible to measure, in a natural situation, the stream of sensory signals and their value for risk assessment, together with the defensive behaviour of the prey animals. The transparent miniature society of fiddler crabs, combined with our extensive knowledge of their visual system and their predator avoidance behaviour, present a unique opportunity to study this link between natural stimuli and the organisation of behaviour. In a first attempt to characterise the visual signals presented by potential predators, I used a synchronized four-camera setup to monitor bird approaches towards an *Uca vomeris* colony while at the same time recording the crabs' escape behaviour. The distinct flight paths of different types of threatening (terns) and non-threatening (e.g. kites and dragonflies) aerial predators were analysed and the visual cues (e.g. retinal elevation, speed and contrast changes) available to the crabs during their escape response were quantified. The critical visual cues predicting a response under natural conditions were compared to those used by the crabs in response to standard dummy predators. The decision criterion combines multiple visual cues – including retinal speed, elevation and visual flicker – and reflects the statistical properties of the different natural signals they experience. The results demonstrate that to understand the structure of visual behaviour we need to understand the visual signals that guide these behaviours under natural circumstances.

IV.2 Introduction

Brains and sensory systems are not general information processing devices, but have evolved to solve particular tasks which are relevant to an animal in its natural environment. The information processing in these systems and the behaviours which they guide thus need to be understood in the context of behaviourally relevant stimuli that an animal might encounter in its natural habitat. In recent years, several studies have examined the neuronal responses of animals in the laboratory when confronted with natural visual scenes (e.g. Baddeley et al., 1997; David et al., 2004; Boeddeker et al., 2005; Kern et al., 2005; van Hateren et al., 2005; Brinkworth et al., 2008). These studies found that properties of neurons often differed dramatically from those elicited by traditional visual stimuli. Similarly, neuron firing rates in dragonflies change radically when recorded outdoors, where light levels and temperature reflect the animals' natural operating conditions (Olberg and Worthington, 2008). These neurophysiological findings have caused a renewed interest in the use of natural and ecologically relevant stimuli for physiological experiments and at the same time highlighted how severely limited our knowledge is about visual signals, their behavioural relevance and their processing under natural circumstances. This is largely due to the fact that it is extremely difficult to reconstruct the natural flow of information in freely behaving animals. For visual information, this requires a detailed knowledge of the animal's visual system, the ability to follow its gaze during natural behaviour, an understanding of the tasks the animal has to solve and finally an experimental setup that makes it possible to record and tightly synchronise the relevant visual signals and the animal's behaviour under natural conditions.

IV.2.1 Predator avoidance in fiddler crabs

As I have outlined in chapter II, fiddler crabs and in particular their predator avoidance response provide an ideal example for such a simultaneous study of visual cues and visually elicited behaviours. The crabs are an important food source for a large number of avian predators that hunt with a wide variety of techniques (Zwarts,

1985; Ens et al., 1993; Iribarne and Martinez, 1999; Land, 1999) and respond to these predators using exclusively visual cues (Hemmi, 2005a, b). In a natural situation, crabs are often forced to take shelter from a passing bird every two or three minutes, which leads to high selective pressure for effective and efficient anti-predator strategies. The crabs' burrow-centred lifestyle in dense colonies makes it possible to record the complete behavioural repertoire of many crabs over extended periods of time with just a single stationary video camera. Our detailed knowledge of the crabs' visual system (Land and Layne, 1995a; Zeil and Al-Mutairi, 1996; Zeil and Hemmi, 2006, chapters II and III), combined with the fact that the crabs do not make any directed eye movements, allows us to quantify the exact visual information that every individual crab has available at any point in time.

Due to the relatively poor resolving power of their eyes, the information that the crabs have available at the time they need to escape from a predator, is extremely limited (Hemmi and Zeil, 2005). Furthermore, their closely-set eyes prevent them from using binocular stereopsis to gain distance information at the distances relevant in predator avoidance (e.g. Collett and Harkness, 1982, Figure II.10B). This gives us the opportunity to examine their anti-predator behaviour using simple dummies (often little plastic balls a few centimetres in diameter) that the crabs cannot distinguish from real predators. Most of our current knowledge about the visual cues guiding crab escape responses is based on their responses to such dummies (Nalbach, 1990; Land and Layne, 1995a; Hemmi, 2005a, b). When approached by a predator – dummy or real – fiddler crabs initiate a multi-staged escape response (Hemmi and Zeil, 2005). Firstly, on detection of the potential threat, they cease any activity and remain still (freeze) while assessing the risk. They then initiate a sudden and fast home run towards their burrow, where they usually remain for a while before finally descending into the burrow. The crabs can interrupt this response cascade at any time to limit the costs of a potential false alarm.

With the incomplete information fiddler crabs have available, they have to solve the challenging task of limiting their responses to the most dangerous stimuli in their environment and avoiding false alarms. Given the fundamentally limited

information, there is no perfect solution and we would therefore expect the criteria that the crabs use to reflect the statistical properties of the different potential signals the crabs face in their environment. In the absence of distance information, other crab species have been shown (under varying experimental conditions) to use different criteria to trigger their home runs. While looming seems to play a role for directly approaching objects and in the laboratory (e.g. Nalbach, 1990; Land and Layne, 1995a; Oliva et al., 2007), the fiddler crab *Uca vomeris* has been shown in extensive dummy predator studies to rely on a decision criterion related to retinal speed (Hemmi, 2005a, b). This was indicated by the fact that the distribution of retinal speeds at the time of response is constant even if the translational speed of the approaching dummy almost triples. However, while retinal speed as a criterion provides a very sensitive early warning system, it is not strictly related to real risk. The retinal speed of a directly approaching object is smaller than that of an object that passes the observer at a certain distance. As has been shown in field experiments, this results in later responses to predators that approach more directly and potentially results in time-consuming false alarms to objects that simply pass by. Other factors that influence the escape response in artificial predation experiments (Hemmi, 2005a, b) are retinal size, elevation, and the direction of motion (crabs are far more responsive to vertical than to horizontal motion). These cues might help alleviate these costs, if they better reflect the signal differences between dangerous and harmless events under natural circumstances.

IV.2.2 Natural visual cues

Despite the information we have on the visual cues that trigger predator avoidance in fiddler crabs, we do not know to what extent they represent the signals normally encountered by crabs when confronted with natural predators. The visual signature of a flying bird in front of a dynamic mangrove background can certainly be very different from that of one of the bird dummies used in recent studies – a small black Styrofoam ball approaching in a straight line. Although the crabs react to these dummies in a way that appears virtually indistinguishable from their responses to real

birds, the visual signatures of different birds could contain additional cues about risk or predator identity that are impossible to identify in a dummy experiment. A real bird flying across the mudflat constantly changes shape (through the beating of its wings), direction, speed and contrast, and all these changes differ depending on the style of the predator's flight manoeuvres. The main natural predators at many beaches in north-eastern Australia, for instance, are gull-billed terns (*Gelochelidon nilotica*, Land, 1999). These relatively small birds regularly scan the mudflats, flying into the wind a few meters above ground at a speed of about 3 m/s. Whenever a tern spots a crab without refuge, it extends its wings to brake in midair, often even flying backwards a metre or two, and then dives down in an attempt to catch the prey (Land, 1999, Figure IV.1). When reaching the end of their path, the birds turn around and fly back down-wind at high speed.

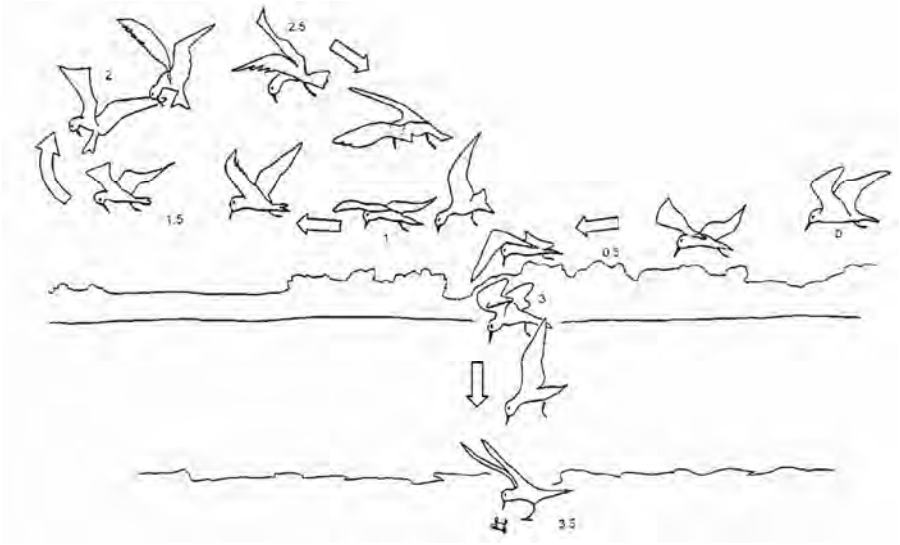

Figure IV.1: The hunting strategy of the gull-billed tern (*Gelochelidon nilotica*). Drawings of a successful attack on a crab. Numbers show times in seconds. The tern began to follow the crab at about 0.5 s, then resumed search between 1 and 1.5 s before returning its gaze to the crab, braking, flying backwards and diving, to land at 3.5 s (from Land, 1999).

Not all birds in the sky, however, are predators. While keeping watch for the subtle, fast and often unreliable signals that indicate an approaching tern, fiddler crabs

should also attempt to monitor, identify, and disregard the signals of a large number of other, harmless flying objects, whether these are distant or departing terns, large birds like kites and eagles that do not hunt fiddler crabs, close-by small insects like migrating butterflies and dragonflies or even mangrove leaves carried past by the wind. To keep the number of false alarms as low as possible, the crabs should employ escape strategies that ensure robust responses to real predators while minimising responses to harmless events.

The aim of this study is to characterise the natural visual signal distribution of real events as they are experienced by crabs in their normal habitat, examine the differences between different classes of birds and illuminate how these signals relate to the behavioural decisions of fiddler crabs under threat. To achieve this, I have used four synchronised cameras to record approaching predators as well as other birds from the view-point of fiddler crabs in the field, while at the same time monitoring the crabs' behaviour and their responses to these events. I extracted elevation, retinal speed and changes in contrast from the videos and explored their effect on the crabs' escape decisions.

IV.3 Materials and methods

IV.3.1 Animals, apparatus and synchronisation

Experiments were conducted with *Uca vomeris* (McNeill) (Ocypodidae: Brachyura: Decapoda) on the intertidal mudflats near Cungulla (19°24'S, 147°6'E), south of Townsville, Queensland, Australia. Four camcorders (Panasonic NV-GS300) were mounted on two vertical steel poles that were placed 192 cm apart on the mudflat (Figure IV.2). The two upper cameras (**crab cameras**) were mounted at a height of 160 cm above ground level and arranged such that they recorded the activity of crabs on two adjacent patches of mudflat, each 1 m^2 in size. The lower cameras (**bird cameras**) were fitted with wide-angle lenses (Raynox Pro semi fish-eye conversion lens 0.3x), mounted with the centre of their lens as close to the ground as possible (13

cm above ground level) and tilted upwards at an angle of approximately 30° to monitor bird approaches from crab-perspective in a visual field of about 50° by 80°.

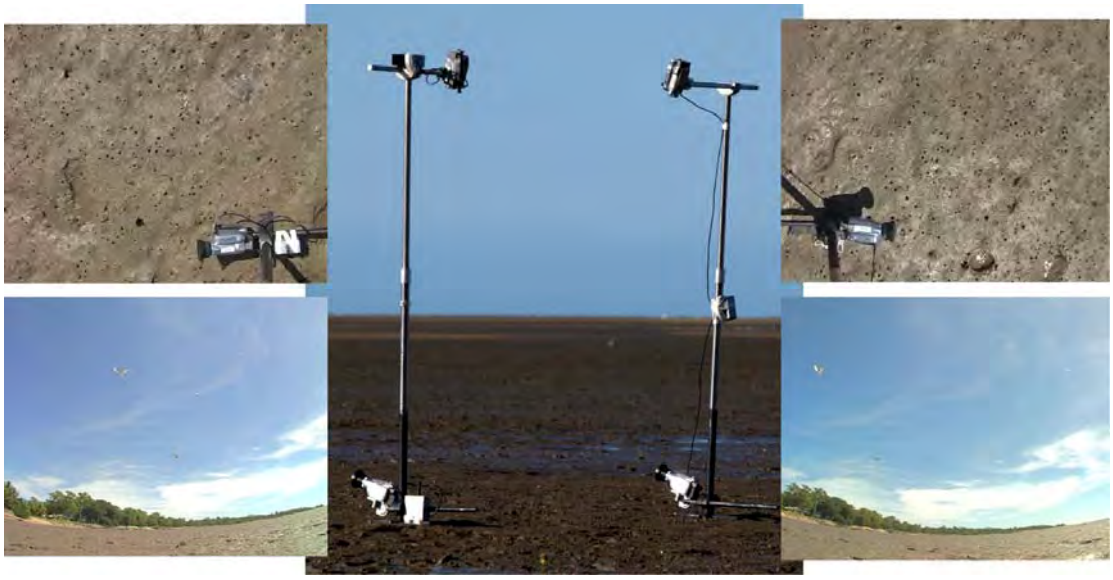

Figure IV.2: The synchronised four-camera setup. The two lower cameras were fitted with fish-eye lenses to observe a field of view of approximately 50° by 80° each. The top cameras pointed down to observe crab behaviour on the mudflat. Sample images are shown next to each camera

Both bird cameras were directed northwards along the beach, into the direction from which most terns approached. Through a central custom-made controller box, all four cameras received a common audio signal. This signal consisted of four tones that alternated in a pre-programmed, pseudo-random sequence which later allowed me to timestamp individual frames recorded by the four cameras to within one millisecond. Activity of birds and crabs were recorded for up to 90 minutes in each session. During this time the setup was observed from at least 10 m away and all bird movements were noted down to ensure that in the subsequent analysis crab reactions to birds outside the cameras' field of view were not mistaken for responses to birds recorded by the cameras.

IV.3.2 Video analysis

The analysis of **crab responses** followed the procedures developed by Hemmi (2005a, b). Film sequences were digitised at 200 ms intervals and cameras were

calibrated for optical and perspective distortions. Crab positions were then tracked using a video analysis program written in C and MATLAB (Jan Hemmi, The Australian National University, see Hemmi and Zeil, 2003a). A home-run response was considered to have started in a given frame when a crab had moved at least 0.66 cm towards its burrow since the previous frame and at least 2 cm during the three-frame interval (600 ms) starting with that frame. For the analysis of timing the positions of both crab and bird in the last frame (200 ms) before the response-criterion was reached were defined as their positions at the time of response.

For the analysis of **bird movements** the above procedure was slightly changed. Videos were digitised at half-frame precision (every 20 ms). The position of all approaching flying animals was then tracked through all frames and their angular elevation and speed were determined. **Elevation**, **horizontal and vertical angular speed** were calculated from the digitised paths. No attempt was made in the calculation of elevation to correct for the difference in height between the crab eyes (about 2-3 cm) and the cameras (13 cm). Even for a close bird at 10 metres distance, this results in a maximum error of 0.75° in elevation. For closer animals, like flies and dragonflies, the error might be significantly larger. However, the geometry of these close approaches means that crabs are likely to see these insects from a completely different vantage point and the information we can deduce, especially about retinal elevation, is limited in such cases.

To define the signal that a single ommatidium pointing at the predator might receive, I calculated average pixel differences in a window of 3x3 pixels around the bird's position. This window size is equivalent to about 0.6°x0.6° apparent size from a crab perspective and is thus smaller than the smallest acceptance angles of fiddler crab eyes (chapter II). However, the crabs' contrast sensitivity and dynamic range are likely to be far superior to those of the video cameras used in this study. For the analysis of response criteria I calculated the **temporal contrast change** at any given time as the maximum change in this signal (average pixel difference) at the bird's current position during the preceding 200 ms. The bird's speed, contrast and change in contrast (produced mainly by its wing beats and orientation relative to the sun), are

the most important characteristics that determine the level of this contrast change value.

IV.3.3 Selection of trials

In the natural setting, the times of bird activity and the directions of their flight paths are difficult to predict. I only analysed those 'predator' approaches that were completely recorded on the bird cameras and discarded all approaches that coincided with the movement of a bird outside the field of view of the cameras. Similarly, when two simultaneous approaches could be observed within the field of view of the camera, I discarded both unless one approach was clearly far more salient (as judged by apparent size, speed and contrast) than all simultaneous events. I recorded a total of 17 experimental sessions and finally analysed the session with the highest number of valid approaches. In this session, I included a total of 37 sequences during which one or more birds were visible. In these 37 sequences I recorded the activity of a total of 62 events (14 terns, 20 kites, 20 insects and 8 others, incl. eagles, crows, herons and gulls) and the responses of 10 crabs. In their natural environment, crabs do not only react to birds, but also to one another and to other events outside of my control. To reduce such responses to a minimum, the following criteria were used to allow sequences to be included in the final analysis: (1) there was no crab-crab interaction; (2) crabs were at least 5 cm away from their burrow; (3) the crabs had to be within the recording area at the start of their response. A total of 127 home runs and 14 underground responses met these criteria and were included in the final analysis.

IV.3.4 Statistical analysis

The individual decisions (home run/no home run) of 10 crabs were evaluated for all 200 ms time intervals fulfilling the above criteria. A total of 14618 such frames, (including the 128 responses and 14490 non-responses) were evaluated in a generalised linear mixed model in R (2.9; using the *glmer* function of the *lme4* package). I took into account the individual variance between crabs (crab identity) and between individual birds (bird identity) by treating them as random factors. The

GLMM used the *logit* as a link function. The final model was selected by sequentially fitting parameters of interest and including only those parameters that reached significance at a 5% level when added to the final model.

IV.4 Results

The level of predation as well as the presence of other flying objects during the experiment was high. In the 80 minutes examined, the sum of all bird recording times was 12.4 minutes. This includes all frames where a valid bird was visible in at least one of the two cameras. Considering that my cameras covered about 90° of azimuth, and taking into account that bird presence might vary in different viewing directions, the total for the whole visual field could be three or four times as high. The fact that the crabs are thus exposed to a bird somewhere in their visual field about 50% of the time only stresses the importance of an effective strategy to distinguish harmless from dangerous events. The crabs appear to be able to do this to some degree. Although terns only contributed 25% to this observation time, they elicited 37% of the responses. Surprisingly, the crabs observed in this study only descended into their respective burrows following 14 out of the 128 home runs. The following analysis therefore deals only with the second stage of the escape response, the home run.

Table IV.1: Recording times and elicited responses. Times are the sum of all times at which the animal was recorded in at least one of the observation cameras. Note that although terns only make up 25% of all observation time, they elicited 37% of all responses.

Type (no.)	Time observed	% of total	Home runs	% of total	Burrow descents
Terns (14)	3min 8s	25.3%	48	37.5%	6
Kites (20)	7min 1s	56.5%	57	44.5%	6
Insects (20)	43s	5.7%	11	8.5%	0
Migrants (8)	1min 32s	12.4%	12	9.4%	2
	12min 25s		128		14

IV.4.1 Description of and responses to different signals categories

Traditional experimental stimuli in the context of predator avoidance are usually designed in a way that makes them progressively more threatening. A dummy predator, for instance, would be moved towards a colony of crabs until all crabs disappear down their burrow (e.g. Hemmi, 2005a, b). The experimenter can then evaluate the average or cumulative response distance, speed, elevation or any other relevant parameter. A very useful tool in the case of these monotonous parameters is provided by survival curves that display the number of animals that have not responded to a stimulus at a particular time or distance (see Chapter V). For a more threatening stimulus, the curves will be shifted towards earlier times and longer distances.

The parameters of natural bird approaches, on the other hand, are not monotonous. The three parameters I examine here in detail – elevation, retinal speed and change in contrast – usually rise and fall multiple times during each approach. A cumulative analysis like survival curves or a linear model including the maximum 'threat' experienced so far does therefore not hold much merit. To stay as close as possible to the cues which are available and relevant to the crabs on a moment-by-moment basis, I have analysed the probability of response as a function of the maximum elevation, retinal speed and change of contrast experienced in the previous 200 ms[10]. This time window is in agreement with behaviourally and physiologically determined response latencies in the crab *Chasmagnathus* (Oliva et al., 2007) and was used in all dummy studies involving fiddler crabs (Hemmi, 2005a, b; chapter V).

In the following I will describe the differences in visual signals between the four classes of approaches (terns, kites, insects, and migrants) and the crabs' responses. The visual signal will be described in example approach traces (see Appendix F for five additional examples) and histograms displaying the *probability of observation* of the three analysed parameters. This probability is based on the number of crabs that observed a certain parameter value. Observation was assumed

[10] Note that this latency is calculated not from the *response* frame (where movement towards the burrow is first observed, see Methods), but from the *decision* frame (one frame / 200 ms before the response).

whenever a crab was out of and more than 5 cm away from its burrow (to ensure that a home-run could be measured). The crabs' responses will initially be described by their *probability of response*, which is the percentage of crabs that initiated a home-run in the given frame[11]. Based purely on example paths, it is very difficult to interpret response criteria, because parameters are strongly correlated. High speed of a dark bird against a bright background, for example, results in large contrast changes. Similarly, a bird flying at a constant height and speed can either produce high horizontal retinal speeds (when flying past the observer) or high vertical retinal speeds (when flying towards the observer), but not both at the same time. In the latter case, larger speeds are also correlated with higher elevations. As will become clear when considering the following examples, common behaviours like the swooping of terns can also be accompanied by distinct sets of correlated parameters. To tackle the problem of correlated parameters, I will evaluate the crabs' responses in a statistical model. Colours in all following diagrams depend on the approach class: Blue for terns, red for kites, green for insects and orange for migrants. Crab responses are shown as magenta circles for home-runs and crosses for burrow entries.

IV.4.2 Terns

Terns usually fly across the mudflat in low, relatively flat trajectories (e.g. Land, 1999). A typical approach path is shown in Figure IV.3A. The tern (blue line) entered the camera field of view from the right (blue square). It continued to the left at medium speed (blue dots every 200 ms), then swooped down in an attempt to catch a crab far away from the recording site. The swoop was accompanied by a large number of responses, including six home runs within the recording area (the saturation of the blue trace indicates the percentage of crabs away from the burrow. In subsequent panels this number is indicated by the black line). The tern stayed at approximately constant height through most of the sequence and its elevation never exceeded 15° (Figure IV.3B). During the swoop its elevation decreased rapidly to almost 0°.

[11] By this definition, the probability of response to, e.g., a certain speed is independent of the actual distribution of speeds. That is to say, it is the probability of a response given that the speed is observed.

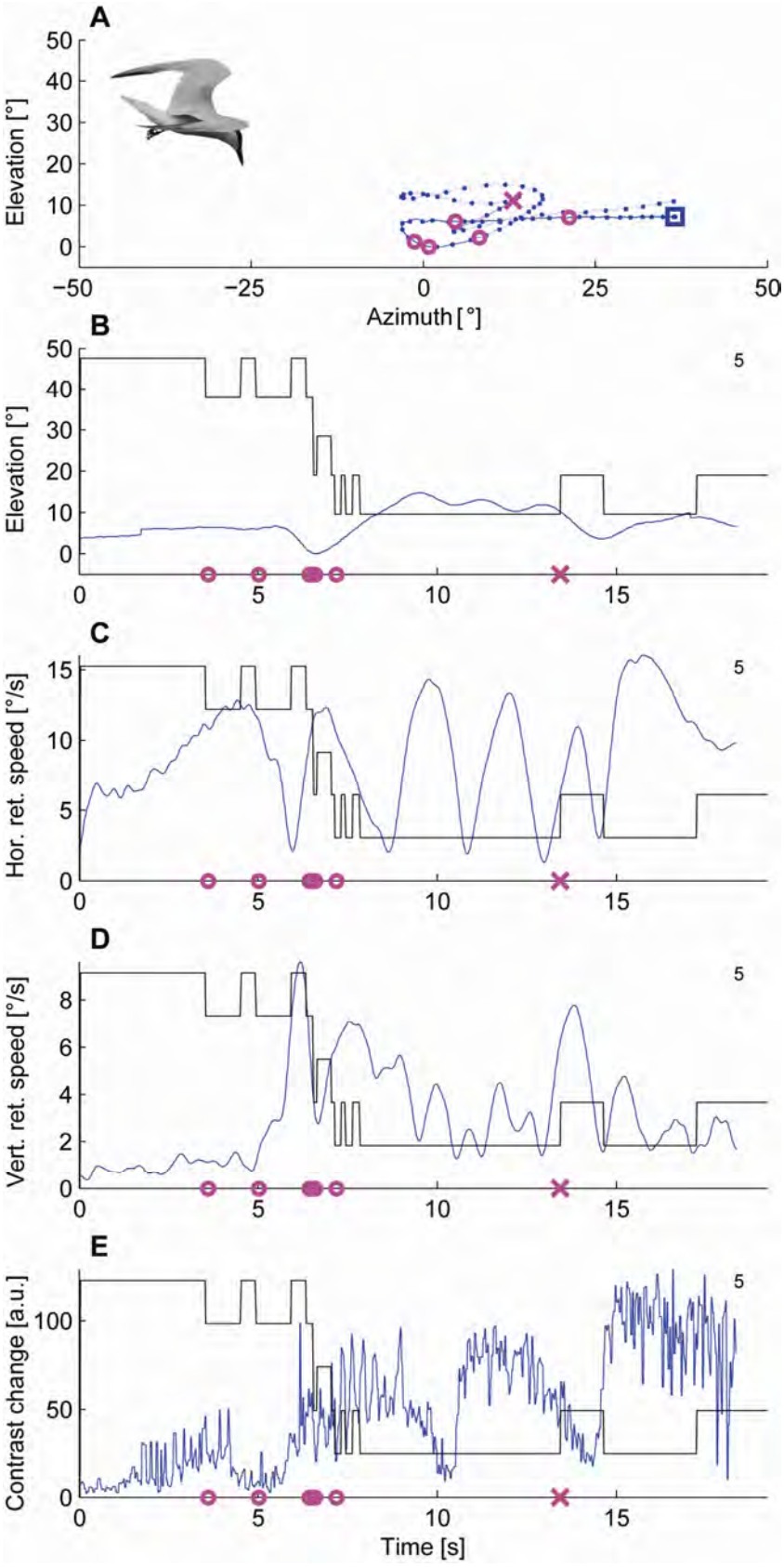

Figure IV.3: Example trace of a tern approach. **(A)** The flight path of the tern during the recording, dots indicate position every 200 ms. High saturation of the trace codes a large relative number of crabs active on the surface (>5 cm away from their burrow). Elevation **(B)**, horizontal retinal speed **(C)**, vertical retinal speed **(D)** and contrast changes **(E)** are displayed over time. The grey line in panels B-E indicates the number of active crabs at any time, the maximum of crabs during the experiment is given by the grey number on the right side of each panel. A magenta circle indicates a home run response of a crab, a magenta cross a burrow entry.

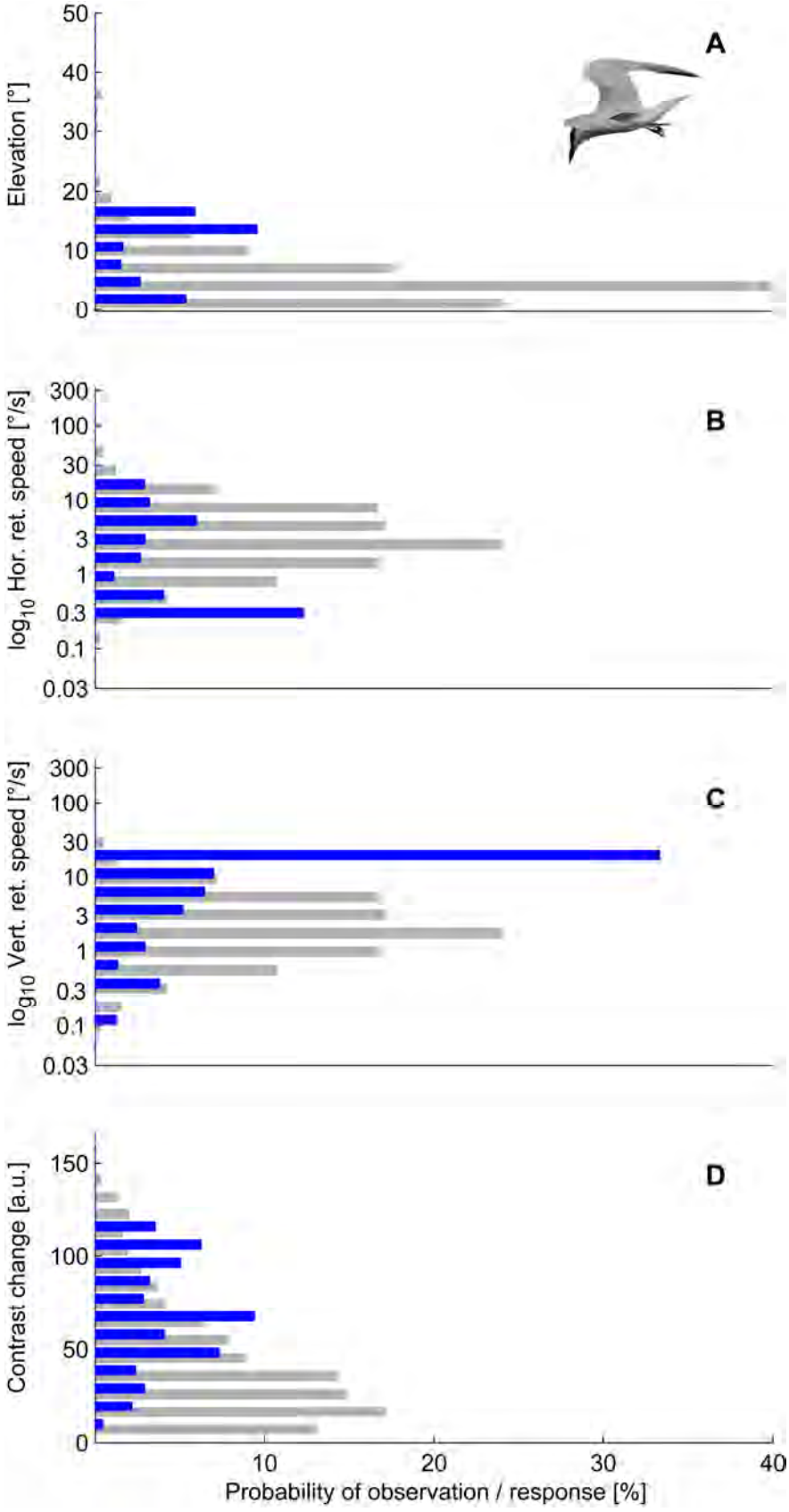

Figure IV.4: Statistics of tern approaches. Grey bars indicate the probability of observation, blue bars the probability of response upon observation (see text). Both probabilities are presented for elevation **(A)**, horizontal retinal speed **(B)**, vertical retinal speed **(C)**, and contrast change **(D)**.

While horizontal retinal speed (Figure IV.3C) changed frequently between about 2 °/s to 12 °/s as the tern changed direction, vertical retinal speed (Figure IV.3D) remained very low during the initial approach and only peaked at almost 10 °/s during the swoop. Note that the swoop is preceded by a sudden horizontal deceleration. The spreading of the wings during the swoop also causes a large change in contrast (Figure IV.3E). In conclusion, while horizontal retinal speed seems a poor predictor of responses in this approach, elevation, vertical retinal speed and contrast change provide large signals correlated with the tern's swoop.

Figure IV.4 summarises the approaches of the 14 terns observed in this study. The grey histogram illustrates the ***probability of observation*** of certain parameter values normalised to the number of crabs that observe the condition while being a potential home-runner by being more than 5 cm away from their burrow. In other words, for a crab that is away from its burrow while a bird is present somewhere, this is the probability to observe this particular condition. The total sum of all bars in this histogram therefore equals 100%. The blue bars, on the other hand, show the ***probability of response*** given that a certain condition has been observed. If there were no correlations between the four different parameters (and others that I did not observe) this measure would directly reflect the crabs' decision criteria. The blue bars therefore do not add up to 100%, but each individual one could theoretically reach 100%, if all crabs had always reacted to the parameter value when they observed it.

Crabs mainly see terns below 20° elevation and responses are most likely at the upper and lower end of this range, i.e. at around 15° and at the horizon (Figure IV.4A). Both horizontal and vertical retinal speeds of up to 30 °/s are common and higher vertical speeds are much more likely to be followed by a response (Figure IV.4B,C). Horizontal retinal speed, on the other hand, seems to be negatively correlated with response probability. Considering the example in Figure IV.3 suggests why this might be so. Low horizontal speeds occur during the swoops, when terns dive straight down towards their prey. The reason then, why crabs react to low horizontal speed, is probably that it is correlated with high vertical retinal speeds.

Contrast changes, finally, are usually small. Large changes, especially above 50 units, are more likely to evoke a response (Figure IV.4D).

IV.4.3 Kites

Kites are frequently seen soaring above the edges of the mudflats in search of food. Fiddler crabs, however, are not part of their diet and the crabs should therefore ideally ignore the kites. Figure IV.5 shows a typical example of a flight path of a soaring kite, showing several differences to the terns' flight behaviour. Firstly, flight path are quite straight, with few sharp turns. Retinal speeds are mostly below 5°/s (Figure IV.5B,C), and most of the time the kite is seen at elevations between 10° and 30° (Figure IV.5B). However, the brown plumage of a Brahmini kite against the blue sky and especially against white clouds provides a high contrast and contrast changes are almost as large as in parts of the tern's approach (Figure IV.5E). In this, and many other records of kite approaches it is difficult to identify the response criteria due to the high correlation of parameters. While some responses seem to be preceded by large changes in contrast and vertical retinal speed (e.g. a home run at second 21), others appear to be elicited by a change in horizontal speed combined with high contrast (e.g. several home runs around second 35).

Overall, the distribution of observed parameters and the probabilities of response are quite distinctly different from those observed in terns (Figure IV.6). Elevation is much more widely distributed throughout the visual field of the camera except for the visual horizon (Figure IV.6B). Retinal speeds are generally much lower than in tern approaches (mostly below about 5 °/s), and both components of retinal speed seem to be positively correlated with the probability of response (Figure IV.6C,D). Only contrast changes show a similar situation to that in terns (Figure IV.6E). They are mostly small (even more so than in terns), and large changes are much more likely to predict a response. Again, 50-60 units seem to be a cut-off.

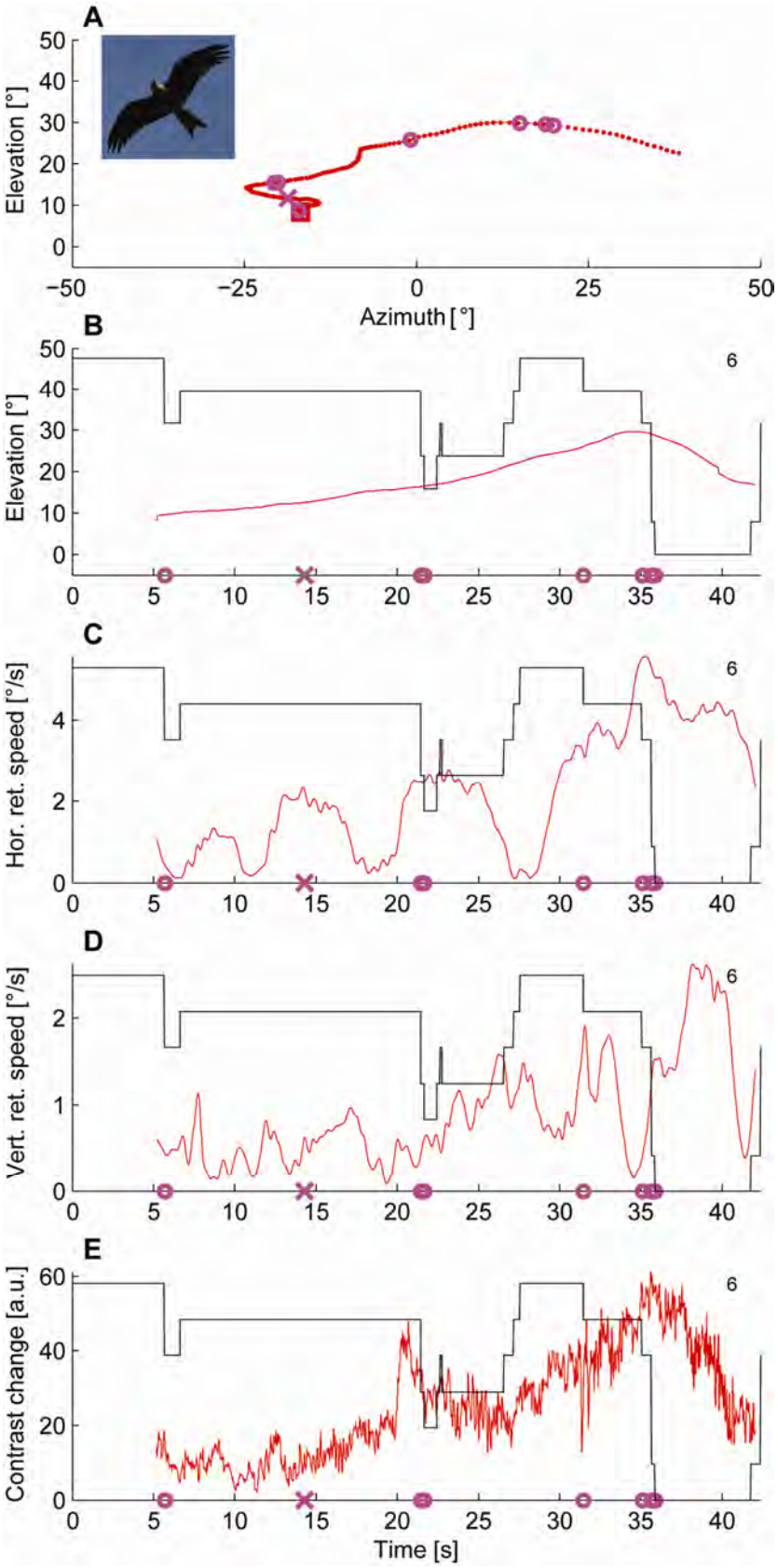

Figure IV.5: Example trace of a kite approach. (A) The flight path of the kite during the recording, dots indicate position every 200 ms. High saturation of the trace codes a large relative number of crabs active on the surface (>5 cm away from their burrow). Elevation **(B)**, horizontal retinal speed **(C)**, vertical retinal speed **(D)** and contrast changes **(E)** are displayed over time. The grey line in panels B-E indicates the number of active crabs at any time, the maximum of crabs during the experiment is given by the grey number on the right side of each panel. A magenta circle indicates a home run response of a crab, a magenta cross a burrow entry.

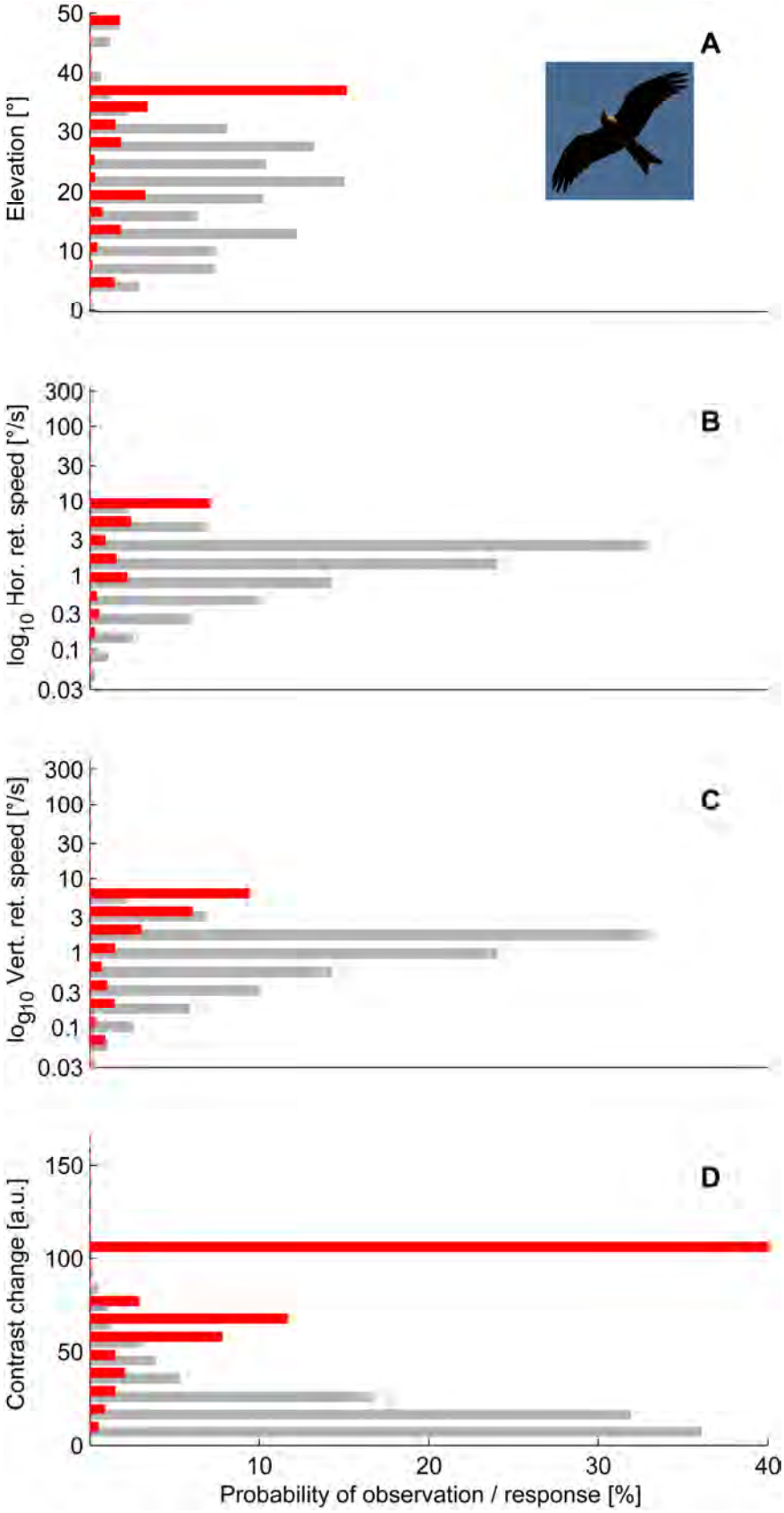

Figure IV.6: Statistics of kite approaches. Grey bars indicate the probability of observation, red bars the probability of response upon observation (see text). Both probabilities are presented for elevation **(A)**, horizontal retinal speed **(B)**, vertical retinal speed **(C)** and contrast change **(D)**.

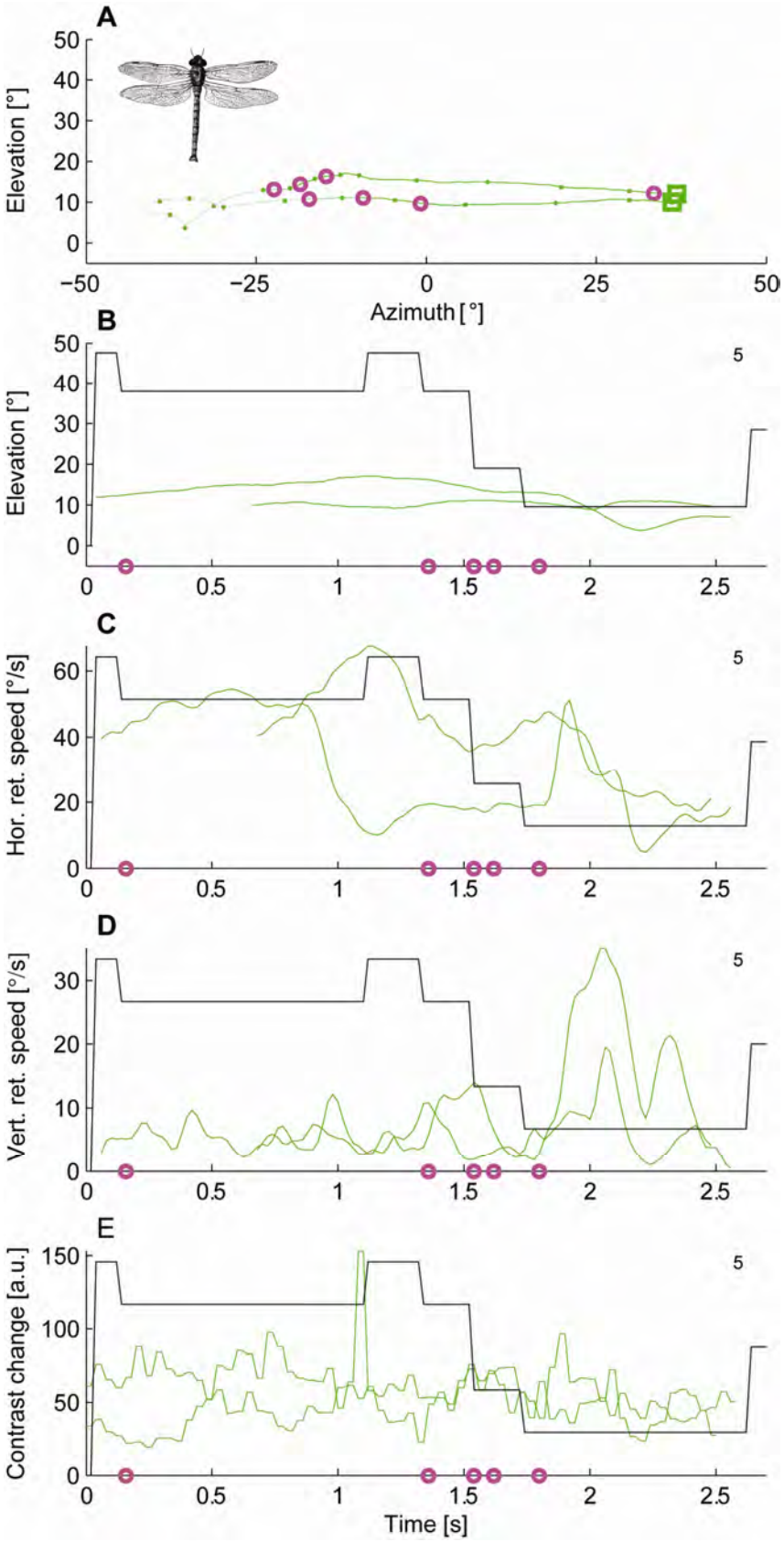

Figure IV.7: Example trace of a dragonfly approach. (A) The flight path of the dragonfly during the recording, dots indicate position every 200 ms. High saturation of the trace codes a large relative number of crabs active on the surface (>5 cm away from their burrow). Elevation **(B)**, horizontal retinal speed **(C)**, vertical retinal speed **(D)** and contrast changes **(E)** are displayed over time. The grey line in panels B-E indicates the number of active crabs at any time, the maximum of crabs during the experiment is given by the grey number on the right side of each panel. A magenta circle indicates a home run response of a crab, a magenta cross a burrow entry.

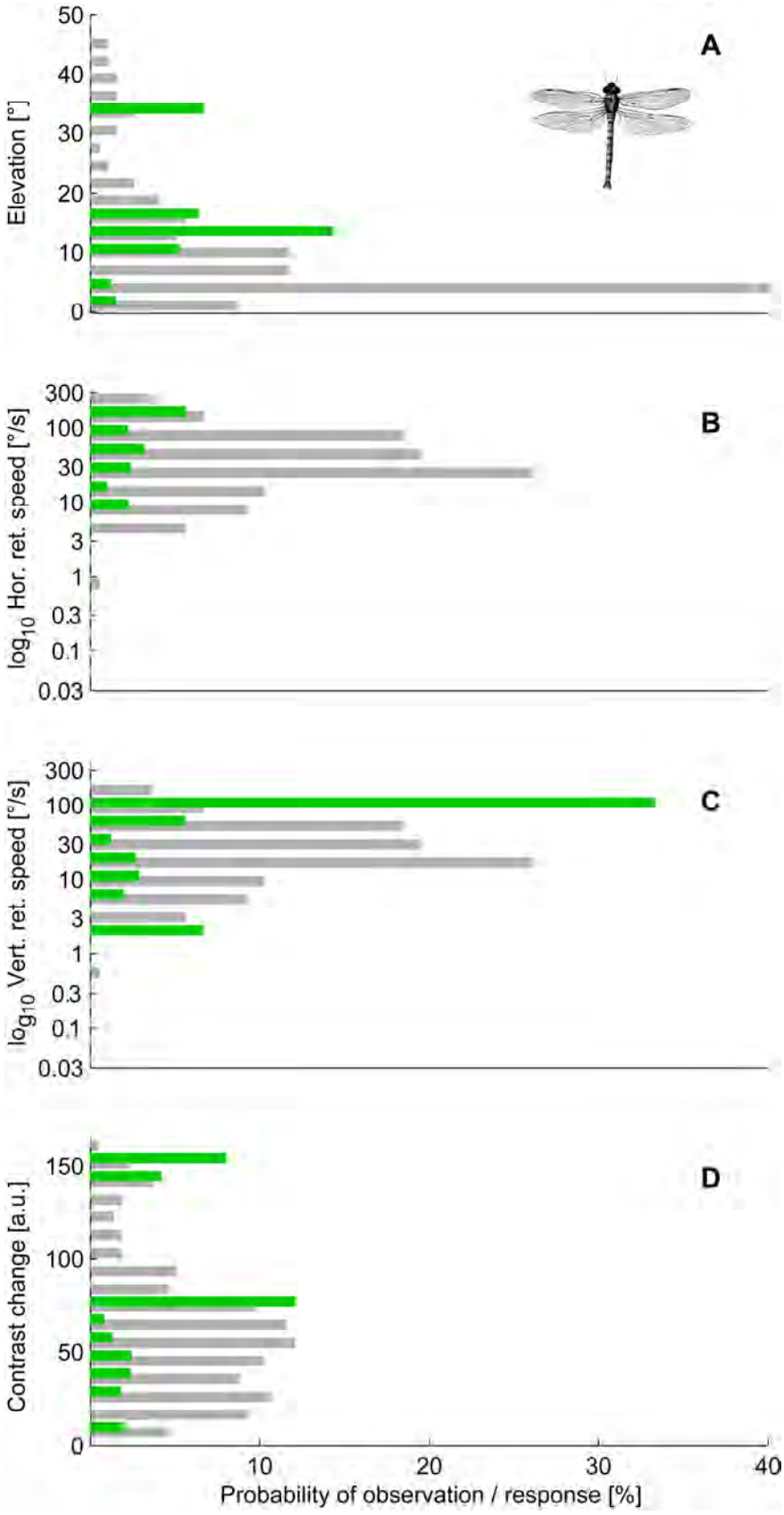

Figure IV.8: Statistics of dragonfly approaches. Grey bars indicate the probability of observation, green bars the probability of response upon observation (see text). Both probabilities are presented for elevation **(A)**, horizontal retinal speed **(B)**, vertical retinal speed **(C)** and contrast change **(D)**.

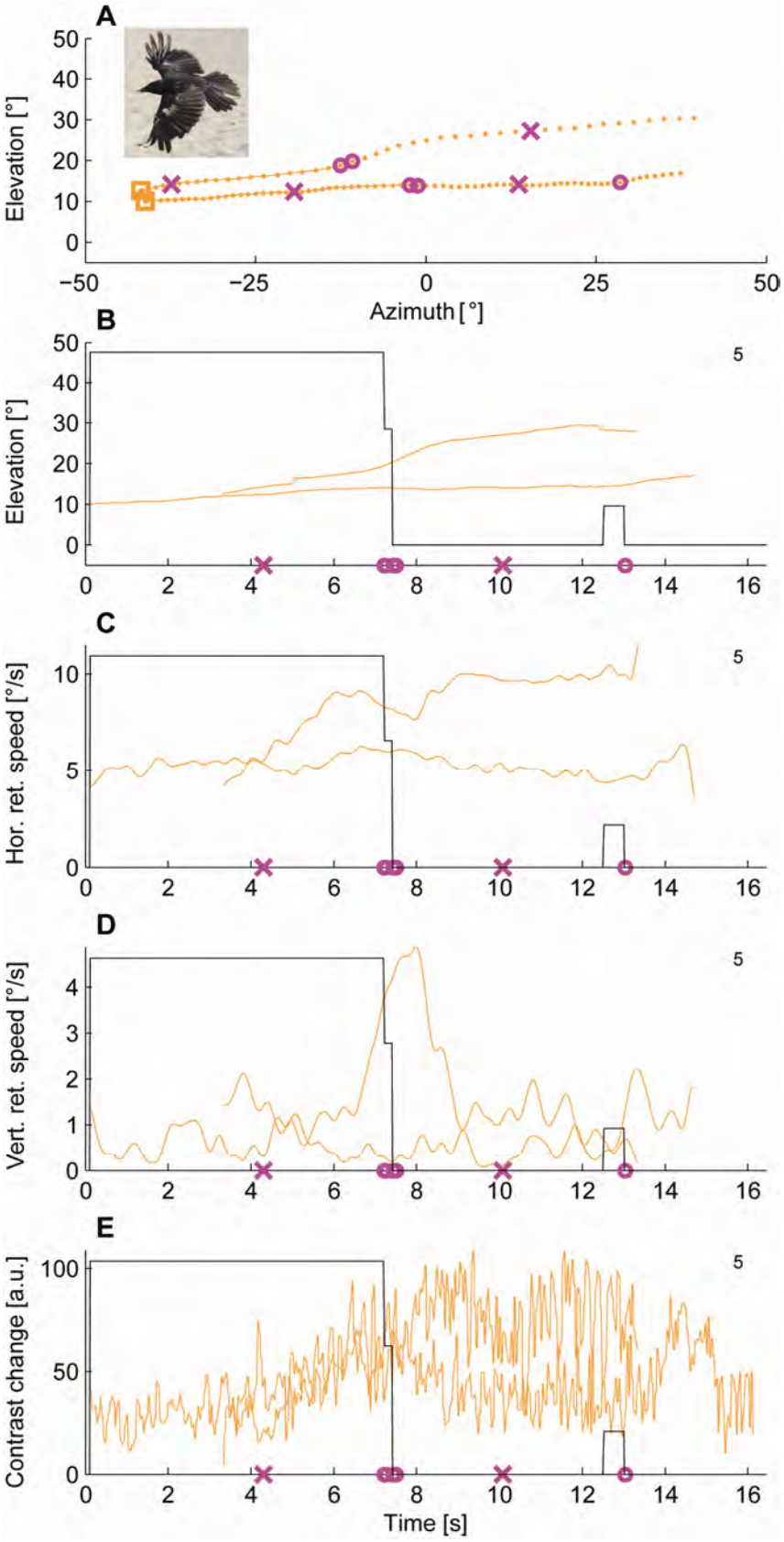

Figure IV.9: Example trace of a crow (migrant) approach. (A) The flight path of the two crows during the recording, dots indicate position every 200 ms. High saturation of the trace codes a large relative number of crabs active on the surface (>5 cm away from their burrow). Elevation **(B)**, horizontal retinal speed **(C)**, vertical retinal speed **(D)** and contrast changes **(E)** are displayed over time. The grey line in panels B-E indicates the number of active crabs at any time, the maximum of crabs during the experiment is given by the grey number on the right side of each panel. A magenta circle indicates a home run response of a crab, a magenta cross a burrow entry.

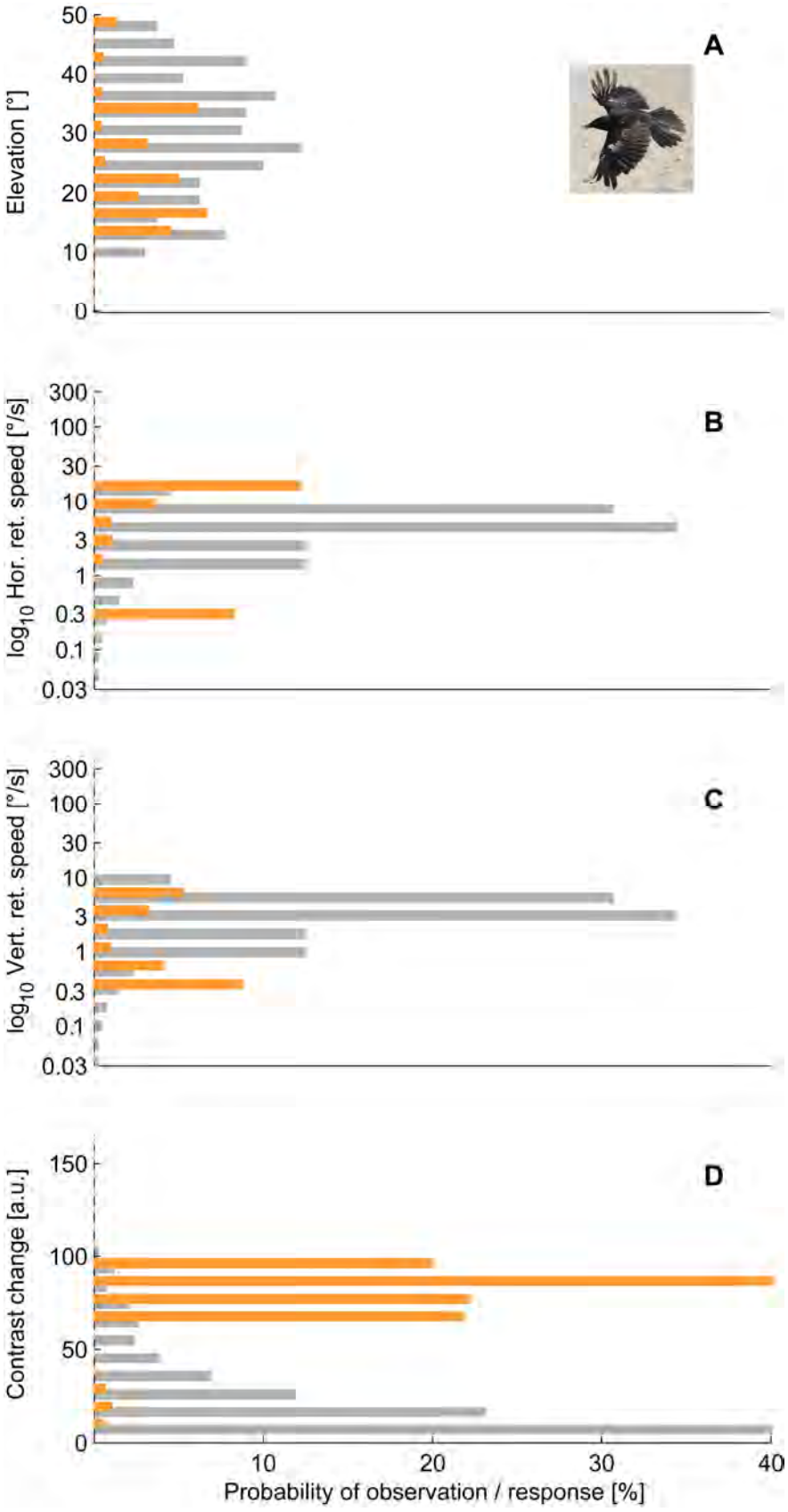

Figure IV.10: Statistics of migrant approaches. Grey bars indicate the probability of observation, orange bars the probability of response upon observation (see text). Both probabilities are presented for elevation **(A)**, horizontal retinal speed **(B)**, vertical retinal speed **(C)** and contrast change **(D)**.

IV.4.4 Dragonflies

Just as large, far-away birds like kites can fool the crabs, small close-by insects like flies and dragonflies often evoke a false alarm. An example flight path of two dragonflies chasing each other (Figure IV.7A) demonstrates the main properties of dragonfly paths as they are seen by crabs. Firstly, encounters are short. The dragonflies in this example passed the camera field of view within 2.5 seconds. The insects fly at a wide range of elevations (Figure IV.7B), retinal speeds are large (up to 60 °/s, Figure IV.7C,D) and contrast changes are very large (50-150 units, Figure IV.7E).

This pattern was common to all 20 recorded dragonfly approaches. In all approaches, elevations were widely distributed and the probability of a response to a certain elevation showed no apparent pattern (Figure IV.8A). Retinal speeds were extremely large (up to 300 °/s) and once again large speeds predicted crab responses (Figure IV.8B,C). Contrast changes were mostly small, although some very high values up to 150 units were observed (Figure IV.8D). Unfortunately, the geometry of the camera setup necessarily limits the scope of inferences that can be drawn from insect observations. Due to the close distance of the dragonflies when they are recorded by the camera or seen by the crabs, the cameras' view (although typical for *a* fiddler crab sitting just behind the camera) is likely different from the view that the *particular* crabs recorded by our camera had. While retinal speeds and contrast will still give an approximation of what the crabs might have experienced, the significance of elevation is hard to judge.

IV.4.5 Migrants (high-flying, passing birds)

Many bird species, including eagles, herons, pelicans and oystercatchers, feed out on the ocean or at the water's edge. When they leave the land for their feeding places, they pass over fiddler crab colonies. Typical flight paths (e.g. Figure IV.9) are very straight, of medium, mostly horizontally dominated, retinal speeds (here between 5-10 °/s), but contrast changes can be quite large. After about 7 seconds in this example of two crows, the closer crow (upper trace in Figure IV.9A) starts speeding up while

increasing the frequency and amplitude of its wing beat. The resulting large change in vertical retinal speed (Figure IV.9D), possibly together with a constant rise of contrast changes (Figure IV.9E) is followed by home-run responses of all five crabs that were active at the time.

To summarise for this approach type (Figure IV.10), elevations are relatively high (10-50 °) and retinal speeds moderate (up to about 20 °/s). Neither of them seems to predict responses. Contrast changes once again confirm the trend seen in terns and kites. Most contrast changes are low, but values above about 50-60 units are highly likely to evoke a response.

IV.4.6 Response criteria

For easier comparison, Figure IV.11 combines the ***probability of observation*** and the ***probability of response*** depending on the four measured parameters for all predator types. Observed **elevation** (Figure IV.11A) interestingly seems to fall into two main groups. Terns and dragonflies are most commonly observed below 10°, while kites and migrants are the dominant signals above 10°. This is reflected in the ***response probabilities*** for terns and dragonflies (Figure IV.11B, blue and green bars). The probability of response is largest at just above ten degrees. However, this probably reflects the fact that for terns (assuming they fly at a roughly constant height) an increase in elevation means that the birds are coming closer. At the same time they would be producing increasingly large vertical retinal speeds, which might be the actual cause of responses. I also examined what this signal looks like through fiddler crab eyes by projecting the birds' positions onto a fiddler crab sampling array (Figure IV.12). The vertical sampling resolution of the fiddler crab eye is dramatically increased in an acute streak at the visual horizon (Figure IV.12 inset). The lowest 10° degrees of azimuth are therefore sampled by approximately the same number of ommatidial rows as the visual space between 10° and 50°. This effect increases the separation of signal groups along the parameter axis of elevation (Figure IV.12A). Rows 0-15 sample practically exclusively terns and insects, while rows 20-35 sample mostly kites and migrants.

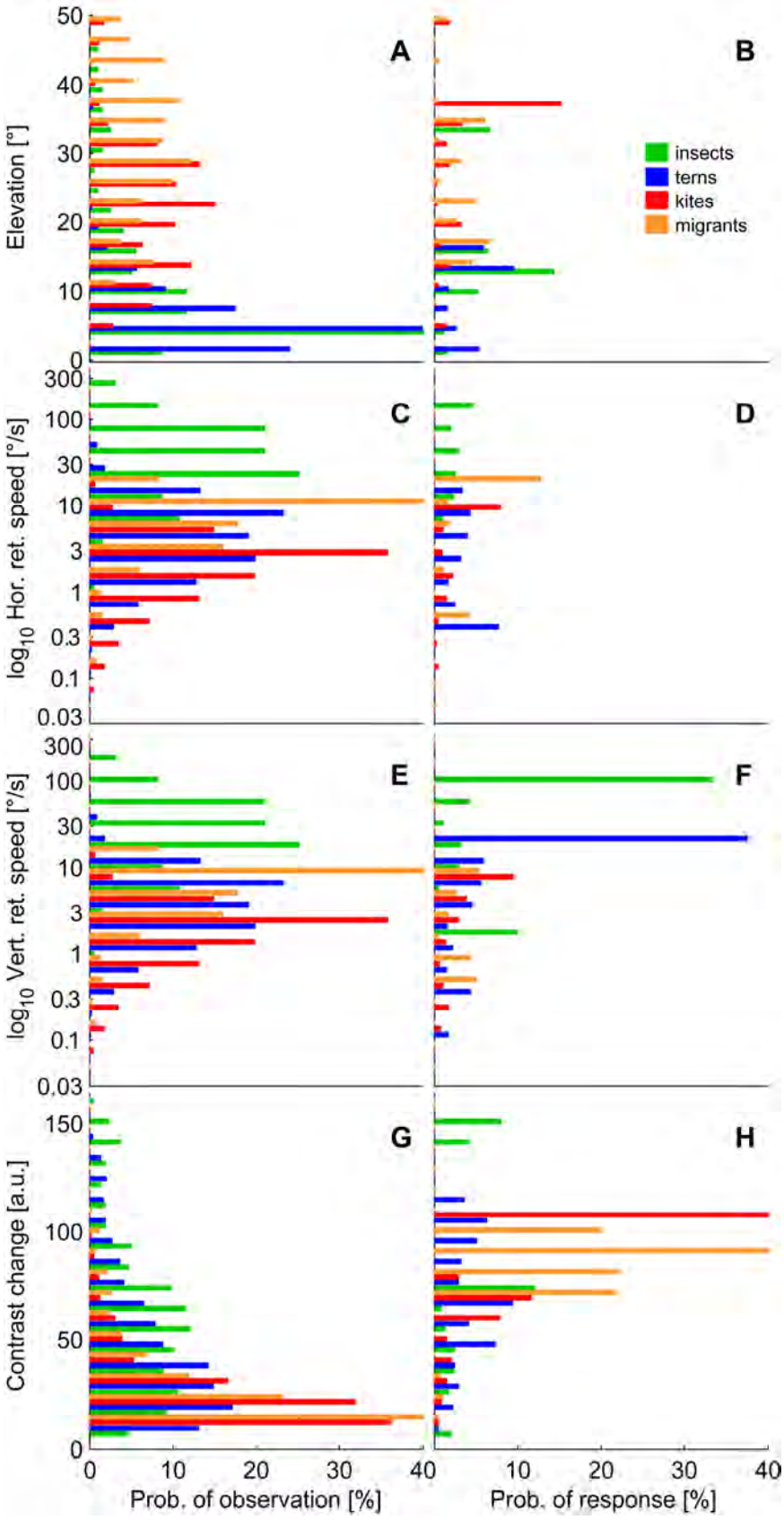
A
B
C
D
E
F
G
H
insects
terns
kites
migrants
Elevation [°]
log10 Hor. ret. speed [°/s]
log10 Vert. ret. speed [°/s]
Contrast change [a.u.]
Prob. of observation [%]
Prob. of response [%]

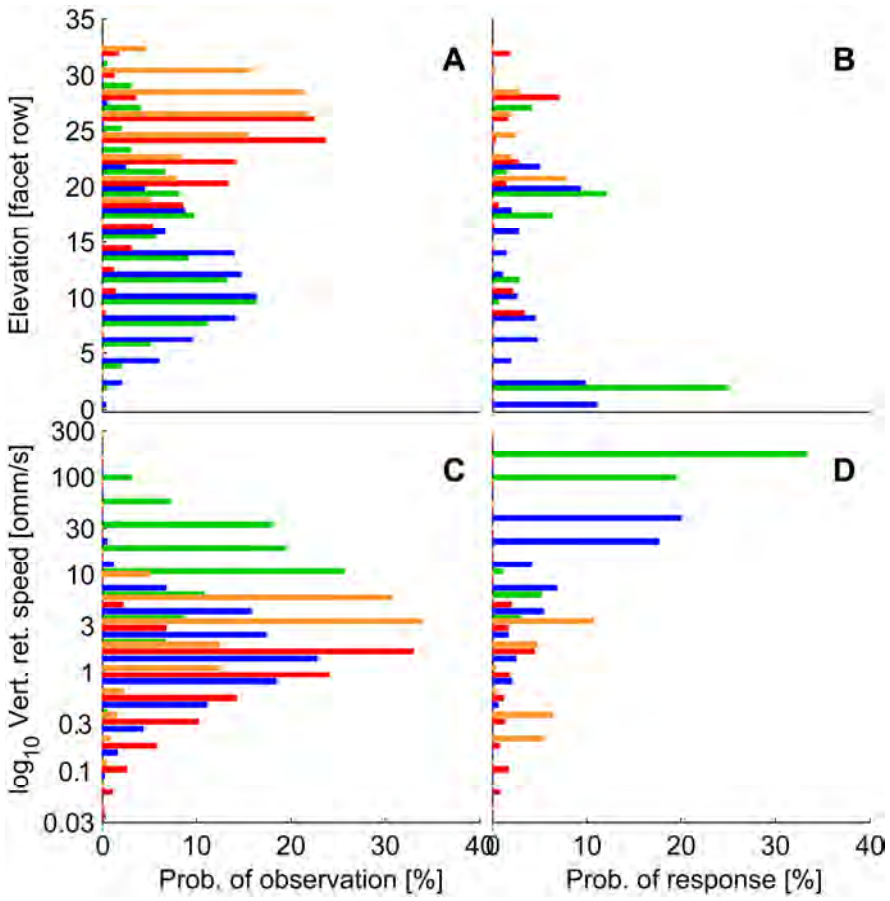

Figure IV.12: Probability histograms considering crab eye optics. All values are calculated in crab eye relevant units, i.e. elevation (**A,B**) in facet rows above the horizon and vertical retinal speeds **(C,D)** as ommatidia per second (omm/s). Left side displays probability of observation, right side probability of response. Note that panel C and D are equivalent parameters to IV.11E and IV.11F. Colours as before, see text for details.

Figure IV.11: Probability histograms combined for all event types. Left side **(A,C,E,G)** displays probability of observation, right side **(B,D,F,H)** probability of response. Colours as before, see text for details.

The ***response probability***, when plotted over facet row (Figure IV.12B), again peaks at the border between these two groups (at about row twenty) and shows an additional large step right at the horizon (rows 0-3). Quite likely, this peak in response probability reflects the swoops of terns, where low elevations are combined with high vertical speeds and large contrast changes through the flicker of the wings.

Vertical and horizontal retinal speeds are distributed in a very similar way, although horizontal speeds are slightly higher on average (Figure IV.11C,E). Dragonflies generally exhibit the highest speeds, followed by migrants, terns and kites. The overlap between groups is large, but interestingly the absolute maximum of vertical speed for terns and insects is higher than for kites and migrants. The ***response probabilities*** (Figure IV.11D,F) are scattered across horizontal speeds, but strongly correlated to vertical retinal speed. Again, this effect is even stronger when vertical resolution is analysed through the crabs' sampling array (Figure IV.12C, D), suggesting that the resolution profile of the crabs' eyes might help separating potential predatory signals into different categories. At speeds above 10 ommatidia per second, which are never reached by kites or migrants, response probability increases drastically.

Contrast changes, finally, are distributed similarly in all four groups (Figure IV.11G). Small contrast changes are very common, while large changes are rare, but seem to occur more often in kites and dragonflies. ***Response probabilities*** are mostly below 5% for low contrast change values. For values above 60 units, I observed much higher response probabilities, surprisingly especially in migrants (Figure IV.11H). Many of these birds have a dark plumage and present a strong contrast change when passing through the visual fields of ommatidia at high horizontal speeds against the background of a bright sky.

IV.4.7 Statistical analysis

To identify the parameters that triggered a crab response and isolate (at least partly) factors that were highly correlated, a generalised linear mixed model (GLMM, R) was applied to individual crab decision (response/non-response) within each

individual 200 ms time frame. Tested parameters included elevation, retinal speeds (logarithmically) and contrast changes. As the effects of contrast change and elevation appear to be more of a step-function than a linear effect (Figures IV.12B and IV.11H), they were included as two-level factors. 'High contrast change' was defined as any contrast change above 60, 'Horizon level' as any elevation below facet row 3. Interactions of up to three parameters were examined, but no interactions achieved significance.

Table IV.2 summarises the results of the statistical analysis. The three parameters that were found to be highly significant were 'High contrast change', 'Horizon', and the vertical retinal speed. All three parameters were positively correlated with the probability of response. There was no indication of an effect of horizontal retinal elevation (GLMM, $Chi^2 = 0.773$, $N = 14618$, $P = 0.38$).

The effect sizes in generalised linear models can be expressed as the logarithm of the odds-ratio. The four predicted probability functions (for the four possible combinations of the 'High contrast change (C)' and 'Horizon (H)') are shown as functions of vertical retinal speed in Figure IV.13A. For low contrasts away from the horizon (C-H-, red line), the predicted probability of response is very low even for large retinal speeds. When contrast is above 60 *or* the signal is seen in the central ommatidial rows at the horizon (C+H-, green line and C-H+, blue line), response probabilities rise up to above 10% at high speeds. Finally, a strongly flickering signal at the horizon (C+H+, black line) will elicit a response with 20-40% certainty at speeds above 10 ommatidia per second. Although these probabilities may seem low, it should be kept in mind that they are calculated and predicted for any 200 ms interval. If the stimulus is experienced for longer than that without changing, probabilities will accumulate. This is explored in Figure IV.13B. If a strong stimulus (fast moving plus flicker at the horizon) is observed for just 1s, the model predicts a probability of response of over 80%.

Table IV.2: Natural visual cues affecting escape decisions. Results of the generalised linear mixed model analysis (GLMM; N = 14618; random model: crab identity + bird identity).

Fixed effects	Effect	*df*	Chi^2	*P*
Horizon level (facet row <4)	1.32	1	57.86	<0.001
High contrast change (>60)	1.30	1	36.01	<0.001
Vertical speed (omm/s, log)	0.637	1	22.45	<0.001

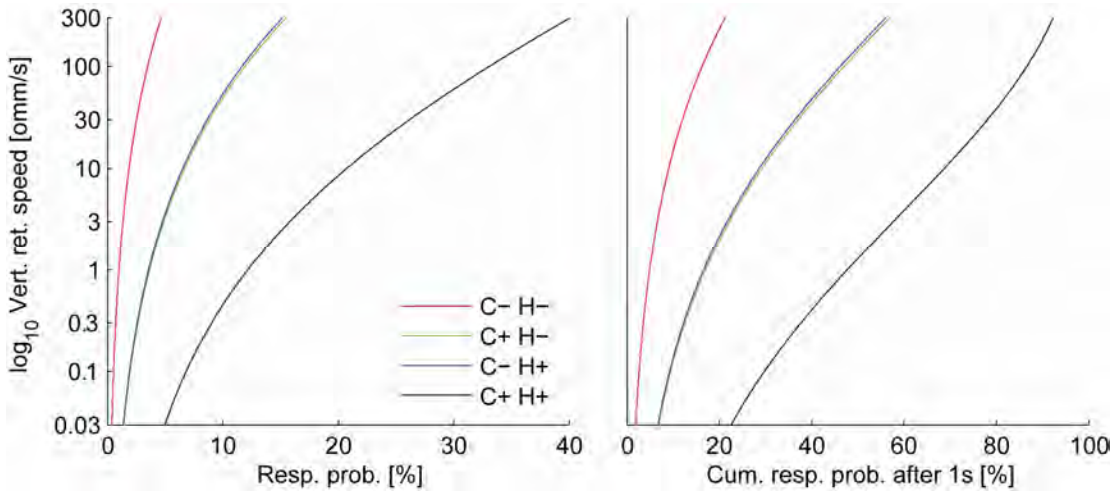

Figure IV.13: GLMM predictions for response probabilities. (A) Predicted response probabilities are shown as a function of vertical retinal speed for all four combinations of the two factors '***H***orizon' and 'High ***C***ontrast Change'. C-H+, for instance, (blue line) indicates the probability curve for low contrast objects at the horizon. **(B)** Accumulated response probabilities after observing the same stimulus for 1 second. Note the difference in axes to (A).

IV.5 Discussion

IV.5.1 Natural signals in the context of predation

The aim of this study was to characterise the signals that fiddler crabs experience in the presence of natural predators in the field and relate them to the visual cues that are known to elicit predator avoidance responses in fiddler crabs. The analysis has illustrated that different birds produce systematically different visual signals. Terns (the crabs' main predators), for instance, produced high retinal speeds, at low elevations and produced large contrast changes through the flicker generated by their beating wings. Kites on the other hand – the most common non-threatening birds in the study area – tended to move at lower apparent speeds, usually at higher elevations, and produced comparatively low contrast changes. The statistics of these signals differ enough for the crabs to potentially make use of these differences and in fact they did so. They responded to terns, their real predator, relatively more often than expected (37% of all home runs were elicited by terns, which only contributed 25% of bird and insect records). Two additional event classes were examined that demonstrate how an evaluation of individual cues can lead to frequent false alarms. Dragonflies occasionally pass over the mudflat in fast, erratic paths. Due to their small size the crabs only see them when they are very close, by which time they produce very large retinal speeds that reliably trigger the crabs' escape response. Migrants on the other hand – i.e. all birds such as eagles, oystercatchers, herons and pelicans that pass over the crabs' colonies to reach their feeding grounds at the water's edge – seem to trigger the crabs' flicker-detection systems, because the fast horizontal motion of these dark birds seen against a bright sky creates large contrast changes. The reason why crabs can afford to react to these birds is that they are comparatively rare and the costs of false alarms in response to their movements apparently do not outweigh the benefits of an early alarm system triggered by retinal speed and flicker.

IV.5.2 Visual cues in natural escape responses

The three main characteristics of the recorded signal that determined the timing of home runs were elevation, vertical retinal speed and large contrast changes. The predictive effect of **elevation** (highest response probabilities at the horizon) was surprising, as its direction was contrary to expectation. Any bird flying at a constant height progressively rises in elevation as it approaches more closely and high elevation should therefore be a good indicator of predation risk. Dummy experiments have also confirmed that fiddler crabs are sensitive to the elevation of a stimulus (Hemmi, 2005b). However, in the interest of a balance between escapes and false alarms, crabs should clearly not react to most stimuli they see above about 20° of elevation, (as many of them are likely to be caused by harmless birds), unless other criteria suggest a real threat. At the horizon, in contrast, almost all observed birds are terns. In combination with a flickering or fast-moving signal, low elevations are therefore a good indicator of a real predator.

Retinal speed is one of the best predictors of home run responses in dummy experiments (Hemmi, 2005b). Both in dummy experiments and in my recorded natural predation events, crabs are much more sensitive to vertical than to horizontal retinal speed. However, while horizontal speed has been clearly shown to trigger responses in dummy experiments, it had no significant predictive effect in this study. This can be understood by considering a simple geometrical argument. As the translational speed of birds is limited, the total sum of its angular components is also limited. To an observer, they can either present a large horizontal component (when they are passing by) or a large vertical component (when they are either flying up, down, or towards the observer). Both components at the same time are rarely high (especially in horizontally flying birds), but they can be both low. High vertical speeds (which are most strongly correlated with real risk) are therefore neither predicted by large nor by low horizontal speeds. The reason, therefore, why horizontal speed did not appear to have a significant effect in this study (while it clearly does so in dummy experiments), is likely its correlation with low vertical speeds. If we assume that the crabs use the same criteria both in dummy experiments

and in response to natural events, the fact that the conclusions we have to draw differ for the two situations highlights the importance of understanding the natural visual signals if we are to understand the hierarchy of response criteria as they apply to the crabs' natural behaviour.

High **contrast changes** appear to be the strongest effect identified in this study. Changes above 60 units increase the response probability dramatically. In many cases such contrast changes are caused by the flicker created by the wing beats of birds (especially terns). In other cases it is caused by a high-contrast bird flying at high speed. Contrast changes therefore include the effects of speed, but carry additional information about flickering objects that are stationary on the retina. One large advantage of flicker as a response criterion is that it can be evaluated from the input of just a single ommatidium, whereas speed, when evaluated by motion detectors, can only be measured by correlating the signals of at least two ommatidia. In the dorsal visual field of fiddler crabs, the acceptance functions of ommatidia are narrow (to increase contrast sensitivity) and sparse (chapter II). Small objects like distant birds will therefore rarely be seen by two neighbouring ommatidia and evaluation by motion detectors will therefore be unreliable, whereas flicker can be evaluated by each ommatidium individually.

A possible alternative explanation for the step function of response probabilities to contrast changes is that the crabs might not be able to perceive lower contrasts and react as soon as they detect a strong flicker signal. However, even though the response probability is low, a number of responses *were* elicited by low contrast signals and the absolute response probability even at very large contrasts is below 50%. This question will be further examined in chapter V by analysing if crabs, in the presence of a strong flickering signal, are still sensitive to other risk factors, such as the distance to their burrow (see below).

Angular size and looming have previously been shown to affect the timing of predator avoidance responses (Nalbach, 1990; Hemmi, 2005b; Oliva et al., 2007). Whether these cues are directly available to fiddler crabs in a natural situation, however, seems doubtful. Most birds change shape and size constantly through the

beating of their wings and through changes in orientation. For this reason it was impossible for me to accurately measure the angular size of birds in the recorded videos. The results of dummy experiments (Hemmi, 2005a, b; chapter V) and my own recordings, however, suggest that the apparent size of birds and dummies rarely exceeds 2° at the time the home run is initiated and thus are seen by only one or two ommatidia. This fact makes it very unlikely that the crabs use retinal size or looming as a decision criterion when responding to flying predators. The same effect might instead be realised through contrast. A bird of larger retinal size will present a higher-contrast signal to an ommatidium and therefore create larger contrast changes if it is moving fast or flickering. Looming might, however, play a role in response to large walking birds, which were not examined in this study, or in cluttered environments, where predators can be much larger by the time they are first seen. It might also play a role at the time the crabs decide to descend into their burrow, when objects are much closer and the crabs have more information available (see below).

Another factor that strongly influences response probability and timing in dummy experiments is a crab's **distance to its burrow**. Crabs that are far away from their refuge are more likely to respond and generally respond earlier (Hemmi, 2005a, b; chapter V). This observation is evidence that the crabs do initiate their home runs at the time they detect the bird, but make a decision based on their estimation of the risk. When they are closer to their burrow and the time needed to run home is therefore shorter, they delay their responses. In this study I have found no effect of crab-burrow distance on home run timing. However, as a large number of low-speed and low-contrast conditions were included in the model, no responses would have been expected during these conditions even if the crabs were far away from their burrow. Similarly, some of the signals, such as a swooping tern, were presumably so strong that they would have triggered a home run no matter how far away the crab was from its burrow. In other words, crab-burrow distance modifies response thresholds, but does not trigger responses by itself. It will therefore manifest itself mostly in situations when the response threshold is slowly approached as is the case

in most of the dummy experiments. The effect of burrow distance on response distance to a flickering dummy will be examined in chapter V.

IV.5.3 After the home run

After reaching their burrow at the end of the home run, crabs only rarely continue their escape straight down into their burrow. Instead, they usually remain at the entrance of the burrow, and only descend when the threat persists and the risk increases further. This strategy allows fiddler crabs to stay in relative safety, as the actual burrow descent only takes a fraction of a second, while collecting as much information as possible to make sure that the threat is real. In many cases this allows them to avoid the burrow descent, which is the most costly part of the escape, because it results in the complete loss of visual information (Hemmi and Zeil, 2005). Even in experiments with bird dummies, where the threat often approaches very directly and very fast, crabs are reluctant to descend into their burrow while the simulated predator is approaching (Jan Hemmi, unpublished data; chapter V). However, they often descend into their burrow after the danger has clearly passed (i.e. when the dummy is moving away from the crab and back to its starting position). It appears that they use the opportunity to enter their burrow, for instance to replenish their water reservoir, before they head out onto their next excursion, and thereby prolong the time that they can stay out without having to return.

Interestingly, during the 37 natural predator approaches I analysed, I observed a total of 170 home runs, but only 18 underground responses. This might indicate that in the presence of an unreliable, unpredictable signal, the crabs avoid descending into their burrow while they are not sure about the status of the potential predator. In other words, while the dummies have to clearly and visibly move away from the crabs before they will enter their burrow, natural predators rarely do that. They might not provide sufficient cues to the crabs to convince them of their departure.

In conclusion, the analysis of natural visual stimuli has shown that the visual cues produced by different species of aerial predators differ in their statistical properties

enough to potentially allow the crabs to distinguish between them. The response criteria that crabs use under natural circumstances reflect these properties. Contrast changes (e.g. flicker) were identified as an important visual cue that has not been detected in previous analyses. While, as this study has shown, the analysis of natural events is essential for identifying the visual cues used in natural predator behaviour, these cues are often highly correlated, because they reflect the physical limitations of the predators' behaviour. The effect of flicker will therefore be examined in detail in dummy experiments presented in the following chapter.

Chapter V

The influence of fast contrast changes (flicker) on escape responses

V.1 Summary

Predator avoidance behaviour comes at a cost and prey animals need to balance these costs with the risk of predation. The decisions that are necessary to strike this balance are often based on information that is inherently imperfect and incomplete due to the limited sensory capabilities of the prey animal. Our knowledge, however, about how prey animals solve the challenging task of limiting their responses to the most dangerous stimuli in their environment, is very limited. Using dummy predators I have examined the contribution of visual flicker (a response criterion identified from an analysis of responses to natural visual stimuli) to the predator avoidance response of the fiddler crab *Uca vomeris*. The results illustrate that crabs let both purely black and purely white dummies approach significantly closer than a rotating black-and-white (flickering) dummy. Furthermore, while in black dummies higher speed elicits earlier responses, there was no difference between the responses to the flickering dummy and a second dummy that flickered at the same frequency, but moved twice as fast. These results indicate that fast contrast changes like flicker provide a very strong cue that can override other important response criteria. By combining and adjusting the weights of these response criteria in a way that relates to the actual risk in their natural environment, crabs may be able to detect threats and prevent false alarms in a more effective and efficient way and therefore limit the impact of their lack of complete information about the risk of predation.

V.2 Introduction

Prey animals constantly have to make life-or-death decisions. While making sure to escape all real predatory threats, they also have to avoid false alarms because of their many associated costs. Such costs can be energetic, informational or through missed mating, social or feeding opportunities. Due to the limitations of sensory systems and the conflicting demands of other behaviours, however, the information that animals have available to make these decisions is usually imperfect and incomplete (Sih, 1992; Koops and Abrahams, 1998; Lima, 1998; Martin and Lopez, 1999; Luttbeg, 2002; Koops, 2004; Hemmi, 2005a, b). Many small animals, for instance, cannot reliably determine important risk-related cues like distance, approach direction or speed of an approaching predator (Collett and Harkness, 1982; Hemmi, 2005a, b; Hemmi and Zeil, 2005). In the absence of these cues they have to rely on simple rules-of-thumb to provide them with an estimate of the risk of predation (Bouskila and Blumstein, 1992; Koops and Abrahams, 1998; Welton et al., 2003).

In addition to the constraints imposed by the visual system, the reliability of visual cues can be drastically reduced in a natural situation by the unpredictable nature of environmental background noise (Peters et al., 2008). On the positive side, however, differences in the appearance and specific behaviours of common dangerous and harmless animals might add additional cues to the signal that – although not strictly related to risk – could help determine the potential identity and risk posed by a particular moving object. In my previous analysis (chapter IV) I have compared the signals that dangerous and harmless flying animals present to fiddler crabs. The results showed that the statistics of these natural signals differ enough for the crabs to potentially make use of these differences to distinguish between dangerous and harmless events, and in fact the crabs did so. They responded to terns, their real predator, relatively more often than expected (37% of all responses were in response to terns, which only made up 25% of recorded signal time). The analysis also demonstrated that the crabs use a complex response criterion which apart from elevation and vertical retinal speed of an object (which are cues known from previous

dummy experiments), is also sensitive to fast changes in contrast. Using this combination of parameters might help crabs distinguish between their predators and birds that are harmless to the crabs, like kites. One large advantage of such a multiple-cue response trigger is that it is extremely adaptable to changes in predator strategies or even the appearance of a new predator. The contributing parameters can be individually adjusted to changing noise conditions and different parameters can reflect different balances between risk-sensitivity and the prevention of false alarms. Contrast changes, for example, can be measured in one individual ommatidium and therefore provide possibly one of the earliest, safest, but least specific response criteria. The information contained in this cue confounds retinal speed with the flicker of an object and cannot distinguish between vertical and horizontal components of speed. As vertical retinal speed is generally a better indicator of risk (it might originate from an approaching object), the risk of false alarms is quite high for contrast changes. Directional speed measurements, however, that could determine such differences between horizontal and vertical components, can only be performed when the signal is seen by two neighbouring ommatidia. Combining both (and several other) cues can thus provide an adaptable and sensitive response system.

In natural signals, visual cues are often highly correlated because they reflect the physical limitations of the behaviour of predators. In many birds, for instance, high speeds are correlated with the flicker produced by their wing beat. Similarly, a horizontally flying bird will reach both higher retinal speeds and higher retinal elevations as it approaches. From recordings of natural stimuli, such as the ones I presented in chapter IV, it is therefore difficult to tease apart individual response criteria. Due to the complex structure of natural bird approaches, it was also not possible to determine how sensitive crabs are to other indicators of risk, such as their own distance to the refuge of their burrow, when presented with a sudden, strong stimulus. The role flicker plays in the fiddler crab predator avoidance system, and how it influences the crabs' risk-sensitivity, therefore needs to be determined in controlled dummy experiments, where stimulus conditions can be manipulated precisely and independently of each other.

The aims of this study are therefore threefold: (1) To show that flicker is used as a response criterion by demonstrating that crabs let purely black and purely white dummies approach significantly closer than an otherwise identical flickering dummy; (2) to examine how flicker interacts with another important response criterion, retinal speed, by comparing the effect of speed separately in black and in flickering dummies; and (3) to illustrate that flicker does not trigger an immediate 'panic' response at the time of detection, but is used as part of a multi-factorial information criterion to estimate the threat an approaching object posed and to make decisions about a safe home run timing.

V.3 Materials and methods

V.3.1 Animals, apparatus and video analysis

The experimental setup was identical to that described in chapter IV with the exception of the stimulus presentation. Dummy predators consisted of 4 cm diameter plastic spheres with a deep, narrow groove around their centre (Figure V.1A). A metal axle was inserted through the centre of the dummy, and two loops at its ends were threaded onto two parallel monofilament lines that were tightly strung between two metal poles about 6-8 m apart on the mudflat. The dummy was moved along this track by a non-stretch polyfilament fishing line, which was wound around the dummy's central groove. The line was wrapped around the poles at both ends of the track and around another pole close to the operator, who was about six metres away from the crabs (Figure V.1B). Here the line was wrapped around an aluminium wheel that was turned by a battery-driven drill allowing the operator to move the dummy at a constant speed, and around an optical encoder, which recorded the movement of the dummy and saved it on an SD card. This made it possible to reconstruct the exact position of the dummy even when it was outside the field of view of the video cameras used to record crab responses.

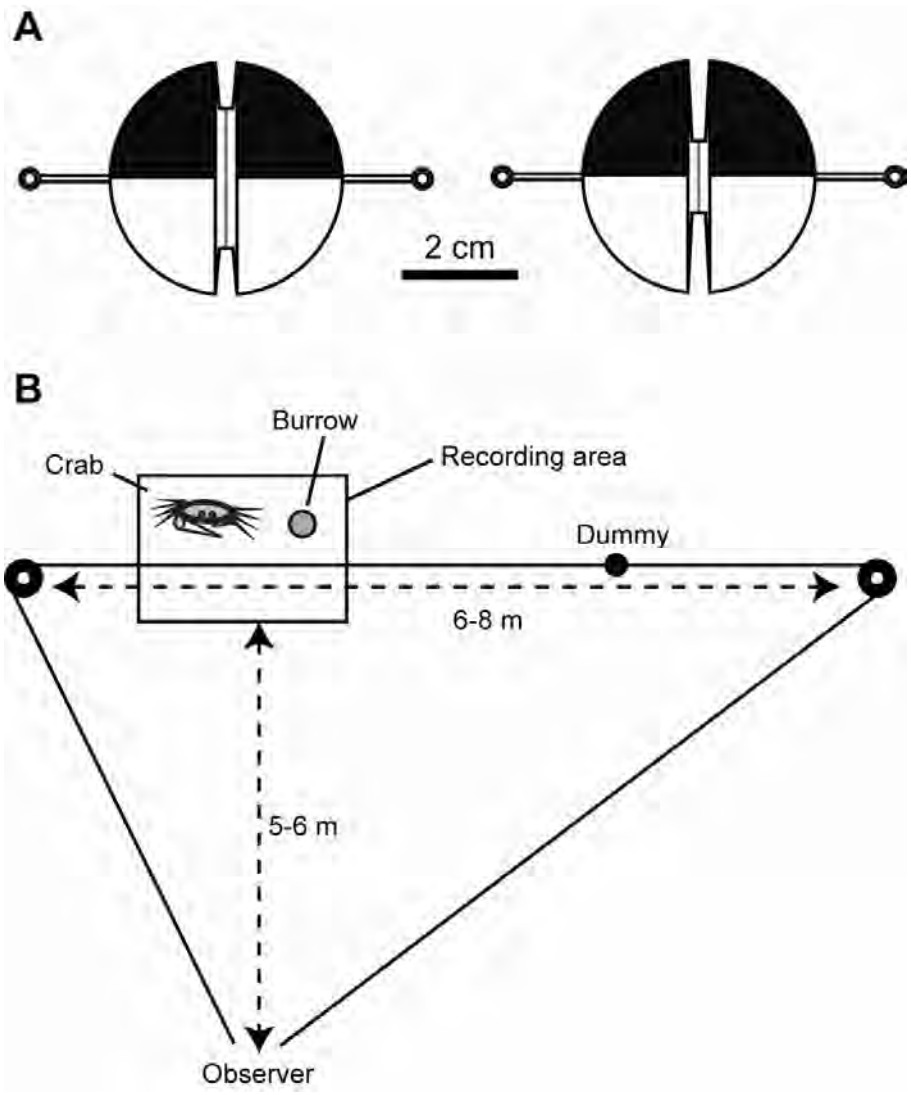

Figure V.1: Experimental setup. (A) Design of the flickering dummy. The loops on both ends were threaded onto two fishing lines. A third line was wrapped around the dummy inside the central groove and used to translate and rotate it. By halving the inner diameter (right), the dummy could be run half as fast and still rotate at the same frequency. **(B)** The experimental setup from a bird's-eye view, showing the observer, the crabs, the camera's field of view and the stimulus apparatus (modified after Hemmi, 2005a).

Winding the fishing line around the dummy's central groove meant that the dummy rotated around its axle at a frequency dependent on its translational velocity and on the inner diameter of the groove. To simulate the flicker of flapping bird wings, I painted several of these dummies white on one hemisphere and black on the other

(Figure V.IA). By varying the inner diameter, I could change translational speed while keeping the flicker frequency constant.

V.3.2 Selection of trials and statistical analysis

The criteria for the selection of trials were similar to those described in chapter IV. For the calculation of total response probability I included only trials where (i) there was no crab or bird interference, (ii) the crab was more than 5 cm away from its burrow at the start of the trial (to decrease the probability that a response was too short to be scored and because crab behaviour changes close to the burrow) and (iii) the crab was inside the recording area at the start of the trial. A total of 184 trials met these criteria. For the analysis of response distance I also included recorded responses of crabs that were less than 5 cm away from their burrow. This increased the total number of crab responses to 220 that were included in the final analysis.

The data were collected from a total of seven setups. Two setups each were dedicated to slow vs. fast black dummies and slow vs. fast flickering dummies, while one setup each examined black vs. flicker, white vs. flicker and horizontal vs. vertical rotation. The dummy presentations within a setup were organised in blocks of three trials. Each block contained a random permutation of two repetitions of one condition and one presentation of the other condition. Consecutive blocks alternated in the condition which was repeated twice, resulting in a final design where no more than three consecutive repetitions of the same stimulus condition could occur and the total number of presentations was the same for each condition. Up to twelve blocks were presented within one setup.

For the statistical analysis, linear mixed models (REML) were calculated in R (2.9). I took into account individual variance between crabs (crab identity) and between individual dummy presentations (trial identity) by including them as random factors in the model. Models were selected by sequentially fitting parameters, and parameters were only included if they were significant at a 5% level when fitted to the model last. All REML models were graphically checked for outliers and a normal error distribution.

V.4 Results

The crabs responded to all dummies in their customary way. At detection of the dummy they froze, i.e. they stopped all activity and observed. Shortly afterwards they started a sudden, fast home run to their burrow, where they again stopped and waited. Only when the threat increased further, they descended into their burrows where they stayed for a certain period of time before returning back to the surface and resuming their normal activity. The overall probability that a crab responded to a dummy with a home run was so high (mean of 89.7% over all setups) that it was not possible to identify which factors affected response probability. However, the response distance, i.e. the three-dimensional distance between the dummy and the crab at the time of response, was strongly influenced by several parameters.

V.4.1 Flicker triggers earlier home runs

The crabs' response distance to a black-and-white, flickering dummy was compared to that in response to a purely black dummy (as used in most previous dummy studies) or a purely white dummy (as an intensity control). The crabs initiated their home runs much earlier in response to the flickering dummy than when approached by either the black or white dummy (Table V.1 and V.2). The linear mixed model shows that, on average, they let the black dummy (Figure V.2A, blue line) approach 44.3 cm closer than a flickering dummy presented in the same session (Figure V.2A, red line). The difference to a white dummy was even larger. The crabs reacted to the flickering stimulus more than one metre earlier (Figure V.2B). In both experiments, the crabs responded earlier when they were further away from their burrow (Figure V.2A,B), indicating that they are sensitive to the risk of predation. For every centimetre the crabs moved away from their burrow, the response distance increased by an average of 2.5 cm in the black-dummy experiment and 6.0 cm in the white-dummy experiment. In addition, in the white-dummy experiment they responded later to dummies that approached more directly, as evident by the variable crab-track distance (the distance between the crab and the closest point on the dummy track;

Figure V.2B). This paradoxical effect is common in the crabs' predator response and is explained by the fact that crabs respond earlier to faster dummies and less directly approaching predators move at higher retinal speeds (Hemmi, 2005a, b; Hemmi and Zeil, 2005). There was no evidence of an interaction between any of the parameters.

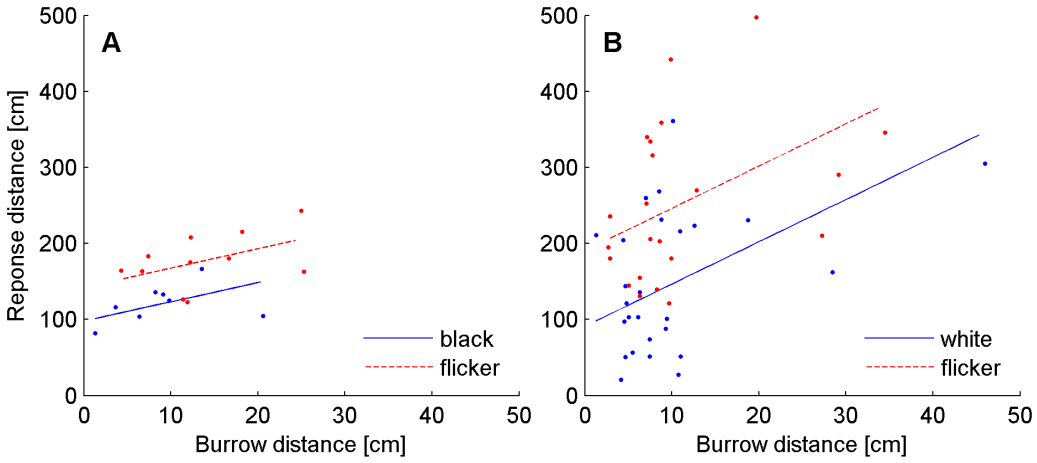

Figure V.2: Crabs respond earlier to flickering dummies than to black or white dummies. The red dashed line shows the model prediction for the flickering dummy, the solid blue line the prediction for the black **(A)** or white **(B)** dummy.

Table V.1: Black vs. flickering dummy. Results of the linear mixed model analysis (REML; $N = 19$; random model: crab identity + trial identity). Crab-burrow distance was measured at the time of response.

Fixed effects	Effect	*df*	Chi^2	*P*
Flicker	44.3	1	6.789	0.009
Crab-burrow distance	2.54	1	7.366	0.007

Table V.2: **White vs. flickering dummy.** Results of the linear mixed model analysis (REML; $N = 48$; random model: crab identity + trial identity). Crab-burrow distance and crab-track distance were measured at the time of response.

Fixed effects	Effect	*df*	Chi^2	*P*
Flicker	109.6	1	18.45	<0.001
Crab-burrow distance	5.95	1	16.42	<0.001
Crab-track distance	4.33	1	12.66	<0.001

V.4.2 Flicker overrides speed dependence

Similarly to earlier studies, crabs responded significantly earlier to the faster of two non-flickering, black dummies that were otherwise identical (Table V.3, Figure V.3A, Hemmi, 2005a, b). A change of average dummy speed from 18.5 cm/s to 33.7 cm/s increased the average response distance by 48.5 cm. Response distance was again influenced by the crab-burrow distance (Table V.3). The crabs responded on average at a 1.9 cm longer distance for every centimetre they were away from their burrow. In these experiments, there was no effect of how directly the dummy approached (crab-track distance, $Chi^2 = 0.62$, $N = 82$, $P = 0.430$).

To test whether the crabs are still sensitive to the speed of the approaching dummy in the presence of flicker, I compared their responses to two flickering dummies with inner diameters that differed by a factor of 2 (Figure V.3). When the dummy with the larger inner diameter was pulled across the mudflat at twice the speed of the other dummy, both dummies rotated and flickered at the same frequency of about 4.8 Hz. The speeds used were approximately the same as in the black-dummy speed experiment. There was no indication that the crabs' response distance to these dummies depended on the translation speed of the dummy (Table V.4, Figure V.3B). The effect of flicker seems to override the effect of speed in this case. However, flicker does not seem to be so threatening to the crabs that they respond immediately after detecting the dummies. The crabs were still clearly sensitive to other indicators of risk. Their response distance strongly depended on their distance

from the refuge of their burrow. The effect was in fact stronger than in either of the previous experiments (as can be seen from the much steeper slope in Figure V3.B when compared to Figures V2 and V3.A). For every centimetre that they were away from their burrow, they responded at a 7.89 cm larger distance to the dummy. The total range of observed crab-burrow distances was also smaller than previously. The crabs seemed to be reluctant to move far away from their burrows during this experimental session. The reason for this observation and for the stronger effect of crab-burrow distance might be that the flickering dummies appear generally more threatening to the crabs. Constant exposure to two flickering dummies might make them less willing to take any risk. Another factor influencing response distance was again the crab-track distance at the time of response (3.25 cm per centimetre away from the track). When crabs were further away from the track (and were therefore approached less directly), they responded earlier.

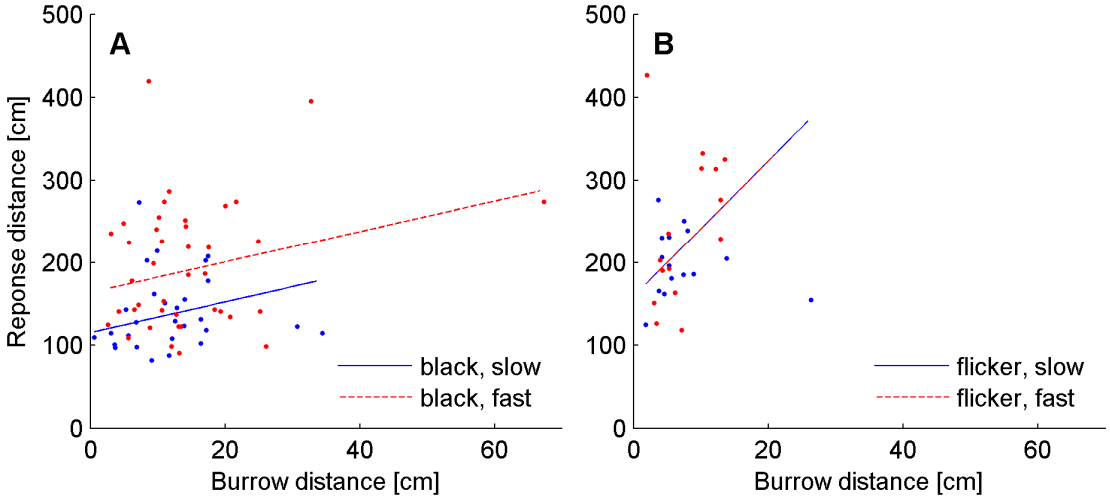

Figure V.3: Responses depend on the speed of a black dummy, but not on the speed of a flickering dummy. The red dashed line shows the model prediction for the fast dummy, the solid blue line the prediction for the slow dummy. **(A)** When approached by black dummies, fiddler crabs clearly respond to the faster dummy earlier. **(B)** When both dummies are flickering (here at 4.8 Hz) the crabs treat them both equally, irrespective of their speed.

Table V.3: Black fast vs. black slow dummy. Results of the linear mixed model analysis (REML; *N* = 82; random model: crab identity + trial identity). Crab-burrow distance was measured at the time of response.

Fixed effects	Effect	*df*	Chi^2	*P*
Speed	48.5	1	9.61	0.002
Crab-burrow distance	1.86	1	6.63	0.010

Table V.4: Flickering fast vs. flickering slow dummy. Results of the linear mixed model analysis (REML; *N* = 47; random model: crab identity + trial identity). Crab-burrow distance was measured at the time of response.

Fixed effects	Effect	*df*	Chi^2	*P*
Crab-burrow distance	7.89	1	14.74	<0.001
Crab-track distance	3.25	1	8.64	0.003
Speed	---	1	1.08	0.298

V.4.3 Motion detectors are (probably) not involved

Although my dummies were not truly flickering, but rotating, at the average distances at which the crabs responded the 4 cm diameter dummies would have only occupied a visual angle of between 0.5° (at about 4 m response distance) and 2° (at about 1 m). The crabs would thus likely have seen them with just one or two ommatidia. To further exclude the possibility that the internal motion of the dummy was the real cue that the crabs used, I compared the responses to a horizontally and a vertically flickering dummy (Figure V.4). There was no indication of a difference between the two flicker directions (Chi^2 = 0.02, *N* = 24, *P* = 0.886). The only factor affecting response distance was the crab-burrow distance (8.34 cm per 1 centimetre distance to the burrow; Table V.5).

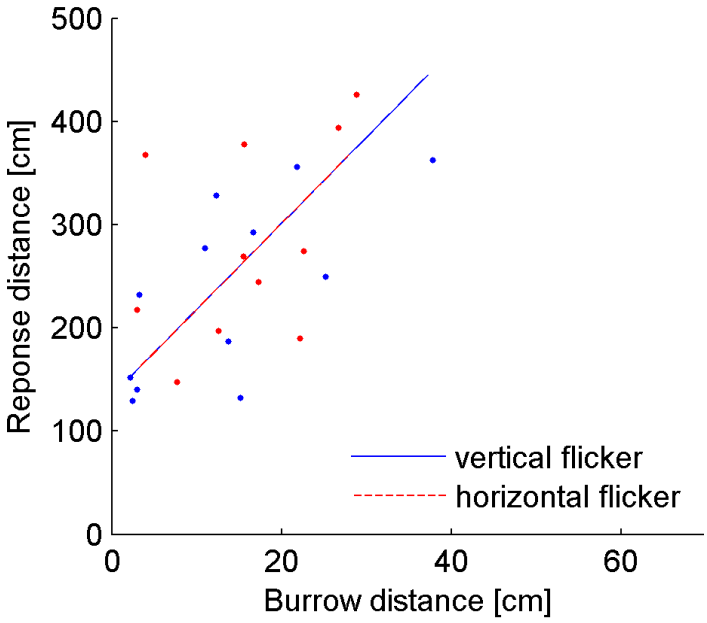

Figure V.4: Crabs responded to flicker, not to the internal motion of dummies. There was no difference between the responses to a horizontally flickering and a vertically flickering dummy. The only variable affecting response distance was the crabs' distance to their burrows.

Table V.5: Horizontally vs. vertically flickering dummy. Results of the linear mixed model analysis (REML; N = 24; random model: crab identity + trial identity). Crab-burrow distance was measured at the time of response.

Fixed effects	Effect	*df*	Chi^2	*P*
Crab-burrow distance	8.34	1	16.8	<0.001
Flicker direction	---	1	0.02	0.886

V.5 Discussion

V.5.1 Flicker as a response cue

My experiments were designed to confirm that fiddler crabs use flicker as a visual cue for escape decisions, to examine the interaction of flicker with speed (another known predictor of the crabs' response timing), and to examine if in the presence of a strong flickering signal, crabs are still sensitive to other risk factors such as their distance to their burrow. The results illustrate that crabs respond significantly earlier to a flickering black-and-white dummy than to either black or white dummies (Figure V.6, first and second experiment), indicating that the flickering dummy is more visible or that they perceive the flickering dummy as more dangerous. While black dummies elicit earlier responses at higher speed, there was no difference between the responses to two flickering dummies that translated at different speeds (Figure V.6, third and fourth experiment). These results indicate that fast contrast changes like flicker can override otherwise important signal properties like speed. However, the crabs remained aware of the differences in risk depending on their distance from the burrow. This effect was strongest when they were exposed to two flickering dummies. Lastly, there was no difference between the crabs' responses to a horizontally and a vertically flickering dummy (Figure V.6, fifth experiment). As crabs are more sensitive to vertical motion, they should have responded significantly earlier to the latter if they had used the dummies rotating motion as a cue. The crabs thus responded to the flicker signal, not the internal motion of the flicker dummies.

The strong influence of flicker on the crabs' escape response can be explained by the likely role it plays in the detection of natural predators. The fact that rapid changes in brightness can be evaluated by a single ommatidium makes flicker an excellent early, albeit very unspecific cue. Fast, constant, high-contrast flicker, such as my dummy produced, probably rarely occurs in natural circumstances. When it does occur it might indicate a directly approaching close predator. For this reason, crabs cannot afford to ignore such a strong cue. This might also be the reason for the large number of false alarms observed in chapter IV that were due to the swoop of a

distant tern or the passage of a fast, dark (harmless and distant) bird seen against the bright sky. Both of these signals create strong flicker and in the absence of unambiguous additional information, the crabs have to assume that the threat is real.

This is not to suggest, however, that the crabs are not aware of other risk factors when exposed to a flicker stimulus. On the contrary, my results clearly show that their response threshold depends on their distance to the burrow. Interestingly, this dependence is much stronger when the crabs are confronted with a flickering dummy than with a black dummy. In all experiments that included at least one flickering dummy, the effect of crab-burrow distance was stronger than in the speed experiment with two black dummies and far stronger than previously found in dummy experiments (Hemmi, 2005a, b). In the experiments that featured two flickering dummies, burrow distance had an even stronger effect than in the ones that involved only a single flicker dummy. The absolute distance the crabs moved away from their burrow also decreased with increasing number of flickering dummies. Although we would have to test all these effects against each other in a single experiment, taken together my results give a clear indication. Crabs seem to be more 'scared' in the presence of a flickering dummy, they stay closer to their burrow and they are more likely to respond earlier when they are away from the burrow.

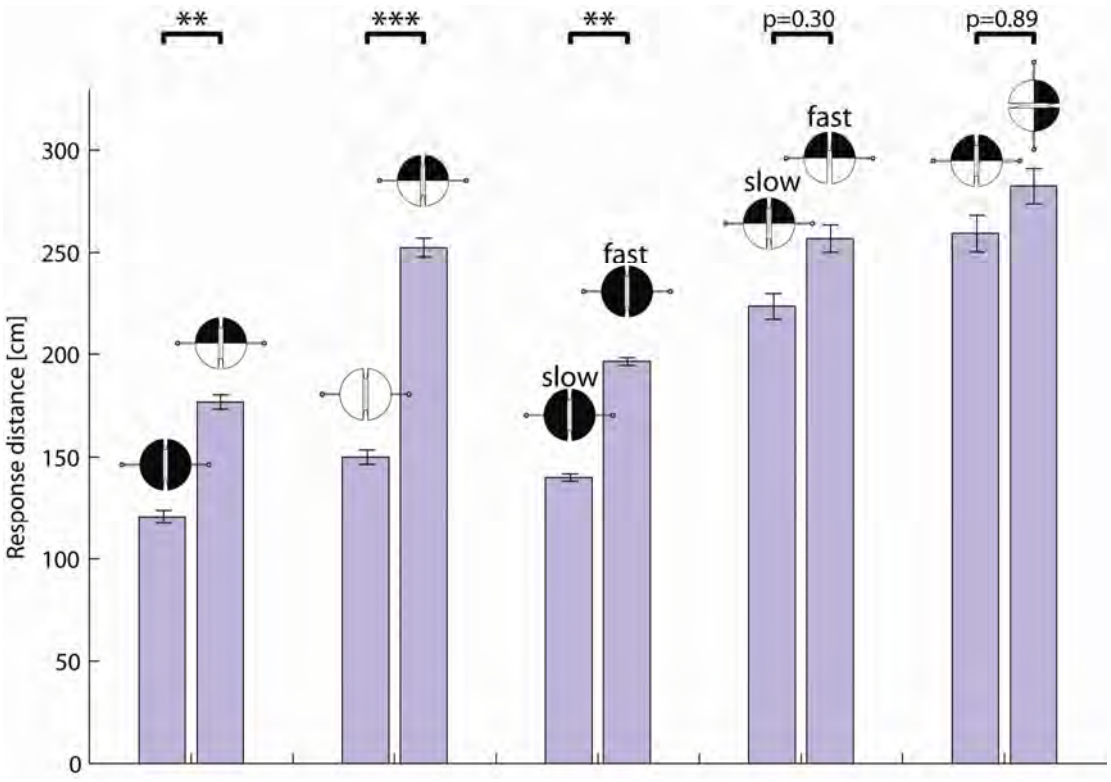

Figure V.5: Summary of the five dummy experiments: Crabs respond significantly earlier to a rotating black-and-white (flickering) dummy than to either black (first bar pair) or white dummies (second pair). While a black dummy at higher speed elicits earlier responses (third pair), there was no difference between the responses to two flickering dummies that translated at different speeds (fourth pair). In a control experiment for the rotating motion of the dummy, no indication was found of a difference between horizontal and vertical rotation (last bar pair), indicating that flicker, not motion are evaluated by the crabs (see text).

An additional piece of supporting evidence might be provided by the slightly paradoxical response to the speed of flickering dummies. Although the crabs responded to these dummies irrespective of their speed, they responded earlier (i.e. at a larger response distance) the less directly the dummy approached. This observation is surprising, as this effect is usually interpreted as a result of the larger retinal speed the crabs experience when approached indirectly. In this case, however, the crabs did not seem to react to the speed of the dummy, but instead relied solely on the flicker signal. Additionally, my dummies rotated around an axis perpendicular to the dummy track. When seen further from the side (i.e. at a large crab-track distance), the contrast of the flicker signal would actually be smaller. A possible explanation for this

apparent paradox is that the crabs further away from the track could actually be reacting to the responses of other crabs that are closer to the track. If all crabs reacted at the same time, the crabs closer to the track would in fact be closer to the dummy. Although these crab-crab interactions seem to have little or no effect in experiments with black dummies (Hemmi, 2005a, b), the flickering dummies might be so stressful for the crabs that they are much more responsive to the movements of others. This hypothesis is supported by the observation that, when working with flickering dummies, crab response 'waves' – a relatively common occurrence where large groups of crabs seem to respond to each other and a 'wave' of home runs passes through the crab colony in response to a very close bird or strong stimulus – are much more common than with black dummies. One way of demonstrating these crab-crab interactions would be to show a statistical effect of group size on response timing (Hemmi, 2005b). If crabs respond to each other, they should be more likely to do so when there are more crabs on the surface. Unfortunately, my data sets are not large enough to test this effect.

V.5.2 Flicker as part of a multiple-cue response criterion

In the presence of perfect information, animals could use a few simple criteria to make decisions about their escape responses. If, for example, the distance and translational speed of the predator were known, a prey animal could calculate a safe escape time at which it would have just enough time to reach its refuge (e.g. Kramer and Bonenfant, 1997). For fiddler crabs, like for many other small animals, this information is not available. Decisions therefore have to be based on unreliable or incomplete information that is only weakly correlated with risk. To deal with this problem, fiddler crabs combine several visual cues that on their own are poor predictors of risk, into a complex decision criterion that could be described as the **visibility or salience** of an approaching object. By combining multiple cues, their relative weights can be adjusted to form a robust predator avoidance strategy that can help distinguish more reliably between dangerous and harmless events. Although in their natural environment the crabs at my study site still respond frequently to kites,

the most common visual disturbance in their habitat, they do so much less often than expected by the frequency of their appearance. An added advantage of the combination of multiple cues is that it is more difficult for predators to adjust to this strategy. Additional cues that can potentially trigger a response constitute in effect additional 'lines of defence'. If, for instance, crabs relied solely on a speed response threshold, predators would have the opportunity to develop a strategy of approaching in slow, straight paths directly towards their target, thereby minimising the retinal motion they create. The prey animal would be forced to reduce its thresholds, thereby again increasing the risk of false alarms. Finally, a multiple-cue strategy might be more adaptable in an environment with frequent motion noise and many diverse predator types. It allows for selective habituation of separate cues while still remaining responsive (Hemmi and Zeil, 2005). If, for instance, the crabs experience strong constant flicker due to jittering leaves of a nearby mangrove tree, they can safely choose to ignore flicker in this part of the visual field and identify predators by their strong motion signature.

In conclusion, the results of this study show that fiddler crabs rely strongly on flicker as a pragmatic criterion for the early identification of potential threats. In response to a flickering dummy, crabs respond significantly earlier and seem to decrease their total level of activity. This effect is probably due to the extremely limited information content of flicker cues. Although likely one of the earliest criteria available to the crabs, it provides little information about distance, speed, heading or identity of a predator. Without additional, more informative cues, the crabs therefore decide to stay close to safety. The fiddler crab example demonstrates how in the absence of complete information, a multiple-cue response strategy may help to reliably balance risks and costs of anti-predator behaviour. We do not know at this point how the crabs implement this strategy, on what level the different criteria are combined and how easily the weighting between their contributions can be changed. However, by combining a number of early and unspecific cues with more complex cues that take longer to obtain, the crabs are able to more closely reflect the statistical properties of their natural predators and thereby reduce the number of false alarms.

Chapter VI

Summary and conclusions

If we are to fully understand the design and efficacy of an animal's visual system then we must consider first what the signals are that the animal is exposed to in its natural environment and how its behavioural strategies affect what visual information it can collect. Similarly, if we want to understand the structure of visually guided behaviour, we have to take into account the statistical properties of relevant natural signals and the limitations imposed by the visual system. Throughout this thesis, I have presented evidence of this tight link between the design of the visual system, the visually guided behaviour and the relevant natural visual signals for the fiddler crab *Uca vomeris*.

Firstly, I have examined the first stage of visual processing, the sampling by the compound eye's ommatidial array. I have presented the first full eye map for any crustacean and my results have demonstrated that the specialisations of different regions of the *Uca vomeris* eye reflect different information content and differences in the behavioural relevance of the corresponding parts of the visual field. While the lateral visual field features the largest facets to facilitate maximum contrast resolution for the detection of territory intruders, the frontal visual field is finely tuned to provide maximum resolution for short-wavelength signals. This region seems to be adapted for the individual recognition of conspecifics by their blue carapace patterns. In the dorsal visual field resolution is extremely low, but lenses are comparatively large. This results in narrow angular acceptance functions and in a drastic undersampling of the visual field at all elevations above about 15°. On the other hand, these narrow acceptance functions provide good contrast sensitivity for the detection of small objects such as approaching birds. The undersampling of the dorsal visual field might be one reason why fiddler crabs use visual flicker as an early response criterion in predator avoidance (see below).

To analyse the second stage of visual sampling, the light absorption by photoreceptors, I have developed the first intracellular electrophysiological preparation for fiddler crabs. I used this new preparation to determine *Uca vomeris'* spectral sensitivities and found evidence of an unusual trichromatic colour vision system featuring a UV receptor type and a wide variety of blue receptors that are most likely created by the co-expression of two short-wavelength sensitive pigments.

This variety in blue receptor types could be an additional adaptation for the processing of carapace patterns. The new electrophysiological preparation also allowed me to demonstrate the polarisation sensitivity of photoreceptors and to record light responses from interneurons in the optical neuropils.

The accurate eye model developed so far now allowed me to accurately predict the information that fiddler crabs have available in a natural situation. I recorded natural bird approaches while simultaneously monitoring crab behaviour. I then filtered the recorded visual signal through the fiddler crab sampling array and examined the cues that the crabs have available to make their escape decisions. The results indicated that the resolution profile of the eye might actually help in separating dangerous from harmless events, as it emphasized a difference in the statistical properties of kites and terns. The cues extracted from the natural signal were compared to those the crabs used in previous dummy-predator experiments. This analysis revealed visual flicker as a response criterion that had not previously been identified.

To investigate the importance of flicker as a response cue for fiddler crab predator avoidance, I designed a flickering dummy to test this cue in controlled experiments. The results demonstrated that the crabs were clearly responsive to flicker. The cue was so strong that it overrode the effect of speed, which had previously been shown to greatly influence the distance to which crabs let a predator approach before initiating a home run. In a natural environment flicker appears to be important as a pragmatic, unspecific, early-response cue that, when combined with other, more difficult to obtain but also more specific cues, might contribute to an adaptable, robust predator avoidance system. The fact that (in contrast to speed), flicker can be evaluated by just a single ommatidium might play an important role for fiddler crabs in overcoming the disadvantages of their heavily undersampled dorsal visual field.

My PhD has focussed on one particular behavioural context, the anti-predator response of fiddler crabs. By approaching the subject from many different directions and on different levels of analysis, it has been a fascinating journey that has thrown

up many new and unexpected connections between the animal's behaviour and its visual system and the results have implications far beyond the predatory context.

Appendices

Appendix A – Virtual wholemount of a crab retina

After recording micrographs of the fiddler crab eye from a large number of positions around the eye (chapter II), we used natural irregularities in the eye as markers to identify individual facets that were visible in adjacent images. With at least three such common facets for each pair of neighbouring images we could individually label all 6925 observed facets, relate them to their neighbours and combine them with the measured pseudopupil positions into a single map similar to a retinal wholemount (Figure A.1). The area of every facet was measured as the area of its Voronoi cell (the cell containing all points that are closer to this than to any other facet).

Figure A.1: Fiddler crab 'virtual' retinal wholemount. Each dot indicates the measured centre of one ommatidium, while the hexagons surrounding them indicate the borders of facets. This map can be viewed as a virtual representation of what the sensory surface would look like when 'peeled off' the eye. Note that, especially in the dorsal eye, where the eye curves strongly, strips of ommatidia can't be connected anymore in this flat representation. This causes distortions and 'rips' which are the main source of unusual facet shapes in the map. Large black dots represent the centres of all measured pseudopupils. Colours code facet area, measured directly from the hexagons.

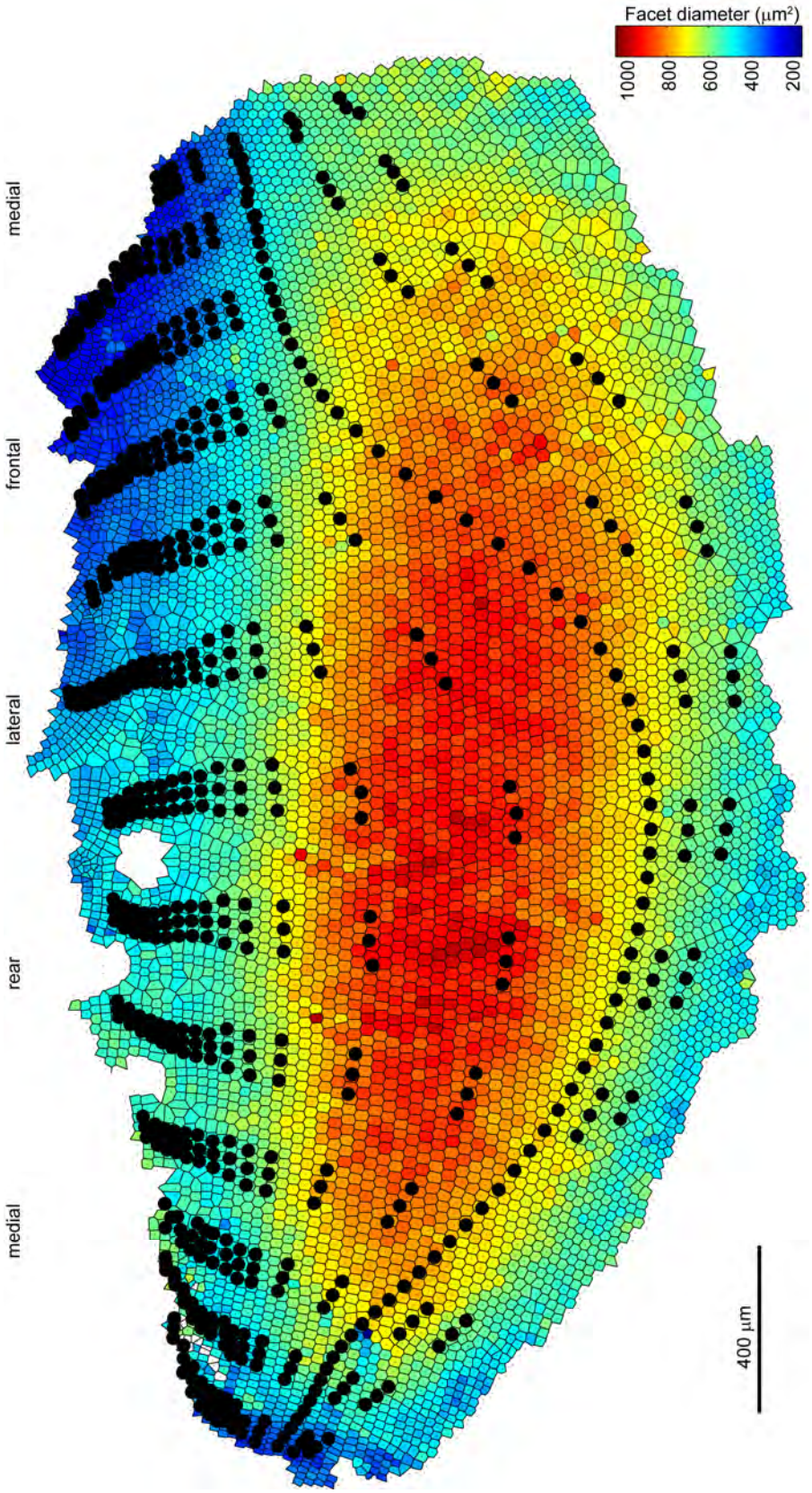
Facet diameter (μm²)
1000
800
600
400
200
medial
frontal
lateral
rear
medial
400 μm

Appendix B: Detailed analysis of frontal and lateral resolution profiles

The width and height of peak of sampling resolution depend critically on the exact measurement of the movement of a large pseudopupil within a very small angular movement of the microscope (chapter II). For instance, the pseudopupil of the eye picture in Figure II.2 (inset) spans about 40 facet rows. An error in the estimation of its centre by just one facet could lead to an error in peak resolution of 0.1 c/°. To more accurately estimate peak height and width and the difference between lateral and frontal visual field, we repeated the measurements along frontal and lateral transects in an additional three and five animals respectively. Although these animals were of very different size (14-22 mm carapace width), the resolution profiles were very similar across animals, but different between lateral and frontal visual field (Figure B.1A). We thus averaged pseudopupil positions over all five animals. Pseudopupil elevation increases with the facet row that coincides with the pseudopupil centre in an inverse sigmoidal relationship (Figure B.1A). We shifted the centre of this curve (which determines the peak of vertical resolution) to coincide in all animals and then fitted a spline through this curve (separately for frontal and lateral visual field). The stiffness of this spline critically determines height and shape of the resulting resolution curve (Figure A1B, solid lines). At high stiffness the fit is practically a linear fit through the data points resulting in a flat resolution profile and large spline residuals. With decreasing stiffness the spline follows the data more closely and the shape that the spline forces onto the resolution profile is reduced (Figure B.1B, dashed line). As a consequence, peak resolution increases until at very low stiffness the curve becomes less smooth and develops secondary peaks due to small variances in the data (Figure B.1B, dotted line). Importantly, irrespective of stiffness, the frontal peak resolution was always higher than the lateral resolution. Using an intermediate stiffness value (0.8, Figure B.1B) we finally obtained an average peak resolution of 1.54 c/° frontally and 1.36 c/° laterally (Figure B.1C).

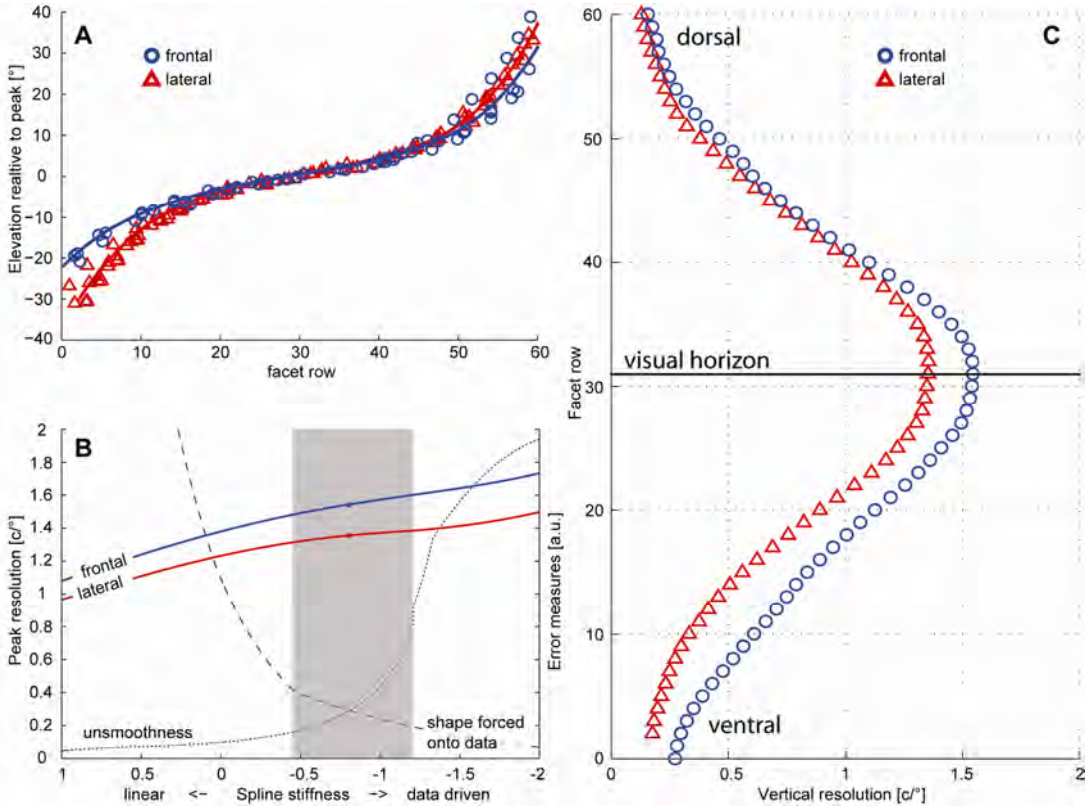

Figure B.1: Analysis of frontal and lateral resolution peaks. (A) Centre positions of pseudopupils measured along a vertical transect in the frontal (circles) and lateral (triangles) visual field of six *U. vomeris* (3 males, 3 females, cw 14-22 mm). Facet row numbers are arbitrary and were shifted to overlay smoothed 0° pseudopupil positions. Positions were fitted with a thin-plate spline using a large range of stiffness constants (here shown for -0.8 in the units of panel **B**). To adjust for lower measurement accuracy, stiffness was linearly increased with distance from 0° elevation. **(B)** Maximum resolution (solid lines) resulting from splines with different stiffness constants. Two error measures characterise the goodness of fit (dashed and dotted line, see text for explanation). Note that in the range where both errors are acceptable (grey bar), peak resolution hardly changes and that frontal resolution is always higher than lateral resolution. **(C)** Vertical sampling resolution resulting from a spline with stiffness constant -0.8 over facet row. Individual points represent individual facets along a vertical transect.

Appendix C – A brief overview of crustacean phylogeny

The following page contains a brief summary of crustacean phylogeny (following Martin and Davis, 2001) centred on fiddler crabs (genus *Uca*). In some clades I have included example species. These should include all non-fiddler-crab species that are mentioned in this thesis, mainly in chapter III, and also some species that might be familiar even to the reader who is not entirely familiar with the enormous breadth of crustacean diversity (like myself). The common names given to some of the groups are in no way official or necessarily represent the whole group. The aim is once again to give an orientation guide for those unfamiliar with crustacean taxonomy/phylogeny.

Apart from this, certain groups are marked with symbols representing, to my knowledge, all groups or species in which (i) colour vision has been proved behaviourally, (ii) spectral sensitivities have been measured intracellularly and (iii) UV pigments have been found. The relevance of the first two as relevant criteria for the analysis of a colour vision system are discussed in chapter III. Note that despite the enormous diversity within the Crustacea (over 52,000 descibed species, Martin and Davis, 2001), all three of these are exceedingly rare, especially clades in which all three have been shown.

Figure C.1 (modified after Kashiyama et al., 2009) complements this description with a schematic from a recent molecular phylogeny of crustacean opsins. It demonstrates the genetic origin of the brachyuran crabs' LWS and MWS opsins, and I have modified it to speculate where the UV opsin might originate (see chapter III).

⊗ behav. colour vision
⊗ intracell. spectral sens.
⊗ UV pigments

Subphylum **Crustacea**
⊗⊗⊗ Class **Branchiopoda**: incl. *Daphnia*, *Artemia*, *Triops*
Class **Remipedia**: blind cave inhabitants
Class **Cephalocarida** (horse-shoe shrimps)
Class **Maxillopoda**: incl. barnacles and copepods
Class **Ostracoda** (seed shrimp): small marine organism, zooplankton
Class **Malacostraca:** two thirds of extant crustacean species
Subclass **Phyllodarida**: 40 species of marine filter feeders
Subclass **Hoplocarida**
⊗⊗⊗ Order **Stomatopoda** (mantis shrimps, incl. *Pseudosquilla*, *Gonodactylus*)
Subclass **Eumalacostraca**
Superorder **Syncarida**
⊗⊗ Superorder **Peracarida**: large group incl. Isopoda (incl. *Ligia*) and Amphipoda
Superorder **Eucarida**
Order **Euphausiacea** (krill)
Order **Amphionidacea**: only one planktonic species
Order **Decapoda**
Suborder **Dendrobranchiata** (prawns)
Suborder **Pleocyemata**
Infraorder **Stenopodidea**
⊗⊗ Infraorder **Caridea** (shrimp, incl. *Janicella*, *Oplophorus* and *Crangon*)
⊗ Infraorder **Astacidea**: incl. Nephropidae (lobsters), Astacoidea (e.g. *Orconectes* and *Procambarus*) and Parastacoedea (crayfish), *Cherax* (yabby)
Infraorder **Thalassinidea**: incl *Trypaea* (marine yabby)
⊗ Infraorder **Palinura**: incl Palinuridae (spiny lobsters, incl. *Panulirus*)
⊗ Infraorder **Anomura**: incl. Paguroidea (hermit crabs)
Infraorder **Brachyura** (crabs)
Section **Dromiacea**
Section **Eubrachyura**
⊗ Subsection **Heterotremata**: incl *Cancer*, *Carcinus*, *Callinectes*, *Scylla* (mud crab)
Subsection **Thoracotremata**
Superfamily **Pinnotheroidea** (pea crabs)
⊗ Superfamily **Grapsoidea**: incl semi-terrestrial crabs *Leptograpsus*, *Hemigrapsus*, *Pachygrapsus*, *Sesarma*, *Chasmagnathus*, *Gecarcinus*
Superfamily **Ocypodoidea**
Family **Camptandriidae**
Family **Mictyridae** (soldier crabs)
Family **Palicidae** (stilt crabs)
Family **Ocypodidae**
Subfamily **Dotillinae**: incl *Scopimera* (sand bubblers)
Subfamily **Heloecinae**: incl. *Heloecius*
Subfamily **Macrophthalminae:** incl. *Macrophthalmus*
Subfamily **Ocypodinae**
Genus ***Ocypode*** (ghost crabs)
Genus ***Ucides***
⊗⊗⊗ Genus ***Uca*** (fiddler crabs)

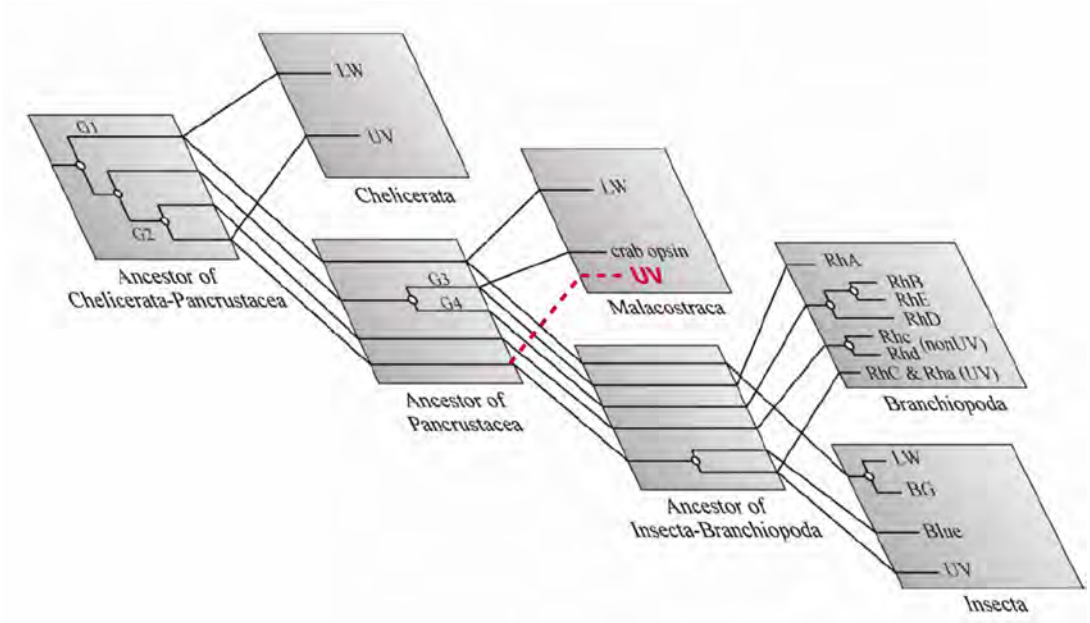

Figure C.1: Hypothetical origin of the crab UV opsin. Figure modified after Kashiyama et al., (2009). While the insect UV and insect blue receptors have a common ancestor with the UV in Chelicerata and Branchiopoda, the Malacostraca (incl. crabs) are assumed to have lost this pigment. The results of this theses (chapter III) challenge this hypothesis.

Appendix D – Photoreceptor spectral sensitivities

This appendix contains the analysis from raw data to initial fits of visual pigment templates for all 21 photoreceptors I recorded spectral sensitivities from. A detailed description of the analysis can be found in paragraph III.4.2.

Figures D.1-D.21: Spectral sensitivity analysis in *Uca vomeris* photoreceptors. (A) Evaluation of spectral runs. Means (± s.e.m.) of scaled spectral response curves (blue for upwards, red for downwards sweeps) are overlayed on mean voltage traces (grey and black lines, off-set to position response peaks at corresponding wavelengths). Approximate response latency between light stimulus (black bars) and response peak (black lines) is shown for four example wavelengths. **(B)** Equivalent analysis for intensity runs. A sigmoidal V/log(I)-function was fitted to the responses (dotted line) and applied to transform spectral responses into sensitivities. **(C)** The spectral sensitivity function (black dots ± s.e.m.) with two model fits: One with the best fitting single photopigment (plus the UV pigment in PR8,22,23, dashed red line), and a second one assuming two pigments at 410 nm and 460 nm (blue line, again plus UV pigment with λ_{max} at 345 nm in UV cells).

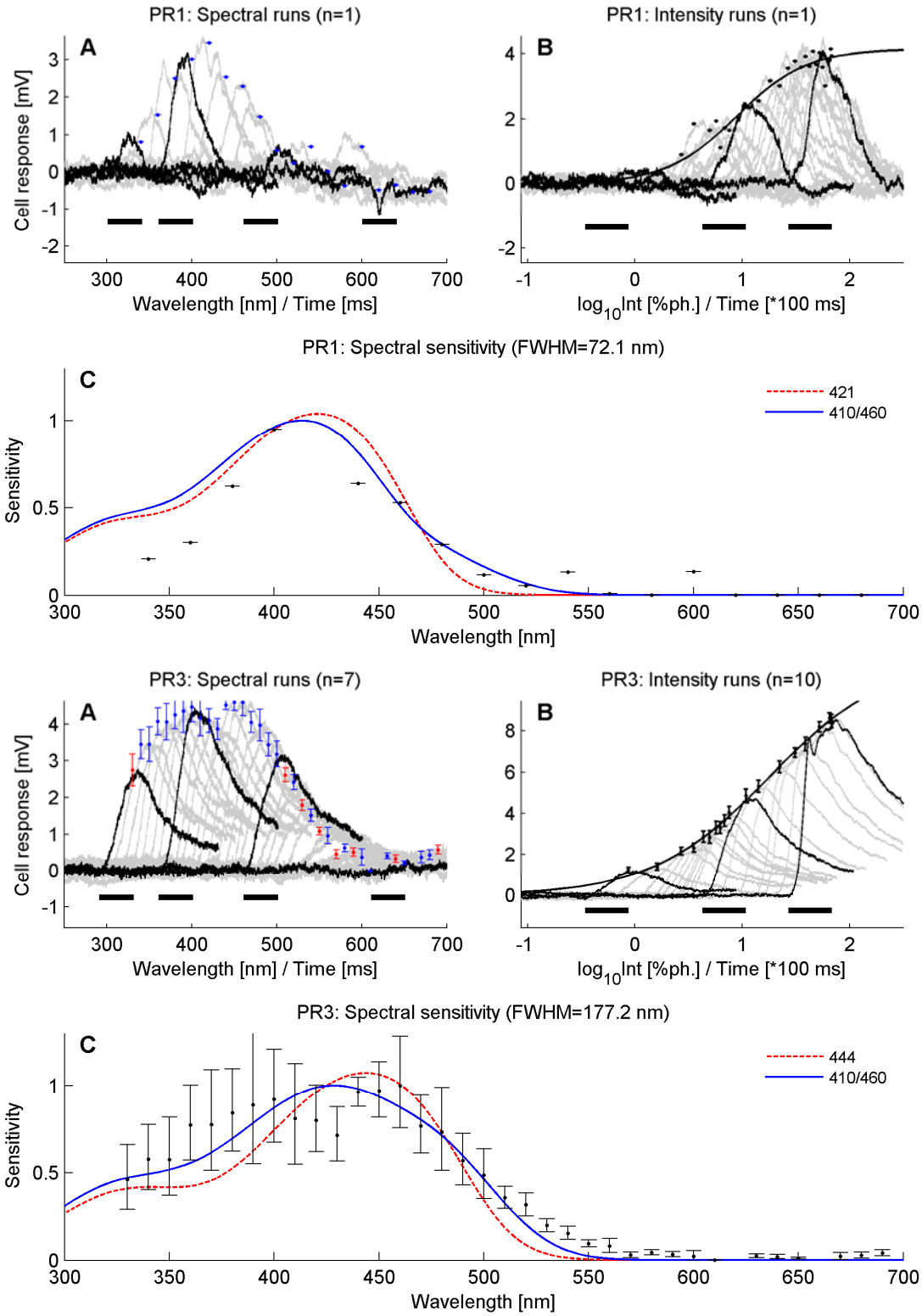
PR1: Spectral runs (n=1)
A
Cell response [mV]
Wavelength [nm] / Time [ms]
PR1: Intensity runs (n=1)
B
log10Int [%ph.] / Time [*100 ms]
PR1: Spectral sensitivity (FWHM=72.1 nm)
C
421
410/460
Sensitivity
Wavelength [nm]
PR3: Spectral runs (n=7)
A
Cell response [mV]
Wavelength [nm] / Time [ms]
PR3: Intensity runs (n=10)
B
log10Int [%ph.] / Time [*100 ms]
PR3: Spectral sensitivity (FWHM=177.2 nm)
C
444
410/460
Sensitivity
Wavelength [nm]

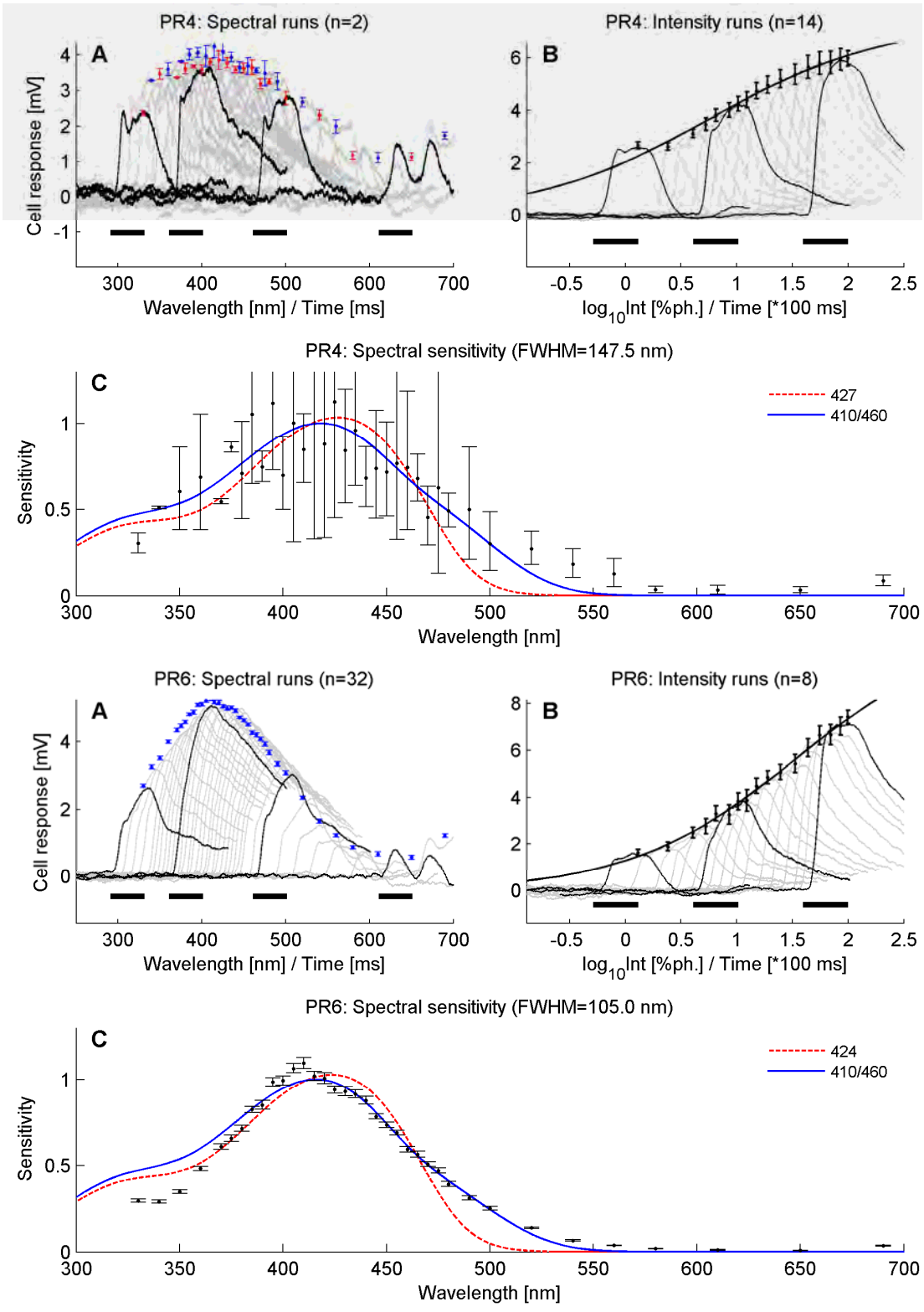
PR4: Spectral runs (n=2)
A
Cell response [mV]
Wavelength [nm] / Time [ms]
PR4: Intensity runs (n=14)
B
log10Int [%ph.] / Time [*100 ms]
PR4: Spectral sensitivity (FWHM=147.5 nm)
C
427
410/460
Sensitivity
Wavelength [nm]
PR6: Spectral runs (n=32)
A
Cell response [mV]
Wavelength [nm] / Time [ms]
PR6: Intensity runs (n=8)
B
log10Int [%ph.] / Time [*100 ms]
PR6: Spectral sensitivity (FWHM=105.0 nm)
C
424
410/460
Sensitivity
Wavelength [nm]

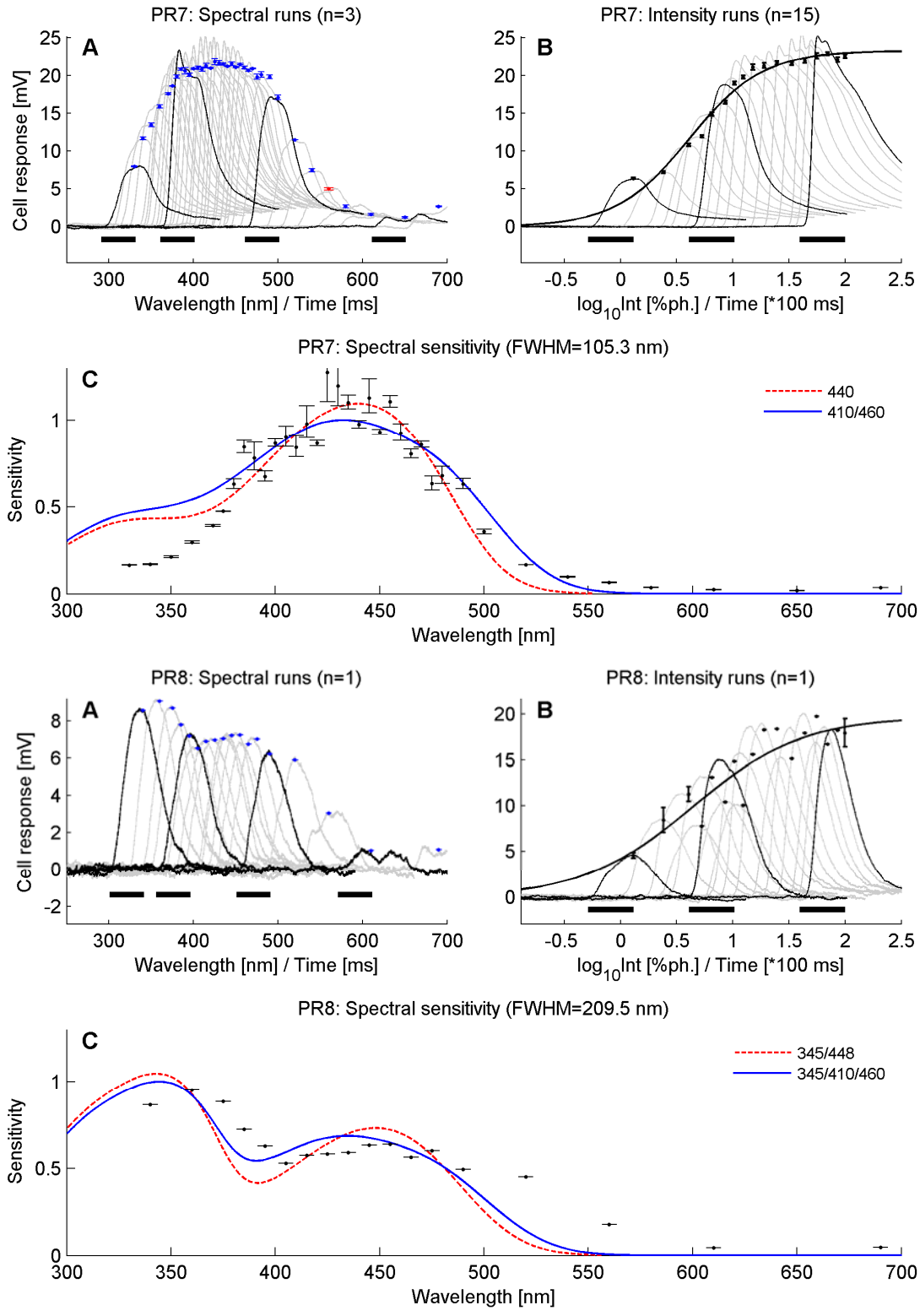
PR7: Spectral runs (n=3)
A
Cell response [mV]
Wavelength [nm] / Time [ms]
PR7: Intensity runs (n=15)
B
log10Int [%ph.] / Time [*100 ms]
PR7: Spectral sensitivity (FWHM=105.3 nm)
C
440
410/460
Sensitivity
Wavelength [nm]
PR8: Spectral runs (n=1)
A
Cell response [mV]
Wavelength [nm] / Time [ms]
PR8: Intensity runs (n=1)
B
log10Int [%ph.] / Time [*100 ms]
PR8: Spectral sensitivity (FWHM=209.5 nm)
C
345/448
345/410/460
Sensitivity
Wavelength [nm]

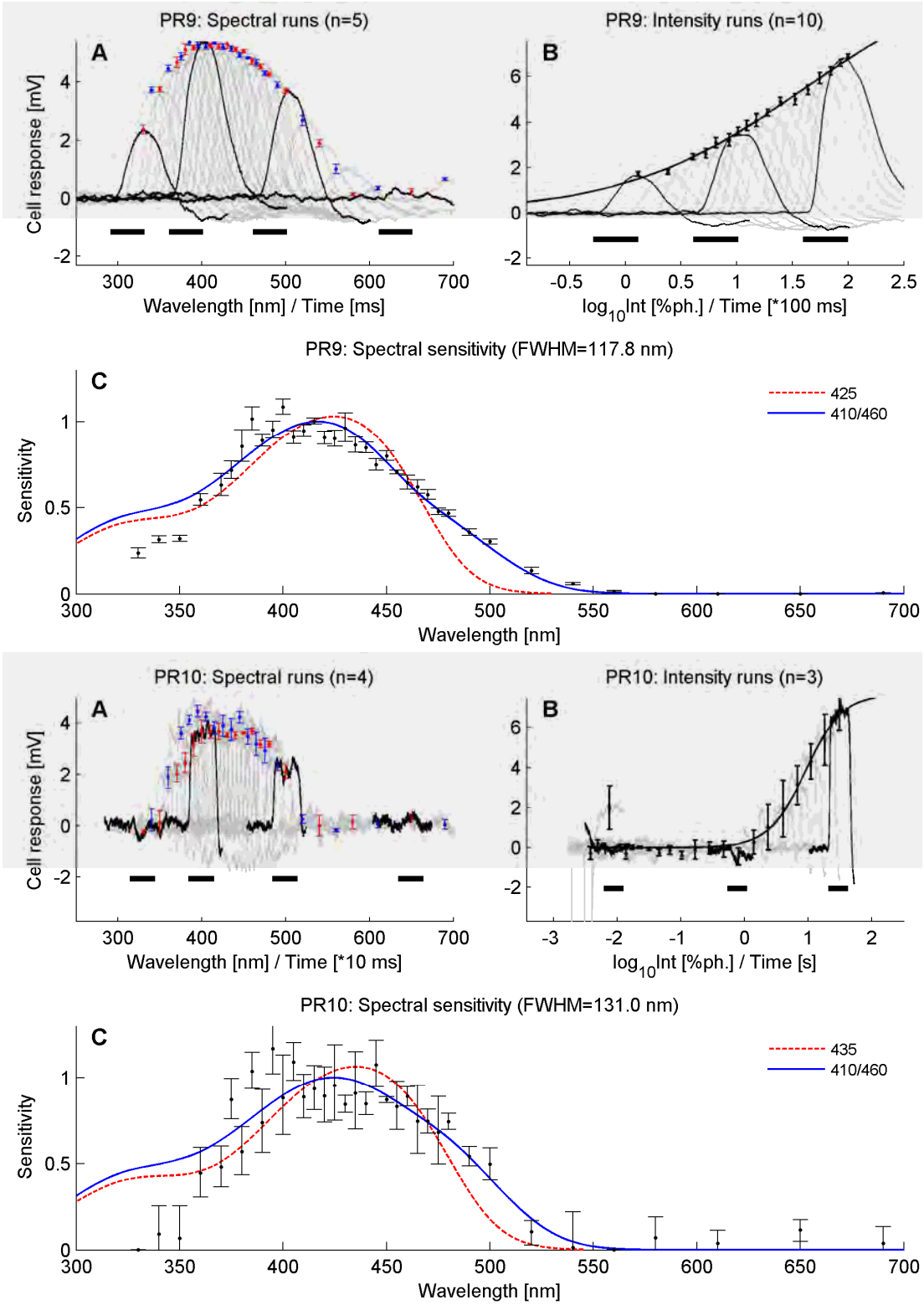
PR9: Spectral runs (n=5)
A
Cell response [mV]
Wavelength [nm] / Time [ms]
PR9: Intensity runs (n=10)
B
log10Int [%ph.] / Time [*100 ms]
PR9: Spectral sensitivity (FWHM=117.8 nm)
C
425
410/460
Sensitivity
Wavelength [nm]
PR10: Spectral runs (n=4)
A
Cell response [mV]
Wavelength [nm] / Time [*10 ms]
PR10: Intensity runs (n=3)
B
log10Int [%ph.] / Time [s]
PR10: Spectral sensitivity (FWHM=131.0 nm)
C
435
410/460
Sensitivity
Wavelength [nm]

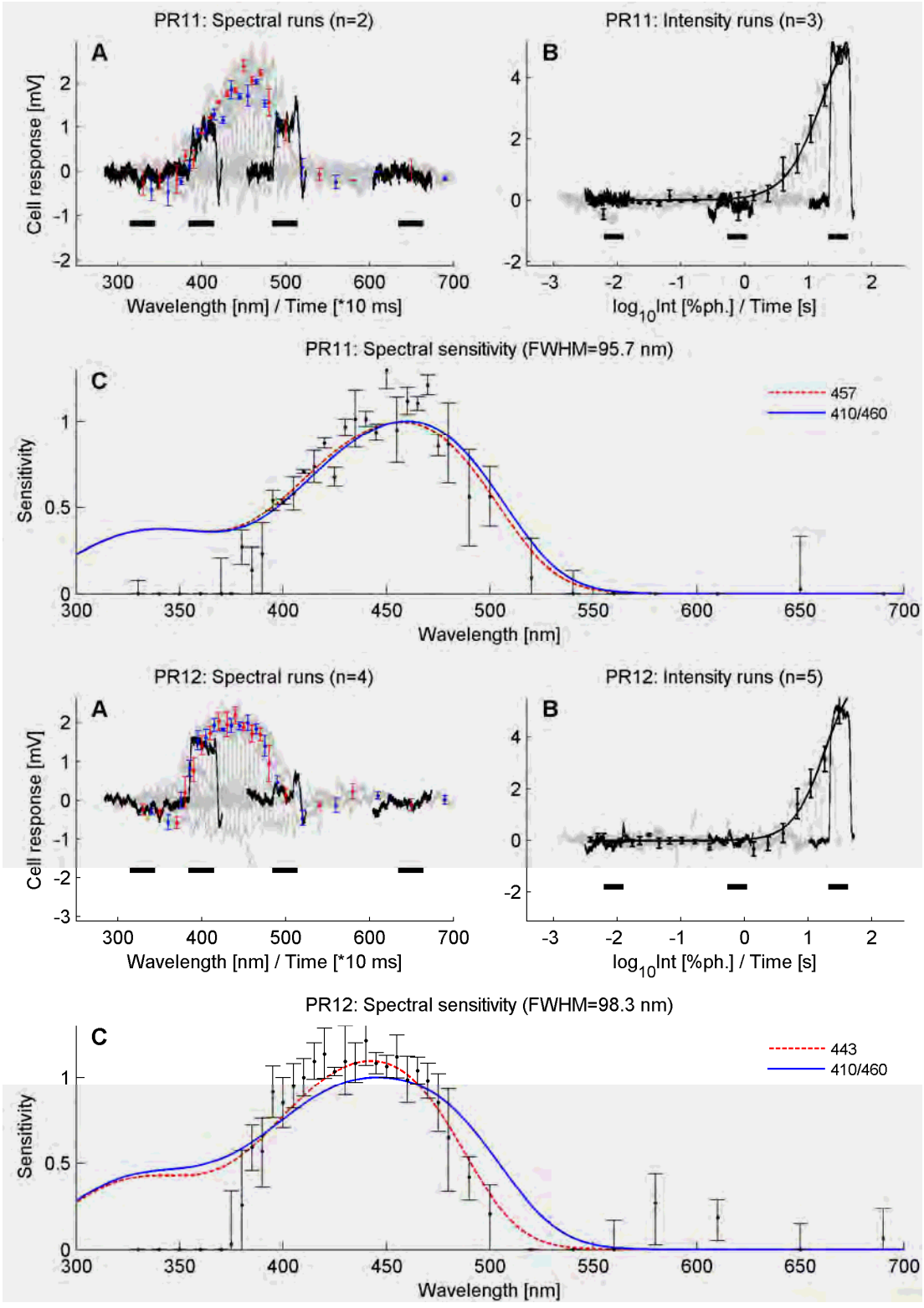
PR11: Spectral runs (n=2)
A
Cell response [mV]
Wavelength [nm] / Time [*10 ms]
PR11: Intensity runs (n=3)
B
log10Int [%ph.] / Time [s]
PR11: Spectral sensitivity (FWHM=95.7 nm)
C
457
410/460
Sensitivity
Wavelength [nm]
PR12: Spectral runs (n=4)
A
Cell response [mV]
Wavelength [nm] / Time [*10 ms]
PR12: Intensity runs (n=5)
B
log10Int [%ph.] / Time [s]
PR12: Spectral sensitivity (FWHM=98.3 nm)
C
443
410/460
Sensitivity
Wavelength [nm]

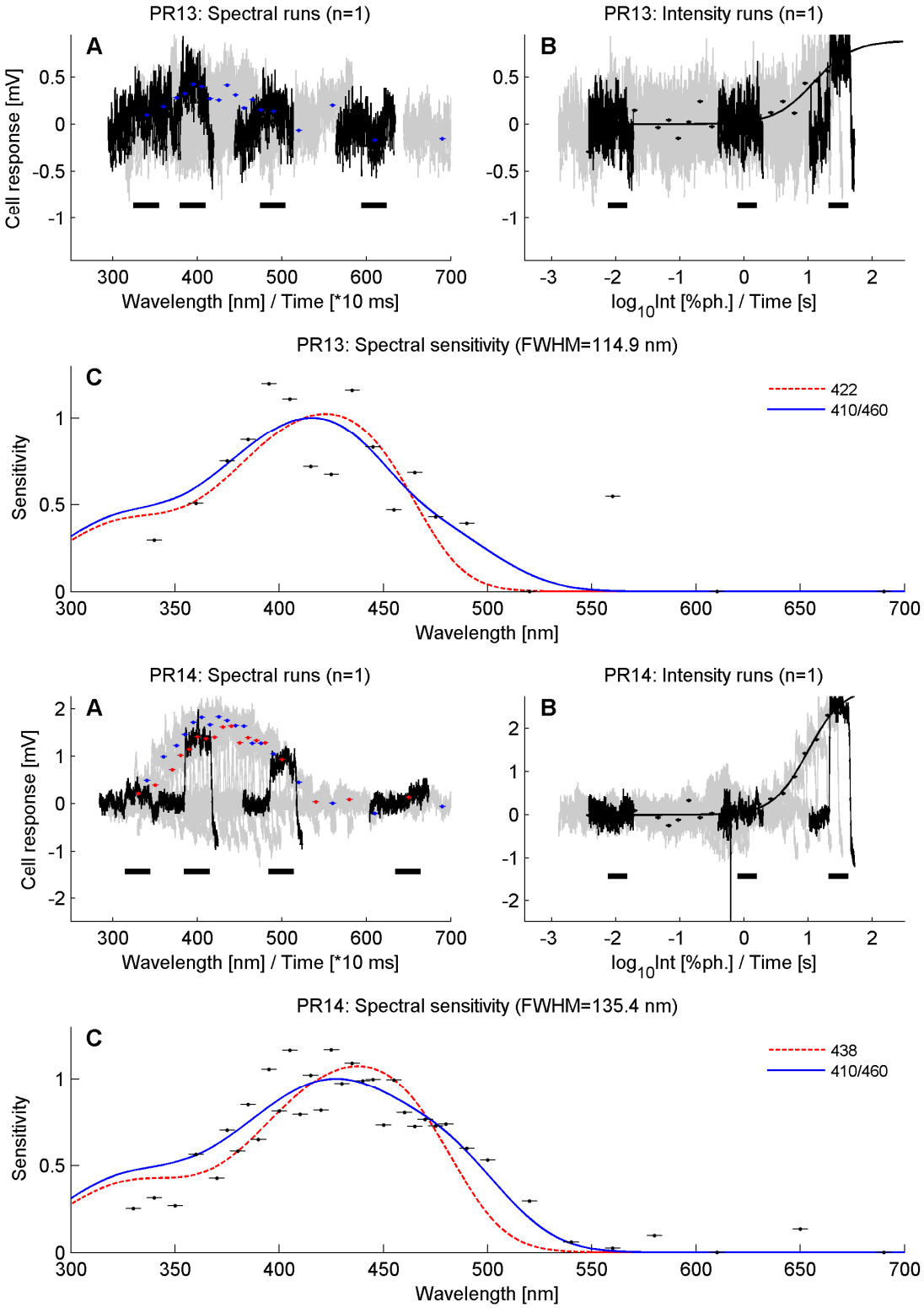
PR13: Spectral runs (n=1)
A
Cell response [mV]
Wavelength [nm] / Time [*10 ms]
PR13: Intensity runs (n=1)
B
log10Int [%ph.] / Time [s]
PR13: Spectral sensitivity (FWHM=114.9 nm)
C
422
410/460
Sensitivity
Wavelength [nm]
PR14: Spectral runs (n=1)
A
Cell response [mV]
Wavelength [nm] / Time [*10 ms]
PR14: Intensity runs (n=1)
B
log10Int [%ph.] / Time [s]
PR14: Spectral sensitivity (FWHM=135.4 nm)
C
438
410/460
Sensitivity
Wavelength [nm]

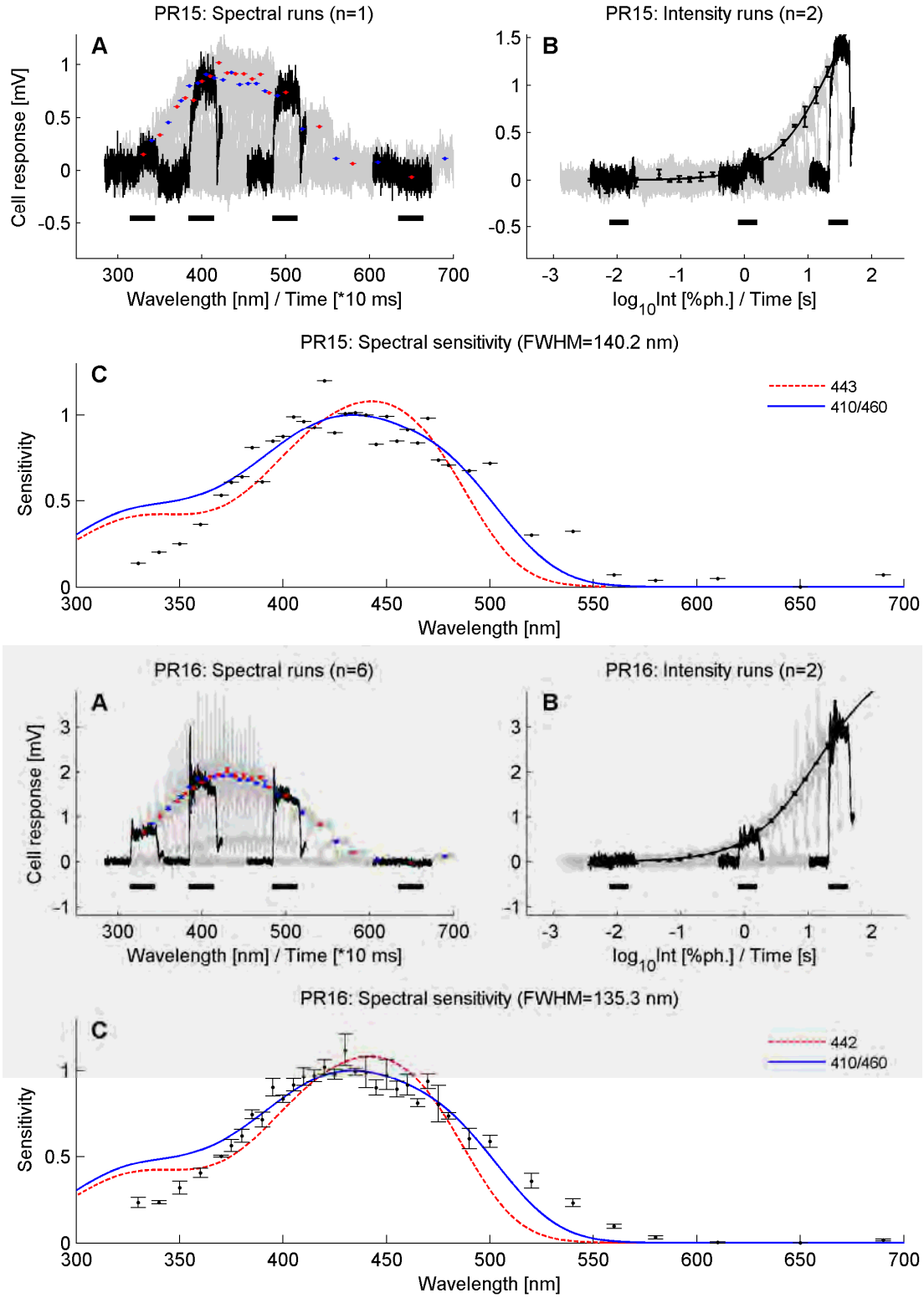
PR15: Spectral runs (n=1)
A
Cell response [mV]
Wavelength [nm] / Time [*10 ms]
PR15: Intensity runs (n=2)
B
log10Int [%ph.] / Time [s]
PR15: Spectral sensitivity (FWHM=140.2 nm)
C
443
410/460
Sensitivity
Wavelength [nm]
PR16: Spectral runs (n=6)
A
Cell response [mV]
Wavelength [nm] / Time [*10 ms]
PR16: Intensity runs (n=2)
B
log10Int [%ph.] / Time [s]
PR16: Spectral sensitivity (FWHM=135.3 nm)
C
442
410/460
Sensitivity
Wavelength [nm]

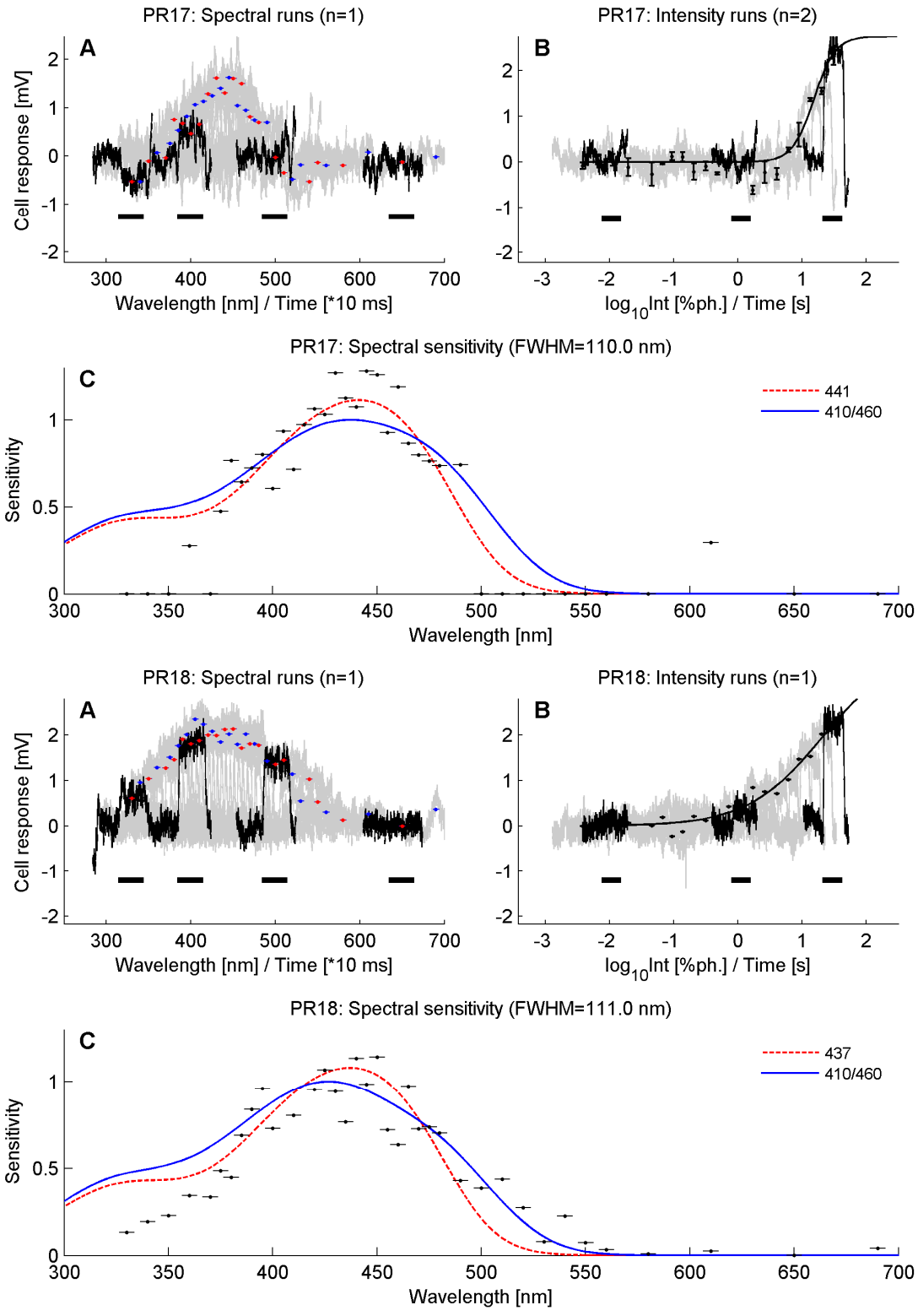
PR17: Spectral runs (n=1)
A
Cell response [mV]
Wavelength [nm] / Time [*10 ms]
PR17: Intensity runs (n=2)
B
log10Int [%ph.] / Time [s]
PR17: Spectral sensitivity (FWHM=110.0 nm)
C
441
410/460
Sensitivity
Wavelength [nm]
PR18: Spectral runs (n=1)
A
Cell response [mV]
Wavelength [nm] / Time [*10 ms]
PR18: Intensity runs (n=1)
B
log10Int [%ph.] / Time [s]
PR18: Spectral sensitivity (FWHM=111.0 nm)
C
437
410/460
Sensitivity
Wavelength [nm]

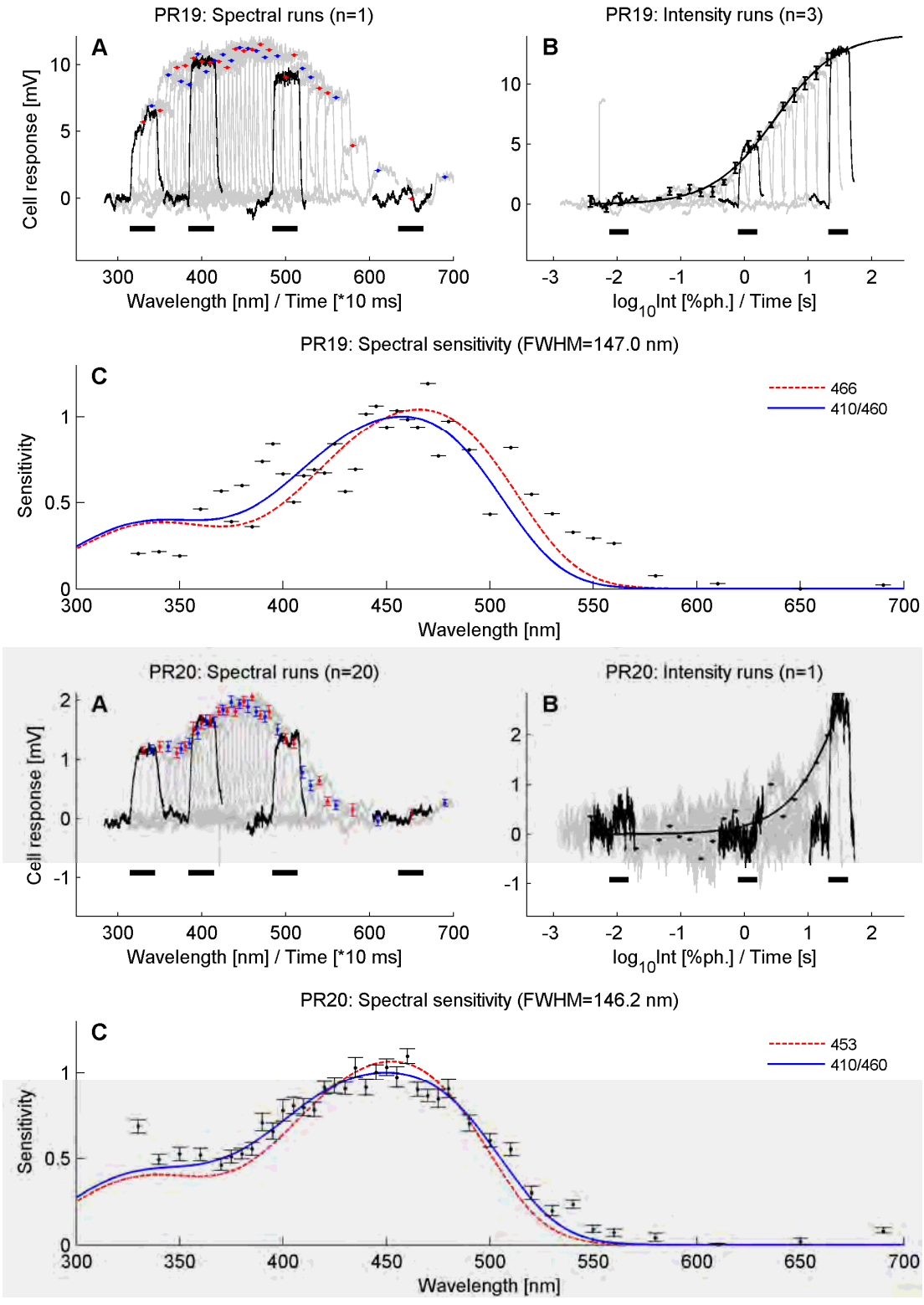
PR19: Spectral runs (n=1)
A
Cell response [mV]
Wavelength [nm] / Time [*10 ms]
PR19: Intensity runs (n=3)
B
log10Int [%ph.] / Time [s]
PR19: Spectral sensitivity (FWHM=147.0 nm)
C
466
410/460
Sensitivity
Wavelength [nm]
PR20: Spectral runs (n=20)
A
Cell response [mV]
Wavelength [nm] / Time [*10 ms]
PR20: Intensity runs (n=1)
B
log10Int [%ph.] / Time [s]
PR20: Spectral sensitivity (FWHM=146.2 nm)
C
453
410/460
Sensitivity
Wavelength [nm]

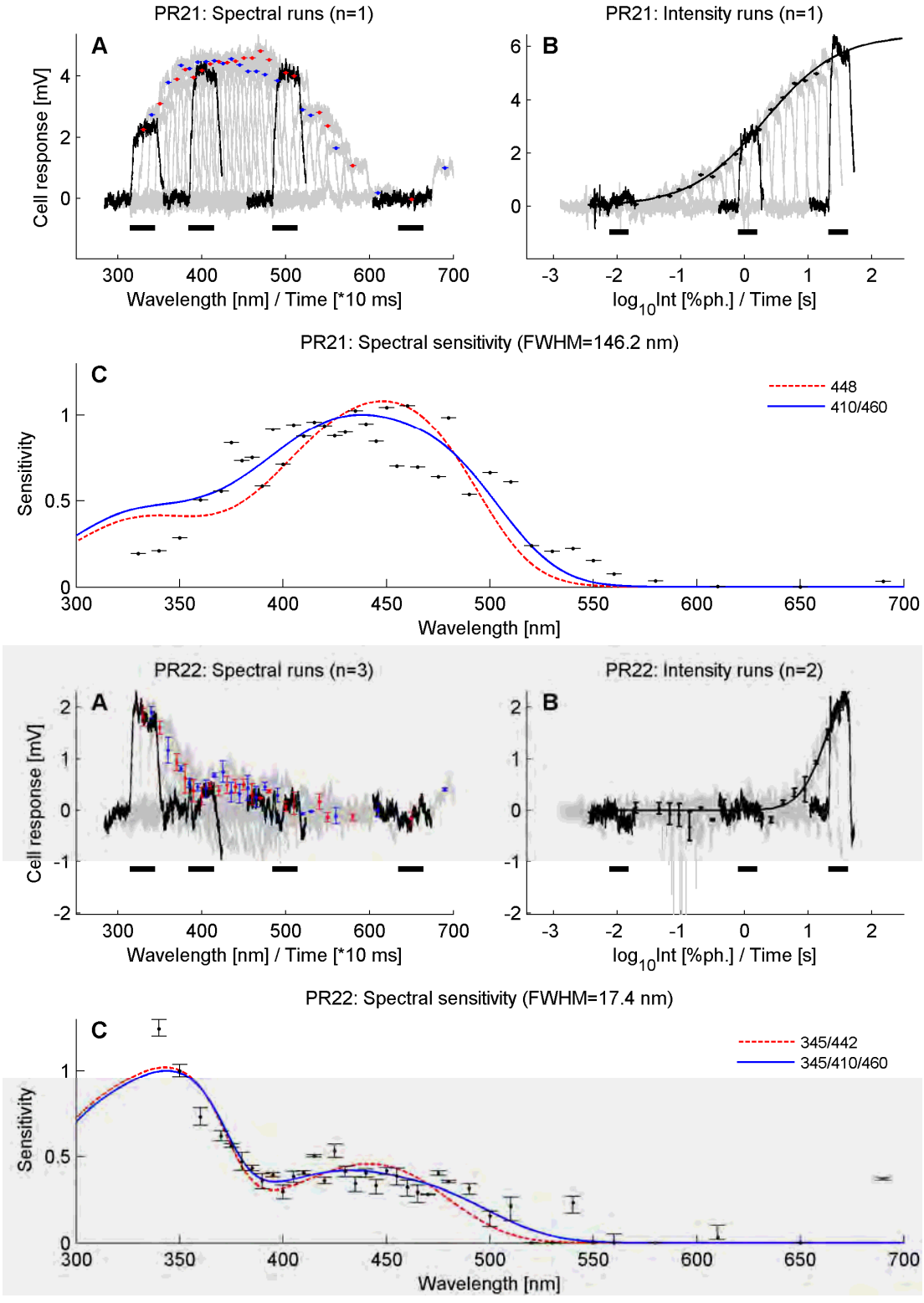
PR21: Spectral runs (n=1)
A
Cell response [mV]
Wavelength [nm] / Time [*10 ms]
PR21: Intensity runs (n=1)
B
log10Int [%ph.] / Time [s]
PR21: Spectral sensitivity (FWHM=146.2 nm)
C
448
410/460
Sensitivity
Wavelength [nm]
PR22: Spectral runs (n=3)
A
Cell response [mV]
Wavelength [nm] / Time [*10 ms]
PR22: Intensity runs (n=2)
B
log10Int [%ph.] / Time [s]
PR22: Spectral sensitivity (FWHM=17.4 nm)
C
345/442
345/410/460
Sensitivity
Wavelength [nm]

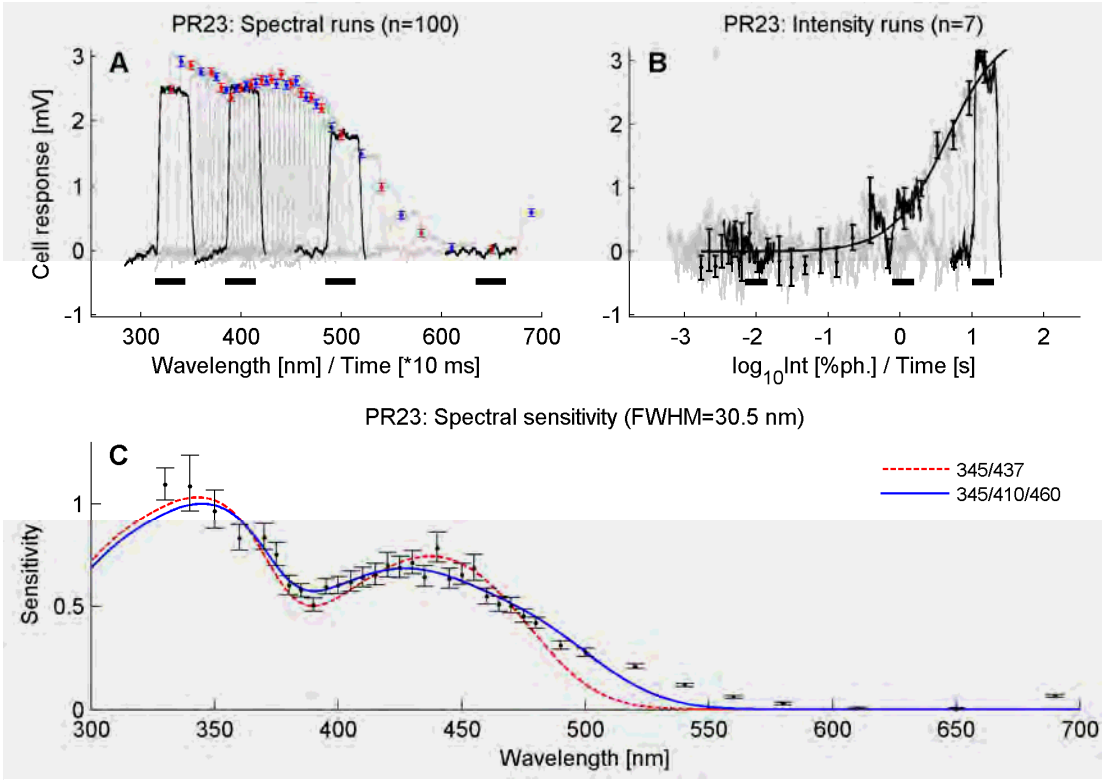
PR23: Spectral runs (n=100)
A
Cell response [mV]
Wavelength [nm] / Time [*10 ms]
PR23: Intensity runs (n=7)
B
log10Int [%ph.] / Time [s]
PR23: Spectral sensitivity (FWHM=30.5 nm)
C
345/437
345/410/460
Sensitivity
Wavelength [nm]

Appendix E – Mathematical details

E.1 A hyperbolic function is equivalent to a sigmoidal function

A proof of the equivalence of Equations III.1 and III.2:

$$\frac{V}{V_{\max}} = \frac{1}{1+\frac{e^{-\ln(I)*n}}{b_1}} = \frac{1}{1+\frac{(e^{\ln(I)})^{-n}}{b_1}} = \frac{1}{1+\frac{(I)^{-n}}{b_1}} = \frac{1}{1+\frac{1}{b_1 I^n}} = \frac{1}{\frac{b_1 I^n+1}{b_1 I^n}} = \frac{b_1 I^n}{b_1 I^n+1} = \frac{(b_2 I)^n}{(b_2 I)^n+1},$$

(Eq. III.1) (Eq. III.2)

where the fit parameter n is the same in both fits and $b_2 = ln(b_1)$.

E.2 Full mathematical detail of two-pigment analysis

To examine which combination of two pigments gives the best overall fit to our measured spectral sensitivities, we determined the normalised average residual. For this purpose the spectral sensitivities of all cells with more than one spectral run were fitted using Equations III.6 and III.7 under the following rules and assumption:

- Rhabdom length l = 150 μm, absorption coefficient α = 0.006 μm^{-1}
- Only residuals above a cut-off wavelength were considered to limit the fit to the peak and the long-wavelength tail of spectral sensitivities, as the UV-tail can be extremely variably and presumably heavily influenced by optical filters. The cut-off wavelength λ_{co} was set to 20 nm below the peak of the shorter-wavelength fitted pigment, or to 370 nm, whichever one was lower.
- The normalised residual $\bar{\varepsilon}$ for each fit was then calculated as

$$\bar{\varepsilon} = \frac{1}{n}\sum_{\lambda>\lambda_{co}}\left(\frac{\varepsilon(\lambda)}{S(\lambda_{\max})}\right)^2 \qquad \text{(E.II)}$$

where $\varepsilon(\lambda)$ are the residuals, normalised by $S(\lambda_{max})$, the maximum of the fitted sensitivity function, and n is the number of residuals above cut-off.

Appendix F – Additional bird examples

Five more examples of bird approaches are presented. For a detailed description of the experimental setup and the parameters plotted please see chapter IV.

Figure F.1-5: Flight paths. (A) The flight path during the recording, dots indicate position every 200 ms. The saturation of the trace codes the relative number of crabs active on the surface (>5 cm away from their burrow). Elevation **(B)**, horizontal retinal speed **(C)**, vertical retinal speed **(D)** and contrast changes **(E)** are displayed over time. The grey line in panels B-E indicates the number of active crabs at any time, the maximum of crabs during the experiment is given by the grey number on the right side of each panel. A magenta circle indicates home a run response of a crab, a magenta cross a burrow entry.

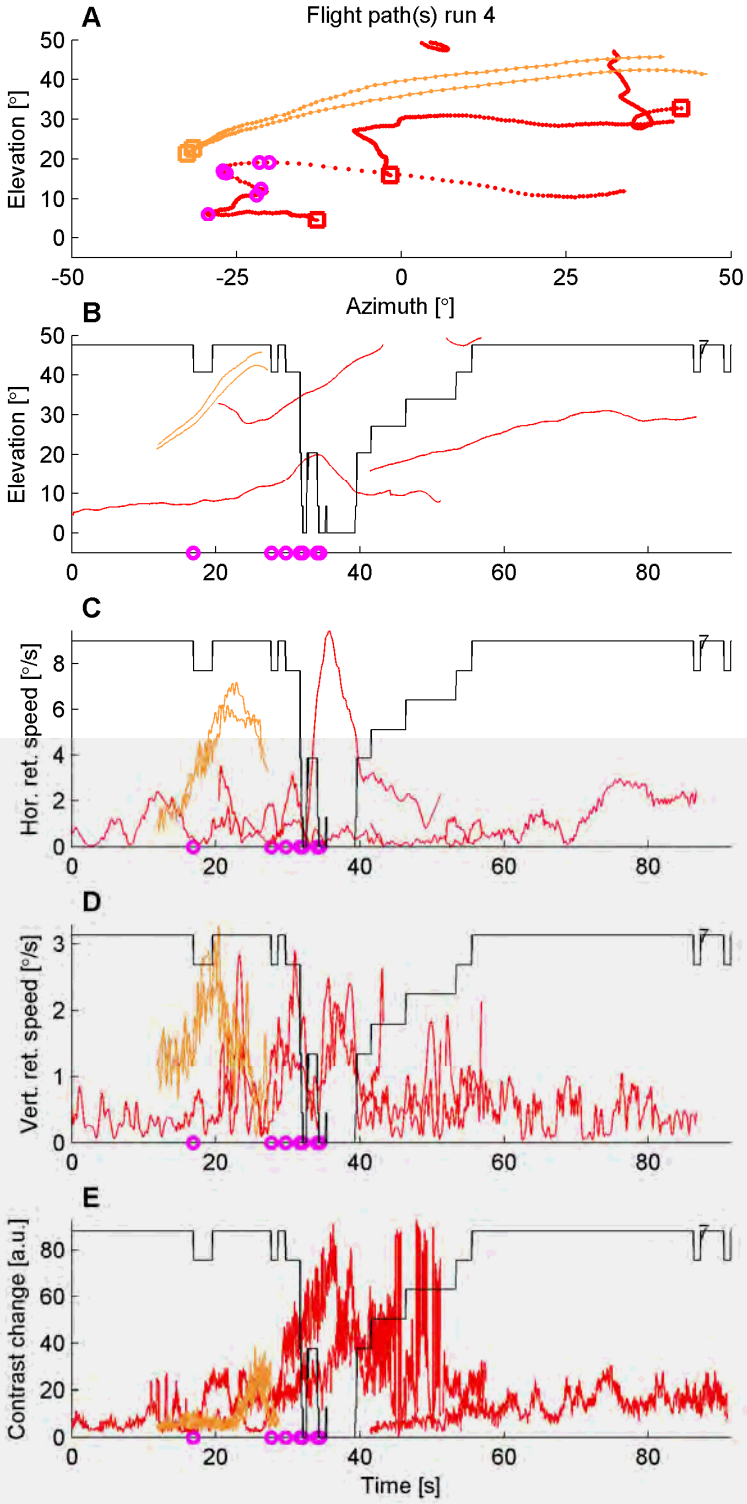
A
Flight path(s) run 4
Elevation [°]
Azimuth [°]
B
Elevation [°]
C
Hor. ret. speed [°/s]
D
Vert. ret. speed [°/s]
E
Contrast change [a.u.]
Time [s]

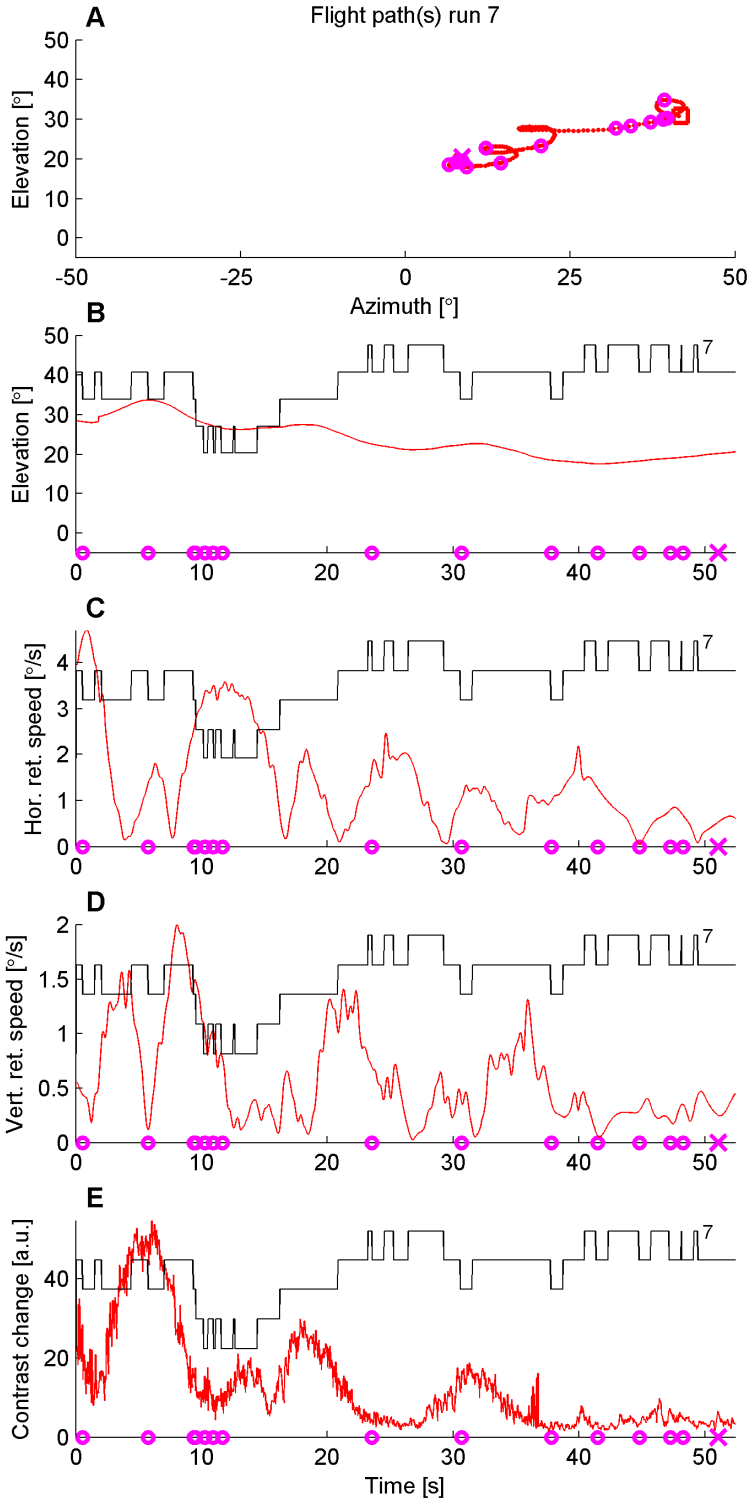
A
Flight path(s) run 7
Elevation [°]
Azimuth [°]
B
Elevation [°]
C
Hor. ret. speed [°/s]
D
Vert. ret. speed [°/s]
E
Contrast change [a.u.]
Time [s]

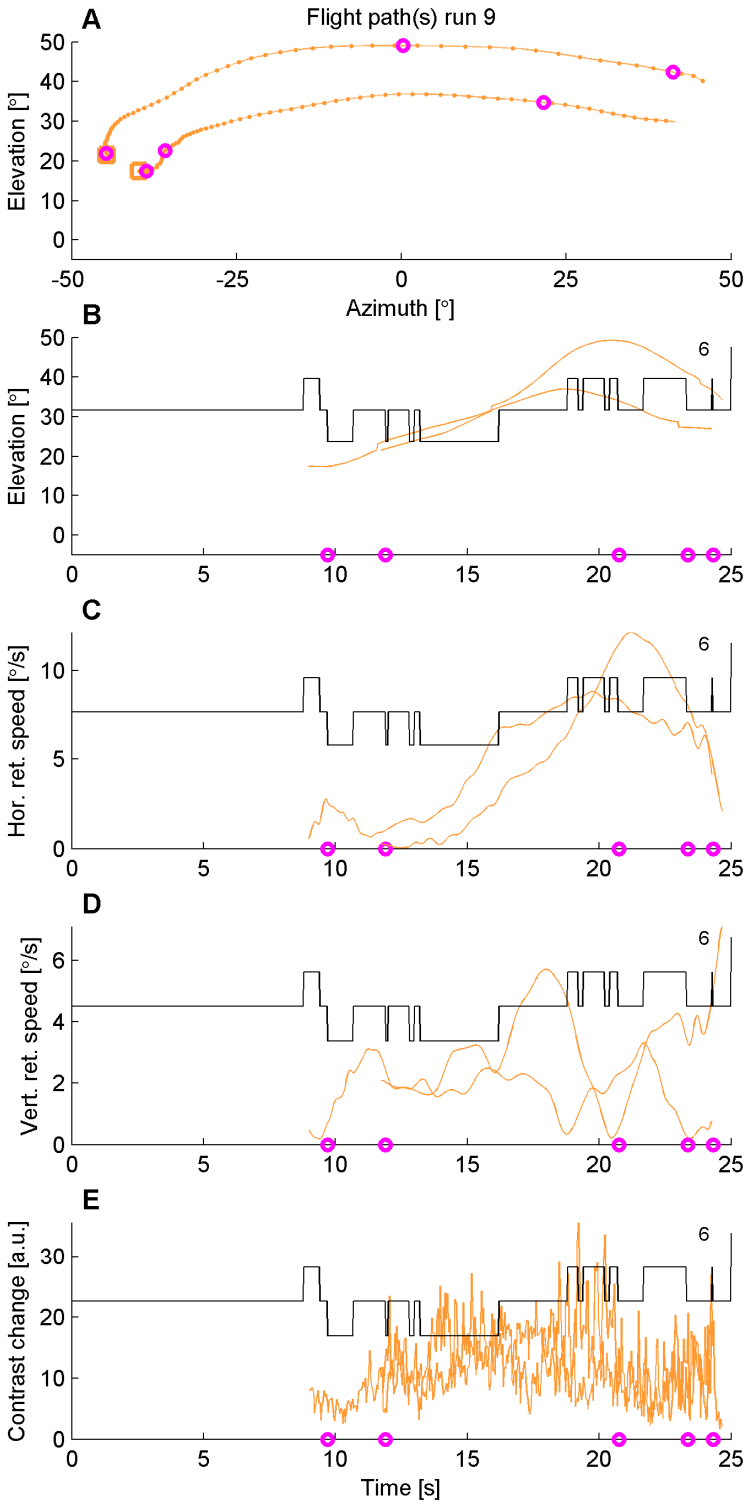
A
Flight path(s) run 9
Elevation [°]
Azimuth [°]
B
Elevation [°]
6
C
Hor. ret. speed [°/s]
6
D
Vert. ret. speed [°/s]
6
E
Contrast change [a.u.]
6
Time [s]

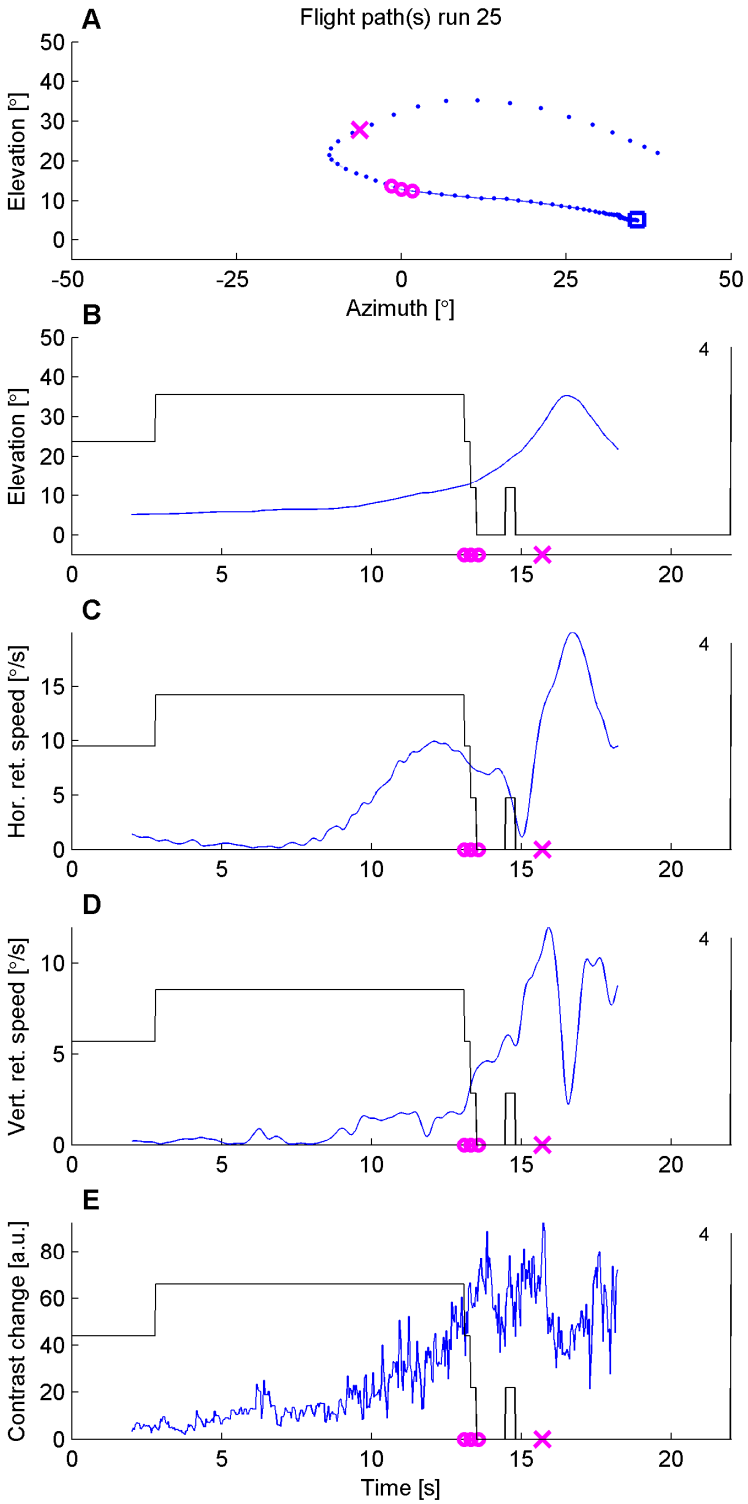
A
Flight path(s) run 25
Elevation [°]
Azimuth [°]
B
Elevation [°]
C
Hor. ret. speed [°/s]
D
Vert. ret. speed [°/s]
E
Contrast change [a.u.]
Time [s]
4

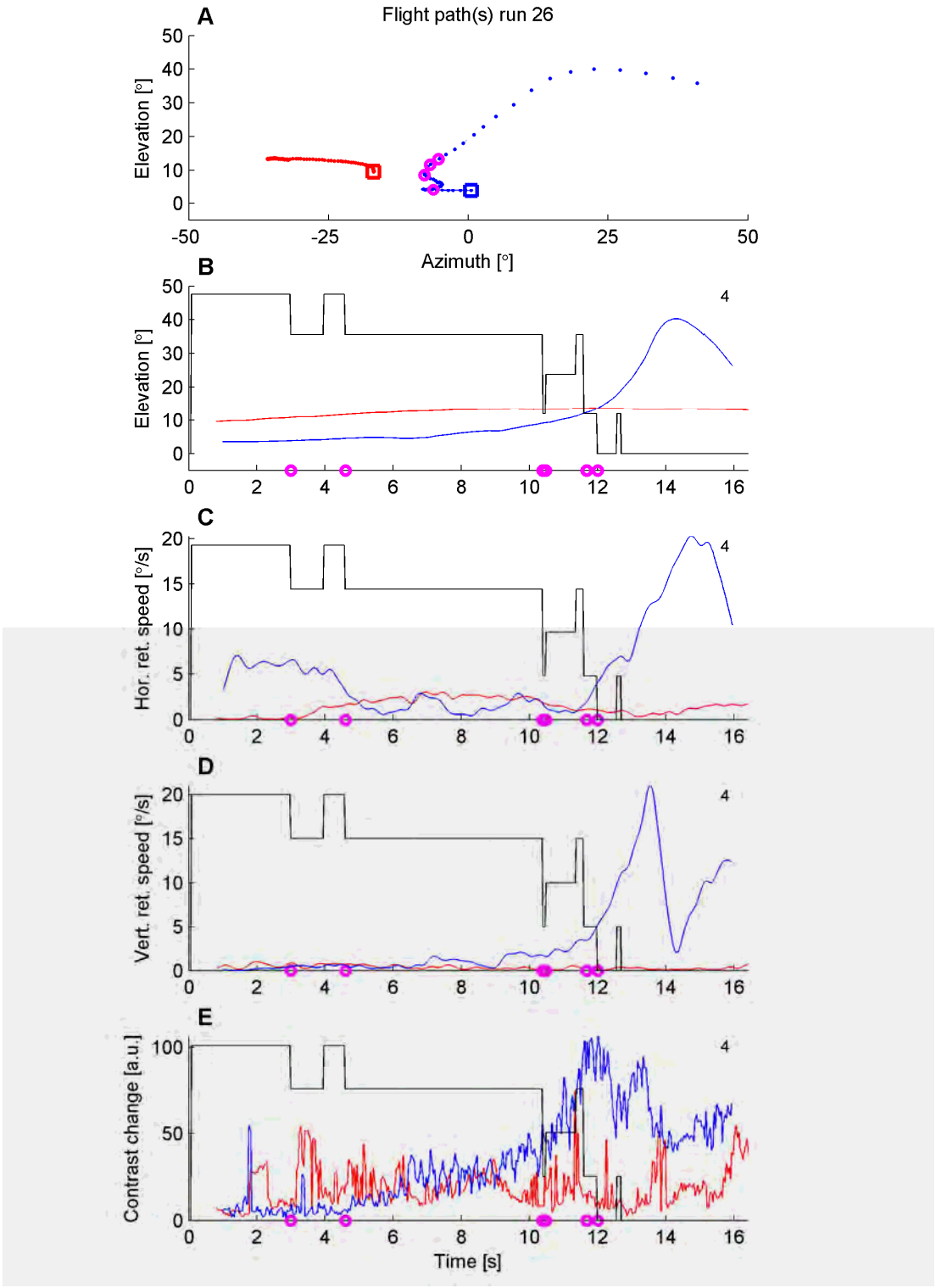
A
Flight path(s) run 26
Elevation [°]
Azimuth [°]
B
Elevation [°]
C
Hor. ret. speed [°/s]
D
Vert. ret. speed [°/s]
E
Contrast change [a.u.]
Time [s]
4

References

Alkaladi, A. (2008). The functional anatomy of the fiddler crab compound eye, PhD thesis. Canberra: The Australian National University.

Alkaladi, A., Anderson, M. C., Deeb, S., Fu, L., Hemmi, J. M., Maleszka, R., Maelszka, J., Das, D. and Zeil, J. (in prep.).

Altevogt, R. and von Hagen, H. O. (1964). Über die Orientierung von *Uca tangeri* (Eydoux) im Freiland. *Z. Morph. Ökol. Tiere* **53**, 636-656.

Arikawa, K. (2003). Spectral organization of the eye of a butterfly, *Papilio*. *J. Comp. Physiol. (A)* **189**, 791-800.

Backwell, P. R. Y. and Passmore, N. I. (1996). Time constraints and multiple choice criteria in the sampling behaviour and mate choice of the fiddler crab, *Uca annulipes*. *Behav. Ecol. Sociobiol.* **38**, 407-416.

Baddeley, R., Abbott, L. F., Booth, M. C., Sengpiel, F., Freeman, T., Wakeman, E. A. and Rolls, E. T. (1997). Responses of neurons in primary and inferior temporal visual cortices to natural scenes. *Proc. R. Soc. Lond. B* **264**, 1775-1783.

Barlow, H. B. (1952). The size of ommatidia in apposition eyes. *J. Exp. Biol.* **29**, 667-674.

Berglund, A., Bisazza, A. and Pilastro, A. (1996). Armaments and ornaments: An evolutionary explanation of traits of dual utility. *Biol. J. Linnean Soc.* **58**, 385-399.

Berón de Astrada, M., Sztarker, J. and Tomsic, D. (2001). Visual interneurons of the crab *Chasmagnathus* studied by intracellular recordings *in vivo*. *J. Comp. Physiol. (A)* **187**, 37-44.

Boeddeker, N., Lindemann, J. P., Egelhaaf, M. and Zeil, J. (2005). Responses of blowfly motion-sensitive neurons to reconstructed optic flow along outdoor flight paths. *J. Comp. Physiol. (A)* **191**, 1143-1155.

Bouskila, A. and Blumstein, D. T. (1992). Rules of thumb for predation hazard assessment: Predictions from a dynamic model. *Am. Nat.* **139**, 161-176.

Brinkworth, R. S. A., Mah, E. L., Gray, J. P. and O'Carroll, D. C. (2008). Photoreceptor processing improves salience facilitating small target detection in cluttered scenes. *J. Vis.* **8**, 8.1-17.

Burkhardt, D., Darnhofer-Demar, B. and Fischer, K. (1973). Zum binokularen Entfernungssehen der Insekten. *J. Comp. Physiol. (A)* **87**, 165-188.

Burton, B. G., Tatler, B. W. and Laughlin, S. B. (2001). Variations in photoreceptor response dynamics across the fly retina. *J. Neurophysiol.* **86**, 950-960.

Chittka, L. (1996). Does bee color vision predate the evolution of flower color? *Naturwissenschaften* **83**, 136-138.

Christy, J. H. (1982). Burrow structure and use in the sand fiddler crab *Uca pugilator* (Bosc). *Anim. Behav.* **30**, 687-694.

Collett, T. S. and Harkness, L. I. K. (1982). Depth vision in animals. In *Analysis of Visual Behaviour* (eds. D. J. Ingle M. A. Goodale and R. J. W. Mansfield), pp. 111-176. Cambridge, MA: MIT Press.

Crane, J. (1975). Fiddler crabs of the world (Ocypodidae: genus *Uca*). Princeton, New Jersey: Princeton University Press.

Cronin, T. W. and Forward, R. B. (1988). The visual pigments of crabs. I. Spectral characteristics. *J. Comp. Physiol. (A)* **162**, 463-478.

Cummins, D. and Goldsmith, T. H. (1981). Cellular identification of the violet receptor in the crayfish eye. *J. Comp. Physiol. (A)* **142**, 199-202.

Cummins, D. R., Chen, D. M. and Goldsmith, T. H. (1984). Spectral sensitivity of the spiny lobster, *Panulirus argus*. *Biol. Bull.* **166**, 269-276.

Dacke, M., Nordstrom, P. and Scholtz, C. H. (2003). Twilight orientation to polarised light in the crepuscular dung beetle *Scarabaeus zambesianus*. *J. Exp. Biol.* **206**, 1535-1543.

Dahmen, H. J. (1991). Eye specialisation in waterstriders: an adaptation to life in a flat world. *J. Comp. Physiol. (A)* **169**, 623-632.

David, S. V., Vinje, W. E. and Gallant, J. L. (2004). Natural stimulus statistics alter the receptive field structure of V1 neurons. *J. Neurosci.* **24**, 6991-7006.

Detto, T. (2007). The fiddler crab *Uca mjoebergi* uses colour vision in mate choice. *Proc. R. Soc. Lond. B.* **274**, 2785-2790.

Detto, T., Hemmi, J. M. and Backwell, P. R. Y. (2008). Colouration and colour changes of the fiddler crab, *Uca capricornis*: A descriptive study. *PLoS ONE* **3**, e1629.

Detto, T., Backwell, P. R. Y., Hemmi, J. M. and Zeil, J. (2006). Visually mediated species and neighbour recognition in fiddler crabs (*Uca mjoebergi* and *Uca capricornis*). *Proc. R. Soc. Lond. B.* **273**, 1661-1666.

Douglas, R. H. and Marshall, N. J. (1999). A review of vertebrate and invertebrate optical filters. In *Adaptive Mechanisms in the Ecology of Vision* (ed. S. N. e. a. Archer), pp. 95-162. Kluwer: Dordrecht.

Eckert, M. P. and Zeil, J. (2001). Towards an ecology of motion vision. In *Motion Vision: Computational, Neural, and Ecological Constraints* (eds. J. M. Zanker and J. Zeil), pp. 333-369. Berlin Heidelberg New York: Springer Verlag.

Ens, B. J., Klaassen, M. and Zwarts, L. (1993). Flocking and feeding in the fiddler crab (*Uca tangeri*): Prey availability as risk-taking behavior. *Neth. J. Sea. Res.* **31**, 477-494.

Franceschini, N. (1975). Sampling of the visual environment by the compound eye of the fly: Fundamentals and applications. In *Photoreceptor Optics* (eds. A. W. Snyder and R. Menzel), pp. 98-125. Berlin Heidelberg New York: Springer.

Franz, M. O. and Krapp, H. G. (2000). Wide-field, motion-sensitive neurons and matched filters for optic flow fields. *Biol. Cybern.* **83**, 185-197.

Gibson, J. J. (1950). The perception of the visual world. Cambridge: Riverside.

Goldsmith, T. H. and Bruno, M. S. (1973). Behavior of rhodopsin and metarhodopsin in isolated rhabdoms of crabs and lobster. In *Biochemistry and Physiology of Visual Pigments* (ed. H. Langer), pp. 147-153. Berlin Heidelberg New York: Springer.

Govardovskii, V. I., Fyhrquist, N., Reuter, T., Kuzmin, D. G. and Donner, K. (2000). In search of the visual pigment template. *Vis. Neurosci.* **17**, 509-528.

Grossman, Y., Parnas, I. and Spira, M. E. (1979). Differential conduction block in branches of a bifurcating axon. *J. Physiol.* **295**, 283-305.

Hamdorf, K., Paulsen, R. and Schwemer, J. (1973). Photoregeneration and sensitivity control of photoreceptors in invertebrates. In *Biochemistry and Physiology of Visual Pigments* (ed. H. Langer), pp. 155-166. Berlin Heidelberg New York: Springer.

Hardie, R. C. (1979). Electrophysiological analysis of fly retina. I: Comparative properties of R1-6 and R7 and 8. *J. Comp. Physiol. (A)* **129**, 19-33.

Hemmi, J. M. (2005a). Predator avoidance in fiddler crabs. 1. Escape decisions in relation to the risk of predation. *Anim. Behav.* **69**, 603-614.

Hemmi, J. M. (2005b). Predator avoidance in fiddler crabs. 2. The visual cues. *Anim. Behav.* **69**, 615-625.

Hemmi, J. M. and Zeil, J. (2003a). Burrow surveillance in fiddler crabs. I. Description of behaviour. *J. Exp. Biol.* **206**, 3935-3950.

Hemmi, J. M. and Zeil, J. (2003b). Burrow surveillance in fiddler crabs. II. The sensory cues. *J. Exp. Biol.* **206**, 3951-3961.

Hemmi, J. M. and Zeil, J. (2003c). Robust judgement of inter-object distance by an arthropod. *Nature* **421**, 160-163.

Hemmi, J. M. and Zeil, J. (2005). Animals as prey: Perceptual limitations and behavioural options. *Mar. Ecol. Prog. Ser.* **287**, 274-278.

Hemmi, J. M., Marshall, J., Pix, W., Vorobyev, M. and Zeil, J. (2006). The variable colours of the fiddler crab *Uca vomeris* and their relation to background and predation. *J. Exp. Biol.* **209**, 4140-4153.

Horch, K., Salmon, M. and Forward, R. (2002). Evidence for a two pigment visual system in the fiddler crab, *Uca thayeri*. *J. Comp. Physiol. (A)* **188**, 493-499.

How, M. J. and Hemmi, J. M. (2008). Courtship herding in the fiddler crab *Uca elegans*. *J. Comp. Physiol. (A)* **194**, 1053-1061.

How, M. J., Zeil, J. and Hemmi, J. M. (2007). Differences in context and function of two distinct waving displays in the fiddler crab, *Uca perplexa* (Decapoda: Ocypodidae). *Behav. Ecol. Sociobiol.* **62**, 137-148.

How, M. J., Hemmi, J. M., Zeil, J. and Peters, R. (2008). Claw waving display changes with receiver distance in fiddler crabs, *Uca perplexa*. *Anim. Behav.* **75**, 1015-1022.

Hughes, A. (1975). A comparison of retinal ganglion cell topography in the plains and tree kangaroo. *J. Physiol.* **244**, 61-63.

Hughes, A. (1977). The topography of vision in mammals of contrasting life style: Comparative optics and retinal organisation. In *Handbook of Sensory Physiology*, vol. VII/5 (ed. H. Autrum), pp. 613-756. Berlin Heidelberg New York: Springer.

Hyatt, G. W. (1975). Physiological and behavioral evidence for color discrimination by fiddler crabs (Brachyura, Ocypodidae, genus *Uca*). In *Physiological Ecology of Estuarine Organisms* (ed. F. J. Vernberg), pp. 333-365. Columbia, South Carolina: University of South Carolina Press.

Iribarne, O. O. and Martinez, M. M. (1999). Predation on the southwestern Atlantic fiddler crab (*Uca uruguayensis*) by migratory shorebirds (*Pluvialis dominica*, *P. squatarola*, *Arenaria interpres*, and *Numenius phaeopus*). *Estuaries* **22**, 47-54.

Jordão, J. M., Cronin, T. W. and Oliveira, R. F. (2007). Spectral sensitivity of four species of fiddler crabs (*Uca pugnax*, *Uca pugilator*, *Uca vomeris* and *Uca tangeri*) measured by *in situ* microspectrophotometry. *J. Exp. Biol.* **210**, 447-453.

Kashiyama, K., Seki, T., Numata, H. and Goto, S. G. (2009). Molecular characterization of visual pigments in Branchiopoda and the evolution of opsins in Arthropoda. *Mol. Biol. Evol.* **26**, 299-311.

Kelber, A., Vorobyev, M. and Osorio, D. (2003). Animal colour vision: Behavioural tests and physiological concepts. *Biol. Rev.* **78**, 81-118.

Kern, R., van Hateren, J. H., Michaelis, C., Lindemann, J. P. and Egelhaaf, M. (2005). Function of a fly motion-sensitive neuron matches eye movements during free flight. *PLoS Biol.* **3**, e171.

Kirk, M. D., Waldrop, B. and Glantz, R. M. (1982). The crayfish sustaining fibers. *J. Comp. Physiol. (A)* **146**, 175-179.

Kirschfeld, K., Franceschini, N. and Minke, B. (1977). Evidence for a sensitising pigment in fly photoreceptors. *Nature* **269**, 386-390.

Koller, G. (1927). Über Chromatophorensystem, Farbensinn und Farbenwechsel bei *Crangon vulgaris*. *Z. Vergl. Physiol.* **5**, 191-246.

Koller, G. (1928). Versuche über den Farbensinn der Euparugiden. *Z. Vergl. Physiol.* **8**, 337-353.

Koops, M. A. (2004). Reliability and the value of information. *Anim. Behav.* **67**, 103-111.

Koops, M. A. and Abrahams, M. V. (1998). Life history and the fitness consequences of imperfect information. *Evol. Ecol.* **12**, 601-613.

Körding, K. P., Kayser, C., Einhauser, W. and Konig, P. (2004). How are complex cell properties adapted to the statistics of natural stimuli? *J. Neurophysiol.* **91**, 206-212.

Korte, R. (1965). Durch polarisiertes Licht hervorgerufene Optomotorik bei *Uca tangeri*. *Experientia* **21**, 98.

Kramer, D. L. and Bonenfant, M. (1997). Direction of predator approach and the decision to flee to a refuge. *Anim. Behav.* **54**, 289-295.

Krapp, H. G. and Gabbiani, F. (2005). Spatial distribution of inputs and local receptive field properties of a wide-field, looming sensitive neuron. *J. Neurophysiol.* **93**, 2240-2253.

Labhart, T. (1980). Specialized photoreceptors at the dorsal rim of the honeybee's compound eye: Polarizational and angular sensitivity. *J. Comp. Physiol. (A)* **141**, 19-30.

Labhart, T. and Meyer, E. P. (1999). Detectors for polarized skylight in insects: a survey of ommatidial specializations in the dorsal rim area of the compound eye. *Microsc. Res. Tech.* **47**, 368-379.

Land, M. and Nilsson, D. E. (2002). Animal eyes. Oxford: Oxford University Press.

Land, M. and Nilsson, D. E. (2006). General-purpose and special-purpose visual systems. In *Invertebrate Vision* (eds. E. Warrant and D. E. Nilsson). Cambridge: Cambridge University Press.

Land, M. F. (1981). Optics and vision in invertebrates. In *Handbook of Sensory Physiology*, vol. VII/6B (ed. H. Autrum), pp. 471-592. Berlin Heidelberg New York: Springer.

Land, M. F. (1989). Variations in the structure and design of compound eyes. In *Facets of Vision* (eds. D. G. Stavenga and R. C. Hardie), pp. 90-111. Berlin Heidelberg New York: Springer.

Land, M. F. (1997). Visual acuity in insects. **42**, 147-177.

Land, M. F. (1999). The roles of head movements in the search and capture strategy of a tern (Aves, Laridae). *J. Comp. Physiol. (A)* **184**, 265-272.

Land, M. F. and Layne, J. E. (1995a). The visual control of behavior in fiddler crabs. 1. Resolution, thresholds and the role of the horizon. *J. Comp. Physiol. (A)* **177**, 81-90.

Land, M. F. and Layne, J. E. (1995b). The visual control of behavior in fiddler crabs. 2. Tracking control systems in courtship and defense. *J. Comp. Physiol. (A)* **177**, 91-103.

Layne, J. E., Barnes, W. J. P. and Duncan, L. M. J. (2003a). Mechanisms of homing in the fiddler crab *Uca rapax*. 1. Spatial and temporal characteristics of a system of small-scale navigation. *J. Exp. Biol.* **206**, 4413-4423.

Layne, J. E., Barnes, W. J. P. and Duncan, L. M. J. (2003b). Mechanisms of homing in the fiddler crab *Uca rapax*. 2. Information sources and frame of reference for a path integration system. *J. Exp. Biol.* **206**, 4425-4442.

Liang, T. (2008). Visual cues influencing escape responses in fiddler crabs (*Uca vomeris*), Honours thesis. Canberra: The Australian National University.

Lima, S. L. (1998). Nonlethal effects in the ecology of predator-prey interactions: What are the ecological effects of anti-predator decision-making? *Bioscience* **48**, 25-34.

Lipetz, L. E. (1971). The relation of physiological and psychological aspects of sensory intensity. In *Handbook of Sensory Physiology*, vol. I (ed. W. R. Loewenstein), pp. 191-225. Berlin Heidelberg New York: Springer.

Loew, E. R. and Lythgoe, J. N. (1985). The ecology of colour vision. *Endeavour* **9**, 170-174.

Lubbock, J. (1888). On the senses, instincts and intelligence of animals with special reference to insects. London: Kegan Paul.

Luttbeg, B. (2002). Assessing the robustness and optimality of alternative decision rules with varying assumptions. *Anim. Behav.* **63**, 805-814.

Lythgoe, J. N. (1979). The ecology of vision. Oxford: Oxford University Press.

Lythgoe, J. N. and Partridge, J. C. (1989). Visual pigments and the acquisition of visual information. *J. Exp. Biol.* **146**, 1-20.

Mark, R. F., James, A. C. and Sheng, X. M. (1993). Geometry of the representation of the visual field on the superior colliculus of the wallaby (*Macropus eugenii*). I. Normal projection. *J. Comp. Neurol.* **330**, 303-314.

Marshall, J., Cronin, T. W. and Kleinlogel, S. (2007). Stomatopod eye structure and function: A review. *Arthropod Struct. Dev.* **36**, 420-448.

Marshall, N. J., Jones, J. P. and Cronin, T. W. (1996). Behavioural evidence for colour vision in stomatopod crustaceans. *J. Comp. Physiol. (A)* **179**, 473-481.

Martin, F. G. and Mote, M. I. (1982). Color receptors in marine crustaceans: A second spectral class of retinular cell in the compound eyes of *Callinectes* and *Carcinus*. *J. Comp. Physiol. (A)* **145**, 549-554.

Martin, J. and Lopez, P. (1999). When to come out from a refuge: risk-sensitive and state-dependent decisions in an alpine lizard. *Behav. Ecol.* **10**, 487-492.

Martin, J. W. and Davis, E. (2001). An updated classification of the recent Crustacea. Los Angeles, California: Natural History Museum of Los Angeles County.

Matić, T. and Laughlin, S. B. (1981). Changes in the intensity-response function of an insect's photoreceptors due to light adaptation. *J. Comp. Physiol. (A)* **145**, 169-177.

Menzel, R. (1974). Colour receptors in insects. In *The Compound Eye and Vision in Insects* (ed. G. A. Horridge), pp. 121-153. Oxford: Clarendon Press.

Menzel, R. (1975). Polarization sensitivity in insect eyes with fused rhabdoms. In *Photoreceptor Optics* (eds. A. W. Snyder and R. Menzel), pp. 372-387. Berlin Heidelberg New York: Springer.

Menzel, R. (1979). Spectral sensitivity and color vision in invertebrates. In *Handbook of Sensory Physiology*, vol. VII/6A (ed. H. Autrum), pp. 503-580. Berlin Heidelberg New York: Springer.

Menzel, R., Ventura, D. F., Hertel, H., Desouza, J. M. and Greggers, U. (1986). Spectral sensitivity of photoreceptors in insect compound eyes: Comparison of species and methods. *J. Comp. Physiol. (A)* **158**, 165-177.

Naka, K. I. and Rushton, W. A. (1966a). S-potentials from luminosity units in the retina of fish (Cyprinidae). *J. Physiol.* **185**, 587-599.

Naka, K. I. and Rushton, W. A. (1966b). S-potentials from colour units in the retina of fish (Cyprinidae). *J. Physiol.* **185**, 536-555.

Nalbach, H. O. (1990). Visually elicited escape in crabs. In *Frontiers in Crustacean Neurobiology* (eds. K. Wiese W. D. Krent J. Tautz H. Reichert and B. Mulloney), pp. 165-172. Basel: Birkhäuser Verlag.

Nalbach, H. O., Zeil, J. and Forzin, L. (1989). Multisensory control of eye-stalk orientation in space: Crabs from different habitats rely on different senses. *J. Comp. Physiol. (A)* **165**, 643-649.

Niven, J. E. and Laughlin, S. B. (2008). Energy limitation as a selective pressure on the evolution of sensory systems. *J. Exp. Biol.* **211**, 1792-1804.

Olberg, R. and Worthington, A. (2008). Looming-sensitive neurons in the dragonfly predict time-to-contact. In *2nd International Conference on Invertebrate Vision*. Bäckaskog Castle, Sweden.

Oliva, D., Medan, V. and Tomsic, D. (2007). Escape behavior and neuronal responses to looming stimuli in the crab *Chasmagnathus granulatus* (Decapoda: Grapsidae). *J. Exp. Biol.* **210**, 865-880.

Ooi, T. L., Wu, B. and He, Z. J. J. (2001). Distance determined by the angular declination below the horizon. *Nature* **414**, 197-200.

Osorio, D. and Vorobyev, M. (2005). Photoreceptor spectral sensitivities in terrestrial animals: adaptations for luminance and colour vision. *Proc. R. Soc. Lond. B.* **272**, 1745-1752.

Osorio, D. and Vorobyev, M. (2008). A review of the evolution of animal colour vision and visual communication signals. *Vision Res.* **48**, 2042-2051.

Peters, R., Hemmi, J. and Zeil, J. (2008). Image motion environments: Background noise for movement-based animal signals. *J. Comp. Physiol. (A)* **194**, 441-456.

Petrowitz, R., Dahmen, H., Egelhaaf, M. and Krapp, H. G. (2000). Arrangement of optical axes and spatial resolution in the compound eye of the female blowfly *Calliphora*. *J. Comp. Physiol. (A)* **186**, 737-746.

Pope, D. S. (1998). The fiddler crab claw waving display: Function and evolution of a sexually selected signal. Durham, NC: Duke University.

Porter, M. L., Cronin, T. W., McClellan, D. A. and Crandall, K. A. (2007). Molecular characterization of crustacean visual pigments and the evolution of pancrustacean opsins. *Mol. Biol. Evol.* **24**, 253-268.

Rajkumar, P., Rollmann, S. M. and Layne, J. E. (2008). Sequence & expression of opsins in fiddler crab, *Uca pugilator*. In *2nd International Conference on Invertebrate Vision*. Bäckaskog Castle, Sweden.

Rossel, S. (1996). Binocular vision in insects: How mantids solve the correspondence problem. *Proc. Natl. Acad. Sci. USA* **93**, 13229-13232.

Sakamoto, K., Hisatomi, O., Tokunaga, F. and Eguchi, E. (1996). Two opsins from the compound eye of the crab *Hemigrapsus sanguineus*. *J. Exp. Biol.* **199**, 441-450.

Salmon, M. (1984). The courtship, aggression and mating system of a "primitive" fiddler crab (*Uca vocans*: Ocypodidae). *Trans. Zool. Soc. Lond.* **37**, 1-50.

Sandeman, D. C. (1969). Integrative properties of a reflex motoneuron in the brain of the crab *Carcinus maenas*. *J. Comp. Physiol. (A)* **64**, 450-464.

Schwind, R. (1989). Size and distance perception in compound eyes. In *Facets of Vision*, pp. 425-444. Berlin Heidelberg New York: Springer Verlag.

Scott, S. and Mote, M. I. (1974). Spectral sensitivity in some marine Crustacea. *Vision Res.* **14**, 659-663.

Shaw, S. R. (1969). Interreceptor coupling in ommatidia of drone honeybee and locust compound eyes. *Vision Res.* **9**, 999-1029.

Sih, A. (1992). Prey uncertainty and the balancing of antipredator and feeding needs. *Am. Nat.* **139**, 1052-1069.

Simoncelli, E. P. and Olshausen, B. A. (2001). Natural image statistics and neural representation. *Annu. Rev. Neurosci.* **24**, 1193-1216.

Smith, K. C. and Macagno, E. R. (1990). UV photoreceptors in the compound eye of *Daphnia magna* (Crustacea, Branchiopoda). A fourth spectral class in single ommatidia. *J. Comp. Physiol. (A)* **166**, 597-606.

Smolka, J. and Hemmi, J. M. (2008). How the fiddler crab eye sees the world. In *2nd International Conference on Invertebrate Vision*. Bäckaskog Castle, Sweden.

Snyder, A. W. (1979). Physics of vision in compound eyes. In *Handbook of Sensory Physiology*, vol. VII/6A (ed. H. Autrum), pp. 225-313. Berlin Heidelberg New York: Springer.

Snyder, A. W., Menzel, R. and Laughlin, S. B. (1973). Structure and function of the fused rhabdom. *J. Comp. Physiol. (A)* **87**, 99-135.

Sparks, D. L. (2005). An argument for using ethologically "natural" behaviors as estimates of unobservable sensory processes. Focus on "Sound localization performance in the cat: the effect of restraining the head". *J. Neurophysiol.* **93**, 1136-1137.

Srinivasan, M. V. (1993). How insects infer range from visual motion. *Rev. Oculomot. Res.* **5**, 139-156.

Stavenga, D. G. (1979). Pseudopupils of compound eyes. In *Handbook of Sensory Physiology*, vol. VII/6a (ed. H. Autrum), pp. 357-439. Berlin Heidelberg New York: Springer.

Stavenga, D. G. (2002). Colour in the eyes of insects. *J. Comp. Physiol. (A)* **188**, 337-348.

Stavenga, D. G. (2003a). Angular and spectral sensitivity of fly photoreceptors. I. Integrated facet lens and rhabdomere optics. *J. Comp. Physiol. (A)* **189**, 1-17.

Stavenga, D. G. (2003b). Angular and spectral sensitivity of fly photoreceptors. II. Dependence on facet lens F-number and rhabdomere type in *Drosophila*. *J. Comp. Physiol. (A)* **189**, 189-202.

Stavenga, D. G. (2004). Angular and spectral sensitivity of fly photoreceptors. III. Dependence on the pupil mechanism in the blowfly Calliphora. *J. Comp. Physiol. (A)* **190**, 115-129.

Storz, U. C. and Paul, R. J. (1998). Phototaxis in water fleas (*Daphnia magna*) is differently influenced by visible and UV light. *J. Comp. Physiol. (A)* **183**, 709-717.

Stowe, S. (1980). Spectral sensitivity and retinal pigment movement in the crab *Leptograpsus variegatus* (Fabricius). *J. Exp. Biol.* **87**, 73-98.

Sztarker, J., Strausfeld, N. J. and Tomsic, D. (2005). Organization of optic lobes that support motion detection in a semiterrestrial crab. *J. Comp. Neurol.* **493**, 396-411.

Sztarker, J., Strausfeld, N., Andrew, D. and Tomsic, D. (2009). Neural organization of first optic neuropils in the littoral crab *Hemigrapsus oregonensis* and the semiterrestrial species *Chasmagnathus granulatus*. *J. Comp. Neurol.* **513**, 129-150.

van Hateren, J. H., Kern, R., Schwerdtfeger, G. and Egelhaaf, M. (2005). Function and coding in the blowfly H1 neuron during naturalistic optic flow. *J. Neurosci.* **25**, 4343-4352.

von Hagen, H. O. (1967). Nachweis einer kinästethischen Orientierung bei *Uca rapax*. *Z. Morph. Ökol. Tiere* **58**, 301-320.

Wahba, G. (1990). Spline models for observational data. Philadelphia: Society for Industrial and Applied Mathematics.

Wald, G., Brown, P. K. and Gibbons, I. R. (1963). The problem of visual excitation. *J. Opt. Soc. Am.* **53**, 20-35.

Walls, G. L. (1942). The vertebrate eye and its adaptive radiation. Bloomfield Hills, Michigan: Cranbook Press.

Warrant, E. J. and McIntyre, P. D. (1993). Arthropod eye design and the physical limits to spatial resolving power. *Prog. Neurobiol.* **40**, 413-461.

Warrant, E. J. and Nilsson, D. E. (1998). Absorption of white light in photoreceptors. *Vision Res.* **38**, 195-207.

Welton, N. J., McNamara, J. M. and Houston, A. I. (2003). Assessing predation risk: Optimal behaviour and rules of thumb. *Theor. Pop. Biol.* **64**, 417-430.

Wiersma, C. A. and Yamaguchi, T. (1967a). Integration of visual stimuli by the crayfish central nervous system. *J. Exp. Biol.* **47**, 409-431.

Wiersma, C. A. and Yamaguchi, T. (1967b). The integration of visual stimuli in the rock lobster. *Vision Res.* **7**, 197-203.

Yamaguchi, T. and Tabata, S. (2004). Territory usage and defence of the fiddler crab, *Uca lactea* (De Haan) (Decapoda, Brachyura, Ocypodidae). *Crusteceana* **77**, 1055-1080.

Zeil, J. (1983). Sexual dimorphism in the visual system of flies: The free flight behaviour of male Bibionidae (Diptera). *J. Comp. Physiol. (A)* **150**, 395-412.

Zeil, J. (1998). Homing in fiddler crabs (*Uca lactea annulipes* and *Uca vomeris*: Ocypodidae). *J. Comp. Physiol. (A)* **183**, 367-377.

Zeil, J. and Al-Mutairi, M. M. (1996). The variation of resolution and of ommatidial dimensions in the compound eyes of the fiddler crab *Uca lactea annulipes* (Ocypodidae, Brachyura, Decapoda). *J. Exp. Biol.* **199**, 1569-1577.

Zeil, J. and Hofmann, M. (2001). Signals from 'crabworld': Cuticular reflections in a fiddler crab colony. *J. Exp. Biol.* **204**, 2561-2569.

Zeil, J. and Layne, J. E. (2002). Path integration in fiddler crabs and its relation to habitat and social life. In *Crustacean Experimental Systems in Neurobiology* (ed. K. Wiese), pp. 227-246. Berlin Heidelberg New York: Springer.

Zeil, J. and Hemmi, J. M. (2006). The visual ecology of fiddler crabs. *J. Comp. Physiol. (A)* **192**, 1-25.

Zeil, J., Nalbach, G. and Nalbach, H. O. (1986). Eyes, eye stalks and the visual world of semi-terrestrial crabs. *J. Comp. Physiol. (A)* **159**, 801-811.

Zeil, J., Nalbach, G. and Nalbach, H. O. (1989). Spatial vision in a flat world: Optical and neural adaptations in arthropods. In *Neurobiology of Sensory Systems* (eds. R. N. Singh and N. J. Strausfeld), pp. 123-137. New York: Plenum.

Zwarts, L. (1985). The winter exploitation of fiddler cabs *Uca tangeri* by waders in Guinea-Bissau. *Ardea* **73**, 3-12.